

Novel approaches to measure physiological and behavioral responses to stress

Dissertation

for the award of the degree

'Doctor rerum naturalium' (Dr. rer. nat.)

of the Georg-August-Universität Göttingen

within the Systems Neuroscience doctoral program of the
Göttingen Graduate School for Neurosciences, Biophysics, and Molecular
Biosciences (GGNB) and of the Georg-August University School of Science
(GAUSS)



submitted by

Jan Sören Seidel

born in Bad Kreuznach

Göttingen, 2019

THESIS ADVISORY COMMITTEE

Prof. Dr. Dr. Hannelore Ehrenreich (Supervisor)

Clinical Neuroscience, Max Planck Institute of Experimental Medicine, Göttingen

Prof. Dr. Lars Penke

Georg Elias Müller Institute of Psychology, Georg-August University, Göttingen

Prof. Klaus-Armin Nave, Ph.D.

Neurogenetics, Max Planck Institute of Experimental Medicine, Göttingen

MEMBERS OF THE EXAMINATION BOARD

Prof. Dr. Dr. Hannelore Ehrenreich (Supervisor, Referee)

Clinical Neuroscience, Max Planck Institute of Experimental Medicine, Göttingen

Prof. Dr. Lars Penke (Co-referee)

Georg Elias Müller Institute of Psychology, Georg-August University, Göttingen

Prof. Klaus-Armin Nave, Ph.D.

Neurogenetics, Max Planck Institute of Experimental Medicine, Göttingen

Prof. Dr. Annekathrin Schacht

Georg Elias Müller Institute of Psychology, Georg-August University, Göttingen

Prof. Dr. Susann Boretius

Functional Imaging, German Primate Center, Göttingen

Prof. Dr. Walter Paulus

Department of Clinical Neurophysiology, University Medical Center, Göttingen

Date of submission of thesis: October 22nd 2019

Date of the oral examination: December 2nd 2019

DECLARATION OF AUTHORSHIP

I hereby declare that the thesis “Novel approaches to measure physiological and behavioral responses to stress” has been written independently and with no other sources and aids than quoted.

Jan Sören Seidel

Göttingen, October 22nd 2019

Dedicated to Ida, Emil, & Anton

may you always see the world as it should be seen

full of wonders

ACKNOWLEDGEMENTS

First and foremost I want to thank my supervisor, Prof. Hannelore Ehrenreich, for the opportunity to pursue research in the fascinating field of Clinical Neurosciences. Her supportive attitude, her guidance, and the way she approaches research questions and associated issues have always been a great source of inspiration for me.

Further, I am grateful for all the scientific input given by my Thesis Advisory Committee members, Prof. Lars Penke and Prof. Klaus-Armin Nave, that improved the quality of my work.

I want to thank PD. Dr. Martin Begemann for the amazing time we spent together. So much I have learned during our trips, the examinations of patients, and our numerous discussions. Your kind nature and your respectful interaction with other people, whether they are patients, colleagues, or just strangers in Café Central, will be kept in good memory.

I am very grateful to Dr. Marina Mitjans, her guidance and help, and, of course, for the great and productive cooperations over the years. Besides others, I highly appreciate her contribution to the Violent Aggression project. Likewise, I want to thank Dr. Vikas Bansal and Fabian Bockhop for their help and assistance.

Further, I thank all the students I had the honor to supervise over the course of my PhD. I hope, I have not been the only one who learned a lot working with you.

Moreover, I want to thank every single one in the Clinical Neuroscience group for all the moments, both great and sometimes tough, we experienced together as a team.

Also, I want to acknowledge the help and contribution of the Light Microscopy Facility team, namely Dr. Mišo Mitkovski, Katharina Schneider, and Heiko Röhse, for their participation in our work on infrared thermography.

And, last, but definitely not least, I want to express my deepest gratitude to my family, my partner, and my friends for all the support, encouragement, and heads-ups given over the years.

TABLE OF CONTENTS

1	INTRODUCTION TO THE THESIS WORK	1
1.1	The perception of danger affects body, cognition, and behavior in multiple ways	1
1.2	Stress can have severe implications on medical and psychological wellbeing	2
1.3	Aggression is a natural behavioral response to stressful events	2
1.4	Aggression is a consequence of the interplay between genetics and the environment	3
1.5	Schizophrenia is a severe psychiatric condition associated with stress and aggression	4
1.6	Stress leads to autonomous responses in animals and humans	5
1.7	Infrared thermography is a non-invasive, contact-free technique to measure body surface temperature	7
1.8	IRT has several advantages over 'conventional' physiological measurement techniques	11
1.9	Limitations of modern IRT in research context	12
2	SCOPE OF THE PRESENT WORK	15
3	PROJECT I: VIOLENT AGGRESSION PREDICTED BY MULTIPLE PRE-ADULT ENVIRONMENTAL HITS	17
3.1	Overview of project I	17
3.2	Original publication	19
4	PROJECT II: VASCULAR RESPONSE TO SOCIAL COGNITIVE PERFORMANCE MEASURED BY INFRARED THERMOGRAPHY: A TRANSLATIONAL STUDY FROM MOUSE TO MAN	37
4.1	Overview of project II	37
4.2	Original publication	39
5	SUMMARY AND CONCLUSIONS	57

BIBLIOGRAPHY	61
A APPENDIX	69
A.1 Accepted co-authorships	69
A.2 List of publications	87

LIST OF FIGURES

- 1.1 Example of the process of IRT recording and following data extraction . . . 9
- 1.2 Facial areas exhibit different thermal patterns over the course of IRT . . . 11

LIST OF ABBREVIATIONS

&	and
°C	<i>degree Celsius</i>
°K	<i>degree Kelvin</i>
µm	<i>micrometer</i>
ANS	<i>autonomous nervous system</i>
CGAS	<i>candidate gene association study/studies</i>
DNA	<i>deoxyribonucleic acid</i>
e.g.	<i>for example (abbr. of latin: exempli gratia)</i>
et al.	<i>and others (abbr. of latin: et alii)</i>
FRT	<i>Face Recognition Test</i>
GRAS	<i>Göttingen Research Association for Schizophrenia</i>
GWAS	<i>genome-wide association study/studies</i>
HDAC	<i>histone deacetylase</i>
HPA axis	<i>hypothalamic-pituitary-adrenal axis</i>
i.e.	<i>that is (abbr. of latin: id est)</i>
IRT	<i>infrared thermography</i>
MAOA	<i>monoamine oxidase A</i>
mK	<i>millikelvin</i>
mRNA	<i>messenger ribonucleic acid</i>
PTSD	<i>posttraumatic stress disorder</i>
VASS	<i>Violent Aggression Severity Score</i>
VTNR	<i>variant number tandem repeat</i>
WCST	<i>Wisconsin Card Sorting Test</i>

1 INTRODUCTION TO THE THESIS WORK

What and who we are is determined by numerous factors. Besides hereditary traits, the experiences we make over the course of our lives affect us in both positive, but sometimes also negative ways. Stress, defined as the actual or anticipated perception of a threat to homeostasis or wellbeing (Ulrich-Lai & Herman, 2009), plays an important role in an organism's ability to adapt to adverse environmental events. In order to mitigate the impact of hazardous conditions, it is crucial to show an adequate physiological and behavioral stress response (Hollon, Burgeno, & Phillips, 2015).

1.1 The perception of danger affects body, cognition, and behavior in multiple ways

Threats to one's physical or psychological integrity come in different flavors (Bhatnagar, Vining, Iyer, & Kinni, 2006; Juruena, 2014). Their perception typically leads to certain alterations of endogenous processes in order to initiate adaptive behavioral actions and to restore homeostasis (Smith & Vale, 2006). In rodents and humans, the hypothalamic-pituitary-adrenal (HPA) axis is most relevant in mediating stress responses. As soon as a potential threat is detected, the paraventricular nucleus of the hypothalamus releases both corticotropin-releasing hormone and vasopressin, triggering the production and secretion of adrenocorticotrophic hormone by the anterior pituitary gland and, ultimately, of glucocorticoids as well as mineralocorticoids by the adrenal cortex (Aguilera, 2011; Joseph & Whirledge, 2017; Smith & Vale, 2006). This endocrinological cascade is associated with many changes in the peripheral and central nervous system in order to prepare for autonomous and behavioral responses (Ulrich-Lai & Herman, 2009).

During the stress responses, to increase chances of survival, important body functions, such as the cardiovascular activity, respiration, or metabolic rate, are enhanced, while other, less critical functions are inhibited (Joseph & Whirledge, 2017). Furthermore, to prevent the risk of lethal blood loss, autonomous nervous system (ANS)-regulated vasoresponses change the volume of arterial blood vessels, typically decreasing blood flow to peripheral body parts (Engert et al., 2014). Physiological research takes advantage of such alterations

in ANS activity to gain insight into the organism's stress response (Cardone & Merla, 2017; Ermatinger, Brugger, & Burkart, 2019). Moreover, levels of hormones that are released via the HPA axis can be analyzed to determine the intensity of perceived stress. In particular glucocorticoids, as the downstream product of the HPA axis (i.e., cortisol in humans, corticosterone in mice and rats), are commonly employed as biological stress markers (Boehringer et al., 2015; Hellhammer, Wust, & Kudielka, 2009).

1.2 Stress can have severe implications on medical and psychological wellbeing

While stress is commonly perceived as unpleasant and adverse, it fulfills an evolutionary purpose and can enhance our physical and psychological functionality (Hollon et al., 2015; McEwen, 2007). However, intense or long-lasting periods of stress may have a negative impact on, or may even be the cause of, somatic diseases as well as psychological and cognitive states (Hollon et al., 2015; Yaribeygi, Panahi, Sahraei, Johnston, & Sahebkar, 2017). Stress is further linked to dysfunctional behavioral patterns and unfavorable coping mechanisms, such as substance abuse (Piazza & Le Moal, 1998). With regard to psychiatric conditions, stressful experiences have an at least modulating impact on the development and course of many, if not all, psychiatric syndromes, including posttraumatic stress disorder (PTSD), major depression, and schizophrenia (Agid, Kohn, & Lerer, 2000).

1.3 Aggression is a natural behavioral response to stressful events

Stress typically leads to characteristic physiological and behavioral responses. One important possible reaction to a threat is aggression, exhibited by many different species, with humans being no exception (Veroude et al., 2016; Waltes, Chiocchetti, & Freitag, 2016). In general, aggression can be defined as an overt behavior that has the intention of inflicting physical damage or harm to other living beings (Miczek, Fish, De Bold, & De Almeida, 2002; Nelson & Trainor, 2007). However, former work suggests distinct subgroups of aggression (e.g., reactive versus proactive; overt versus covert; physical versus relational), with variations in the incidence of these subtypes in relation to context, age, and gender (Björkqvist, 2018; Österman et al., 1998; Veroude et al., 2016). While adaptive in certain situations, when exhibited repeatedly, over longer phases, or out of context aggression

constitutes a serious problem for society as a whole, both due to individual consequences and economical costs (Blair, 2016). Thus, a closer look at factors modulating the expression of aggressive responses to stress is desirable.

1.4 Aggression is a consequence of the interplay between genetics and the environment

Over the last decades, genetic and environmental factors that may cause or modulate aggression have extensively been investigated. For instance, twin and adoption studies emphasize that, besides a strong hereditary impact, the relevance of environmental factors should not be underestimated. In particular, the non-shared environment plays an at least moderate role in aggressive behavior. However, due to differences in age and gender of the investigated individuals as well as operationalization of aggression phenotypes over studies, the amount of estimated genetic and environmental influence varies (Veroude et al., 2016). Accordingly, genome-wide association studies (GWAS), which aimed to identify gene variants relevant for aggressive phenotypes, could not achieve genome-wide significances (Mick et al., 2014; Tiihonen et al., 2015; Waltes et al., 2016). Approaches of candidate gene association studies (CGAS), on the other hand, targeted and identified several genes possibly connected to aggression. In particular, genes that influence monoaminergic neurotransmission (Veroude et al., 2016; Waltes et al., 2016) seem to be of importance.

Research genuinely relying on genetic readouts neglects the interplay between genes and the environment, which seems to serve as an important modulator of the development of aggressive behavior and related disorders. In an influential study, Caspi and colleagues (2002) prospectively examined the impact of a variant number tandem repeat (VNTR) polymorphism in the promoter region of the *monoamine oxidase A (MAOA)* gene on the occurrence of antisocial problems in men. The *MAOA* gene is located on the X chromosome and expresses an enzyme that metabolizes monoamines, such as serotonin, dopamine, or noradrenaline. These neurotransmitters have been linked to aggression (Brunner, Nelen, Breakefield, Ropers, & van Oost, 1993). In 2002, Caspi et al. reported that low *MAOA* activity, due to the VNTR polymorphism, is linked to a higher risk of antisocial behavior. However, this higher risk could only be observed in individuals who additionally suffered

from maltreatment during childhood, highlighting the importance of both genes and adverse environmental factors in the explanation of problematic behavior patterns (Caspi et al., 2002). Their findings have been replicated multiple times (Byrd & Manuck, 2014; Kim-Cohen et al., 2006), suggesting a robust gene \times environment interaction effect on aggression. Epigenetic analyses try to combine both genetic and environmental research by investigating the effects of environmental factors on the expression of genes via, besides others, DNA methylation, chromatin modification, or histone acetylation and deacetylation (Palumbo, Mariotti, Iofrida, & Pellegrini, 2018).

Studies examined a huge number of potentially relevant environmental risk factors with respect to aggressive behavior. However, such work often focuses on not clearly defined environmental experiences (e.g., childhood maltreatment). More importantly, risk factors are often assessed in an isolated manner, ignoring possible additive effects (Raine, 2002). Furthermore, several other parameters moderate aggressive behavior, such as age and gender (Björkqvist, 2018; Österman et al., 1998). Moreover, an altered state of mind, typically found in psychiatric conditions, such as schizophrenia, is prominently linked to increased aggressive potential. In fact, aggression does occur more frequently in patients with schizophrenia compared to individuals without. Yet, just a minority of patients actually exhibits aggressive behavior, often moderated by additional factors (Fazel, Gulati, Linsell, Geddes, & Grann, 2009; Sariaslan, Lichtenstein, Larsson, & Fazel, 2016).

1.5 Schizophrenia is a severe psychiatric condition associated with stress and aggression

Schizophrenia is a chronic mental disease, which usually starts in early adulthood and severely impairs cognitive functions, affect, and behavior of patients. It is characterized by both positive symptoms, like sensory hallucinations, delusions, and disordered thoughts as well as negative symptoms, such as poverty of speech (alogia), reduction of emotions and motivation, and social withdrawal (American Psychological Association, 2013; Howes & Murray, 2014). With a lifetime prevalence of approximately 1%, schizophrenia is one of the very common psychiatric disorders, with highly heterogeneous interindividual disease patterns (Howes & Murray, 2014). Schizophrenia negatively affects an individual's

ability of daily living and quality of life in manifold ways. Moreover, due to high direct and indirect costs, schizophrenia is not only a burden for patients and their personal environment but also for society (Knapp, Mangalore, & Simon, 2004; van Os & Kapur, 2009).

Both genetic and environmental risk factors have been associated with schizophrenia (Belbasis et al., 2018; Schizophrenia Working Group of the Psychiatric Genomics Consortium, 2014; Brown, 2011; van Os & Kapur, 2009), but our knowledge concerning its development is limited. As an approach to overcome weaknesses of many genetic and environmental studies, our group established the Göttingen Research Association for Schizophrenia (GRAS) data collection as a multicenter assessment of patients suffering from schizophrenia or schizoaffective disorder (Begemann et al., 2010; Ribbe et al., 2010). In a recent study, our group used the potential of the GRAS data collection to investigate the impact of well-defined environmental risk factors on the age of disease onset in a sample of 750 male patients with schizophrenia (Stepniak et al., 2014). We reported that the amount of adverse risk factors experienced before adulthood is strongly related to the age of onset of schizophrenia. Moreover, extreme group comparisons revealed a 10 years earlier disease onset in patients with a high, in relation to those with a low, risk load. Contrary to the remarkable effects of the environment on disease onset, polygenic risk scores did not reveal notable results. Having these large additive environmental effects on the development of schizophrenia in mind, we were wondering whether models of accumulated environmental risk factors, experienced in critical phases of development (i.e., before adulthood) could improve our understanding of the relationship between environmental stressors and aggression in both individuals from the general population and patients suffering from schizophrenia.

1.6 Stress leads to autonomous responses in animals and humans

As discussed before, autonomic responses to negative environmental experiences are an important readout of stress, not only in animal studies but also in human research (Ulrich-Lai & Herman, 2009). Stress is not only relevant when it occurs in an intense way or in critical stages of development. Chronic mild stress can influence our somatic and

psychological wellbeing and daily life functioning (Won & Kim, 2016; Yaribeygi et al., 2017). Therefore, it is worthwhile to take a closer look at the physiological and behavioral responses to more subtle forms of stress.

Animal models of stress commonly rely on the assessment of behavioral reactions within stress-inducing settings. Depending on the experimental scenario, different behavior can be observed, including fight-or-flight reactions, freezing, or situational avoidance (Benus, Koolhaas, & van Oortmerssen, 1992; de Boer, 2018; Harro, 2018; Toth & Neumann, 2013). In addition, to get deeper insights into endogenous processes, techniques to investigate physiological reactions to stress are available. The latter range from blood corticosterone levels and core body temperature, often measured via a surgically introduced probe, to posthumous analyses of hypothalamic Fos expression (Bhatnagar et al., 2006; Keeney, Hogg, & Marsden, 2001; Martinez, Carvalho-Netto, Amaral, Nunes-de Souza, & Canteras, 2008). Such measures, however, are very invasive or distress animals even further, leading to unnatural testing conditions and thus likely biasing the outcome of experiments (Cardone & Merla, 2017). Moreover, invasive assessment techniques raise ethical concerns regarding animal welfare (Gjendal, Franco, Ottesen, Sorensen, & Olsson, 2018; Meyer, Ootsuka, & Romanovsky, 2017).

Compared to animals, human research provides the great advantage to get insight into psychological states by simply asking. Assuming proper usage, psychometric tools, such as psychological questionnaires or interviews, are known to be capable of collecting valid information on an individual's internal processes. However, subjective self-descriptions may not always be the best choice to investigate stress. For instance, the administration of psychometric instruments is not always feasible over the course of an experiment. Furthermore, given answers are commonly biased and are not necessarily in line with data derived from physiological instruments. Therefore, an accompanying implementation of more objective approaches is indicated.

Human body responses to ANS activity are typically measured via a variety of instruments. Modern techniques are capable of accurately capturing a wide spectrum of basal

physiological functions, such as the heart rate, arterial blood pressure, respiration rate, muscle tone, or electrodermal activity (Cardone & Merla, 2017; Engert et al., 2014). Although these valuable tools are important in both neuroscientific research and clinical practice, they all have certain limitations (Ermatinger et al., 2019). Many of these techniques require participants to remain as motionless as possible to prevent measurement artifacts and errors, or they need to apply sensors on the test subjects' bodies (Cardone & Merla, 2017). Such intrusive conditions typically result in an uncomfortable and artificial testing environment. Moreover, certain investigations, such as an exploration of social interactions, are often considerably limited (Cardone & Merla, 2017; Ioannou, Morris, Baker, Reddy, & Gallese, 2017). Furthermore, the application of those techniques is highly challenging in individuals who are not able or willing to follow standard measurement protocols, such as patients suffering from psychiatric conditions (Engert et al., 2014). In summary, methods commonly used in both animal and human stress studies suffer from limitations that weaken and question the validity of reported outcomes. Therefore, besides others, this field of research could substantially benefit from non-invasive, contact-free techniques to reliably measure ANS activity. Modern infrared thermography recording has the potential to fill this gap.

1.7 Infrared thermography is a non-invasive, contact-free technique to measure body surface temperature

Infrared thermography (IRT) was first discovered in 1800 by astronomer William Herschel under the term 'Calorific Rays' while investigating specific radiation emitted by the sun (Herschel, 1800; Rogalski, 2012). In order to quantify the physical property commonly perceived as 'heat', IRT utilizes electromagnetic radiation of a characteristic wavelength outside our visible spectrum of light, namely within a bandwidth of 0.75 to 1000 μm (Lahiri, Bagavathiappan, Jayakumar, & Philip, 2012). Every living being, as well as inanimate objects with a temperature higher than 0 °K, emit radiation within this spectrum, where higher wavelengths are linked to lower temperatures (Tattersall, 2016). As an example, mammals', including humans, body surface constantly emits heat, peaking between 8 and 12 μm . Thus, IRT specialized in recording living beings mostly relies on sensors made of materials sensitive to long-wavelength infrared (Lahiri et al., 2012; Tattersall, 2016).

Today, infrared radiation technology commonly used to detect thermal alterations relies on either cooled (quantum) or uncooled (thermal) detectors (Usamentiaga et al., 2014). Quantum IRT systems utilize the interaction of semiconductors with changes in the energy distribution of electrons due to the stimulation of thermal photons (Cardone & Merla, 2017; Rogalski, 2012). They depend on selective wavelengths and achieve very high measurement precision. Given the high demand for constant cooling, this type of detectors are characterized by high costs, a bulky and heavy design, and a complicated way of usage (Rogalski, 2002). Conversely, cameras with uncooled thermal detectors are calibrated to a certain temperature (e.g., ambient temperature) and are typically independent of photonic wavelength (Rogalski, 2012). In order to translate electromagnetic radiation to electricity and, subsequently, to thermal images, special materials that do not block infrared radiation are employed (Cardone & Merla, 2017; Rogalski, 2002, 2012). When detector parts are hit by thermal radiation, they heat up and alter their electrical properties. In order to create a visible representation of this process, changes in electrical properties can be translated to corresponding pixels. This results in the creation of a monochromatic image with pixel intensities correlating with the respectively detected thermal energy. For a better visual interpretation, monochromatic images can then be converted into false-color images using different color palettes (Alpar & Krejcar, 2017; Ring & Ammer, 2012; Tattersall, 2016). An example of the recording and data quantification process can be found in Figure 1.

In relation to cooled systems, uncooled IRT cameras are characterized by lower thermal sensitivity. Nevertheless, modern cameras still achieve a relatively high spatial (up to 1280×1024 pixels) and temporal resolution (≥ 200 frames per second) and combine a satisfying thermal sensitivity (Noise-Equivalent Temperature Difference of not more than 30 mK at 30 °C ambient temperature) with a sufficiently high testing accuracy (Cardone & Merla, 2017).

At present, IRT plays an important role in different fields, such as the military, law enforcement, search and rescue missions, material sciences, and many more (Jarlier et al., 2011; Rogalski, 2012; Tattersall, 2016; Usamentiaga et al., 2014). In medicine, IRT had its first appearance already in the 1960s. However, technical limitations led scientists and physicians to favor more applicable tools (Lahiri et al., 2012; Ring, 2010). In recent years, technological and manufacturing advancements resulted in a comeback of IRT in both medical research and diagnostic applications. Nowadays, modern IRT presents

itself as a valid, relatively inexpensive and easy-to-use measuring method that is already implemented in diverse areas of medicine, including oncology, dentistry, dermatology, endocrinology, epidemiology, or infectiology (Lahiri et al., 2012; Ring & Ammer, 2012; Usamentiaga et al., 2014).

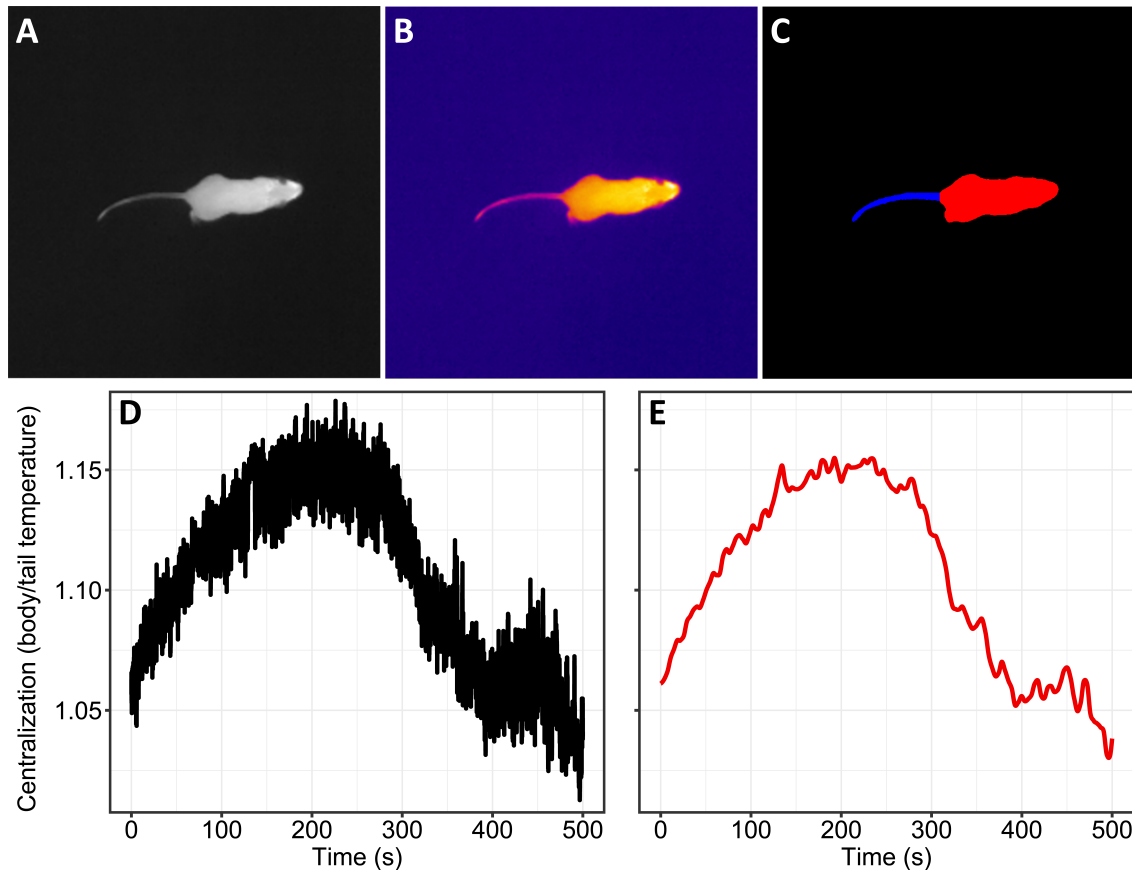


FIGURE 1.1: **Example of the process of IRT recording and following data extraction.**

A: Grayscale image derived from a mouse performing an Open Field paradigm. **B:** Pseudo-colors application makes differences in surface temperature easily visible. **C:** Peripheral (blue) and core (red) body regions are defined for the following data extraction. **D:** Thermal curve of the index of core body divided by periphery (centralization) over the course of 500 seconds. **E:** To reduce noise thermal curve can then be smoothed.

Recently, IRT has found its way into neuroscientific research, including both animal and human subjects (Cardone & Merla, 2017; Ermatinger et al., 2019; Gjendal et al., 2018; Herborn, Jerem, Nager, McKeegan, & McCafferty, 2018; Ioannou, Gallese, & Merla, 2014; Moline et al., 2017; Mufford et al., 2016; Tattersall, 2016). Mammals are endothermic organisms and therefore in need of maintaining stable body temperature by internal regulation processes, including muscular activity (e.g., shivering) to increase body heat and perspiration (i.e., activation of sweat glands) in order to cool down (Mufford et al., 2016; Ring, 2010). But body temperature does not only alter in response to physical parameters like ambient temperature changes. Autonomous activity, for instance, as a response to

stressful experiences, leads to alterations in volumes of blood vessels (i.e., vasoconstriction and vasodilation) in both peripheral and core body regions, culminating in changes in blood flow (flushing; Gjendal et al., 2018; Meyer et al., 2017; Mufford et al., 2016; Yoshihara et al., 2016). Autonomous responses prepare animals for defensive actions in the eye of a physical or predatory threat (e.g., fight-or-flight). Moreover, they provide protection from blood loss due to injury and hence increase the chances of survival (Herborn et al., 2018; Ioannou et al., 2014; Vianna & Carrive, 2005). As a side effect, such highly adaptive physiological alterations concur with changes in temperature of core and peripheral body parts. Remarkably, IRT is capable of quantifying these changes by recording heat emissions from the body surface.

Accordingly, in humans, associations between physiological processes, detectable via measurements of thermal alterations, and psychological or behavioral reactions have long been reported. For instance, already Darwin (1872) described the relationship between facial flushing and emotions, such as anger. Subsequently, other authors reported vasoconstriction or vasodilation as a result of autonomous activity that is strongly linked to thermal changes in both acral and central body parts as well as facial regions (Ioannou et al., 2014, 2017). Notably, in a series of studies Kistler and colleagues (Kistler et al., 1996; Kistler, Mariauzouls, & von Berlepsch, 1998a, 1998b) used Laser Doppler Flowmetry and photoplethysmography techniques to associate sympathetic vasoconstriction and temperature alterations in the fingertips during sympathetically activating procedures, such as watching horror movies, chewing cotton swaps, or receiving an acupuncture treatment. The authors showed that with a delay of approximately 15 seconds, temperature changes reliably occurred in more than 90% of the time. Similarly, Drummond and colleagues used Laser Doppler Flowmetry in order to explore the relationship between blood vessel volume and anger induction in female (Drummond, 1999), and during an embarrassment task in male and female, participants (Drummond & Su, 2012).

The human face is of particular interest for thermal studies. Due to a complex network of blood vessels under its surface, alterations in ANS activity have strong effects on subcutaneous blood flow and, consequently, temperature in different facial regions (Figure 2; Ioannou et al., 2017). Engert et al. (2014) investigated thermal alterations of various

areas of the face in response to physical and social stress, revealing large differences in thermal patterns in relation to the type of stressor experienced. Changes in flushing, due to negative or positive social stimuli, combined with different intensity levels also lead to alteration in surface temperature, with, in particular, the nose consistently reported as highly reactive to affective and social cues (Cardone & Merla, 2017; Engert et al., 2014; Ioannou et al., 2017; Kosonogov et al., 2017).

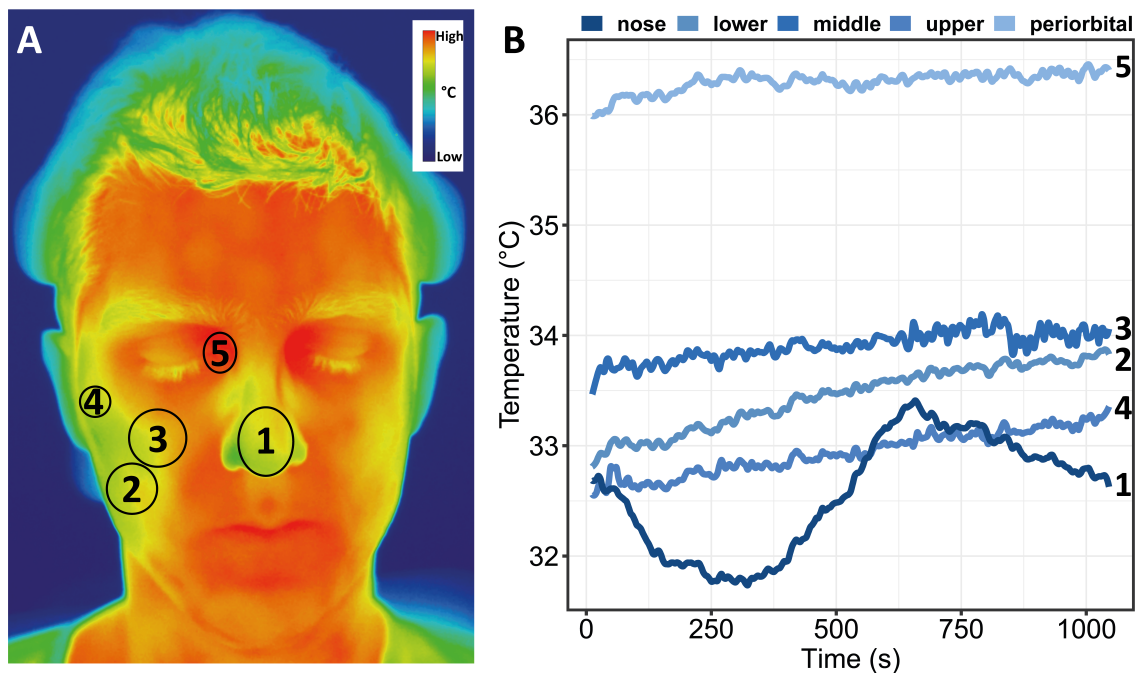


FIGURE 1.2: Facial areas exhibit different thermal patterns over the course of IRT.

A: False-color image of a participant reveals area-specific face surface temperatures. Ellipses denote defined regions of interest for subsequent data extraction, namely nose (1), lower (2), middle (3), and upper (4) cheek, and periorbital area (5). **B:** Quantification of these regions shows different temperatures and also thermal curves during a cognition task with social components, with the nose exhibiting most reactivity.

1.8 IRT has several advantages over 'conventional' physiological measurement techniques

IRT has been proven to have a satisfactorily high accuracy in measuring physiological parameters, such as cardiac pulse, respiratory rate, and cutaneous blood perfusion rate, as compared to state-of-the-art techniques in humans (Cardone & Merla, 2017; Cardone, Pinti, & Merla, 2015; Ermatinger et al., 2019; Ioannou et al., 2014). Additionally, former work showed that IRT is a valid readout of ANS activity in mice (Gjendal et al., 2018). Further, it displays several advantages over other established physiological measuring techniques.

Most importantly, IRT offers an easy to use, non-invasive, and contact-free application mode. This renders it feasible to conduct experiments with almost no restriction in the movements of test subjects, leading to a more naturalistic and ecological testing environment (Ioannou et al., 2014, 2017). Moreover, IRT can record and analyze multiple test subjects simultaneously, remarkably facilitating research of social contexts, deeming IRT as the most suitable method in this research field (Cardone & Merla, 2017). IRT is fully functional even in complete darkness (i.e., in absence of visible light). Accordingly, enhanced measurements under conditions with light as a limiting factor, for instance in testings of nocturnal animals, is possible. Recent work successfully introduced IRT into the assessment of psychiatric patients, making it possible to investigate individuals who have difficulties with the restrictive standard measuring procedures of other methods (Di Giacinto, Brunetti, Sepede, Ferretti, & Merla, 2014; Jian, Chen, Chu, & Huang, 2017; Perpetuini et al., 2019). Taken together, IRT can be seen as a valuable, non-invasive, economical tool to conduct psychophysiological research in more naturalistic contexts.

1.9 Limitations of modern IRT in research context

Even though IRT's validity in displaying surface temperature is generally accepted, its testing reliability depends on controlling of numerous environmental, personal, and technological factors (Fernández-Cuevas et al., 2015). Physical parameters, including ambient temperature and humidity, direct sunlight, or emission from other sources of heat, interfere with IRT. To obtain proper recordings, IRT cameras also need a clear and direct focus on the relevant body surfaces. Moreover, multiple personal factors, comprising gender, age, amount of body fat, diurnal or menstrual cycle, food intake or consumption of psychoactive substances, besides others, display potentially confounding effects and, therefore, have to be taken into account.

Unfortunately, many former studies did not sufficiently control for these issues. Moreover, no overall accepted gold standard in IRT testing has been introduced yet. Hence, numerous different experimental designs, test stimuli, and examined facial regions as well as ways of data extraction and analysis have been utilized (Ermatinger et al., 2019; Ioannou et al., 2014; Ring & Ammer, 2012). Rather small and heterogeneous sample groups further limit

explanatory power. The majority of previous work relies on the analysis of single or short series of IRT images (e.g., before versus after experimental manipulation), examinations of thermal dynamics over the course of longer-lasting time intervals are scarce. Thus, the interpretation of IRT alterations is often limited to unidirectional statements.

2 SCOPE OF THE PRESENT WORK

As discussed in the Introduction, stress is long known to be an internal reaction in the face of danger or threat to physiological or psychological integrity. Typically, stress results in adaptive physiological and behavioral responses, aiming at reducing the impact of perceived threats and, ultimately, to re-establish and maintain homeostasis. Apart from that, chronic or intensive stress experiences, particularly in critical periods of development, can have a negative impact on an individual's physical and psychological health. Furthermore, stress commonly accounts for a broad spectrum of dysfunctional behaviors. Aggression, due to its impact on individuals and society, is a very prominent target of respective investigations. Different models have been postulated to explain the association between stressors and aggression, still, most work focuses on individual risk factors. This weakens power in explaining or predicting aggressive behavior. Likewise, a range of measurement techniques can utilize autonomous responses to stressful experiences. These techniques are invasive, demand applications of body sensors, or require test subjects to remain unnaturally motionless. Such limitations, besides others, may greatly bias the context of measurements. Infrared thermography (IRT) can overcome these issues. However, due to differing quality in controlling for external and personal confounding factors as well as study designs, findings reported from former IRT studies have to be interpreted with caution.

This work seeks to address the discussed issues of former research, using two innovative methodological approaches. Within the **first research project**, we create a robust model of accumulated environmental risk to predict violent aggression in large groups of both schizophrenia patients and individuals from the general population in several independent samples. The **second project** aims to enhance the methodological quality of IRT as a reliable tool in both mice and humans to measure autonomic responses to stress and arousal by utilizing novel approaches in IRT data acquisition, preprocessing, and analyses.

3 PROJECT I: VIOLENT AGGRESSION PREDICTED BY MULTIPLE PRE-ADULT ENVIRONMENTAL HITS

3.1 Overview of project I

Aggression is of great concern for individuals and society as a whole. The identification of factors playing a vital role in its manifestation is useful with respect to the prevention of aggression. Unfortunately, previous research lacks empirically confirmed models capable of predicting aggressive behavior. Notable work highlights the substantial impact of the environment in the development of aggression and antisocial behavior (Caspi et al., 2002; Nelson & Trainor, 2007; Palumbo et al., 2018; Veroude et al., 2016; Waltes et al., 2016). However, studies focusing solely on genetic data (e.g., classical GWAS) neglect the important contribution of the environment to the occurrence of aggressive behavior. Conversely, phenotypical studies attempt to elucidate the role of the environment in aggression. However, such research commonly investigates specific, individual factors instead of assessing a possible additive effect (Raine, 2002).

Aggressive behavior is commonly attributed to patients suffering from mental disorders, such as schizophrenia (Fazel et al., 2009; Sariaslan et al., 2016). Albeit the fact that aggression occurs more often in patients with this disorder, compared to individuals without (Fazel et al., 2009; Sariaslan et al., 2016), the relevance of moderating factors remains rather obscure. Our study was conducted to improve our knowledge about negative environmental influences on violent aggression.

In a follow-up to the study by Stepniak et al. (2014), we planned to compare male schizophrenia patients with low and high amounts of adverse environmental experiences before adulthood in a highly matched discovery sample. In doing so, we realized that high-risk patients had a great chance of a record of past or current aggressive behaviors. Thus, we were wondering about a possible connection between adverse environmental risks and the likelihood of displaying aggressive behavior.

As a first approach, we carefully screened all information on the discovery sample patients, collected during GRAS examinations (Begemann et al., 2010; Ribbe et al., 2010), with respect to any aggressive behavior. Based on these data, we created the Violent Aggression Severity Score (VASS) as a highly sensitive readout of any kind of aggressive behavior over the course of the patients' lifetime. Next, we defined environmental risk factors and assessed their relationship with the VASS. In particular, six factors, namely urbanicity (being raised in a big city), migration, physical abuse, sexual abuse, problematic alcohol use, and lifetime consumption of cannabis, revealed effects on aggressive behavior. This observation was consistently reproduced in three independent schizophrenia samples, using a proxy of violent behavior as the target readout. Consequently, we created a model of accumulated risk including the above-mentioned six factors.

We found that, although single risk factors already had a moderate impact on violent aggression readouts, our accumulation models revealed strong associations between violent behavior in relation to the number of risk factors. Interestingly, the described risk was only observed in patients who suffered from such negative experiences before adulthood (i.e., before 18 years of age), indicating that environmental experiences have a harmful impact, especially during the critical developmental period of childhood to adolescence.

Our results suggest that the environment has a strong effect on the manifestation of violent behavior that may be rather independent of patients' mental condition. To investigate this hypothesis, we associated accumulated environmental risk and psychometrically collected aggression trait scores in two general population samples. Again, we found highly significant associations between risk and aggression traits. These findings emphasize not only the environment's influence on violent behavior, but also that our model of accumulated environmental risk can be used to predict aggressive behavior and identify individuals at risk.

Contrary to the large effects attributable to the environment, epigenetic analyses using epigenome-wide association scans remained behind our expectations; patients with different risk loads (low versus high) revealed comparable blood-derived DNA methylation levels. However, peripheral *histone deacetylase 1 (HDAC1)* mRNA levels, a gene encoding an important epigenetic modulator, were significantly higher in individuals who suffered from a high risk load.

3.2 Original publication

Mitjans, M.*, Seidel, J.*, Begemann, M.*, Bockhop, F., Moya-Higueras, J., Bansal, V., Wesolowski, J., Seelbach, A., Ibáñez, M. I., Kovacevic, F., Duvar, O., Fañanás, L., Wolf, H.-U., Ortet, G., Zwanzger, P., Klein, V., Lange, I., Tänzer, A., Dudeck, M., Penke, L., Tebartz van Elst, L., Bittner, R. A., Schmidmeier, R., Freese, R., Müller-Isberner, R., Wiltfang, J., Bliesener, T., Bonn, S., Poustka, L., Müller, J. L., Arias, B., Ehrenreich, H. (2018). Violent aggression predicted by multiple pre-adult environmental hits. *Molecular Psychiatry*, 24(10), 1549-1564.

**Equally contributing authors*

Personal contribution

I was involved in the ongoing process of GRAS patient examinations, thoroughly assessing more than 100 patients suffering from schizophrenia or schizoaffective disorder, and collecting, besides others, detailed information about negative environmental factors experienced before adulthood and aggressive behavior. I updated and organized our phenotypical databases with information while additionally supervising students in the process of data entry. Together with my first author colleagues and under the supervision of Prof. Hannelore Ehrenreich I created variables to investigate both potential environmental risk factors and aggressive behavior of different intensity. I was responsible for the creation and the validation of the Violent Aggression Severity Score (VASS) and for the design of our model of accumulated risk factors of violent aggression. Furthermore, I conducted extensive statistical analyses of all the phenotypical data in addition to comparing *HDAC1* methylation levels in different risk accumulation groups. Moreover, I was responsible for creating *Figure 1* as well as *Tables 1-3* of the final manuscript. Together with my first author colleagues and Prof. Hannelore Ehrenreich I contributed to the *Introduction*, *Methods*, and *Results* sections of the manuscript and interpreted our findings for the *Discussion* section. Finally, I answered questions and requests from editors and reviewers during the process of submission and publication and read and corrected the final version of the manuscript.



Violent aggression predicted by multiple pre-adult environmental hits

Marina Mitjans^{1,2,3} · Jan Seidel¹ · Martin Begemann^{1,4} · Fabian Bockhop¹ · Jorge Moya-Higueras^{3,5} · Vikas Bansal^{1,6} · Janina Wesolowski¹ · Anna Seelbach¹ · Manuel Ignacio Ibáñez^{3,7} · Fatka Kovacevic¹ · Oguzhan Duvar¹ · Lourdes Fañanás^{3,8} · Hannah-Ulrike Wolf¹ · Generós Ortet^{3,7} · Peter Zwanzger⁹ · Verena Klein¹⁰ · Ina Lange¹¹ · Andreas Tänzer¹² · Manuela Dudeck¹³ · Lars Penke¹⁴ · Ludger Tebartz van Elst¹⁵ · Robert A. Bittner¹⁶ · Richard Schmidmeier⁹ · Roland Freese¹⁷ · Rüdiger Müller-Isberner¹⁷ · Jens Wiltfang⁴ · Thomas Bliesener¹⁸ · Stefan Bonn^{2,6} · Luise Poustka¹⁹ · Jürgen L. Müller^{4,20} · Bárbara Arias^{3,8} · Hannelore Ehrenreich^{1,2}

Received: 1 November 2017 / Revised: 19 February 2018 / Accepted: 21 February 2018 / Published online: 24 May 2018
© The Author(s) 2018. This article is published with open access

Abstract

Early exposure to negative environmental impact shapes individual behavior and potentially contributes to any mental disease. We reported previously that accumulated environmental risk markedly decreases age at schizophrenia onset. Follow-up of matched extreme group individuals (≤ 1 vs. ≥ 3 risks) unexpectedly revealed that high-risk subjects had >5 times greater probability of forensic hospitalization. In line with longstanding sociological theories, we hypothesized that risk accumulation before adulthood induces violent aggression and criminal conduct, independent of mental illness. We determined in 6 independent cohorts (4 schizophrenia and 2 general population samples) pre-adult risk exposure, comprising urbanicity, migration, physical and sexual abuse as primary, and cannabis or alcohol as secondary hits. All single hits by themselves were marginally associated with higher violent aggression. Most strikingly, however, their accumulation strongly predicted violent aggression (odds ratio 10.5). An epigenome-wide association scan to detect differential methylation of blood-derived DNA of selected extreme group individuals yielded overall negative results. Conversely, determination in peripheral blood mononuclear cells of histone-deacetylase1 mRNA as ‘umbrella mediator’ of epigenetic processes revealed an increase in the high-risk group, suggesting lasting epigenetic alterations. Together, we provide sound evidence of a disease-independent unfortunate relationship between well-defined pre-adult environmental hits and violent aggression, calling for more efficient prevention.

Introduction

Early exposure to external risk factors like childhood maltreatment, sexual abuse or head trauma, but also living in urban environment or migration from other countries and cultures, have long been known or suspected to exert adverse effects on individual development and

socioeconomic functioning. Moreover, these environmental risk factors seem to contribute to abnormal behavior and to severity and onset of mental illness [1–11], even though different risk factors may have different impact, dependent on the particular neuropsychiatric disease in focus. On top of these ‘primary’ factors, that are rather inevitable for the affected, ‘secondary’, avoidable risks add to the negative individual and societal outcome, namely cannabis and alcohol abuse [1, 11–16].

Adverse experiences in adulthood, like exposure to violence, traumatic brain injury, or substance intoxication, can act as single triggers to increase the short-term risk of violence in mentally ill individuals as much as in control subjects [16, 17]. However, comprehensive studies, including large numbers of individuals and replication cohorts, on pre-adult accumulation of environmental risk factors and their long-term consequences on human behavior do not exist. In a recent report, we showed that

These authors contributed equally: Marina Mitjans, Jan Seidel, Martin Begemann.

✉ Bárbara Arias
barbara.arias@ub.edu

✉ Hannelore Ehrenreich
ehrenreich@em.mpg.de

Extended author information available on the last page of the article

accumulation of environmental risks leads to a nearly 10-year earlier schizophrenia onset, demonstrating the substantial impact of the environment on mental disease, which by far outlasted any common genetic effects [18]. To search for epigenetic signatures in blood of carefully matched extreme group subjects of this previous study (with ≤ 1 vs. ≥ 3 risk factors) we had to re-contact them. This re-contact led to the unforeseen observation that high-risk subjects had > 5 times higher probability to be hospitalized in forensic units compared to low-risk subjects.

This finding stimulated the present work: Having the longstanding concepts of sociologists and criminologists in mind, we hypothesized that early accumulation of environmental risk factors would lead to increased violent aggression and social rule-breaking in affected individuals, independent of any mental illness. To test this hypothesis, we explored environmental risk before the age of 18 years in 4 schizophrenia samples of the GRAS (Göttingen Research Association for Schizophrenia) data collection [19, 20]. Likewise, risk factors were assessed as available in 2 general population samples. In all cohorts, accumulation of pre-adult environmental hits was highly significantly associated with lifetime conviction for violent acts or high psychopathy and aggression-hostility scores as proxies of violent aggression and rule-breaking. As a first small hint of epigenetic alterations in our high-risk subjects, histone-deacetylase1 (*HDAC1*) mRNA was found increased in peripheral blood mononuclear cells (PBMC).

Methods

Subjects

Schizophrenia

Ethics Committees of Georg-August-University, Göttingen, and participating centers across Germany approved the GRAS study, complying with the Helsinki Declaration. All patients (and/or legal representatives) gave written informed consent. GRAS data collection-I (2005–2010) [19, 20] and -II (2013–2016) consist of schizophrenic and schizoaffective subjects, assigned to: (1) male discovery sample ($N = 134$ extreme group individuals with ≤ 1 or ≥ 3 risk factors, selected/matched from our previous study [18]); (2) male GRAS-I ($N = 606$); (3) male GRAS-II ($N = 320$); (4) female GRAS-I and -II cohorts ($N = 503$).

General population

Replication samples IV ($N = 336$) and V ($N = 229$) consist of individuals from the Spanish general population,

recruited from the Jaume I University in Castelló and drawn from the third wave of an ongoing follow-up study which recruited students from a variety of urban and rural, public and private high schools from Castelló. Ethical approval was obtained from University Ethics Committees; participants provided written informed consent [21, 22].

Sociodemographic and disease-related parameters

The GRAS data collection contains comprehensive information regarding sociodemographic and disease-related parameters, acquired through detailed examination, semi-structured interviews, telephone consultations, questionnaires, and complete collection of hospitalization letters, allowing meticulous double-checking of patients' self-reports [19, 20]. **Chlorpromazine equivalents** as indicator of present medication/disease severity and **past suicide attempts** as measure of severe self-aggression were employed for sample characterization and group comparison. **Premorbid intelligence** was estimated using *MWT-B* (*Mehrfachwahl-Wortschatz-Intelligenztest-B*), and for **current cognitive symptoms**, a cognitive composite score was calculated, based on reasoning (*Leistungsprüfsystem-subtest-3*), executive function (*Trail-Making-B*) and verbal learning and memory (*VLMT*) [18, 19].

Environmental risk exposure

Schizophrenia subjects

Specific information was derived from history-taking and semi-structured interviews with patients and relatives/caretakers (GRAS-Manual) [19, 20] and from *SCID-I*. Each patient was dichotomously classified as having/not having been exposed premorbid and until age 18 years to **severe physical abuse** (comprising unpredictability of violence, injury due to physical reprimand or objects for corporal punishment), **sexual abuse** (forced touches, kissing, attempted or real rape), **migration** (subjects immigrating to Germany), **neurotrauma** (traumatic brain injury of all severity grades), **perinatal complications** (pregnancy, delivery, early postnatal life), **any cannabis consumption** and **alcohol abuse** [23]. To operationalize **urbanicity** until age 18, information on place of residence and relocation was collected from discharge letters, social history, telephone interviews/return mail (questionnaire). Total urbanicity score was dichotomously divided into rural vs. urban residence [18]. In case of contradictory or missing information, patients were excluded from respective analyses. Single risk factors with highest impact over all samples were accumulated to investigate combined influence on aggression.

General population subjects

Physical and sexual abuse was assessed by the shortened version of *Childhood Trauma Questionnaire (CTQ)* [24] and dichotomously recorded (never/any), as was **migration** (not born in Spain), **alcohol** (*Alcohol Use Disorders Identification Test - AUDIT* ≥ 4) [25] and any **cannabis consumption**. Data regarding perinatal complications, neurotrauma and urbanicity were unavailable.

Measures of violent aggression and criminal conduct

Schizophrenia subjects

History of **forensic hospitalization** or **conviction** for battery, sexual assault, manslaughter, murder (at least once in life time) was used as violent aggression proxy. For cross-validation of this dichotomous variable, a continuous measure, the **violent aggression severity score (VASS)**, based on questionnaires, interviews and charts, was generated and applied to the discovery sample. The VASS in turn was cross-validated by an intra-sample ranking of relative aggression severity by 2 independent raters (Fig. 1).

General population subjects

Secondary psychopathy of the *Levenson Self-Report Psychopathy Scale (LSRP)* [26], measuring antisocial aspects of psychopathy (rule-breaking; lack of effort towards socially rewarded behavior), and aggression-hostility factor of the *Zuckerman-Kuhlman Personality Questionnaire, shortened form (ZKPQ-50-CC)* [27], were used as proxies of violent aggression.

Statistical analysis of environmental risk

Group differences for continuous variables were assessed using Mann-Whitney-*U* or Kruskal-Wallis-*H* test for comparison of >2 groups. Frequency differences between groups were assessed using χ^2 -test or Fisher's exact test. As trend tests, Jonckheere-Terpstra or Cochran-Armitage tests were applied. Covariates are explained in display items. Bonferroni correction accounted for multiple testing (*p* values withstanding correction denoted). Statistical analyses were performed using SPSS (v17.0; IBM-Deutschland GmbH, Munich, Germany), or R (v3.3.2; R-Foundation for Statistical Computing, Vienna, Austria).

Methylation Array

Whole blood-derived DNA of extreme group individuals ($N = 134$) was analyzed by Infinium-HumanMethylation450K

(Illumina Inc, CA, USA). Raw intensity data was pre-processed and SWAN (Subset-quantile Within Array Normalization) performed using Bioconductor package Minfi (v1.18.6) [28]. Probes with annotated single-nucleotide polymorphisms (SNPs) in CpG site or at single base extension sites were removed, leaving 467,971 probes total. To identify differentially methylated positions, a linear regression model using limma (v3.28.17) Bioconductor package [29] was fit. Covariates were age, medication and estimated cell proportions (monocytes, granulocytes, CD4T, CD8T, natural killer, and B-cells), calculated using Cell Counts Function in Minfi package [30]. A total of $N = 129$ individuals were finally included for the analyses since two samples were dropped based on separate clustering in principal component analysis and information regarding medication was not available for three samples. All analyses were performed in R.

PBMC isolation and HDAC1 assay

PBMC were isolated from morning blood, collected into CPDA-vials (Citrate-Phosphate-Dextrose-Adenine, Sarstedt, Germany), applying standard Ficoll-Paque-Plus isolation (GE-Healthcare, Munich, Germany). Total RNA extraction was done using miRNeasy Mini-kit (Qiagen, Hilden, Germany). For reverse transcription, 200ng RNA was applied using a mixture of oligo(dT)/hexamers, dNTPs, DTT and 200U SuperscriptIII (Life Technologies GmbH, Darmstadt, Germany). *HDAC1* expression was measured using quantitative real-time PCR. The cDNA was diluted 1:12.5 in 10 μ l reaction-mix, containing 5 μ l of SYBR-green (Life Technologies) and 1pmol/primer:

HDAC1-Fw: 5'-AAATTCTTGCGCTCCATCCG-3'

HDAC1-Rv: 5'-CAGGCCATCGAATACTGGACA-3'

GAPDH-Fw: 5'-CTGACTTCAACAGCGACACC-3'

GAPDH-Rv: 5'-TGCTGTAGCCAAATTCGTTGT-3'

Technical triplicates were run on LightCycler480 (Roche-Diagnostics GmbH, Mannheim, Germany). Relative *HDAC1* expression was calculated by the threshold-cycle method (LightCycler480 Software1.5.0SP3-Roche) and normalization to the housekeeping gene *GAPDH* was performed. After examination for outliers, Student's *t* test was used to compare groups using Prism4 (GraphPad-Software; San Diego, CA, USA).

Results

The environmental risk factors evaluated in this study comprise urbanicity, migration, perinatal complications, physical maltreatment, sexual abuse, traumatic brain injury, cannabis consumption and alcohol abuse. Contacting male extreme group subjects of GRAS (with low vs. high

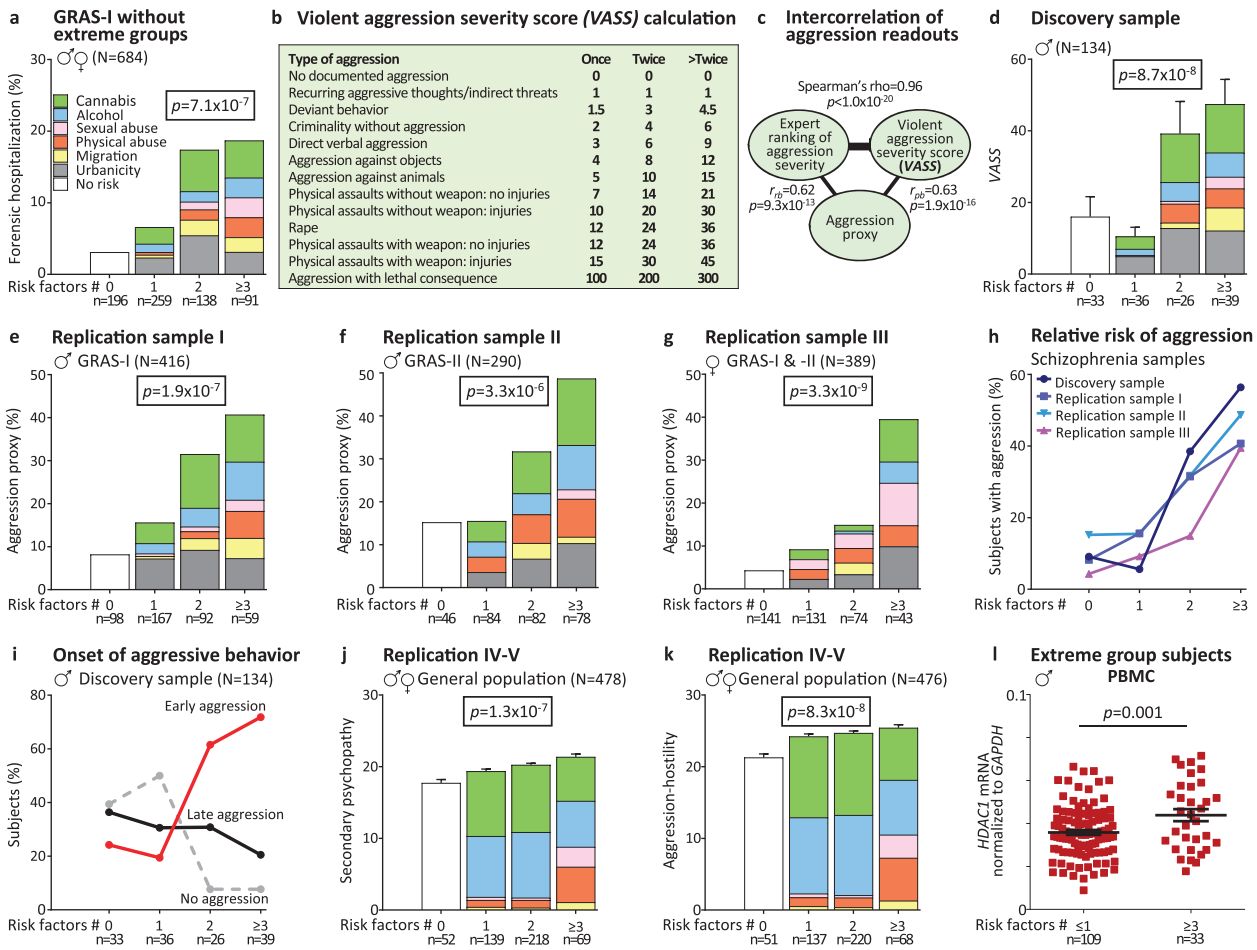


Fig. 1 Multiple environmental hits before adulthood predict violent aggression in mentally ill subjects as well as in the general population – Results from 6 independent samples. **a** Distribution of forensic hospitalization in the discovery sample (see results) suggested a substantial impact of environmental risk accumulation on violent aggression, a finding replicated in the remaining GRAS sample (GRAS-I males and females minus extreme group subjects of the discovery sample). Note the ‘stair pattern’ upon stepwise increase in risk factors; stacked-charts illustrate risk factor composition in the respective groups (including all risk factors of each individual in the respective risk group). Each color represents a particular risk (same legend for **d–g** and **j–k**); χ^2 test (two-sided). **b** Brief presentation of the violent aggression severity score, VASS, ranging from no documented aggression to lethal consequences of violent aggression with relative weight given to severity of aggression and number of registered re-occurrences. **c** Highly significant intercorrelation of violent aggression

measures used in the present paper. **d** Application of VASS to risk accumulation in the discovery sample; Kruskal-Wallis-*H* test (two-sided). **e–g** Schizophrenia replication cohorts I–III: ‘stair pattern’ of aggression proxy in risk accumulation groups; all χ^2 test (one-sided). **h** Comparative presentation of subjects (%) with violent aggression in risk accumulation groups across schizophrenia cohorts. **i** Comparative presentation of subjects (%) with violent aggression before (pre-morbid, ‘early’) or after schizophrenia onset (‘late’) vs. individuals without evidence of aggression (‘no’) in risk accumulation groups of the discovery sample. **j–k** General population replication cohorts IV and V: ‘stair pattern’ of aggression proxies, *LSRP* secondary psychopathy score (**j**) and aggression-hostility factor of *ZKPQ-50-CC* (**k**) in risk accumulation groups; Kruskal-Wallis-*H* test (one-sided). **l** *HDAC1* mRNA levels in PBMC of male extreme group subjects as available for analysis; Student’s *t* test (one-sided)

environmental risk before age 18; discovery sample; $N=134$) [18] for a planned epigenetic follow-up, we found 27% of high-risk individuals in forensic units in contrast to only 6% of low-risk subjects ($p < 0.001$; χ^2 -test, two-sided). This finding was replicated in the remaining GRAS-I sample (GRAS-I males and females minus extreme group subjects), where a stepwise increase in lifetime prevalence of forensic hospitalization was seen upon risk accumulation (Fig. 1a).

This observation made us wonder whether we would find a strong intercorrelation between the here investigated

environmental risks. To test for multicollinearity between the risk factors included in the accumulation models, we calculated the variance inflation factor (VIF) for each sample. Our results suggest that none of the included factors significantly collinears with any other (for each sample $VIF \leq 1.28$), allowing us to include them in our models.

We hypothesized that forensic hospitalization reflects violent aggression. To quantify this trait, and in absence of established instruments for comprehensive retrospective analysis of violent aggression, we generated the VASS

(Fig. 1b). Information for VASS was extracted for all discovery individuals ($N = 134$) from detailed history, available in the GRAS database [19, 20], and additional extensive chart study based on original medical documents over lifetime. VASS ranges from no documented aggression to lethal consequences of violent aggression. Relative weight is given to severity of aggression and number of registered re-occurrences. For first cross-validation of this new tool, an intra-sample expert ranking of relative aggression severity in the discovery sample was performed by 2 independent psychologists (unaware of environmental risk status of subjects under study), yielding Spearman's $\rho = 0.97$ for interrater reliability and $\rho = 0.96$ for intercorrelation with VASS (Fig. 1c). Inspection of VASS values in the discovery sample upon risk accumulation again demonstrates the 'stair pattern' (Fig. 1d).

Since not all information was available as detailed for the schizophrenia replication samples of GRAS-I and -II as for the discovery sample, we introduced a dichotomous aggression proxy, including history of forensic hospitalization and/or conviction for battery, sexual assault, manslaughter or murder (at least once in lifetime). Intercorrelation with VASS and expert ranking, respectively, resulted in $r_{pb} = 0.63$ (point-biserial) and $r_{rb} = 0.62$ (rank-biserial) (Fig. 1c). Applying this proxy to replication samples I-III (GRAS-I males without discovery sample, GRAS-II males, GRAS-I&II females), consistently yielded the 'stair pattern' upon risk accumulation, even though at slightly lower level in females (Fig. 1e-g). The percentage of subjects with documented aggression increases with the number of risk factors, strikingly similar in all schizophrenia cohorts (Fig. 1h). Important for future preventive measures in *at-risk* subjects is the observation that a single risk factor (independent of its kind) is still compensated for (Fig. 1h). When comparing subjects with 0 vs. ≥ 3 environmental factors over all schizophrenia samples, the odds ratio for violent aggression (based on aggression proxy) amounts to 10.5. Details on sociodemographic and disease-related variables, as well as on the various highly intercorrelating measures of violent aggression in the environmental risk accumulation groups in discovery and replication samples are given in Tables 1 and 2. Whereas no consistent differences in premorbid intelligence, present cognition (cognitive composite), and chlorpromazine equivalents (relative amount of antipsychotics) emerge among groups, age tends to be lower and suicidality to occur more frequently with increasing pre-adult environmental risk exposure in the schizophrenia cohorts, which is not unexpected considering our previous report [18] (Table 1). A remarkable increase in all available measures of violent aggression becomes obvious upon accumulation of environmental risk (final model consisting of urbanicity, migration, physical and sexual abuse, alcohol and

cannabis), reflected by highly significant p values in group and trend statistics throughout samples (Table 2).

For analyzing onset of aggressive behavior, the extensive information on aggression available in the discovery sample was exploited. Early aggression (any aggression documented before age 18 years and well before schizophrenia onset) clearly increased upon ≥ 2 risk factors, whereas aggression seen only later in life seemed independent of early environmental risk (Fig. 1i). Therefore, we hypothesized that violent aggression upon risk accumulation may be unrelated to mental disease.

To test this hypothesis, we had the chance to analyze 2 well-characterized independent samples (replication IV and V; Tables 1 and 2) of young individuals from the Spanish general population. Since data on criminal conduct could not be obtained in these cohorts, we had to use alternative, psychometrically validated instruments as aggression proxies, namely *LSRP* secondary psychopathy score [26], measuring rule-breaking and lack of effort towards socially rewarded behavior, and the aggression-hostility factor of *ZKPQ-50-CC* [27]. Urbanicity as risk factor was unavailable in these samples (reducing the model to 5 of the 6 risk factors explored in schizophrenia, that is migration, physical maltreatment, sexual abuse, alcohol and cannabis). We also note that subjects were younger and as academics probably higher educated as compared to the disease cohorts. Despite these mitigating facts, and despite employing individuals of another country, the expected 'stair pattern' still emerged clearly for both proxies, likely suggesting generalizability of these findings (Fig. 1j,k; Tables 1 and 2). Data given here for the general population samples (replications IV and V) are based on both males and females. In addition, evaluating men and women separately (taking both general population cohorts together) yielded significant results for both genders (Table 2 bottom).

Addressing the composition of risk factors among groups across cohorts, we obtained a comparable pattern throughout schizophrenia samples (stacked-charts; Fig. 1a,d-g). In the general population subjects, particularly alcohol and cannabis consumption (classified as 'secondary hits') predominated (Fig. 1j,k) which also seem to play an appreciable role in schizophrenia cohorts. Therefore, we wondered whether separate analysis of risk accumulation, integrating only primary vs. only secondary hits, would still result in significant effects on aggression. For all schizophrenia samples individually, group difference and trend remained highly significant (not shown). Taking all schizophrenia subjects together ($N > 1200$), the aggression proxy yields for the accumulation model, built on primary risks only (urbanicity, migration, physical and sexual abuse), $p = 4.5 \times 10^{-17}$ ($\chi^2 = 75.28$) and $p < 2.2 \times 10^{-16}$ ($\chi^2 = 68.28$), for group differences and trend, respectively. The corresponding results for secondary risk factors (alcohol,

Table 1 Presentation of environmental risk groups in discovery and replication samples: sociodemographic and disease-related measures

	No risk factors	1 risk factor	2 risk factors	≥3 risk factors	<i>p</i> value (<i>H/χ</i> ²)
Discovery sample^a (<i>N</i> = 121–134)					
Male schizophrenic subjects					
	<i>n</i> = 30–33	<i>n</i> = 32–36	<i>n</i> = 24–26	<i>n</i> = 35–39	
Age (years) ^b	33.09 (10.24)	35.68 (11.23)	31.47 (8.27)	32.46 (8.66)	<i>p</i> = 0.630 (<i>H</i> = 1.73)
Premorbid intelligence <i>MWT-B</i> ^c	103.23 (16.57)	101.09 (11.80)	104.48 (14.36)	97.42 (14.91)	<i>p</i> = 0.172 (<i>H</i> = 5.00)
Cognitive composite score ^d	−0.05 (1.13)	−0.49 (1.07)	0.22 (0.72)	0.03 (1.00)	<i>p</i> = 0.651 (<i>H</i> = 1.64)
Chlorpromazine equivalents	751.09 (696.52)	771.87 (1227.51)	674.28 (508.49)	648.83 (569.38)	<i>p</i> = 0.769 (<i>H</i> = 1.13)
Suicidality ^e	11 (33.3%)	8 (23.5%)	9 (34.6%)	14 (36.8%)	<i>p</i> = 0.651 (<i>χ</i> ² = 1.64)
Replication sample I (<i>N</i> = 392–411)					
GRAS I male schizophrenic subjects					
	<i>n</i> = 91–98	<i>n</i> = 156–166	<i>n</i> = 91–92	<i>n</i> = 53–59	
Age (years) ^b	46.94 (12.26)	39.65 (12.50)	34.51 (10.18)	32.85 (8.38)	<u><i>p</i> = 1.6 × 10^{−5}</u> (<i>H</i> = 24.87)
Premorbid intelligence <i>MWT-B</i> ^c	105.35 (17.09)	103.32 (15.87)	101.00 (14.26)	99.23 (15.10)	<i>p</i> = 0.085 (<i>H</i> = 6.61)
Cognitive composite score ^d	0.15 (1.12)	0.75 (1.01)	0.10 (0.93)	−0.01 (0.89)	<i>p</i> = 0.873 (<i>H</i> = 0.70)
Chlorpromazine equivalents	611.92 (571.29)	703.38 (585.70)	686.03 (608.01)	836.07 (622.14)	<i>p</i> = 0.059 (<i>H</i> = 7.43)
Suicidality ^e	23 (24.2%)	57 (34.5%)	33 (36.6%)	33 (55.9%)	<u><i>p</i> = 0.001</u> (<i>χ</i> ² = 16.11)
Replication sample II (<i>N</i> = 238–290)					
GRAS II male schizophrenic subjects					
	<i>n</i> = 36–46	<i>n</i> = 68–84	<i>n</i> = 67–82	<i>n</i> = 67–78	
Age (years) ^b	45.57 (15.02)	42.17 (13.83)	38.50 (14.08)	35.75 (10.52)	<i>p</i> = 0.011 (<i>H</i> = 11.20)
Premorbid intelligence <i>MWT-B</i> ^c	98.09 (14.46)	102.29 (16.03)	100.48 (13.36)	96.39 (9.29)	<i>p</i> = 0.184 (<i>H</i> = 4.84)
Cognitive composite score ^d	−0.23 (1.24)	−0.08 (1.03)	−0.01 (0.84)	−0.08 (0.96)	<i>p</i> = 0.816 (<i>H</i> = 0.94)
Chlorpromazine equivalents	629.15 (513.31)	747.35 (629.02)	689.31 (717.18)	713.84 (532.66)	<i>p</i> = 0.629 (<i>H</i> = 1.74)
Suicidality ^e	8 (20.5%)	12 (14.6%)	25 (31.6%)	25 (34.2%)	<i>p</i> = 0.018 (<i>χ</i> ² = 10.08)
Replication sample III (<i>N</i> = 345–386)					
GRAS I-II female schizophrenic subjects					
	<i>n</i> = 125–140	<i>n</i> = 118–130	<i>n</i> = 65–71	<i>n</i> = 37–43	
Age (years) ^b	43.44 (11.75)	46.67 (12.90)	40.84 (12.71)	36.53 (11.31)	<u><i>p</i> = 0.003</u> (<i>H</i> = 13.83)
Premorbid intelligence <i>MWT-B</i> ^c	103.53 (14.19)	104.04 (14.28)	102.96 (15.84)	99.10 (15.41)	<i>p</i> = 0.147 (<i>H</i> = 5.37)
Cognitive composite score ^d	0.03 (0.96)	0.09 (0.99)	0.24 (0.99)	−0.21 (1.00)	<i>p</i> = 0.164 (<i>H</i> = 5.11)
Chlorpromazine equivalents	536.52 (579.61)	564.04 (506.21)	620.48 (628.30)	650.87 (477.23)	<i>p</i> = 0.167 (<i>H</i> = 5.07)
Suicidality ^e	45 (33.6%)	59 (46.5%)	33 (46.5%)	22 (53.7%)	<i>p</i> = 0.052 (<i>χ</i> ² = 7.72)
Replication sample IV (<i>N</i> = 299)					
General population					
	<i>n</i> = 39	<i>n</i> = 83	<i>n</i> = 133	<i>n</i> = 44	
Age (years)	26.44 (4.81)	25.93 (2.46)	25.56 (3.50)	25.25 (3.64)	<i>p</i> = 0.117 (<i>H</i> = 5.89)
Gender, female/male (% male)	29/10 (25.6%)	51/32 (38.6%)	78/55 (41.4%)	18/26 (59.1%)	
Replication sample V (<i>N</i> = 177–183)					
General population					
	<i>n</i> = 13	<i>n</i> = 54–56	<i>n</i> = 86–89	<i>n</i> = 24–25	
Age (years)	20.54 (0.88)	20.63 (0.98)	20.85 (1.12)	20.88 (1.15)	<i>p</i> = 0.696 (<i>H</i> = 1.44)
Gender, female/male (% male)	7/6 (46.2%)	41/15 (26.8%)	56/33 (37.1%)	20/5 (20.0%)	

Data are uncorrected means (SD) or *n* (%); for statistical analysis, Kruskal-Wallis-*H*, χ^2 , or Fisher's exact test was used, all *p* values two-sided; Bonferroni-corrected *p* values <0.01 are considered significant and underlined; because of missing data, sample sizes vary;

^anote regarding discovery sample: extreme groups of our previous study [18] differ slightly due to elimination of birth complications and neurotrauma, but inclusion of alcohol in the present study;

^bcorrected for age at disease onset;

^c*MWT-B*=*Mehrfachwahl-Wortschatz-Intelligenztest-B*;

^dcognitive composite score consists of reasoning (*Leistungsprüfung-subtest-3*), executive function (*Trail-Making Test B*), verbal learning & memory test (*VLMT*) [18]; corrected for age, *PANSS* negative score, and chlorpromazine equivalents (standardized residuals after linear regression);

^esuicidality=individuals with past suicide attempts

Table 2 Effect of environmental risk factor accumulation on measures of aggressive behavior in schizophrenic and general population subjects

	No risk factors	1 risk factor	2 risk factors	≥3 risk factors	p value (χ^2/H)	p value (χ^2/J) ^a
Discovery sample^b (N = 134)	n = 33	n = 36	n = 26	n = 39		
Male schizophrenic subjects	1 (3.0%)	1 (2.8%)	6 (23.1%)	14 (35.9%)	$p = 5.4 \times 10^{-5}$ ($\chi^2 = 20.82$)	$p = 1.5 \times 10^{-5}$ ($\chi^2 = 18.71$)
History of forensic hospitalization	3 (9.1%)	2 (5.6%)	10 (38.5%)	22 (56.4%)	$p = 4.9 \times 10^{-7}$ ($\chi^2 = 32.14$)	$p = 1.3 \times 10^{-7}$ ($\chi^2 = 27.80$)
Aggression proxy ^c	16.03 (32.17)	10.49 (15.50)	39.21 (45.38)	47.45 (43.14)	$p = 8.7 \times 10^{-8}$ ($H = 35.70$)	$p = 9.2 \times 10^{-8}$ ($J = 4671.5$)
Violent aggression severity score (VASS)	8 (24.2%)	7 (19.4%)	16 (61.5%)	28 (71.8%)	$p = 1.8 \times 10^{-6}$ ($\chi^2 = 29.51$)	$p = 7.4 \times 10^{-7}$ ($\chi^2 = 24.52$)
Aggression before schizophrenia ^d						
Replication sample I (N = 411–416)						
GRAS I male schizophrenic subjects	n = 96–98	n = 165–167	n = 91–92	n = 59		
History of forensic hospitalization	5 (5.2%)	14 (8.5%)	21 (23.1%)	12 (20.3%)	$p = 0.0001$ ($\chi^2 = 19.51$)	$p = 4.7 \times 10^{-5}$ ($\chi^2 = 15.25$)
Aggression proxy ^e	8 (8.2%)	26 (15.6%)	29 (31.5%)	24 (40.7%)	$p = 1.9 \times 10^{-7}$ ($\chi^2 = 32.71$)	$p = 8.9 \times 10^{-9}$ ($\chi^2 = 31.73$)
Replication sample II (N = 289–290)						
GRAS II male schizophrenic subjects	n = 46	n = 84	n = 81–82	n = 78		
History of forensic hospitalization	5 (10.9%)	10 (11.9%)	26 (32.1%)	32 (41.0%)	$p = 6.8 \times 10^{-6}$ ($\chi^2 = 25.26$)	$p = 8.6 \times 10^{-7}$ ($\chi^2 = 22.88$)
Aggression proxy ^f	7 (15.2%)	13 (15.5%)	26 (31.7%)	38 (48.7%)	$p = 3.3 \times 10^{-6}$ ($\chi^2 = 26.74$)	$p = 4.6 \times 10^{-7}$ ($\chi^2 = 24.10$)
Replication sample III (N = 389–392)						
GRAS I–II female schizophrenic subjects	n = 141–142	n = 131–133	n = 74	n = 43		
History of forensic hospitalization	1 (0.7%)	4 (3.0%)	4 (5.4%)	6 (14.0%)	$p = 0.002$ ($\chi^2 = 16.49$)	$p = 7.5 \times 10^{-5}$ ($\chi^2 = 14.37$)
Aggression proxy ^g	6 (4.3%)	12 (9.2%)	11 (14.9%)	17 (39.5%)	$p = 3.3 \times 10^{-9}$ ($\chi^2 = 40.96$)	$p = 3.5 \times 10^{-9}$ ($\chi^2 = 33.56$)
Replication sample IV (N = 293–295)						
General population	n = 38–39	n = 81–83	n = 129–131	n = 43–44		
Secondary psychopathy score, <i>LSRP</i> ^h	17.46 (3.25)	19.12 (3.52)	20.17 (3.49)	20.57 (3.18)	$p = 4.6 \times 10^{-5}$ ($H = 21.94$)	$p = 1.1 \times 10^{-5}$ ($J = 1837.1$)
Aggression-hostility score, <i>ZKPQ</i> ⁱ	21.18 (3.68)	24.05 (3.27)	24.51 (4.07)	24.91 (3.62)	$p = 3.4 \times 10^{-5}$ ($H = 21.28$)	$p = 4.5 \times 10^{-4}$ ($J = 17550.5$)
Replication sample V (N = 183)						
General population	n = 13	n = 56	n = 89	n = 25		
Secondary psychopathy score, <i>LSRP</i> ^h	18.54 (3.89)	19.73 (3.63)	20.38 (3.17)	22.76 (3.33)	$p = 0.0009$ ($H = 15.01$)	$p = 0.0003$ ($J = 6721$)
Aggression-hostility score, <i>ZKPQ</i> ⁱ	21.62 (3.10)	24.50 (4.95)	25 (4.23)	26.32 (3.41)	$p = 0.004$ ($H = 11.61$)	$p = 0.003$ ($J = 6438$)
General population, replication samples IV & V together						
General population, males	n = 16	n = 46–47	n = 86–88	n = 31		
Secondary psychopathy score, <i>LSRP</i> ^h	17.25 (4.46)	19.57 (3.16)	20.42 (3.31)	20.39 (2.93)	$p = 0.022$ ($H = 8.06$)	$p = 0.011$ ($J = 6253.5$)
Aggression-hostility score, <i>ZKPQ</i> ⁱ	20.38 (2.94)	23.63 (3.30)	25.09 (4.16)	24.90 (3.77)	$p = 3.29 \times 10^{-5}$ ($H = 21.98$)	$p = 1.02 \times 10^{-4}$ ($J = 6821$)
General population, females	n = 35–36	n = 91–92	n = 132	n = 37–38		
Secondary psychopathy score, <i>LSRP</i> ^h	17.94 (2.88)	19.26 (3.76)	20.15 (3.40)	22.16 (3.55)	$p = 8.35 \times 10^{-7}$ ($H = 29.60$)	$p = 9.6 \times 10^{-8}$ ($J = 19223.5$)
Aggression-hostility score, <i>ZKPQ</i> ⁱ	21.71 (3.71)	24.54 (4.34)	24.45 (4.11)	25.86 (3.42)	$p = 1.20 \times 10^{-4}$ ($H = 19.28$)	$p = 0.0013$ ($J = 17067$)

Urbanicity, migration, physical abuse, sexual abuse, problematic alcohol use, and cannabis use are included in the accumulation model; data are uncorrected means (SD) or n (%); for statistical analysis, Kruskal-Wallis- H , χ^2 , or Fisher's exact test was used; p values <0.01 are considered significant and underlined; because of missing data, sample sizes vary;

^ato test for statistical trends, the Cochran-Armitage trend (qualitative traits) or Jonckheere-Terpstra trend (quantitative traits) test was used; for replication samples, testing was one-sided;

^bnote regarding discovery sample: extreme groups of our previous study [18] differ slightly due to elimination of birth complications and neurotrauma, but inclusion of alcohol in the present study;

^cany conviction for battery, sexual assault, manslaughter, murder, or a history of forensic hospitalization;

^ddeviant behavior, criminality, verbal, physical, or sexual aggression, at least half a year (mean=13.69 years, SD=10.10) before first psychotic episode;

^e*LSRP*=Levenson Self-Report Psychopathy Scale; ^f*ZKPQ-50-CC*=Zuckerman-Kuhlman Personality Questionnaire;

^gtwo-sided Fisher's exact test for group size estimations <5.

cannabis) in schizophrenia are $p = 6.6 \times 10^{-19}$ ($\chi^2 = 83.71$) and $p < 2.2 \times 10^{-16}$ ($\chi^2 = 83.40$). Analogously, taking all general population subjects together ($N > 530$), we obtain for *LSRP* with primary risks (urbanicity not available) $p = 0.002$ ($H = 12.65$) and $p = 0.0003$ ($J = 33774.5$), and with secondary risks $p = 1.3 \times 10^{-4}$ ($H = 17.92$) and $p = 5.3 \times 10^{-5}$ ($J = 42412.5$) for group differences and trend. Also here, significance was already reached with separate analysis of both cohorts (not shown).

For deciding on the accumulation model, we had initially screened all individual risk factors of our 'primary plus secondary risk factor model' separately in both schizophrenia and general population cohorts to get an estimation of their relative impact (Tables 3a,3b,3c). Perinatal complications and neurotrauma before the age of 18 years were unavailable for general population subjects. Since these risks showed the lowest overall impact on aggression proxies in schizophrenia, we decided not to include them in our present accumulation model.

Finally, we performed an epigenome-wide association scan to detect differential methylation of blood-derived DNA of selected extreme group individuals (discovery sample; $N = 134$; Fig. 1a), originally planned as epigenetic follow-up study [18]. This scan turned out to be negative. In fact, contrasting subjects either with high vs. low number of environmental hits or according to *VASS* median split yielded a single methylation difference upon lowering the Bonferroni threshold to 10^{-6} (Table 4). Similarly, when looking in an exploratory fashion (small/unbalanced group sizes) at individual risk factors separately, results were essentially negative (Table 4). Hits associated with migration were likely related to ethnicity rather than environmental risk, as reported recently [31]. The power of our sample size - even though in the range of suggestions [32] and despite extreme group comparison - may not have been sufficient to detect differences, also due to a vast underlying heterogeneity of individual methylation sites. Even the search for methylation differences of aggression-related candidate genes [33–35] turned out negative (not shown), putting the relative weight of phenotypical consequences (here violent aggression) vs. common methylation results in humans into perspective. In contrast, determining *HDAC1* mRNA levels in PBMC available from male extreme group subjects (≤ 1 vs. ≥ 3 risks) revealed a highly significant difference ($p = 0.001$), with higher levels in the high-risk ($N = 33$) compared to the low-risk group ($N = 109$) (Fig. 11). This transcript encodes an enzyme of the histone deacetylase complex which serves as an overarching regulator of epigenetic processes. Indeed, peripheral *HDAC1* mRNA levels seem to be a more robust readout of epigenetic modifications in small sample sizes [36] as compared to specific methylation sites in the epigenome-wide association scan, and suggest lasting epigenetic alterations.

Discussion

The present work was initiated based on the observation in a schizophrenia cohort that accumulation of environmental risk factors before adulthood promotes the likelihood of later forensic hospitalization, interpreted as indicator of violent aggression. This interpretation and the effect of risk accumulation were consolidated using direct scoring of aggression over lifetime or, as aggression proxies, forensic hospitalization and conviction for battery, sexual assault, manslaughter or murder, or respective psychopathology measures in 4 independent schizophrenia cohorts and 2 general population samples. Importantly, our data support the concept of a disease-independent development of violent aggression in subjects exposed to multiple pre-adult environmental risk factors.

Whereas a vast amount of literature on single environmental risk factors reports consequences for abnormal behavior and mental illness, publications on pre-adult risk accumulation are scarce and mostly based on closely interrelated social/familial risk factors. Also, risk and consequence are often not clearly defined. Studies including larger, comprehensively characterized datasets and replication samples do not exist. The present work is the first to provide sound evidence, based on 6 separate cohorts, of a disease-independent relationship between accumulation of multifaceted pre-adult environmental hits and violent aggression. The overall societal damage is enormous, and we note that mentally ill individuals who re-enter the community from prison are even more at risk for unemployment, homelessness, and criminal recidivism [37]. These results should encourage better precautionary measures, including intensified research on protective factors which is still underrepresented [2, 38–40].

In the psychosociological literature, the so-called externalizing behavior in childhood includes hostile and aggressive physical behavior toward others, impulsivity, hyperactivity, and noncompliance with limit-setting [41, 42]. The respective risk factors are all highly plausible, yet often theoretical, and derived from 4 broad domains: child risk factors (e.g., adverse temperament, genetic and gender risk), sociocultural risks (e.g., poverty, stressful life events), parenting and caregiving (e.g., conflict and violence at home, physical abuse), and children's peer experiences (e.g., instable relationships, social rejection). A full model of the development of conduct problems has been suggested to include at least these 4 domains [41, 43, 44]. The risk factors analyzed in the present study are perhaps somewhat clearer defined but partially related to and overlapping across these domains. Urbanicity, migration, cannabis and alcohol reflect sociocultural input but also peer experience, and physical or sexual abuse belong to the parenting/caregiver aspect.

Table 3a Effect of single environmental risk factors on measures of aggressive behavior in schizophrenic and general population subjects

	Perinatal hit		Urbanicity		Migration		p value (χ^2/Z)
	No	Yes	Rural	Urban	No	Yes	
	n (%)	n (%)					
Discovery sample (N = 134)							
Male schizophrenic subjects	n = 77	n = 57	n = 66	n = 68	n = 114	n = 20	
History of forensic hospitalization	12 (15.6%)	10 (17.5%)	7 (10.6%)	15 (22.1%)	12 (10.5%)	10 (50.0%)	$p = 0.0001^{\dagger}$ ($\chi^2 = 19.32$)
Aggression proxy ^a	18 (23.4%)	19 (33.3%)	11 (16.7%)	26 (38.2%)	21 (18.4%)	16 (80.0%)	$p = 1.3 \times 10^{-8}$ ($\chi^2 = 32.28$)
Violent aggression severity score (VASS)	23.01 (37.43)	35.17 (39.23)	22.86 (38.29)	33.35 (38.35)	23.16 (33.73)	56.83 (51.12)	$p = 0.0005$ ($Z = -3.46$)
Aggression before schizophrenia ^b	25 (32.5%)	34 (59.6%)	24 (36.4%)	35 (51.5%)	46 (40.4%)	13 (65.0%)	$p = 0.0005$ ($Z = -3.46$)
Replication sample I (N = 438-606)							
GRAS I male schizophrenic subjects	n = 374-381	n = 222-223	n = 262-266	n = 176-178	n = 542-550	n = 56	
History of forensic hospitalization	51 (13.6%)	25 (11.3%)	28 (10.7%)	25 (14.2%)	59 (10.9%)	17 (30.4%)	$p = 1.6 \times 10^{-5}$ ($\chi^2 = 17.35$)
Aggression proxy ^a	81 (21.3%)	48 (21.5%)	43 (16.2%)	45 (25.3%)	102 (18.5%)	27 (48.2%)	$p = 1.2 \times 10^{-7}$ ($\chi^2 = 26.70$)
Replication sample II (N = 316-320)							
GRAS II male schizophrenic subjects	n = 219-220	n = 99	n = 182-183	n = 134	n = 282-283	n = 37	
History of forensic hospitalization	55 (25.1%)	25 (25.3%)	41 (22.5%)	39 (29.1%)	65 (23.0%)	15 (40.5%)	$p = 0.011$ ($\chi^2 = 5.33$)
Aggression proxy ^a	64 (29.1%)	28 (28.3%)	45 (24.6%)	47 (35.1%)	76 (26.9%)	16 (43.2%)	$p = 0.019$ ($\chi^2 = 4.29$)
Replication sample III (N = 424-503)							
GRAS I-II female schizophrenic subjects	n = 269-300	n = 200	n = 267-268	n = 157-159	n = 450-454	n = 49	
History of forensic hospitalization	11 (3.7%)	5 (2.5%)	6 (2.2%)	7 (4.4%)	14 (3.1%)	2 (4.1%)	$p = 0.474^{\dagger}$ ($\chi^2 = 0.14$)
Aggression proxy ^a	33 (11.1%)	23 (11.5%)	25 (9.4%)	20 (12.7%)	48 (10.7%)	8 (16.3%)	$p = 0.117$ ($\chi^2 = 1.42$)
Replication sample IV-V (N = 513-551)							
General population	NA	NA	NA	NA	n = 517-521	n = 25-26	
Secondary psychopathy score - LSRP ^c	NA	NA	NA	NA	19.79 (3.53)	20.96 (3.30)	$p = 0.047$ ($Z = -1.68$)
Aggression-hostility score - ZKPQ ^d	NA	NA	NA	NA	24.25 (4.04)	24.81 (4.55)	$p = 0.344$ ($Z = -0.40$)

Data are uncorrected means (SD) or n (%); for statistical analysis, Mann-Whitney-U, χ^2 , or Fisher's exact test was used; significant p values are underlined; for replication samples, testing was one-sided; because of missing data, sample sizes vary;

^aany conviction for battery, sexual assault, manslaughter and murder, or a history of forensic hospitalization;

^bdeviant behavior, criminality, verbal, physical, or sexual aggression at least half a year (mean=13.69 years, SD=10.10) before first psychotic episode;

^cLSRP=Levenson Self-Report Psychopathy Scale;

^dZKPQ-50=Zuckerman-Kuhlman Personality Questionnaire;

[†]Fisher's exact test upon group size estimations <5; NA=information not available.

Table 3b Effect of single environmental risk factors on measures of aggressive behavior in schizophrenic and general population subjects (continued)

	Neurotrauma		Physical abuse		Sexual abuse		<i>p</i> value (χ^2/Z)
	No	Yes	No	Yes	No	Yes	
Discovery sample (N = 134)							
Male schizophrenic subjects	n = 66	n = 68	n = 112	n = 22	n = 123	n = 11	
History of forensic hospitalization	5 (7.6%)	17 (25.0%)	16 (14.3%)	6 (27.3%)	19 (15.4%)	3 (27.3%)	$p = 0.388^{\dagger}$ ($\chi^2 = 1.03$)
Aggression proxy ^a	10 (15.2%)	27 (39.7%)	28 (25.0%)	9 (40.9%)	32 (26.0%)	5 (45.5%)	$p = 0.176^{\dagger}$ ($\chi^2 = 1.91$)
Violent aggression severity score (VASS)	16.42 (27.03)	39.60 (44.39)	24.71 (36.73)	45.89 (43.35)	26.19 (35.98)	50.50 (57.95)	$p = 0.071$ ($Z = -1.80$)
Aggression before schizophrenia ^b	16 (24.2%)	43 (63.2%)	45 (40.2%)	14 (63.6%)	51 (41.5%)	8 (72.7%)	$p = 0.059^{\dagger}$ ($\chi^2 = 4.01$)
Replication sample I (N = 567-606)							
GRAS I male schizophrenic subjects	n = 263-265	n = 304-307	n = 535-543	n = 63	n = 547-555	n = 38	
History of forensic hospitalization	40 (15.2%)	31 (10.2%)	60 (11.2%)	16 (25.4%)	67 (12.2%)	8 (21.1%)	$p = 0.098^{\dagger}$ ($\chi^2 = 2.46$)
Aggression proxy ^a	59 (22.3%)	60 (19.5%)	107 (19.7%)	22 (34.9%)	118 (21.3%)	10 (26.3%)	$p = 0.232$ ($\chi^2 = 0.54$)
Replication sample II (N = 293-320)							
GRAS II male schizophrenic subjects	n = 144	n = 175-176	n = 216-217	n = 102	n = 271-272	n = 22	
History of forensic hospitalization	36 (25.0%)	44 (25.1%)	45 (20.8%)	34 (33.3%)	66 (24.4%)	7 (31.8%)	$p = 0.223$ ($\chi^2 = 0.61$)
Aggression proxy ^a	42 (29.2%)	50 (28.4%)	51 (23.5%)	40 (39.2%)	76 (27.9%)	8 (36.4%)	$p = 0.200$ ($\chi^2 = 0.71$)
Replication sample III (N = 494-502)							
GRAS I-II female schizophrenic subjects	n = 319-322	n = 177-178	n = 433-437	n = 65	n = 397-400	n = 97-98	
History of forensic hospitalization	11 (3.4%)	5 (2.8%)	10 (2.3%)	6 (9.2%)	10 (2.5%)	6 (6.1%)	$p = 0.073^{\dagger}$ ($\chi^2 = 3.32$)
Aggression proxy ^a	32 (10.0%)	24 (13.6%)	41 (9.5%)	15 (23.1%)	34 (8.6%)	22 (22.7%)	$p = 4.2 \times 10^{-5}$ ($\chi^2 = 15.46$)
Replication sample IV-V (N = 513-551)							
General population	NA	NA	n = 453-456	n = 95-96	n = 505	n = 42-44	
Secondary psychopathy score - LSRP ^c	NA	NA	19.65 (3.49)	20.68 (3.37)	19.72 (3.44)	21.07 (3.90)	$p = 0.013$ ($Z = -2.23$)
Aggression-hostility score - ZKPQ ^d	NA	NA	24.08 (4.01)	25.07 (4.23)	24.19 (4.12)	24.83 (3.30)	$p = 0.128$ ($Z = -1.13$)

Data are uncorrected means (SD) or n (%); for statistical analysis, Mann-Whitney-U, χ^2 , or Fisher's exact test was used; significant *p* values are underlined; for replication samples, testing was one-sided; because of missing data, sample sizes vary;

^aany conviction for battery, sexual assault, manslaughter and murder, or a history of forensic hospitalization;

^bdeviant behavior, criminality, verbal, physical, or sexual aggression at least half a year (mean=13.69 years, SD=10.10) before first psychotic episode;

^cLSRP=Levenson Self-Report Psychopathy Scale;

^dZKPQ-50-CC=Zuckerman-Kuhlman Personality Questionnaire;

[†]Fisher's exact test upon group size estimations <5; NA=information not available

Table 3c Effect of single environmental risk factors on measures of aggressive behavior in schizophrenic and general population subjects (continued)

	Problematic alcohol use		Cannabis use		<i>p</i> value (χ^2/Z)
	No	Yes	No	Yes	
Discovery sample (N = 134)					
Male schizophrenic subjects	n = 102	n = 32	n = 66	n = 68	
History of forensic hospitalization	14 (13.7%)	8 (25.0%)	4 (6.1%)	18 (26.5%)	<u>$p = 0.001$</u> ($\chi^2 = 10.17$)
Aggression proxy ^a	25 (24.5%)	12 (37.5%)	9 (13.6%)	28 (41.2%)	<u>$p = 0.0004$</u> ($\chi^2 = 12.71$)
Violent aggression severity score (VAAS)	25.60 (38.59)	36.41 (37.79)	16.30 (27.82)	39.72 (43.85)	<u>$p = 1.1 \times 10^{-5}$</u> ($Z = -4.39$)
Aggression before schizophrenia ^b	37 (36.3%)	22 (68.8%)	18 (27.3%)	41 (60.3%)	<u>$p = 0.0001$</u> ($\chi^2 = 14.82$)
Replication sample I (N = 575–582)					
GRAS I male schizophrenic subjects	n = 472–477	n = 103–104	n = 319–323	n = 257–259	
History of forensic hospitalization	60 (12.7%)	15 (14.6%)	28 (8.8%)	42 (16.3%)	<u>$p = 0.003$</u> ($\chi^2 = 7.63$)
Aggression proxy ^a	91 (19.1%)	35 (33.7%)	48 (14.9%)	73 (28.2%)	<u>$p = 4.1 \times 10^{-5}$</u> ($\chi^2 = 15.50$)
Replication sample II (N = 293–294)					
GRAS II male schizophrenic subjects	n = 204	n = 89–90	n = 146	n = 147–148	
History of forensic hospitalization	39 (19.1%)	35 (39.3%)	23 (15.8%)	51 (34.7%)	<u>$p = 9.5 \times 10^{-5}$</u> ($\chi^2 = 13.92$)
Aggression proxy ^a	48 (23.5%)	38 (42.2%)	29 (19.9%)	57 (38.5%)	<u>$p = 0.0002$</u> ($\chi^2 = 12.35$)
Replication sample III (N = 466–490)					
GRAS I–II female schizophrenic subjects	n = 436–440	n = 30	n = 401–405	n = 85	
History of forensic hospitalization	12 (2.7%)	3 (10.0%)	9 (2.2%)	7 (8.2%)	<u>$p = 0.011^{\dagger}$</u> ($\chi^2 = 8.04$)
Aggression proxy ^a	40 (9.2%)	11 (36.7%)	32 (8.0%)	23 (27.1%)	<u>$p = 2.3 \times 10^{-7}$</u> ($\chi^2 = 25.44$)
Replication sample IV–V (N = 513–551)					
General population	n = 163–165	n = 361–363	n = 156–158	n = 357	
Secondary psychopathy score – <i>LSRP</i> ^c	18.89 (3.56)	20.37 (3.37)	19.27 (3.59)	20.04 (3.48)	<u>$p = 0.013$</u> ($Z = -2.24$)
Aggression-hostility score – <i>ZKPQ</i> ^d	23.15 (3.91)	24.90 (4.06)	23.31 (4.47)	24.64 (3.78)	<u>$p = 0.0005$</u> ($Z = -3.47$)

Data are uncorrected means (SD) or n (%); for statistical analysis, Mann-Whitney-*U*, χ^2 , or Fisher's exact test was used; significant *p* values are underlined; for replication samples, testing was one-sided; because of missing data, sample sizes vary;

^aany conviction for battery, sexual assault, manslaughter and murder or a history of forensic hospitalization;

^bdeviant behavior, criminality, verbal, physical, or sexual aggression at least half a year (mean = 13.69 years, SD = 10.10) before first psychotic episode;

^c*LSRP* = *Levenson Self-Report Psychopathy Scale*;

^d*ZKPQ-50-CC* = *Zuckerman-Kuhlman Personality Questionnaire*;

[†]Fisher's exact test upon group size estimations <5; NA = information not available

Table 4 Comparison of methylation data from whole blood-derived DNA of selected extreme group individuals (schizophrenia discovery sample; $N = 134$)

Factor	n	Number of significant CpG sites ^a		$p < 10^{-6}$
		$p < 10^{-8}$	$p < 10^{-7}$	
High vs. low # of environmental hits	64	0	0	0
VASS	Low	65	0	1
	High	64	0	cg23980294 ^b
(Median split)	65	0	0	0
Perinatal hit	Yes	55	0	0
	No	74	0	1
Urbanicity	Yes	63	0	cg08446900 ^c
	No	66	0	+73 ^d
Migration	Yes	19	5	+12
	No	110	cg19078576, cg24719005, cg06809544, cg25146017, cg17275700	cg15916004, cg17714025, cg14326196, cg11236526, cg15858239, cg18952796, cg12969644, cg13895765, cg12204732, cg12892004, cg19927816, cg05641882
Neurotrauma	Yes	65	0	0
	No	64	0	0
Physical abuse	Yes	22	0	0
	No	107	0	0
Sexual abuse	Yes	10	0	1
	No	119	0	cg03051003 ^e
Alcohol	Yes	32	0	0
	No	97	0	0
Cannabis	Yes	65	0	0
	No	64	0	0

number; VASS = violent aggression severity score

^acomparisons with age, medication and cell counts as covariates^bCpG site in *TRAPPC11* gene 5'UTR, not previously associated^cCpG site in *RARA* gene (body), previously associated with tobacco smoking [56]^dtotal amount of migration-associated CpG sites at threshold 10^{-6} amounts to 90 CpG sites [$5 (<10^{-8})+12(<10^{-7})+73(<10^{-6})$]^eCpG site not previously associated (intergenic)

Certainly, there are many more, still undiscovered risk and numerous protective factors, potentially explaining why ‘only’ 40–50% of high-risk individuals in our schizophrenia samples fulfill criteria of violent aggression. We note that this study does not include genetic data analysis or correction for any genetic impact. The genetic influence on aggression, however, may be of considerable relevance for the individual [45–49], even though highly heterogeneous as for essentially all behavioral traits. Heritability of aggression, estimated from twin studies, reaches >60% [50, 51]. In fact, 50% of individuals with violent aggression upon pre-adult risk accumulation in the present study means another 50% without detectable aggression. This consistent finding across samples likely indicates that genetic predisposition is prerequisite for whichever behavioral consequence. Individuals without genetic predisposition and/or with more protective factors (genetic and environmental) may not react with violent aggression to accumulated environmental risk. Importantly, the obvious gender effect may be a matter of degree rather than of pattern. In fact, the etiology of externalizing behavior problems is similar for girls and boys [41, 52], as is the consequence of risk accumulation in the present study for males and females.

The risk factors of the sociological domains seem to be stable predictors over time, to some degree interchangeable, pointing to many pathways leading to the same outcome (principle of equifinality) [41]. The interchangeability is highly interesting also with respect to potential biological mechanisms. It appears that any of the here investigated hits alone, independent of its kind, can be compensated for but that higher risk load increases the probability of violent aggression. Also for that reason, we are weighing risk factors equally in the present study. This could theoretically create some bias. However, to be able to estimate the true effect size of each specific factor separately on violent aggression and subsequently weigh all factors in a more proper way, much larger samples sizes would be needed that are presently not available anywhere in the world.

In contrast to the marginal influence of genome-wide association data on mental disease in GRAS [18, 53], the accumulated environmental impact on development of violent aggression is huge, reflected by odds ratios of > 10. When striking at a vulnerable time of brain development, namely around/before puberty, the environmental input may ‘non-specifically’ affect any predisposed individual. The hypothetical biological mechanisms underlying this accumulation effect in humans may range from alterations in neuroendocrine and neurotransmitter systems, neuronal/synaptic plasticity and neurogenesis to changes in the adaptive immune system and interference with developmental myelination, affecting brain connectivity and network function [9, 10, 54, 55].

Our approach to detect methylation changes in blood using an epigenome-wide association scan was unsuccessful despite matched extreme group comparison, likely due to the small sample size (although in the suggested range [32]), and perhaps the etiological/pathogenetic complexity of accumulated risks. Changes in brain, not accessible here for analysis, can certainly not be excluded. Interestingly, however, *HDAC1* mRNA levels in PBMC of male extreme group subjects were increased in the high-risk compared to the low-risk group. This finding confirms peripheral *HDAC1* mRNA levels as a more robust readout of epigenetic alterations in relatively small sample sizes [36], as compared to specific methylation sites in epigenome-wide association scans or even in candidate genes. To gain further mechanistic insight and thereby develop - in addition to prevention measures - novel individualized treatment concepts [36], animal studies modeling risk accumulation seem unavoidable.

To conclude, this study should motivate sociopolitical actions, aiming at identifying individuals-at-risk and improving precautionary measures. Effective violence prevention strategies start early and include family-focused and school-based programs [2, 16, 38]. Additional risk factors, interchangeable in their long-term consequences, like urbanicity, migration, and substance abuse, should be increasingly considered. Health care providers are essential for all of these prevention concepts. More research on protective factors and resilience should be launched. Animal studies need to be supported that model risk accumulation for mechanistic insight into brain alterations leading to aggression, and for developing new treatment approaches, also those targeting reversal of epigenetic alterations. As a novel concept, scientific efforts on ‘*phenotyping of the environment*’ [11] should be promoted to achieve more fundamental risk estimation and more effective prevention in the future.

Acknowledgements This work was supported by the Max Planck Society, the Max Planck Förderstiftung, the DFG (CNMPB), EXTRABRAIN EU-FP7, the Niedersachsen-Research Network on Neuroinfectiology (N-RENNT), and EU-AIMS. The research of EU-AIMS receives support from the Innovative Medicines Initiative Joint Undertaking under grant agreement n°115300, resources of which are composed of financial contribution from the European Union’s Seventh Framework Programme (FP7/2007–2013), from the EFPIA companies, and from Autism Speaks. Moreover, support from Centro de Investigación en Red de Salud Mental (CIBERSAM); Instituto de Salud Carlos III (PI16/00998), Comissionat per a Universitats i Recerca del DIUE (2014SGR1636) and Spanish Ministry of Economy and Competitiveness (ES-EUEpiBrain, SAF2015-71526-REDT) is gratefully acknowledged. We thank all subjects for participating in the study, and all the many colleagues who have contributed over the past decade to the GRAS data collection.

Author Contributions: Concept, design and supervision of the study: HE, MM, JS. Data acquisition/analysis/interpretation: MB, JS, MM,

FB, JMH, VB, JWE, AS, MII, FK, OD, LF, HW, GO, PZ, VK, IL, AT, MD, LP, LTVE, RAB, RS, RF, RMI, JW, TB, SB, LUP, JLM, BA, HE. Drafting manuscript and figures: HE, JS, MM, BA. All authors read and approved the final version of the manuscript.

Compliance with ethical standards

Conflict of interest The authors declare that they have no conflict of interest.

Open Access This article is licensed under a Creative Commons Attribution 4.0 International License, which permits use, sharing, adaptation, distribution and reproduction in any medium or format, as long as you give appropriate credit to the original author(s) and the source, provide a link to the Creative Commons license, and indicate if changes were made. The images or other third party material in this article are included in the article's Creative Commons license, unless indicated otherwise in a credit line to the material. If material is not included in the article's Creative Commons license and your intended use is not permitted by statutory regulation or exceeds the permitted use, you will need to obtain permission directly from the copyright holder. To view a copy of this license, visit <http://creativecommons.org/licenses/by/4.0/>.

References

- McDonald C, Murray RM. Early and late environmental risk factors for schizophrenia. *Brain Res Rev.* 2000;31:130–7.
- Raine A. Biosocial studies of antisocial and violent behavior in children and adults: a review. *J Abnorm Child Psychol.* 2002;30:311–26.
- Read J, van Os J, Morrison AP, Ross CA. Childhood trauma, psychosis and schizophrenia: a literature review with theoretical and clinical implications. *Acta Psychiatr Scand.* 2005;112:330–50.
- van Os J, Kenis G, Rutten BPF. The environment and schizophrenia. *Nature.* 2010;468:203–12.
- Brown AS. The environment and susceptibility to schizophrenia. *Prog Neurobiol.* 2011;93:23–58.
- Lederbogen F, Kirsch P, Haddad L, Streit F, Tost H, Schuch P, et al. City living and urban upbringing affect neural social stress processing in humans. *Nature.* 2011;474:498–501.
- Wortzel HS, Arciniegas DB. A forensic neuropsychiatric approach to traumatic brain injury, aggression, and suicide. *J Am Acad Psychiatry.* 2013;41:274–86.
- Orlovska S, Pedersen MS, Benros ME, Mortensen PB, Agerbo E, Nordentoft M. Head injury as risk factor for psychiatric disorders: A nationwide register-based follow-up study of 113,906 persons with headinjury. *Am J Psychiatr.* 2014;171:463–9.
- McEwen BS, Nasca C, Gray JD. Stress effects on neuronal structure: hippocampus, amygdala, and prefrontal cortex. *Neuropsychopharmacology.* 2016;41:3–23.
- Nemeroff CB. Paradise lost: the neurobiological and clinical consequences of child abuse and neglect. *Neuron.* 2016;89:892–909.
- Ehrenreich H. The impact of environment on abnormal behavior and mental disease. *EMBO Rep.* 2017;18:661–5.e201744197-n/a.
- Giancola PR. Alcohol-related aggression during the college years: Theories, risk factors and policy implications. *J Stud Alcohol.* 2002;14:129–39.
- Heinz AJ, Beck A, Meyer-Lindenberg A, Sterzer P, Heinz A. Cognitive and neurobiological mechanisms of alcohol-related aggression. *Nat Rev Neurosci.* 2011;12:400–13.
- Large M, Sharma S, Compton MT, Slade T, Nielssen O. Cannabis use and earlier onset of psychosis. *Arch Gen Psychiatr.* 2011;68:555–61.
- Walsh E, Gilvarry C, Samele C, Harvey K, Manley C, Tattan T, et al. Predicting violence in schizophrenia: a prospective study. *Schizophr Res.* 2004;67:247–52.
- Fazel S, Gulati G, Linsell L, Geddes JR, Grann M. Schizophrenia and violence: systematic review and meta-analysis. *PLoS Med.* 2009;6:e1000120.
- Sariaslan A, Lichtenstein P, Larsson H, Fazel S. Triggers for violent criminality in patients with psychotic disorders. *JAMA Psychiatry.* 2016;73:796–803.
- Stepniak B, Papiol S, Hammer C, Ramin A, Everts S, Hennig L, et al. Accumulated environmental risk determining age at schizophrenia onset: a deep phenotyping-based study. *Lancet Psychiatry.* 2014;1:444–53.
- Begemann M, Grube S, Papiol S, Malzahn D, Krampe H, Ribbe K, et al. Modification of cognitive performance in schizophrenia by complexin 2 gene polymorphisms. *Arch Gen Psychiatr.* 2010;67:879–88.
- Ribbe K, Friedrichs H, Begemann M, Grube S, Papiol S, Kastner A, et al. The cross-sectional GRAS sample: a comprehensive phenotypical data collection of schizophrenic patients. *BMC Psychiatry.* 2010;10:91.
- Alemamy S, Moya J, Ibanez MI, Villa H, Mezquita L, Ortet G, et al. Research Letter: Childhood trauma and the rs1360780 SNP of FKBP5 gene in psychosis: a replication in two general population samples. *Psychol Med.* 2016;46:221–3.
- Ortet G, Ibanez MI, Moya J, Villa H, Viruela A, Mezquita L. Assessing the five factors of personality in adolescents: the junior version of the Spanish NEO-PI-R. *Assessment.* 2012;19:114–30.
- Ribbe K, Ackermann V, Schwitulla J, Begemann M, Papiol S, Grube S, et al. Prediction of the risk of comorbid alcoholism in schizophrenia by interaction of common genetic variants in the corticotropin-releasing factor system. *Arch Gen Psychiatr.* 2011;68:1247–56.
- Bernstein DP, Stein JA, Newcomb MD, Walker E, Pogge D, Ahluvalia T, et al. Development and validation of a brief screening version of the Childhood Trauma Questionnaire. *Child Abuse Negl.* 2003;27:169–90.
- Babor T, DeLaFuentes J, Saunders J, Grant M. The alcohol use disorders identification test: guidelines for use in primary health care. Vol. PSA. World Health Organization; Geneva, Switzerland, 1992. pp. 1–30.
- Levenson MR, Kiehl KA, Fitzpatrick CM. Assessing psychopathic attributes in a noninstitutionalized population. *J Pers Soc Psychol.* 1995;68:151–8.
- Aluja A, Rossier J, Garcia LF, Angleitner A, Kuhlman M, Zuckerman M. A cross-cultural shortened form of the ZKPQ (ZKPQ-50-cc) adapted to English, French, German, and Spanish languages. *Pers Individ Differ.* 2006;41:619–28.
- Aryee MJ, Jaffe AE, Corrada-Bravo H, Ladd-Acosta C, Feinberg AP, Hansen KD, et al. Minfi: a flexible and comprehensive Bioconductor package for the analysis of Infinium DNA methylation microarrays. *Bioinformatics.* 2014;30:1363–9.
- Ritchie ME, Phipson B, Wu D, Hu Y, Law CW, Shi W, et al. limma powers differential expression analyses for RNA-sequencing and microarray studies. *Nucleic Acids Res.* 2015;43:e47.
- Jaffe AE, Irizarry RA. Accounting for cellular heterogeneity is critical in epigenome-wide association studies. *Genome Biol.* 2014;15:R31.
- Galanter JM, Gignoux CR, Oh SS, Torgerson D, Pino-Yanes M, Thakur N, et al. Differential methylation between ethnic subgroups reflects the effect of genetic ancestry and environmental exposures. *Elife.* 2017;6:e20532.

32. Tsai PC, Bell JT. Power and sample size estimation for epigenome-wide association scans to detect differential DNA methylation. *Int J Epidemiol*. 2015;44:1429–41.
33. Waltes R, Chiochetti AG, Freitag CM. The neurobiological basis of human aggression: a review on genetic and epigenetic mechanisms. *Am J Med Genet B Neuropsychiatr Genet*. 2016;171:650–75.
34. Gunter TD, Vaughn MG, Philibert RA. Behavioral genetics in antisocial spectrum disorders and psychopathy: a review of the recent literature. *Behav Sci Law*. 2010;28:148–73.
35. Kolla NJ, Matthews B, Wilson AA, Houle S, Bagby RM, Links P, et al. Lower monoamine oxidase-A total distribution volume in impulsive and violent male offenders with antisocial personality disorder and high psychopathic traits: an [(11)C] harmine positron emission tomography study. *Neuropsychopharmacology*. 2015;40:2596–603.
36. Bahari-Javan S, Varbanov H, Halder R, Benito E, Kaurani L, Burkhardt S, et al. HDAC1 links early life stress to schizophrenia-like phenotypes. *Proc Natl Acad Sci USA*. 2017;114:E4686–94.
37. Swanson J. Mental illness, release from prison, and social context. *JAMA*. 2016;316:1771–2.
38. Sumner SA, Mercy JA, Dahlberg LL, Hillis SD, Klevens J, Houry D. Violence in the United States: status, challenges, and opportunities. *JAMA*. 2015;314:478–88.
39. Stoddard SA, Whiteside L, Zimmerman MA, Cunningham RM, Chermack ST, Walton MA. The relationship between cumulative risk and promotive factors and violent behavior among urban adolescents. *Am J Commun Psychol*. 2013;51:57–65.
40. van der Laan AM, Veenstra R, Bogaerts S, Verhulst FC, Ormel J. Serious, minor, and non-delinquents in early adolescence: the impact of cumulative risk and promotive factors. The TRAILS Study. *J Abnorm Child Psychol*. 2010;38:339–51.
41. Deater-Deckard K, Dodge KA, Bates JE, Pettit GS. Multiple risk factors in the development of externalizing behavior problems: group and individual differences. *Dev Psychopathol*. 1998;10:469–93.
42. McMahon RJ. Diagnosis, assessment, and treatment of externalizing problems in children - the role of longitudinal data. *J Consult Clin Psych*. 1994;62:901–17.
43. Herrenkohl TI, Maguin E, Hill KG, Hawkins JD, Abbott RD, Catalano RF. Developmental risk factors for youth violence. *J Adolesc Health*. 2000;26:176–86.
44. Loeber R, Pardini D, Homish DL, Wei EH, Crawford AM, Farrington DP, et al. The prediction of violence and homicide in young men. *J Consult Clin Psych*. 2005;73:1074–88.
45. Mason DA, Frick PJ. The heritability of antisocial-behavior - a metaanalysis of twin and adoption studies. *J Psychopathol Behav Assess*. 1994;16:301–23.
46. Mednick SA, Gabrielli WF Jr, Hutchings B. Genetic influences in criminal convictions: evidence from an adoption cohort. *Science*. 1984;224:891–4.
47. Coccaro EF, Bergeman CS, Kavoussi RJ, Seroczynski AD. Heritability of aggression and irritability: a twin study of the Buss-Durkee aggression scales in adult male subjects. *Biol Psychiatry*. 1997;41:273–84.
48. Miles DR, Carey G. Genetic and environmental architecture of human aggression. *J Pers Soc Psychol*. 1997;72:207–17.
49. Rhee SH, Waldman ID. Genetic and environmental influences on antisocial behavior: a meta-analysis of twin and adoption studies. *Psychol Bull*. 2002;128:490–529.
50. DiLalla LF, Gottesman II. Biological and genetic contributors to violence—Widom’s untold tale. *Psychol Bull*. 1991;109:125–9. discussion 130–122
51. Plomin R, DeFries JC, Knopik VS, Neiderhiser J. Behavioral genetics. 6th ed. New York, NY: Worth Publishers; 2013.
52. Zoccolillo M. Gender and the development of conduct disorder. *Dev Psychopathol*. 1993;5:65–78.
53. Ehrenreich H, Mitjans M, Van der Auwera S, Centeno TP, Begemann M, Grabe HJ, et al. OTTO: a new strategy to extract mental disease-relevant combinations of GWAS hits from individuals. *Mol Psychiatry*. 2016;23:476–86.
54. Korosi A, Naninck EFG, Oomen CA, Schouten M, Krugers H, Fitzsimons C, et al. Early-life stress mediated modulation of adult neurogenesis and behavior. *Behav Brain Res*. 2012;227:400–9.
55. Nave KA, Ehrenreich H. Myelination and oligodendrocyte functions in psychiatric diseases. *JAMA Psychiatry*. 2014;71:582–4.
56. Su D, Wang X, Campbell MR, Porter DK, Pittman GS, Bennett BD, et al. Distinct epigenetic effects of tobacco smoking in whole blood and among leukocyte subtypes. *PLoS ONE*. 2016;11:e0166486.

Affiliations

Marina Mitjans^{1,2,3} · Jan Seidel¹ · Martin Begemann^{1,4} · Fabian Bockhop¹ · Jorge Moya-Higueras^{3,5} · Vikas Bansal^{1,6} · Janina Wesolowski¹ · Anna Seelbach¹ · Manuel Ignacio Ibáñez^{3,7} · Fatka Kovacevic¹ · Oguzhan Duvar¹ · Lourdes Fañanás^{3,8} · Hannah-Ulrike Wolf¹ · Generós Ortet^{3,7} · Peter Zwanzger⁹ · Verena Klein¹⁰ · Ina Lange¹¹ · Andreas Tänzer¹² · Manuela Dudeck¹³ · Lars Penke¹⁴ · Ludger Tebartz van Elst¹⁵ · Robert A. Bittner¹⁶ · Richard Schmidmeier⁹ · Roland Freese¹⁷ · Rüdiger Müller-Isberner¹⁷ · Jens Wiltfang⁴ · Thomas Bliesener¹⁸ · Stefan Bonn^{2,6} · Luise Poustka¹⁹ · Jürgen L. Müller^{4,20} · Bárbara Arias^{3,8} · Hannelore Ehrenreich^{1,2}

¹ Clinical Neuroscience, Max Planck Institute of Experimental Medicine, Göttingen, Germany

² DFG Research Center for Nanoscale Microscopy and Molecular Physiology of the Brain (CNMPB), Göttingen, Germany

³ Instituto de Salud Carlos III, Centro de Investigación Biomédica en Red de Salud Mental (CIBERSAM), Madrid, Spain

⁴ Department of Psychiatry & Psychotherapy, University of Göttingen, Göttingen, Germany

⁵ Department of Psychology, Faculty of Education, Psychology and Social Work, University of Lleida, Lleida, Spain

⁶ Center for Molecular Neurobiology, Institute of Medical Systems Biology, University Clinic Hamburg-Eppendorf, Hamburg, Germany

⁷ Department of Basic and Clinical Psychology and Psychobiology, Universitat Jaume I, Castelló, Spain

-
- ⁸ Departament Biologia Evolutiva, Ecologia i Ciències Ambientals, Facultat de Biologia and Institut de Biomedicina (IBUB), Universitat de Barcelona, Barcelona, Spain
- ⁹ KBO-Inn-Salzach-Klinikum, Gabersee, Wasserburg am Inn, Germany
- ¹⁰ KBO-Isar-Amper-Klinikum, Taufkirchen (Vils), Germany
- ¹¹ Competence Center for Forensic Psychiatry, Lower Saxony, MRV Moringen, Germany
- ¹² Department of Forensic Psychiatry & Psychotherapy, KRH, Wunstorf, Germany
- ¹³ Forensic Psychiatry and Psychotherapy, University of Ulm, Ulm, Germany
- ¹⁴ Institute of Psychology, University of Göttingen, Göttingen, Germany
- ¹⁵ Department of Psychiatry & Psychotherapy, University of Freiburg, Freiburg, Germany
- ¹⁶ Department of Psychiatry & Psychotherapy, University of Frankfurt, Frankfurt, Germany
- ¹⁷ Vitos Forensic Psychiatric Hospital, Haina, Germany
- ¹⁸ Criminological Research Institute of Lower Saxony, Hannover, Germany
- ¹⁹ Department of Child and Adolescent Psychiatry & Psychotherapy, University of Göttingen, Göttingen, Germany
- ²⁰ Asklepios Hospital for Forensic Psychiatry & Psychotherapy, Göttingen, Germany

4 PROJECT II: VASCULAR RESPONSE TO SOCIAL COGNITIVE PERFORMANCE MEASURED BY INFRARED THERMOGRAPHY: A TRANSLATIONAL STUDY FROM MOUSE TO MAN

4.1 Overview of project II

Physiological measurements play an important role in psychological and neuroscientific research. Recently, advances in the field of infrared thermography (IRT) resulted in increased implementation attempts of this technology in studies investigating stress and arousal (Ermatinger et al., 2019; Gjendal et al., 2018; Herborn et al., 2018; Ioannou et al., 2014). Modern IRT is characterized by both high spatial and temporal resolution (Cardone & Merla, 2017; Ioannou et al., 2014; Jarlier et al., 2011) and, due to its non-invasive and contact-free application method, can be employed where other 'conventional' techniques reach their limits (Ermatinger et al., 2019; Ioannou et al., 2014). However, various IRT studies suffer from diverse weaknesses, due to small and heterogeneous samples, insufficient control of the many environmental and personal confounding factors (Fernández-Cuevas et al., 2015), or suboptimal data extraction methods (Ioannou et al., 2014). Consequently, this leads to inconsistencies in findings (Ermatinger et al., 2019), limiting explanatory power.

This project seeks to enhance our knowledge of modern IRT technology and its potential in the assessment of stress, both in mice and men. We developed novel approaches to explore alterations in body surface temperature at defined regions of interest as readout of autonomous activity. Importantly, we took great effort to avoid the numerous pitfalls that typically occur in experimental IRT research (Cardone & Merla, 2017; Fernández-Cuevas et al., 2015; Ioannou et al., 2014). This way, we intended to enhance the quality of collected data and analyses, ensuring robust study conclusions.

The starting point of this work was the rather unexpected observation that mice exhibited abnormal social behavior during a modified Y-maze sociability test (Brimberg et al., 2016; Lai & Johnston, 2002) four weeks after completing the SocioBox test of complex social recognition (Krueger-Burg et al., 2016). Intrigued by that finding we conducted more experiments, using mice, separated by sex, under two different conditions. While the experimental groups underwent the normal SocioBox paradigm, control groups stayed in the empty box. Four weeks afterward, all mice performed the Y-maze sociability test. As we were wondering whether groups differ regarding their autonomous activity, in addition to potentially distinct sociability behavior, we recorded body surface temperature via IRT. As hypothesized, experimental mice, in contrast to control animals, exhibited higher central body, compared to tail, temperatures over the course of the SocioBox experiment. Further, during the experimental test condition, thermal readouts were negatively associated with time spent interacting with the unfamiliar stimulus mouse, indicating that increased physiological arousal, as determined via IRT, interferes with recognition abilities.

In accordance with our initial findings, the Y-maze sociability test revealed both different behavioral as well as thermal readouts between experimental and control animals: While control mice showed a high motivation to interact with an unfamiliar conspecific, compared to a lifeless object, experimental group mice demonstrated a reduced social engagement. Moreover, experimental mice displayed higher body, compared to tail, temperatures. The evaluation of a possible relationship between thermal readouts during SocioBox and sociability during Y-maze showed that experimental mice with a higher thermal centralization during SocioBox spent less time interacting with a conspecific. Our findings suggest that the amount of physiological arousal experienced during the SocioBox is associated with a reduced motivation for social engagement, possibly inducing social avoidance behavior, which is maintained for at least four weeks.

In order to clarify whether the SocioBox is associated with overall behavioral changes, after the Y-maze sociability test all mice performed a paradigm of novelty-induced freezing. Importantly, comparisons in the degree of freezing behavior over time uncovered similar patterns between experimental and control mice. Based on these findings, we assume that the SocioBox is not only a promising instrument to assess complex social recognition memory in mice, it also seems to have a negative effect on social interaction behavior,

indicating a potential value as a novel model of isolated social anxiety (Toth & Neumann, 2013). IRT can be used to reliably record body temperature as an additional readout of physiological arousal, not revealed by conventional behavioral tests alone.

Subsequently, we evaluated the applicability of IRT in a human study, translating our findings from mice to man. Therefore, we created the Face Recognition Test (FRT), a social memory task using neutral male faces as stimuli (Kulke, Janßen, Demel, & Schacht, 2017), that resembles, in its design, the SocioBox paradigm. We then employed IRT to explore temperature alterations between the FRT and the Wisconsin Card Sorting Test (WCST), a widely used test of executive functioning that employs abstract symbols (Heaton, Chelune, Talley, Kay, & Curtiss, 2003), in a homogenous group of healthy men. In order to acquire solid data, novel approaches of automated extraction were employed. The analyses of thermal alterations over time in defined areas of the face revealed that the majority of participants showed a characteristic thermal pattern during the FRT but not in the WCST. Interestingly, salivary cortisol level changes were not different between the two tests and correlated rather mildly with thermal values. This suggests that IRT provides higher sensitivity than an established readout of physiological stress (Engert et al., 2014), at least within the context of the conducted social experiment.

4.2 Original publication

Seidel, J.*, Bockhop, F.*, Mitkovski, M.*, Martin, S., Ronnenberg, A., Krueger-Burg, D., Schneider, K., Röhse, H., Wüstefeld, L., Cosi, F., Bröking, K., Schacht, A., Ehrenreich, H. (2020). Vascular response to social cognitive performance measured by infrared thermography: A translational study from mouse to man. *FASEB BioAdvances*, 2, 18-32.

**Equally contributing authors*

Personal contribution

I was, with the exception of the experimental data acquisition in mice, significantly involved in all aspects of both animal and human studies. Under the supervision of Prof. Hannelore Ehrenreich, and with contributions from my co-author colleagues, I was responsible for the design, conduction, and evaluation of the human experiments. In mice, and

analogous in humans, I contributed to the process of quantitative data generation, which encompassed conversions of raw videos, identification and assignment of appropriate regions of interest as relevant readouts, and extraction of thermal and behavioral data for later analyses. Under the supervision of Prof. Hannelore Ehrenreich, I generated standardized preprocessing routines to obtain well-organized data in order to calculate new, intraindividually adjusted IRT readouts with the potential to methodologically enhance future thermal imaging research. I conducted and interpreted extensive statistical analyses, including behavioral, thermal, and cortisol level readouts. With contributions from my first-author colleagues, I wrote the *Methods* and *Results* sections as well as the *Figure legends*, created the *Display items* and was involved in the design of the *Supplementary videos* for the final manuscript. Together with my supervisor, I searched for relevant literature and wrote the *Introduction* and *Discussion* sections of the manuscript.

Vascular response to social cognitive performance measured by infrared thermography: A translational study from mouse to man

Jan Seidel¹ | Fabian Bockhop¹ | Miso Mitkovski² | Sabine Martin¹ |
 Anja Ronnenberg¹ | Dilja Krueger-Burg³ | Katharina Schneider² | Heiko Röhse² |
 Liane Wüstefeld¹ | Filippo Cosi⁴ | Kai Bröking² | Annekathrin Schacht⁵ |
 Hannelore Ehrenreich¹

¹Clinical Neuroscience, Max Planck Institute of Experimental Medicine, Göttingen, Germany

²Light Microscopy Facility, Max Planck Institute of Experimental Medicine, Göttingen, Germany

³Department of Molecular Neurobiology, Max Planck Institute of Experimental Medicine, Göttingen, Germany

⁴Biomedical Physics Group, Max Planck Institute for Dynamics and Self-Organization, Göttingen, Germany

⁵Department of Affective Neuroscience and Psychophysiology, Georg-Elias-Müller-Institute of Psychology, Georg-August University, Göttingen, Germany

Correspondence

Hannelore Ehrenreich, Clinical Neuroscience, Max Planck Institute of Experimental Medicine, Hermann-Rein-Str.3, 37075 Göttingen, Germany.
 Email: ehrenreich@em.mpg.de

Funding information

Max Planck Society; DFG Research Center for Nanoscale Microscopy and Molecular Physiology of the Brain (CNMPB)

Abstract

To assess complex social recognition in mice, we previously developed the *SocioBox* paradigm. Unexpectedly, 4 weeks after performing in the *SocioBox*, mice displayed robust social avoidance during Y-maze sociability testing. This unique “sociophobia” acquisition could be documented in independent cohorts. We therefore employed infrared thermography as a non-invasive method of stress-monitoring during *SocioBox* testing (presentation of five other mice) versus empty box. A higher *Centralization Index* (body/tail temperature) in the *SocioBox* correlated negatively with social recognition memory and, after 4 weeks, with social preference in the Y-maze. Assuming that social stimuli might be associated with characteristic thermo-responses, we exposed healthy men (N = 103) with a comparably high intelligence level to a standardized test session including two cognitive tests with or without social component (face versus pattern recognition). In some analogy to the *Centralization Index* (within-subject measure) used in mice, the *Reference Index* (ratio nose/malar cheek temperature) was introduced to determine the autonomic facial response/flushing during social recognition testing. Whereas cognitive performance and salivary cortisol were comparable across human subjects and tests, the *Face Recognition Test* was associated with a characteristic *Reference Index* profile. Infrared thermography may have potential for discriminating disturbed social behaviors.

KEYWORDS

flushing, IRT, social stimulus, stress, temperature, vasoactivity

Abbreviations: *BSI*, Brief Symptom Inventory; *FRT*, Face Recognition Test; *HPA*, Hypothalamic-Pituitary-Adrenal Axis; *IRT*, Infrared Thermography; *LOESS*, Locally Estimated Scatterplot Smoothing; *LPS*, Leistungsprüfsystem; *mK*, Millikelvin; *NEO-FFI*, NEO-Five-Factor Inventory; *NETD*, Noise Equivalent Thermal Difference; *ROI*, Regions Of Interest; *SIAS*, Social Interaction Anxiety Scale; *SPS*, Social Phobia Scale; *STAI*, State-Trait Anxiety Inventory; *WCST*, Wisconsin Card Sorting Test.

Jan Seidel, Fabian Bockhop and Miso Mitkovski are equally contributing first authors.

This is an open access article under the terms of the Creative Commons Attribution-NonCommercial License, which permits use, distribution and reproduction in any medium, provided the original work is properly cited and is not used for commercial purposes.

© 2019 The Authors.

1 | INTRODUCTION

An association of emotions during unaccustomed social interactions with facial flushing in humans has long been recognized.¹⁻³ The autonomic nervous system response during such social interactions—highly conserved across mammals and perceived like “stress”—leads to altered vasoactivity in peripheral and core body regions. The resulting blood flow changes via vasoconstriction and vasodilation, respectively, affect local body temperature.⁴⁻¹⁰ Exposure to an embarrassment task, for instance, led to an increase in facial blood flow in both male and female participants, measured via Laser Doppler Flowmetry.¹¹ Using this technique, temperature changes upon sympathetic vasoconstriction, occurring with a delay of 5-15 s,¹²⁻¹⁴ can be reliably detected. Negative as well as positive social stimuli provoke alterations in surface temperature of various facial areas, with the nose consistently reported as highly reactive to affective and social cues.^{12,15-18}

These observations advocate infrared thermography (IRT) as a highly attractive method of contact-free and non-invasive measurement of naturally emitted electromagnetic radiation with a wavelength between 0.75-1000 μm , commonly interpreted as “heat”.¹⁹ Modern IRT recording systems are characterized by high spatial and temporal resolutions and require almost no restrictions in movement of test subjects, allowing a more natural/ecological testing environment.^{9,15,20} Because of its high accuracy, relative ease of use, and minimal inconvenience for the subjects, IRT has already been implemented in different fields of medical research and practice.^{19,21}

While the validity of IRT for assessing surface temperature is generally accepted and has led to several pivotal publications,^{4,6,7,16,22-28} its broader applicability in the future will depend on controlling environmental, subject-related, and technological factors²⁹ as well as improved reliability and reproducibility. So far, no overall accepted, dependable state-of-the-art procedure for IRT testing in social behavior diagnostics has been introduced. Numerous different experimental designs, test stimuli, facial/body target regions, and data extraction/analysis procedures have been reported.^{9,21} Often, single or short series of IRT images (before versus after experimental condition) are described, based on rather small and heterogeneous samples, whereas data on thermal dynamics over longer time intervals are scarce. Interpretation of thermal alterations is frequently limited to single directional statements, for instance increase or decrease or unaltered temperature.

In the present translational study, we employ and adapt IRT for more reliable, internally controlled measurement of a social stimulus-related autonomic vaso-response. We start with an unexpected discovery in mice, namely induction of “sociophobia” upon inescapable interaction in a social recognition test, where the *Centralization Index* (ratio body/tail temperature) serves as continuous “whole body stress readout”. We then extend these findings to human subjects,

exposed to social versus non-social cognitive tasks in a highly standardized fashion. Here, the *Reference Index* (ratio nose/malar cheek temperature) is introduced to determine the autonomic facial response/flushing during social recognition testing. We report a novel non-invasive “sociophobia” model in mice, characterized by a pronounced thermo-reaction during induction and on retrieval, and a typical facial thermo-response in men under cognitive challenge containing a social component.

2 | MATERIALS AND METHODS

2.1 | Mouse studies

2.1.1 | Mice

All experiments were approved by and conducted in accordance with the regulations of the local Animal Care and Use Committee (Niedersächsisches Landesamt für Verbraucherschutz und Lebensmittelsicherheit, LAVES). C57BL/6JRj mice were used as experimental mice, C3H/HeNcrI as stimulus mice (Charles River). Animals were group-housed in standard cages (36.5 \times 20.7 \times 14 cm, 4-5 mice per cage of the same gender and strain), in rooms separated by gender and strain (to avoid olfactory contact), and kept on a 12 h light-dark cycle (lights off at 7 PM) at 20-22°C. Food and water were provided ad libitum.

2.1.2 | SocioBox test for complex social recognition memory and recording

A detailed description of the *SocioBox* as a multiple social recognition task is provided elsewhere³⁰ (see also Figure 1). Experiments were conducted during light phase of the day (10-15 lux, 23.5°C room temperature), with male or female C57BL/6JRj experimental mice (N = 45 in total) and gender-matched C3H/HeNcrI as stimulus mice (Figure 1A). Male mice were 13-15, female 20-22 weeks old. Prior to test session, experimental and stimulus mice had been habituated separately (in absence of any other mice) to the *SocioBox* for 3 consecutive days. The following test sessions consisted of three phases, namely exposure 1, exposure 2, and recognition test.³⁰ At beginning of test session, the experimental mouse was placed into the central arena inside a white Plexiglas circular partition, spatially and visually separated from stimulus mice. After 5 minutes of recovery (“Initiation stage”), the circular partition was lifted, and the mouse allowed to freely explore the arena, including the stimulus mice in their inserts, for 5 additional minutes (“Interaction stage”). At the end of exposure 1, the mouse was removed and placed back in its transport cage. The arena was cleaned and the mouse then

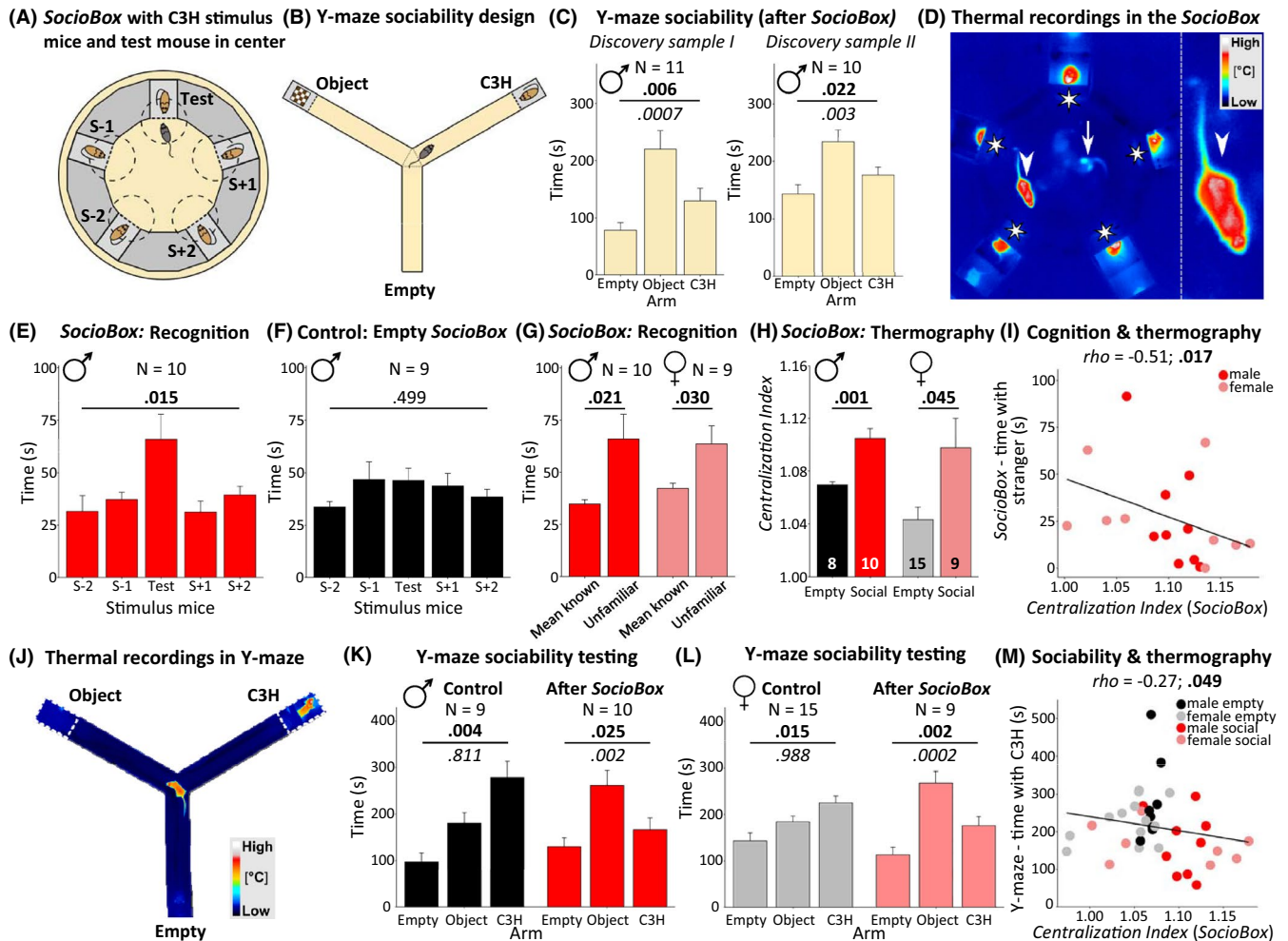


FIGURE 1 Mouse IRT study: *SocioBox* recognition testing induces lasting social avoidance in mice. A, *SocioBox* arena³⁰ with experimental mouse in center (gray), unfamiliar “stranger” (“Test”) and familiar stimulus mice (all brown). Time spent in zones close to each stimulus mouse (circles) is recorded to determine interaction/recognition. B, Y-maze sociability test:³¹ Test mouse starts in center of Y-maze with one arm empty, one containing an object and the third another mouse (C3H). Time spent in each arm is measured. A normal naïve mouse spends most of the time with the other mouse (stair pattern of controls in panel K and L). C, Unexpectedly, 4 weeks after *SocioBox* testing, experimental mice display social avoidance behavior in 2 independent samples: *Discovery I and II*; repeated-measure ANOVA; quadratic-trend analysis (below; italics). D, IRT image of *SocioBox* test with experimental mouse (arrowhead) and stimulus mice (asterisks); white arrow: experimental mouse left trace of urine (evaporation cooling). Magnification on the right illustrates temperature differences in body parts. **Compare video S1**. E, Zone preference of male mice during *SocioBox* recognition testing. Mice with normal recognition memory spend most time with the “stranger” (unfamiliar stimulus mouse). F, Control mice tested in empty *SocioBox* do not show appreciable zone preference; repeated-measure ANOVA. G, Average interaction time with all familiar mice versus time with unfamiliar mouse (stranger); paired Student's *t* tests (one-sided). H, Both genders exhibit in *SocioBox* an increase in *Centralization Index* (body/tail temperature), compared to controls in empty box; unpaired Student's *t* tests (two-sided). Note that due to difficulties in tracking tail ROI ($\geq 25\%$ missing values), 3 animals (1 male, 2 female controls) had to be excluded from thermal analyses. I, *Centralization Index* is negatively correlated with social recognition performance; Spearman's *rho* (one-sided). J, Representative IRT image during Y-maze sociability. K-L, Both genders show robust social avoidance 4 weeks after *SocioBox* compared to the expected stair pattern of control animals; repeated-measure ANOVA; quadratic-trend analysis (below; italics). Due to atypical hypoactive behavior during testing, two female control animals were excluded prior to analyses. M, Social aversion priming: Negative correlation between *Centralization Index* in *SocioBox* and time spent with C3H conspecific in Y-maze 4 weeks later; Spearman's *rho* (one-sided)

again placed in the *SocioBox* center. Exposure 2 followed the same procedure. At the end of exposure 2, one of the five stimulus mice was randomly exchanged for a new, unfamiliar conspecific. Next, the mouse was reintroduced and the recognition test conducted accordingly. During the course of the experiment, a black body-calibrated A655sc IRT camera

with a 13.1 mm focal length lens was used. The system has a noise equivalent thermal difference (NETD) < 30 mK and resolution of 640×480 pixels (FLIR ResearchIR Max software v4.40.2.1, TOPA, Hohenpeissenberg, Germany) and was mounted 110 cm above the arena, recording at a frame-rate of 25 Hz. Care was taken that no direct or indirect heat

emissions from external sources affected recordings. The IRT camera was connected to a computer located in a separate room. Readouts were temperature changes of the mouse, duration of interaction with stimulus mice/recognition of the stranger mouse, and distance traveled (video S1). To ensure that sociability changes are not triggered by the *SocioBox* arena itself, the same procedure was conducted with control mice exposed to an empty *SocioBox* (without stimulus mice).

2.1.3 | Y-maze sociability testing and recording

Y-maze testing was performed as described with slight modifications.³¹ Mice were tested 4 weeks after *SocioBox*/empty box performance on 2 consecutive days at light intensities of 60-70 lux. Day 1 included three habituation trials with an inter-trial-interval of 60 min. The mouse was placed in one of the arms and allowed to explore the empty maze for 10 min per trial. The starting point was rotated through all three arms (dimensions of each arm 46.1 × 8.3 × 13.7 cm). On day 2, an object (6 cm chess piece) and a C3H-stranger mouse, same gender and age, were each presented in an insert, preventing direct access, and positioned at the end of two randomly chosen Y-maze arms while the third arm remained empty (Figure 1B). The mouse was then placed in the empty arm, facing the center, and allowed to explore freely for 10 minutes. All mice underwent the same test procedure. The IRT camera was positioned 130 cm above the maze, readouts were changes in temperature, distance traveled and, to estimate social preference, time spent in each arm (Figure 1J).

2.1.4 | Data extraction and preprocessing

Mouse location and stress readouts during *SocioBox* recognition and Y-maze sociability tests were assessed through an image analysis workflow implementing the software packages Ilastik v.1.3.3b2³² and FIJI,³³ as well as the TrackMate³⁴ FIJI plugin. Thermal readouts of both, body and tail, were extracted by first using the pixel classification workflow of Ilastik. Pixel groups delineating “background”, “body”, and “tail” were annotated to train a Random Forest classifier³² that was used to produce probabilities for the respective classes for each image sequence of the recorded mice. Resulting body and tail probabilities were binarized with FIJI to generate masks, which were then applied to the corresponding, original IRT image sequence as regions of interest (ROI), from which the relative mean body and tail temperatures were obtained.

For the *SocioBox*, five zones were defined in close proximity to each stimulus mouse/empty inset (Figure 1A). Number of frames the respective mouse spent in each zone

was summed up to obtain total interaction time with stimulus mice. Interaction with stranger (unfamiliar mouse) served as readout of social recognition.³⁰ To exclude zone preferences not attributable to experimental setup (eg, room features) during empty *SocioBox* condition, control mouse zone orientations were randomly matched to experimental mouse zones. A similar procedure was employed during Y-maze sociability, counting number of frames in each arm (empty, object, C3H).

After down-sampling (1 Hz) to increase computational speed during following preprocessing steps, frames with missing information (eg, hidden tail) were replaced by the mean of the remaining data points for each mouse. Mice with $\geq 25\%$ missing values were excluded from respective thermographic analysis. To reduce random noise effects we smoothed data sequences of both body and tail separately, using locally estimated scatterplot smoothing (LOESS). By dividing the relative mean temperature of the body ROI by its corresponding tail ROI relative mean temperature at each time point, we created an intraindividually adjusted measure of endogenous arousal: the **Centralization Index**. To evaluate whether potential thermal differences were independent of higher physical activity, we additionally calculated the distance mice traveled in 500 ms intervals for *SocioBox* and Y-maze.

2.2 | Statistical analyses

Both male and female experimental (*SocioBox*) versus control (empty box) mice were analyzed. To reduce the impact of extreme values in statistical analyses while avoiding exclusion, data for each group (empty *SocioBox*, *SocioBox* with stimuli) were winsorized: extreme values <5th and >95th percentiles were set to 5th and 95th percentiles, respectively.³⁵ Total time spent in *SocioBox* zones was analyzed using repeated measure analyses of variance (ANOVA).³⁰ Additionally, for experimental groups, average time spent in zones with familiar mice was compared with time spent with stranger (unfamiliar zone). Due to expected outcome (more time spent with unfamiliar mouse),³⁰ one-sided paired Student's *t* tests were calculated. Differences in mean *Centralization Index* and total distance traveled were compared between conditions via two-sided unpaired Student's *t* tests. Exploring the relationship between *Centralization Index* as readout of physiological reactivity (stress) and recognition performance, Spearman's *rho* was calculated for all experimental mice. Because of initial orientation and adaption to the situation with potentially interfering effects on recognition performance, we used only the second half of *SocioBox* test (minutes 4-5). Hypothesizing that a higher *Centralization Index* is associated with worse performance, analysis was one-sided. For Y-maze sociability, differences in time spent in each arm was tested via repeated-measure ANOVA with following linear and quadratic trend analyses using polynomial contrasts. Both differences in

mean *Centralization Index* and total sum of distances traveled were analyzed with two-sided unpaired Student's *t* tests. Hypothesizing that the *Centralization Index* in Y-maze correlates negatively with sociability, one-sided Spearman's *rho* was calculated, including all test mice. Additionally, to investigate the relationship between severity of experience during *SocioBox* (assumed priming of social aversion) and sociability in Y-maze, we calculated Spearman's *rho* for *Centralization Index* in *SocioBox* and time spent in C3H-arm during Y-maze, again with test mice from all conditions. Expecting a negative correlation, a one-sided test was applied. All statistical analyses were performed using R v3.5.2³⁶ with RStudio v1.1.463 (RStudio Inc, Boston, United States) and significance level of $\alpha = 0.05$. Welch-corrected Student's *t* tests were used, and, in cases of violations of sphericity, Greenhouse-Geisser corrections were applied to repeated-measure ANOVA.

2.3 | Human studies

2.3.1 | Participants

The study was conducted in accordance with the Declaration of Helsinki and approved by the ethics committee of the Georg-Elias-Müller-Institute of Psychology, University of Göttingen. Online screening was set up to attract and assess eligibility of potential participants. Besides providing demographic information and answering questions regarding their ability to identify and memorize faces, interested individuals completed the German versions of Brief Symptom Inventory (BSI)³⁷ and complementary social phobia instruments Social Phobia Scale (SPS) and Social Interaction Anxiety Scale (SIAS)³⁸. As additional readout of personality structure, NEO-Five-Factor Inventory (NEO-FFI)³⁹ was filled out. Those with questionnaire scores within normal limits were invited to the experimental session, aiming to include only mentally healthy individuals without indication of (sub)clinical symptoms. Based upon results of this online screening, a total number of $N = 111$ subjects were invited. However, due to psychiatric conditions, illicit substance consumption shortly before study onset, or technical difficulties during recording, $N = 8$ had to be excluded, leaving a final sample of $N = 103$ participants (see Figure 2A for inclusion process). All subjects were heterosexual, native German men between 18 and 34 years of age with normal or contact lens-corrected vision, no facial piercings or beard, and without history of neuropsychiatric or somatic diseases.

2.3.2 | Experimental procedure

To reduce impact of external factors during IRT recordings^{9,15,29} participants were asked to avoid alcohol

consumption (24 h), physical activity (12 h), and intake of food or activating substances (eg, caffeine, nicotine; 2 h) before test session (Figure 2 and Figure 3). Additionally, they were instructed not to shave or apply facial lotion at testing day. Study participation was compensated with 35€ or course credit. Completing the online screening offered the chance to win 1 of 3 gift cards (10€). All test subjects gave written informed consent and could withdraw participation at any time. Main experiments took place in a 5×3 m²-sized testing room without direct sunlight or ventilation and with normal ambient temperature ($M = 22.94^\circ\text{C}$, $SD = 1.14$) and humidity ($M = 59.62\%$, $SD = 7.34$). Trained experimenters (JS, FB) ensured standardized test conditions during sessions,²⁹ which consisted of an initial assessment, habituation, two IRT-recorded computer tests of cognitive abilities, and a closing assessment (Figure 2B). Individual sessions consistently started at either 09:00 AM or 11:00 AM, total test duration did not exceed 120 minutes. During initial assessment, the participant was welcomed and informed about study procedure, followed by an examination of state-trait anxiety (German version of State-Trait Anxiety Inventory, STAI)⁴⁰ and, thereafter, general face perception abilities via a short prosopagnosia test. IRT-recorded cognitive testing was performed in a 3×2 m²-sized chamber within the experimental room (Figure 3A). One chamber side was not completely closed to allow fresh air supply and communication between subject and experimenters. The participant was seated in a specialized comfortable chair which adapted to his body size and shape, effectively avoiding pressure points (M^cLean REHAtechnik, Duderstadt, Germany). The implemented headrest enabled relaxation of head and neck muscles, while gently minimizing head movements (Figure 3A). The entire setup was highly adaptable to the differing subject shapes and sizes preventing irritation of the vascular system, while ensuring an unobstructed view of the relevant facial features for the IRT camera. Prior to testing, subjects stayed in a relaxed position for 15 minutes to acclimatize to setup (habituation phase).^{15,29} Each participant performed computerized tests of both executive functioning and social cognition in counter-balanced order, separated by a 2 min break. The IRT camera was mounted above the monitor and recorded whole-face images of the participant at 25 Hz from approximately 32 cm distance while the subject performed the tasks.

Executive functioning

Executive functioning as a process of general cognitive abilities was measured via *Wisconsin Card Sorting Test, Computer Version 4 (WCST)*.⁴¹ Subjects are required to virtually classify cards regarding different features (symbol, number, color) via button press to 1 of 4 target decks. No additional instructions are provided. Instead, subjects have to infer sorting strategies from a feedback ("correct"/"incorrect") following each sorting decision. After a series of correct answers

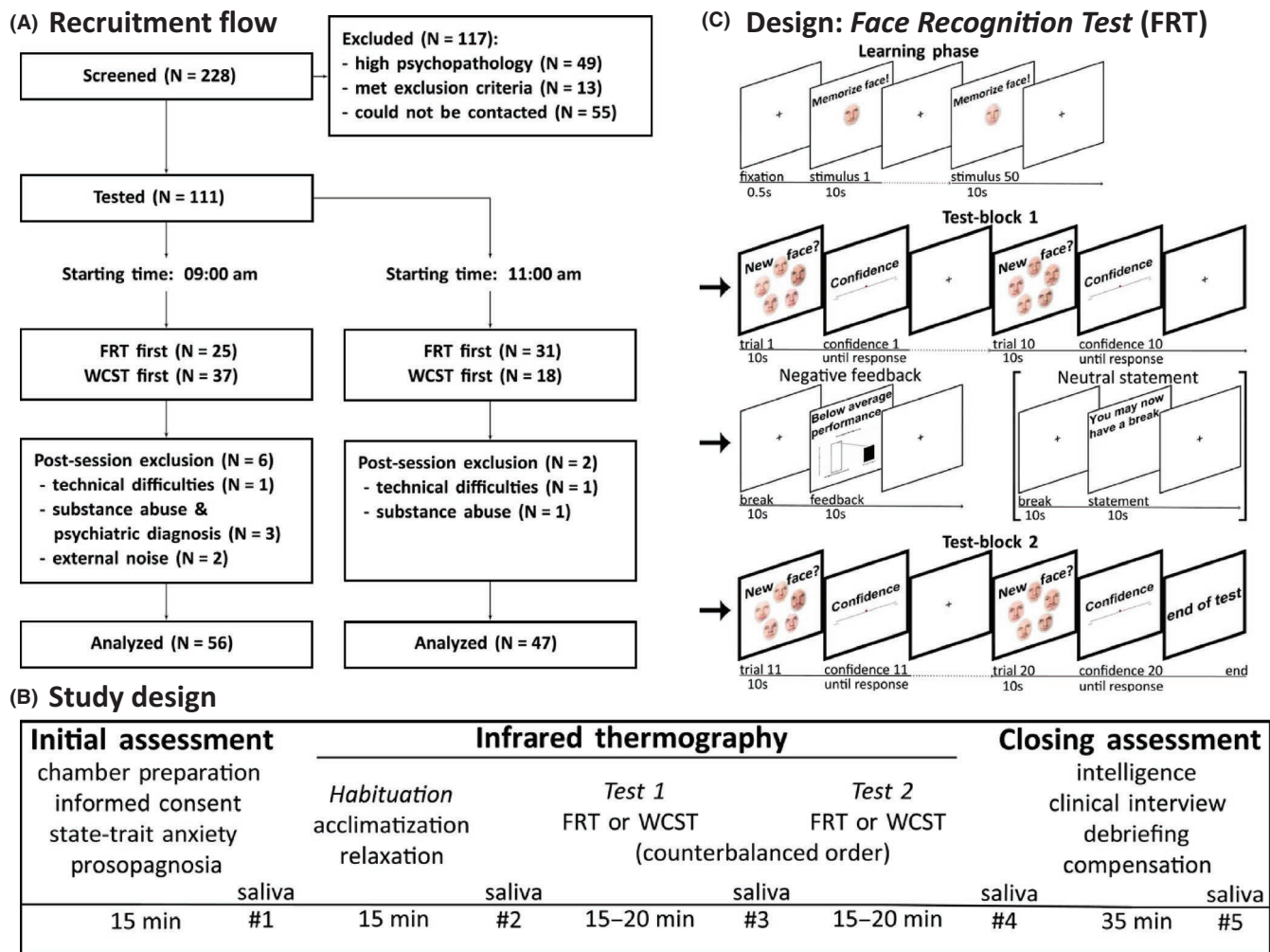


FIGURE 2 IRT of social recognition versus executive function testing in men: Study logistics. A, Recruitment process: To ensure sample homogeneity, pre-experimental online screenings were implemented. A total of 111 individuals completed experimental session, starting at either 09:00 AM or 11:00 AM. After post-session exclusion, 103 subjects remained as final sample. B, Study design: During initial assessment, participants were welcomed and provided with study information, followed by state-trait anxiety and prosopagnosia examinations. Then, IRT-recorded test phase was conducted, starting with habituation and 2 computerized cognition tests (in counterbalanced order: FRT, WCST). At closing assessment, intelligence was measured, and an interview concerning mental and physical health as well as debriefing (explanation of feedback) and, finally, compensation for participation took place. Over the course of experimental session saliva samples for cortisol analysis were collected at 5 different time points in 15–35 min intervals. C, Sketch of the novel, brief *Face Recognition Test* (FRT): Participants are first asked to memorize 50 male stimulus faces (learning phase). Subsequently, test trials containing 5 stimulus faces each are presented; subjects decide whether all are familiar or not, respectively (test-block 1). After 10 trials either a fabricated, negative feedback or an alternative, neutral statement is presented, before concluding with 10 more trials (test-block 2), analogous to test-block 1

of certain length, sorting criteria shift, prompting subjects to adapt.

Social cognition

Social cognition in humans was assessed based on face memory tasks.^{42–44} Analogous to the *SocioBox* recognition test in mice, we created the *Face Recognition Test* (FRT), a computerized measure of social cognitive abilities (face perception, face memory based on internal features, perception of social evaluation). The FRT consists of a learning phase, followed by two test blocks, each separated by a negative feedback or, alternatively, neutral statement (Figure 2C). The test is presented

via PsychoPy v1.85.4⁴⁵ for Python v2.7.⁴⁶ During the learning phase, 50 male faces from the Göttingen Faces Database⁴⁷ with neutral valence, standardized visual features, luminance, and resolution are sequentially presented in random order. Test subjects are instructed to stay calm, focus and memorize the stimulus on screen. Each face is shown once for 10 s at the center of the screen, followed by fixation cross (500 ms). Learning phase lasts 560 s in total. For test-block 1, of the previous 50 stimulus faces, two are randomly replaced with unfamiliar ones. This new set of images is then given in 10 trials. Each trial includes 5 stimuli, randomly presented in a circular order (Figure 2C). Participants indicate via keyboard button press within 20 s if

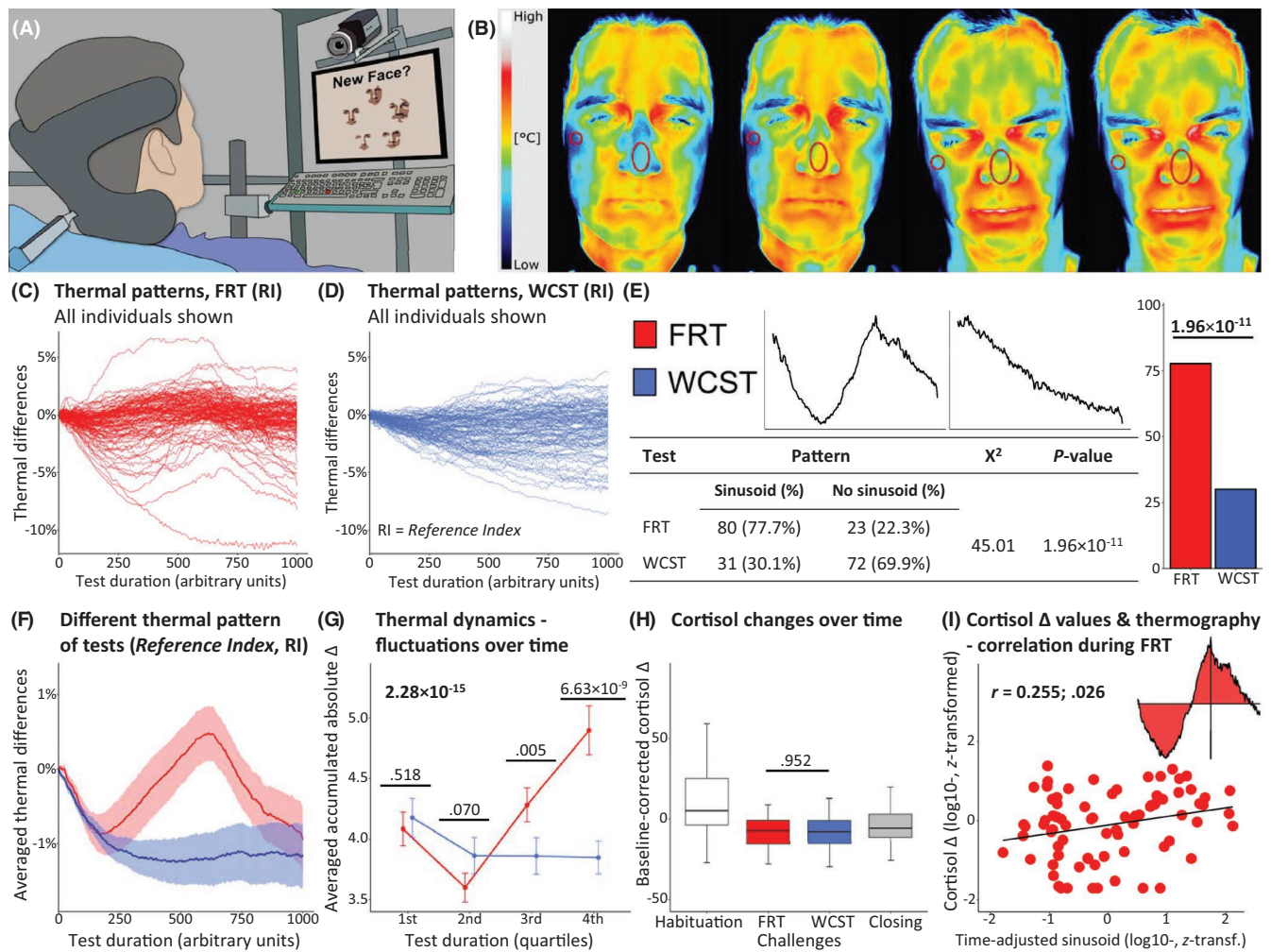


FIGURE 3 Human IRT study during social recognition versus executive function testing: Social cognition stimulus induces a distinct thermo-pattern. A, Illustration of test setup: Participant sits as still as possible in a comfortable orthopedic armchair, with headrest to minimize head movements, and performs FRT (*Face Recognition Test*) while IRT camera (above screen) records facial regions of interest (ROI). B, IRT images of two sample test subjects with nose and right malar cheek ROI (circled in red) used to calculate *Reference Index* (RI). Images taken from early and late FRT session phase, respectively. **Compare video S2**. C-D, Overlays of all participants' normalized *Reference Index* differences from baseline in both tests indicate a sinusoid-shaped thermo-pattern over the course of FRT but not WCST (*Wisconsin Card Sorting Test*). E, Consensus ratings by three examiners (blinded to any test/subject information) revealed that the majority of test subjects exhibited a characteristic *Reference Index* sinusoid pattern during FRT (left example curve) but not WCST (right example curve); χ^2 -test. F, Comparison of *Reference Index* course between tests over time using $M \pm 95\%$ confidence intervals. Groups' thermo-patterns differ significantly where confidence intervals do not overlap. G, Over each test quartile, accumulated absolute changes in *Reference Index* showed differences during second test halves, with higher temperature dynamics in FRT compared to WCST; repeated-measure ANOVA, Bonferroni-adjusted multiple-comparison tests (two-sided). H, Contrary to *Reference Index*, salivary cortisol reactivity was similar between tests, suggesting IRT as a more sensitive tool for measurement of physiological responses in social tasks. Cortisol levels were log10-transformed and normalized to the first sample (baseline); then cortisol Δ values were calculated between sample time points; paired Student's *t* test (two-sided). I, Pearson correlation coefficient revealed mild-to-moderate positive relationship between log10- and z-transformed time-adjusted integrals of *Reference Index* and z-transformed salivary cortisol Δ values during FRT. Only participants with characteristic sinusoid thermal curve and z-score ± 2.58 included (N = 78)

all faces are familiar or not. Each stimulus face is shown only once and trials never contain more than one unfamiliar face. Additionally, after each trial, participants rate confidence in their response on a 5-point Likert scale. Then, after a break of 10 s, either an unprompted, fabricated negative feedback or a neutral statement is included, each lasting for 10 s. Negative feedback is shown graphically and as text (*"your performance is below average"*), the non-threatening alternative is

displayed as text (*"you may now take a break - the second part of the test will start automatically"*). Immediately thereafter, test-block 2 is initiated with the two unfamiliar faces of test-block 1 again exchanged for two new faces and participants perform the same task with confidence judgments, analogous to test-block 1. Closing assessments covered a structured clinical interview on mental and somatic conditions, a nonverbal intelligence assessment (performance test system subtest-3;

“Leistungsprüfsystem Untertest-3”),⁴⁸ monetary compensation and, lastly, a debriefing on the aims of the study. As an additional, biological readout, saliva was collected to measure cortisol levels at five different time points in intervals of around 15-35 min (Figure 2B).

2.3.3 | Data extraction & preprocessing

Tracking information of facial ROI in human subjects was obtained with the DeepLabCut software package⁴⁹ and implemented into a FIJI-based image analysis workflow, allowing for corrections of small head movements not prevented by the headrest. Labels delineating either nose or right cheek (malar region) coordinates (Figure 3B; video S2) in up to 600 images were used to train the DeepLabCut network. Facial regions were selected regarding reactivity to social stimuli, with nose reacting strongly while malar cheek does not. After 10⁶ iterations, the resulting network had converged sufficiently to be evaluated for accuracy and then applied to human IRT recordings in FIJI in order to track and extract relative mean temperatures of the two facial ROI at their respective position and time. The resulting series of temperature values (25 per second) were subsequently down-sampled (1 Hz) for following processing steps. In order to replace missing values we calculated the sequence (ascending/descending) between the last valid data points before and after the missing. Then both ROI frame sequences were smoothed separately using LOESS fitting.

By dividing mean nose ROI temperature of each frame with its corresponding malar cheek ROI, we calculated the *Reference Index*, analogous to the *Centralization Index* in mice. Due to initial temperature differences in respective ROI, *Reference Index* was normalized as percentage change from the very first frame (baseline), and, due to varying individual test length of participants, duration of both tests was normalized to 1000 arbitrary units, both for FRT (Figure 3C) and WCST (Figure 3D). To investigate differences in thermal curve characteristics, two independent evaluators rated in a blinded manner over both tests whether the normalized *Reference Index* curve was initially decreasing and then increasing (sinusoid curve), or was differently shaped (Cohens' $kappa = 0.63$). In case of dissent, a third evaluator made a final decision on the rating.

2.3.4 | Saliva cortisol determination

Saliva was collected at five different time points in intervals of 15-35 minutes (Figure 2B) and stored at -80°C until further use. ELISA was used to detect cortisol levels in saliva samples, according to manufacturer's instruction (Demeditec, Kiel, Germany). To account for circadian cortisol profile differences (ie, cortisol awakening response⁵⁰⁻⁵²) due to experimental starting points (09.00 AM versus 11.00 AM), we

calculated normalized *delta* values (Δ) between sample collection time points: First, all samples were log10-transformed and normalized to percentage alteration from first sample (baseline). Next, differences between consecutive samples were calculated. This way we received adjusted cortisol changes for habituation, FRT, WCST, and closing assessment.

2.3.5 | Statistical analyses

Differences in frequency of sinusoid-curve ratings between FRT and WCST were analyzed using Yates'-corrected *chi*-squared test. To display averaged group differences over total test course, normalized *Reference Index* means and 95% confidence intervals were calculated, highlighting significant differences where confidence intervals do not touch. To additionally investigate thermal dynamics over test quarters, mixed-design ANOVA was calculated, with quarter-sums of absolute *Reference Index* changes per arbitrary unit as dependent variable, test quarters as within- and test as between-factor. Bonferroni-adjusted post-hoc multiple comparison tests were calculated to compare differences between individual test quarters. Cortisol reactivity changes between FRT and WCST were analyzed by comparing cortisol- Δ group values via two-sided paired Student's *t* test. All statistical tests were conducted in R using RStudio, with significance levels set to $alpha = 0.05$. Welch-corrected Student's *t* tests were used, and, in cases of violations of sphericity, Huyn-Feldt corrections were applied to repeated-measure ANOVA.

3 | RESULTS

3.1 | Unexpected discovery: *SocioBox* recognition testing induces lasting social avoidance in mice

To evaluate the social Y-maze test^{31,50} for suitability as routine sociability readout in our mouse behavioral test battery, we used mice which had previously undergone *SocioBox*³⁰ experiments. By serendipity, we this way discovered that 4 weeks after passing through the *SocioBox* paradigm, these mice displayed social avoidance. This unexpected result was fully replicated in a second, independent cohort of former *SocioBox* completers (Figure 1A-C), leading to two first conclusions: (I) By chance, we may have developed a mouse model of social aversion priming/sociophobia, arising from a situation of inescapable social contacts. (II) The *SocioBox* test, even though superior to all other presently available social recognition tests and the first that successfully addresses multiple social contacts in parallel, will have to be treated as a final test in future behavioral test batteries (similar to eg, fear conditioning).

3.2 | IRT as non-invasive tool to measure the vascular response to social cognitive performance in a “sociophobia” inducing setup

To further explore the novel “mouse model of sociophobia”, we employed IRT as a non-invasive method to continuously approximate experienced stress during these inescapable social contacts in the *SocioBox* (Figure 1D-I; video S1). Conveniently, IRT additionally provides monitoring of spatiotemporal dynamics, and thus location information needed for tracking. As expected, in the *SocioBox* recognition test, male mice spent significantly more time in the zone close to the stranger compared to already acquainted stimulus mice ($F_{(4,36)} = 3.58$; $P = .015$; Figure 1E), while control mice (empty *SocioBox*) did not exhibit any zone preference ($F_{(4,32)} = 0.86$; $P = .499$; Figure 1F). These findings were reproduced in female mice (*SocioBox*: $F_{(4,32)} = 3.03$; $P = .032$; empty box: $F_{(4,64)} = 1.21$; $P = .314$). Comparison of mean time spent with stranger versus all known mice yielded equivalent results (male $t_{(9)} = 2.38$; $P = .021$; female: $t_{(8)} = 2.20$; $P = .030$; Figure 1G). Screening the obtained IRT readouts in a few males first, we observed that mice changed their temperature over time in the *SocioBox* in a typical way, namely displayed an increase in body and a decrease in tail temperature (video S1). We therefore introduced a novel descriptive measure, integrating an internal control (within-subject) aspect, the **Centralization Index**. This measure, likely approximating the experienced stress during the task, clearly demonstrates an increase in *SocioBox* mice versus controls for both males ($t_{(10,23)} = -4.44$; $P = .001$) and females ($t_{(10,66)} = -2.27$; $P = .045$; Figure 1H). Importantly, enhanced movement and thus physical activity cannot account for this difference since control mice even had a tendency to move more than *SocioBox* performers ($t_{(36,18)} = 1.90$; $P = .066$). Interestingly, the **Centralization Index** correlated negatively with the time spent with the stranger in the *SocioBox* (Spearman's $\rho = -0.51$; $P = .017$; Figure 1I), indicating that mice with a higher **Centralization Index** (likely reflecting their stress level) perform worse in this social recognition task.

3.3 | Robust induction of social avoidance in the Y-maze sociability test following *SocioBox* recognition testing

Around 4 weeks after *SocioBox* testing, mice were exposed to Y-maze sociability testing, including IRT (Figure 1J). While male control mice exhibited normal social preference ($F_{(2,16)} = 7.88$; $P = .004$; linear trend: $b = 128.32$; $t_{(16)} = 4.85$; $P = .0004$; quadratic trend: $b = 6.44$; $t_{(16)} = 0.24$; $P = .811$), the prior *SocioBox* performers displayed social avoidance behavior, similar to the discovery samples ($F_{(2,18)} = 4.55$;

$P = .025$; linear trend: $b = 25.86$; $t_{(18)} = 0.99$; $P = .334$; quadratic trend: $b = -92.48$; $t_{(18)} = -3.55$; $P = .002$; Figure 1K). Comparable effects were found for female mice in both control ($F_{(2,28)} = 4.89$; $P = .015$; linear trend: $b = 57.70$; $t_{(28)} = 3.80$; $P = .0007$; quadratic trend: $b = 0.23$; $t_{(28)} = 0.02$; $P = .988$) and post-*SocioBox* condition ($F_{(2,16)} = 9.56$; $P = .002$; linear trend: $b = 44.67$; $t_{(20)} = 2.16$; $P = .046$; quadratic trend: $b = -100.52$; $t_{(16)} = -4.87$; $P = .0002$; Figure 1L). These results, together with those of the two discovery samples, point to a robust induction of “sociophobia” by the *SocioBox* recognition test.

After Y-maze sociability testing, we controlled for potential differences in basic anxiety-related conduct. As a simple, non-invasive readout, spatial novelty-induced freezing in the fear-conditioning chamber (without shock) was evaluated. Importantly, neither male nor female *SocioBox* performers differed from empty box controls regarding duration of freezing (males: $F_{(2,36)} = 0.09$; $P = .910$; females: $F_{(2,28)} = 2.96$; $P = .068$, tendency in the opposite direction), excluding an “unspecific global fear behavior” underlying their “sociophobia” phenotype.

The next crucial question was whether we would see a correlation between stress, experienced in the *SocioBox*, as measured by the **Centralization Index**, and the degree of sociability evaluated 4 weeks later in the Y-maze. Indeed, a higher **Centralization Index** was associated with lower sociability (Spearman's $\rho = -0.27$; $P = .049$) (Figure 1M). Together, these results support our hypothesis that inescapable social encounters can induce sociophobia/social aversion in mice.

The **Centralization Index** during Y-maze sociability testing also tended to be increased in *SocioBox* mice ($M = 1.23$, $SD = 0.03$) versus empty box controls ($M = 1.21$, $SD = 0.02$; both genders included; two-sided unpaired Student's t test, $t_{(34,47)} = -1.88$, $P = .068$). Once again, these higher **Centralization Index** values could not be explained by higher physical activity; control animals traveled more than their *SocioBox* counterparts (both genders included; $t_{(36,07)} = 2.81$; $P = .008$).

3.4 | Translational study: IRT as sensitive measure of the vascular response to social cognitive performance in humans

In our mouse experiments, we unexpectedly discovered that stress experienced during an inescapable social encounter (*SocioBox*) likely acts as a “primer” of sociophobia/social aversion. We thus started an IRT study in men, investigating in a translational fashion, whether a simple social component in a cognitive task (face recognition) would already yield thermographic results differing from a “non-social” cognitive test (pattern recognition) (Figure 2A-C; Figure

3A-I; Table 1; video S2). Of a total of $N = 228$ men screened for participation, $N = 111$ were tested, and $N = 103$ finally analyzed. Recruitment flow, study design and *Face Recognition Test* (FRT) are shown in Figure 2A-C.

All 103 subjects displayed high accuracy of face recognition in the prosopagnosia test (part of initial assessment; $M = 97.67\%$, $SD = 6.45$) as prerequisite to perform the study. To ensure that subjects whose session started with FRT did not differ systematically from those with *Wisconsin Card Sorting Test* (WCST) first, we compared sociodemographic, psychopathological, and cognitive data between the two samples (Table 1). Since none of these variables showed any group differences, we combined both samples for the now following analyses of IRT readouts. First, we screened several facial IRT videos of participating subjects, allowing us to determine our regions of interest (ROI), namely nose (highly variable and seemingly responsive, as also described before)^{15,18} and malar region of the cheek (obviously quite stable; compare video S2). We then calculated the *Reference Index*, in some analogy to the *Centralization Index* in mice, by dividing mean nose ROI temperature of each frame with its corresponding malar cheek ROI. Comparing the *Reference Index* course

of all individuals during FRT, we noticed a sinusoid pattern predominating in most subjects (initial decrease, followed by increase) (Figure 3C). In contrast, only a minority of participants seemed to show such pattern during WCST (Figure 3D). To consolidate this first visual impression, independent raters estimated in a blinded fashion all individual thermal curves of both FRT and WCST to determine whether they resembled the characteristic sinusoid shape or not, with high interrater reliability (Cohen's $kappa = 0.63$ between first two raters). Comparisons of pattern frequency (sinusoid versus not) yielded highly significant differences, with 77.7% of participants showing the sinusoid curve during FRT but only 30.1% during WCST ($OR = 7.98$; Figure 3C-E). Interestingly, comparing participants with sinusoid-shaped *Reference Index* curve to those without revealed younger age and less time spent in the educational system together with higher scores in *Social Phobia Scale* (SPS) and *Social Interaction Anxiety Scale* (SIAS)³⁸ as well as lower answer security in FRT (Table 2).

Presentation of the normalized *Reference Index* total course of all subjects for each test ($M \pm 95\%$ confidence interval) illustrates the sinusoid pattern during FRT versus the

TABLE 1 Sociodemographic, psychopathological, and cognitive data of test subjects performing FRT or WCST first

	Total sample N = 103	FRT first N = 52	WCST first N = 51	t/χ^2	P
Neutral statement in FRT	23 (22.33%)	12 (23.08%)	11 (21.57%)	0.03	.854
Years of age	24.58 (3.34)	24.76 (3.49)	24.40 (3.20)	0.55	.584
Years of education	16.83 (2.67)	17.02 (2.86)	16.65 (2.51)	0.65	.520
BMI	24.15 (2.97)	23.75 (1.95)	24.53 (3.67)	-1.25	.216
LPS-3 (T)	61.52 (5.53)	61.58 (6.20)	61.46 (4.81)	0.10	.918
STAI state	32.41 (5.08)	32.90 (5.62)	31.90 (4.45)	1.00	.318
STAI trait	32.85 (6.94)	33.79 (7.47)	31.90 (6.27)	1.39	.168
SPS sum	6.22 (4.51)	5.75 (4.35)	6.71 (4.67)	-1.08	.285
SIAS sum	15.95 (8.05)	15.38 (7.88)	16.53 (8.25)	-0.72	.473
BSI sum (T)	45.81 (9.07)	46.21 (9.58)	45.39 (8.59)	0.46	.649
NEO-Openness	32.20 (6.50)	33.06 (6.68)	31.33 (6.25)	1.35	.179
NEO-Conscientiousness	32.31 (7.21)	33.38 (7.09)	31.22 (7.23)	1.54	.127
NEO-Extraversion	29.21 (6.61)	29.15 (6.06)	29.27 (7.19)	-0.09	.927
NEO-Agreeableness	31.21 (6.93)	31.08 (7.44)	31.35 (6.45)	-0.20	.841
NEO-Neuroticism	15.61 (7.45)	16.12 (8.01)	15.10 (6.87)	0.69	.490
FRT error percentage	42.28 (12.04)	41.06 (12.58)	43.53 (11.46)	-1.04	.300
FRT duration (s)	969.12 (64.88)	975.24 (68.86)	962.74 (60.48)	0.98	.332
FRT confidence	3.40 (0.52)	3.44 (0.47)	3.36 (0.57)	0.78	.437
WCST error percentage	18.35 (9.43)	17.29 (9.01)	19.43 (9.82)	-1.15	.251
WCST duration (s)	621.15 (161.36)	612.04 (146.99)	630.44 (175.80)	-0.58	.566

Note: Data represent uncorrected means (SD) or N (%). Student's *t* tests and Pearson's *chi*-squared tests for independent comparisons were employed for analyses. Abbreviations: BMI, Body Mass Index; BSI, Brief Symptom Inventory; FRT, *Face Recognition Test*; LPS-3, Leistungsprüfsystem-3 (performance test system subtest-3); SIAS, Social Interaction Anxiety Scale; SPS, Social Phobia Scale; STAI, State-Trait Anxiety Inventory; WCST, *Wisconsin Card Sorting Test*.

TABLE 2 Sociodemographic, psychopathological, and cognitive data of subjects with/without sinusoid-shaped thermal curve during FRT

	Total sample N = 103	No sinusoid N = 23	Sinusoid N = 80	t/χ^2	<i>P</i>
Neutral statement in FRT	23 (22.33%)	5 (21.74%)	18 (22.50%)	<0.01	>.999
Presenting FRT first	52 (50.49%)	12 (52.17%)	40 (50.00%)	<0.01	>.999
Starting at 09:00 AM	56 (54.37%)	9 (39.13%)	47 (58.75%)	2.04	.154
Years of age	24.58 (3.34)	26.16 (3.90)	24.13 (3.03)	2.31	.028
Years of education	16.83 (2.67)	18.24 (2.99)	16.43 (2.46)	2.41	.024
BMI	24.15 (2.97)	24.92 (4.72)	23.92 (2.21)	0.92	.366
LPS-3 (<i>T</i>)	61.52 (5.53)	62.41 (4.24)	61.26 (5.84)	1.04	.302
STAI state	32.41 (5.08)	31.57 (6.27)	32.65 (4.70)	-0.77	.447
STAI trait	32.85 (6.94)	30.17 (7.35)	33.63 (6.66)	-2.03	.051
SPS sum	6.22 (4.51)	4.09 (3.41)	6.84 (4.62)	-3.13	.003
SIAS sum	15.95 (8.05)	12.91 (5.85)	16.83 (8.40)	-2.54	.014
BSI sum (<i>T</i>)	45.81 (9.07)	44.04 (9.48)	46.31 (8.94)	1.02	.313
NEO-Openness	32.20 (6.50)	33.00 (5.90)	31.98 (6.68)	0.71	.481
NEO-Conscientiousness	32.31 (7.21)	33.35 (8.05)	32.01 (6.97)	0.72	.476
NEO-Extraversion	29.21 (6.61)	30.57 (6.40)	28.83 (6.66)	1.14	.262
NEO-Agreeableness	31.21 (6.93)	31.13 (6.77)	31.24 (7.02)	-0.07	.948
NEO-Neuroticism	15.61 (7.45)	14.26 (8.25)	16.00 (7.21)	-0.92	.367
FRT error percentage	42.28 (12.04)	40.22 (12.20)	42.88 (12.01)	-0.92	.362
FRT duration (s)	969.12 (64.88)	951.94 (69.46)	975.79 (62.48)	-1.49	.147
FRT confidence	3.40 (0.52)	3.65 (0.55)	3.33 (0.49)	2.48	.018
WCST error percentage	18.35 (9.43)	16.96 (6.72)	18.75 (10.08)	-1.00	.323
WCST duration (s)	621.15 (161.36)	594.41 (139.00)	636.83 (169.32)	-1.23	.225

Note: Data represent uncorrected means (SD) or N (%). Student's *t* tests or Pearson's *chi*-squared tests for independent comparisons were employed for analyses. *P* values < .05 are indicated in bold.

Abbreviations: BMI, Body Mass Index; FRT, Face Recognition Test; WCST, Wisconsin Card Sorting Test; LPS-3, Leistungsprüfsystem-3 (performance test system subtest-3); STAI, State-Trait Anxiety Inventory; SPS, Social Phobia Scale; SIAS, Social Interaction Anxiety Scale; BSI, Brief Symptom Inventory. Because of the exploratory nature of the study, no *P*-value adjustments were conducted.

continuous decrease followed by a plateau during WCST (Figure 3F). Mean temperature changes over test quartiles as another readout of thermal dynamics were likewise found significantly different, with greater fluctuations in the second half of FRT (quartile \times condition-interaction: $F_{(3,612)} = 30.17$; $P = 2.28 \times 10^{-15}$; Figure 3G). Taken together, these data may point to an association of the sinusoid pattern with the emotional perception of the social task component.

Somewhat surprisingly, salivary cortisol alterations as “classical stress measures” did not differ during FRT and WCST ($t_{(101)} = -0.06$; $P = .952$; Figure 3H). This may question the validity of cortisol measurements for determining the specific stress caused by a social test component which can be sensitively detected by IRT. Nevertheless, cortisol reactivity during FRT correlated mildly positively with the time-adjusted integrals of *Reference Index* during FRT (Pearson correlation coefficient; $r = 0.255$; $P = .026$; Figure 3I), indicating at least a slight “typical” stress reaction during FRT.

Contrary to our expectations, no differences were found upon presentation of negative feedback versus neutral statement during FRT, neither in *Reference Index* curve ratings ($\chi^2_{(1)} < 0.01$; $P > .999$), nor average *Reference Index* curve shape, nor post-feedback temperature dynamics (fluctuations during 3rd and 4th test quartile, repeated-measure ANOVA interaction effect: $F_{(1,101)} = 2.38$; $P = .126$), nor any other variable (two-sided unpaired Student's *t* tests; all $P > .05$). This suggests that the negative feedback did not have any relevant impact on these measures.

4 | DISCUSSION

The present translational study demonstrates that IRT can be applied as a convenient, easy-to-apply, non-invasive technology to sensitively and reliably assess physiological reactivity (“flushing”) in social contexts in humans and mice.

By implementing IRT within the *SocioBox* paradigm, we replicated and extended our previous findings that normal mice are able to easily recognize an unfamiliar stranger out of five stimulus mice. Strikingly, 4 weeks after performing this challenging social cognitive task, mice displayed abnormal social interaction in the Y-maze sociability test, namely distinct social avoidance. This unforeseen “sociophobia” following inescapable exposure to five conspecifics in the relatively narrow environment of the *SocioBox* was robustly reproduced several times in both genders. Control mice in the same narrow box without conspecifics (“empty”) did not acquire this phenotype nor show any appreciable change in their basal anxiety behavior, as evaluated by spatial novelty-induced spontaneous freezing. Importantly, performance in the *SocioBox* as inducer of sociophobia was characterized by a higher overall *Centralization Index*, that is, higher temperature in central compared to peripheral body parts (tail), suggesting an increase in the experienced stress. Eye, body, or tail have previously been reported as stress-responsive IRT zones in mice.⁴ Considering body and tail temperature of mice in IRT simultaneously, as introduced here with the *Centralization Index*, seems to constitute a promising robust measure of autonomous responses/social stress. Interestingly, the *Centralization Index* during *SocioBox* correlated negatively with the time spent with the stranger mouse in the social recognition task as well as the succeeding sociability test, indicating that the degree of stress influences cognitive performance (*SocioBox*) as well as severity of social avoidance (Y-maze). Hence, the *SocioBox* paradigm may serve not only as a superior test of complex social recognition memory,³⁰ but also as a reliable inducer of social avoidance, thereby delivering a novel non-invasive animal model of “sociophobia”.⁵¹ As a consequence, the *SocioBox* test has to be used as a final test in a behavioral battery, similar to fear conditioning.

This unexpectedly strong relation between social cognition testing and IRT readouts in mice raised the obvious translational question whether the addition of a social component to a cognitive task would yield characteristic IRT data also in human individuals that differ from those obtained during a non-social test. In human IRT, thermo-patterns depend strongly on stimuli used and facial ROI targeted.^{9,16,20,29} We focused on the nose because of its high reactivity to social cues.^{9,12,15-17,20} Since the introduction of the *Centralization Index* in mice had proven to be a reproducible, sensitive and widely environment-independent measure, we established a similar readout in human subjects. The *Reference Index*, again providing an “internal” (ie, within-subject) control by relating the responsive facial area (nose) to a rather temperature-stable zone (malar cheek) turned out to be a suitable tool to adjust for sources of IRT readout noise (eg, slight differences in ambient temperature, humidity, camera accuracy).^{9,29}

Indeed, in the translational human study, we saw a characteristic sinusoid-shaped thermal curve with initial decrease

in the majority of test subjects during the social FRT. In contrast, over the course of WCST, as non-social pattern recognition test, this typical curve was widely absent, with the temperature overall decreasing. However, not all participants responded with this characteristic social thermo-pattern, in the following referred to as “non-responders”. Contrasting participants that exhibited the typical sinusoid-shaped thermo-pattern in FRT with the “non-responders” revealed interesting and plausible differences: younger age, less time spent in the educational system, higher scores in social phobia questionnaires (though still within the normal range), and less secure feedback-answers regarding their perceived own performance during FRT. Together, these differing items may point to lower experienced stress,¹⁵ that is, to a more “relaxed attitude” toward social test settings.

Whereas IRT analyses revealed differences between social/non-social tests, salivary cortisol levels, an established standard measure of the hypothalamus-pituitary-adrenal (HPA) stress response, did not. To exclude potential bias due to different starting times of our test sessions (9.00 AM or 11.00 AM), falling into the cortisol diurnal profile/awakening response,⁵²⁻⁵⁴ we employed normalized cortisol changes (*delta* values) between time points of sample collection. Comparing subject groups separated by starting time or order of test presentation (FRT or WCST first) did not reveal differences in *delta* cortisol values. These negative cortisol findings are in agreement with previous investigations on the potential of IRT in physical and social stress paradigms, compared to recognized stress markers.¹⁶ While thermal readouts in various facial regions were sensitive to stress-induced mood changes, conventional stress markers, such as cortisol, were not,¹⁶ suggesting a different origin (less HPA-related, more autonomic/catecholaminergic) and time course (fast versus delayed) of the experienced stress. Taken together, IRT seems to have a higher discriminative power for assessment of social cognition-related stress than cortisol.

Somewhat surprising, the fabricated negative feedback within FRT (“*your performance is below average*”), compared to the neutral statement (“*you may now take a break—second part of test will start automatically*”) did not induce any measurable differences in thermograms. This may be due to a lower than expected socially threatening/embarrassing impact, the shortness of presentation (only 10 s each)¹³ with test-block 2 following immediately thereafter, or doubts of subjects regarding feedback authenticity. Finally, temperature alterations in connection with such ultra-brief negative feedback may belong to different underlying processes.²⁰ Neither nose nor malar cheek may be optimal for exploring respective facial thermo-reactions.

In recent years, the potential of IRT as a valid research tool alongside traditional physiological approaches has been increasingly explored.^{9,15,17} However, IRT did not instantaneously turn out as a straightforward and easy-to-apply

method. IRT is sensitive to numerous interfering factors, arising from environmental (eg, ambient temperature, humidity, room size, radiation) and individual sources (eg, gender, age, amount of brown adipose tissue, physical activity, food or substance intake). Further inconsistencies and reliability problems were caused by suboptimal study design, such as small or heterogeneous samples, artifacts due to manual ROI definition or quantification, or camera signal noise.^{9,29} Many studies did not sufficiently control for these methodological issues, leading to weak internal consistencies.^{9,29}

In the present study, considerable effort was made to limit the impact of such interfering factors. As for the animal part, inbred mice were housed under controlled conditions and tested under standardized settings. In the human part, healthy male individuals with highly comparable sociodemographic characteristics were included. Large enough (N = 45 mice, N = 103 humans) test samples and standardized testing and recording procedures under constant ambient conditions were used as suggested by Fernández-Cuevas and colleagues.²⁹ While various studies analyzed single or short series of images due to technological or memory-storage limitations,⁹ we used relatively long IRT video recordings (5–10 minutes for mice; >15 minutes per human participant and test) with high spatial and temporal resolution, and novel methods of data extraction and analysis. *Centralization Index* and *Reference Index* were introduced here as sensitive and widely environment-independent measures, providing internal (within-subject) control in the assessment of thermo-reactions in social contexts. Automated tracking and preprocessing algorithms delivered examiner-independent, objective and clean data extraction and organization, while imputations, smoothing, and winsorizing of data were conducted to reduce the impact of IRT camera inaccuracy, noise, and missing data.

Recently, IRT has also been employed for subjects diagnosed with mild posttraumatic stress disorder, Alzheimer's disease, or schizophrenia,^{55–57} underlining that psychological/psychiatric research might profit from the contact-free, non-invasive IRT of freely moving and interacting subjects. In fact, deficits in social interaction/cognition of various origins are frequently seen in neuropsychiatry and often difficult to diagnose cross-sectionally. The current study on healthy individuals may stimulate future standardized social interaction testing using IRT in disease states, thereby opening new avenues for differential diagnostic approaches.

To summarize, based on a unique translational IRT study from mouse to man, we suggest that inclusion of a social component in a cognitive task specifically alters local body or face temperature, indicating a defined vascular response to this particular category of stress. These rather clear-cut findings were only possible on the ground of highly standardized and innovative experimental conditions, including IRT videos over an extended period to long-term monitor temperature alterations, unusually large, homogeneous subject

samples, novel measures of internally (within-subject) controlled temperature over time, that is, *Centralization* and *Reference Index* and, finally, novel approaches to data acquisition, preprocessing, and analyses.

ACKNOWLEDGEMENTS

This study was supported by the Max Planck Society and the DFG Research Center for Nanoscale Microscopy and Molecular Physiology of the Brain (CNMPB).

CONFLICT OF INTEREST

The authors declare no competing financial or other interests.

AUTHOR CONTRIBUTIONS

Concept, study design and supervision: HE together with MM & AS. Experimental design and interpretation: JS and FB together with HE & AS. Data acquisition and analysis: JS, FB, MM, SM, AR, DKB, KS, HR, LW, FC, KB, AS & HE. Drafting manuscript: HE together with JS, FB, MM & AS. Drafting display items: JS, FB, MM & HE. All authors read and approved the final version of the manuscript.

DATA AVAILABILITY STATEMENT

Full data availability will be provided. Accession codes will be available before publication.

REFERENCES

1. Darwin CR. *The expression of the emotions in man and animals*. London: John Murray; 1872.
2. Leary MR, Britt TW, Cutlip WD 2nd, Templeton JL. Social blushing. *Psychol Bull*. 1992;112:446–460.
3. Drummond PD. The effect of adrenergic blockade on blushing and facial flushing. *Psychophysiology*. 1997;34:163–168.
4. Gjendal K, Franco NH, Ottesen JL, Sorensen DB, Olsson IAS. Eye, body or tail? Thermography as a measure of stress in mice. *Physiol Behav*. 2018;196:135–143.
5. Meyer CW, Ootsuka Y, Romanovsky AA. Body temperature measurements for metabolic phenotyping in mice. *Front Physiol*. 2017;8:520.
6. Mufford JT, Paetkau MJ, Flood NJ, Regev-Shoshani G, Miller CC, Church JS. The development of a non-invasive behavioral model of thermal heat stress in laboratory mice (*Mus musculus*). *J Neurosci Methods*. 2016;268:189–195.
7. Herborn KA, Jerem P, Nager RG, McKeegan DEF, McCafferty DJ. Surface temperature elevated by chronic and intermittent stress. *Physiol Behav*. 2018;191:47–55.
8. Vianna DM, Carrive P. Changes in cutaneous and body temperature during and after conditioned fear to context in the rat. *Eur J Neurosci*. 2005;21:2505–2512.
9. Ioannou S, Gallese V, Merla A. Thermal infrared imaging in psychophysiology: potentialities and limits. *Psychophysiology*. 2014;51:951–963.
10. Drummond PD. Facial flushing during provocation in women. *Psychophysiology*. 1999;36:325–332.
11. Drummond PD, Su D. The relationship between blushing propensity, social anxiety and facial blood flow during embarrassment. *Cogn Emot*. 2012;26:561–567.

12. Esposito G, Nakazawa J, Ogawa S, et al. Baby, you light-up my face: culture-general physiological responses to infants and culture-specific cognitive judgements of adults. *PLoS ONE*. 2014;9:e106705.
13. Kistler A, Mariauzouls C, von Berlepsch K. Fingertip temperature as an indicator for sympathetic responses. *Int J Psychophysiol*. 1998;29:35-41.
14. Yoshihara K, Tanabe HC, Kawamichi H, et al. Neural correlates of fear-induced sympathetic response associated with the peripheral temperature change rate. *NeuroImage*. 2016;134:522-531.
15. Cardone D, Merla A. New Frontiers for Applications of Thermal Infrared Imaging Devices: Computational Psychophysiology in the Neurosciences. *Sensors (Basel)* 2017;17:E1042.
16. Engert V, Merla A, Grant JA, Cardone D, Tusche A, Singer T. Exploring the use of thermal infrared imaging in human stress research. *PLoS ONE*. 2014;9(3):e90782.
17. Kosonogov V, De Zorzi L, Honore J, et al. Facial thermal variations: a new marker of emotional arousal. *PLoS ONE*. 2017;12:e0183592.
18. Ermatinger FA, Brugger RK, Burkart JM. The use of infrared thermography to investigate emotions in common marmosets. *Physiol Behav*. 2019;211:112672.
19. Lahiri BB, Bagavathiappan S, Jayakumar T, Philip J. Medical applications of infrared thermography: a review. *Infrared Phys Technol*. 2012;55:221-235.
20. Ioannou S, Morris PH, Baker M, Reddy V, Gallese V. Seeing a blush on the visible and invisible spectrum: a functional thermal infrared imaging study. *Front Hum Neurosci*. 2017;11:525.
21. Ring EF, Ammer K. Infrared thermal imaging in medicine. *Physiol Meas*. 2012;33:R33- R46.
22. Garbey M, Sun N, Merla A, Pavlidis I. Contact-free measurement of cardiac pulse based on the analysis of thermal imagery. *IEEE Trans Biomed Eng*. 2007;54:1418-1426.
23. Murthy R, Pavlidis I. Noncontact measurement of breathing function. *IEEE Eng Med Biol Mag*. 2006;25:57-67.
24. Merla A, Di Donato L, Romani GL, Proietti M, Salsano F. Comparison of thermal infrared and laser doppler imaging in the assessment of cutaneous tissue perfusion in scleroderma patients and healthy controls. *Int J Immunopathol Pharmacol*. 2008;21:679-686.
25. Pavlidis I, Tsiamirtzis P, Shastri D, et al. Fast by nature - how stress patterns define human experience and performance in dexterous tasks. *Sci Rep*. 2012;2.
26. Krzywicki AT, Berntson GG, O'Kane BL. A non-contact technique for measuring eccrine sweat gland activity using passive thermal imaging. *Int J Psychophysiol*. 2014;94:25-34.
27. Jarlier S, Grandjean D, Delplanque S, et al. Thermal Analysis of Facial Muscles Contractions. *IEEE Transactions on Affective Computing*. 2011;2:2-9.
28. Salazar-Lopez E, Dominguez E, Juarez Ramos V, et al. The mental and subjective skin: Emotion, empathy, feelings and thermography. *Conscious Cogn*. 2015;34:149-162.
29. Fernández-Cuevas I, Bouzas Marins JC, Arnáiz Lastras J, et al. Classification of factors influencing the use of infrared thermography in humans: A review. *Infrared Phys Technol*. 2015;71:28-55.
30. Krueger-Burg D, Winkler D, Mitkovski M, et al. The sociobox: a novel paradigm to assess complex social recognition in male mice. *Front Behav Neurosci*. 2016;10:151.
31. Brimberg L, Mader S, Jeganathan V, et al. Caspr2-reactive antibody cloned from a mother of an ASD child mediates an ASD-like phenotype in mice. *Mol Psychiatry*. 2016;21:1663-1671.
32. Sommer C, Straehle C, Kothe U, Hamprecht FA. Ilastik: Interactive learning and segmentation toolkit. *IEEE*. 2011;230-233.
33. Schindelin J, Arganda-Carreras I, Frise E, et al. Fiji: an open-source platform for biological-image analysis. *Nat Methods*. 2012;9:676-682.
34. Tinevez JY, Perry N, Schindelin J, et al. TrackMate: An open and extensible platform for single-particle tracking. *Methods*. 2017;115:80-90.
35. Wilcox RR. Winsorized Robust Measures. 2017; 1-2.
36. R Core Team. *R: A language and environment for statistical computing*. Vienna: R Foundation for Statistical Computing; 2018.
37. Franke GH. *BSI - Brief Symptom Inventory - deutsche Fassung*. Göttingen: Beltz; 2000.
38. von Consbruch K, Stangier U, Heidenreich T. *Skalen zur Sozialen Angststörung (SOZAS)*. Göttingen: Hogrefe; 2016.
39. Borkenau P, Ostendorf F. *NEO-Fünf-Faktoren Inventar (NEO-FFI) nach Costa und McCrae*. Göttingen: Hogrefe; 1993.
40. Grimm J. State-Trait Anxiety Inventory nach Spielberger. Deutsche Lang- und Kurzversion: Methodenforum der Universität Wien; 2009.
41. Heaton KH, Chelune GJ, Talley JL, Kay G, Curtiss G. *Wisconsin Card Sorting Test: computer version 4 (WCST: CV4) research edn*. San Antonio, TX: Harcourt Assessment; 2003.
42. Duchaine BC, Weidenfeld A. An evaluation of two commonly used tests of unfamiliar face recognition. *Neuropsychologia*. 2003;41:713-720.
43. Herzmann G, Danthiir V, Schacht A, Sommer W, Wilhelm O. Toward a comprehensive test battery for face cognition: Assessment of the tasks. *Behav Res Methods*. 2008;40:840-857.
44. Warrington EK. *Recognition memory test: Manual*. Berkshire, UK: NFER-Nelson; 1984.
45. Peirce JW. PsychoPy—Psychophysics software in Python. *J Neurosci Methods*. 2007;162:8-13.
46. Van Rossum G. Python 2.7.10 Language Reference. Samurai Media Limited; 2015.
47. Kulke L, Janßen L, Demel R, Schacht A. Validating the Goettingen Faces Database. Open Science Framework; 2017.
48. Horn W. *L-P-S Leistungsprüfsystem*. Göttingen: Hogrefe; 1983.
49. Mathis A, Mamidanna P, Cury KM, et al. DeepLabCut: markerless pose estimation of user-defined body parts with deep learning. *Nat Neurosci*. 2018;21:1281-1289.
50. Lai WS, Johnston RE. Individual recognition after fighting by golden hamsters: a new method. *Physiol Behav*. 2002;76:225-239.
51. Toth I, Neumann ID. Animal models of social avoidance and social fear. *Cell Tissue Res*. 2013;354:107-118.
52. Boehringer A, Tost H, Haddad L, et al. Neural correlates of the cortisol awakening response in humans. *Neuropsychopharmacology*. 2015;40:2278-2285.
53. Fries E, Dettenborn L, Kirschbaum C. The cortisol awakening response (CAR): facts and future directions. *Int J Psychophysiol*. 2009;72:67-73.
54. Clow A, Hucklebridge F, Stalder T, Evans P, Thorn L. The cortisol awakening response: More than a measure of HPA axis function. *Neurosci Biobehav Rev*. 2010;35:97-103.
55. Jian BL, Chen CL, Chu WL, Huang MW. The facial expression of schizophrenic patients applied with infrared thermal facial image sequence. *BMC Psychiatry*. 2017;17:229.
56. Di Giacinto A, Brunetti M, Sepede G, Ferretti A, Merla A. Thermal signature of fear conditioning in mild post traumatic stress disorder. *Neuroscience*. 2014;266:216-223.

57. Perpetuini D, Cardone D, Chiarelli AM, et al. Autonomic impairment in Alzheimer's disease is revealed by complexity analysis of functional thermal imaging signals during cognitive tasks. *Physiol Meas*. 2019;40:034002.

SUPPORTING INFORMATION

Additional supporting information may be found online in the Supporting Information section.

How to cite this article: Seidel J, Bockhop F, Mitkovski M, et al. Vascular response to social cognitive performance measured by infrared thermography: A translational study from mouse to man. *FASEB BioAdvances*. 2020;2:18–32. <https://doi.org/10.1096/fba.2019-00085>

5 SUMMARY AND CONCLUSIONS

As discussed and reported, we found strong associations between the amount of defined adverse environmental risk factors experienced before adulthood and violent aggression in patients suffering from schizophrenia. Environmental risk accumulation is further linked to aggression severity scores in two general population samples. Moreover, while we could not find epigenome-wide differences in DNA methylation, an examination of *HDAC1* mRNA expression levels revealed significant group differences in relation to environmental risk load (high versus low). These results explicitly suggest that an accumulation of negative environmental experiences during childhood and adolescence has a substantial influence on aggression, which may be even more relevant with respect to the exhibition of aggressive behavior than a person's mental condition.

It is important to note that we do not report a direct, causal relation between these risk factors and aggression; neither living in a large city, migrating to another country, nor consuming cannabis once in life will transform anybody into a threat to others. However, these factors constitute valid predictors in the complex interplay of genetics and environmental experiences, with the ultimate outcome of aggressive phenotypes. Against this backdrop, the reported model lets us predict the likelihood of aggressive behavior manifestation and makes the identification of individuals at risk possible. Some of the reported risk factors are easily avoidable, such as consumption of certain substances, whereas negative effects of others may be possible to mitigate.

Future research should aim to replicate our findings and extend them to different contexts. It is yet not clear whether our model's large effects are specific to aggression phenotypes or if it has more general implications. Possibly, there are other, equally or even more important, factors not included in our current model. Similarly, some of the identified risk factors could be characterized more clearly, to improve its accuracy even further. For instance, concerning the risk factor *Migration*, our model does not distinguish between individuals seeking refuge and those who migrated due to educational or occupational

reasons. Likewise, it might be beneficial to differentiate the risk factor *Lifetime cannabis consumption* further with respect to the severity of consumption or used cannabis type (Schoeler et al., 2016). However, the standard model revealed already large and solid effects over all examined groups.

Notably, model modifications for more specific research questions seem to be feasible and can easily be achieved. Currently, we are working on modifications of the standard model in order to apply it in different contexts. For example, we investigate the relationship between environmental risk and psychopathology in a group of young asylum seekers. In this approach, the standard model is modified to take the special, detrimental experiences commonly reported by persons fleeing their countries due to war or expulsion, into account. Within a second project, we assess the relationship of our model with the consumption of multiple illicit drugs (i.e., polytoxicomania). In both cases, the model of accumulated environmental risk exhibits promising results (*in preparation*).

Our work on the utilization of infrared thermography (IRT), on the other hand, resulted not only in the development of a new model of social avoidance ('social phobia') in mice but also improved our knowledge about the potentials of IRT recordings in both animal and human experiments. By introducing new thermal readouts as well as innovative routines of automated data acquisition, processing, and analysis we were able to deepen our insight into socially-induced temperature alterations over longer time periods. In this context, the many confounders that can undermine the reliability of thermal assessments have been considerably taken into account. The number of studies employing IRT in psychophysiological or neuroscientific context is growing fast, rendering reliable and state-of-the-art recording and quantification techniques more and more important.

IRT offers great prospects for research and applications, in particular when the usage of other measurement techniques is limited. This involves, besides others, settings where assessed individuals are not able to act in accordance with application protocols of other techniques or are not willing to cooperate. In such situations, IRT can increase our range of possibilities, due to its contact-free and non-invasive application mode.

In particular, physiological research involving patients suffering from mental conditions can benefit greatly from IRT research. As shown by several recent studies, IRT can be successfully utilized in experiments with patient groups (Di Giacinto et al., 2014; Jian et al., 2017; Perpetuini et al., 2019). Additionally, IRT may prove itself to be a valuable supporting tool in diagnostical approaches of different psychiatric conditions exhibiting similar phenotypes. IRT may detect distinct thermal patterns and enable a more reliable discrimination of patients in regard to psychiatric diseases as well as individuals from the general population. Accordingly, IRT can potentially be used in therapeutical contexts, for example as a contact-free, more flexible measure of physiological states during the treatment of disorders that are associated with stress and arousal.

Taken together, this work aimed at improving our knowledge on behavioral and autonomous reactions to stressful experiences. The robust findings we reported along with our methodological suggestions have implications both for research and society.

BIBLIOGRAPHY

- Agid, O., Kohn, Y., & Lerer, B. (2000). Environmental stress and psychiatric illness. *Biomedicine & Pharmacotherapy*, *54*(3), 135-141. doi: 10.1016/s0753-3322(00)89046-0
- Aguilera, G. (2011). Hpa axis responsiveness to stress: implications for healthy aging. *Experimental Gerontology*, *46*(2-3), 90-5. doi: 10.1016/j.exger.2010.08.023
- Alpar, O., & Krejcar, O. (2017). Quantization and equalization of pseudocolor images in hand thermography. In I. Rojas & F. Ortuño (Eds.), *Bioinformatics and biomedical engineering* (pp. 397–407). Cham: Springer International Publishing.
- Begemann, M., Grube, S., Papiol, S., Malzahn, D., Krampe, H., Ribbe, K., ... Ehrenreich, H. (2010). Modification of cognitive performance in schizophrenia by complexin 2 gene polymorphisms. *Archives Of General Psychiatry*, *67*(9), 879-88. doi: 10.1001/archgenpsychiatry.2010.107
- Belbasis, L., Kohler, C. A., Stefanis, N., Stubbs, B., van Os, J., Vieta, E., ... Evangelou, E. (2018). Risk factors and peripheral biomarkers for schizophrenia spectrum disorders: an umbrella review of meta-analyses. *Acta Psychiatrica Scandinavica*, *137*(2), 88-97. doi: 10.1111/acps.12847
- Benus, R. F., Koolhaas, J. M., & van Oortmerssen, G. A. (1992). Individual strategies of aggressive and non-aggressive male mice in encounters with trained aggressive residents. *Animal Behaviour*, *43*(4), 531-540. doi: 10.1016/s0003-3472(05)81013-9
- Bhatnagar, S., Vining, C., Iyer, V., & Kinni, V. (2006). Changes in hypothalamic-pituitary-adrenal function, body temperature, body weight and food intake with repeated social stress exposure in rats. *Journal of Neuroendocrinology*, *18*(1), 13-24. doi: 10.1111/j.1365-2826.2005.01375.x
- American Psychological Association. (2013). *Diagnostic and statistical manual of mental disorders* (5th Revised ed.). Washington, DC: Author.
- Schizophrenia Working Group of the Psychiatric Genomics Consortium. (2014). Biological insights from 108 schizophrenia-associated genetic loci. *Nature*, *511*(7510), 421-7. doi: 10.1038/nature13595
- Björkqvist, K. (2018). Gender differences in aggression. *Current Opinion in Psychology*, *19*, 39-42. doi: 10.1016/j.copsyc.2017.03.030

- Blair, R. J. (2016). The neurobiology of impulsive aggression. *Journal of Child and Adolescent Psychopharmacology*, 26(1), 4-9. doi: 10.1089/cap.2015.0088
- Boehringer, A., Tost, H., Haddad, L., Lederbogen, F., Wust, S., Schwarz, E., & Meyer-Lindenberg, A. (2015). Neural correlates of the cortisol awakening response in humans. *Neuropsychopharmacology*, 40(9), 2278-85. doi: 10.1038/npp.2015.77
- Brimberg, L., Mader, S., Jeganathan, V., Berlin, R., Coleman, T. R., Gregersen, P. K., ... Diamond, B. (2016). Caspr2-reactive antibody cloned from a mother of an asd child mediates an asd-like phenotype in mice. *Molecular Psychiatry*, 21(12), 1663-1671. doi: 10.1038/mp.2016.165
- Brown, A. S. (2011). The environment and susceptibility to schizophrenia. *Progress in Neurobiology*, 93(1), 23-58. doi: 10.1016/j.pneurobio.2010.09.003
- Brunner, H. G., Nelen, M., Breakefield, X. O., Ropers, H. H., & van Oost, B. A. (1993). Abnormal behavior associated with a point mutation in the structural gene for monoamine oxidase a. *Science*, 262(5133), 578-80. doi: 10.1126/science.8211186
- Byrd, A. L., & Manuck, S. B. (2014). Maa, childhood maltreatment, and antisocial behavior: meta-analysis of a gene-environment interaction. *Biological Psychiatry*, 75(1), 9-17. doi: 10.1016/j.biopsych.2013.05.004
- Cardone, D., & Merla, A. (2017). New frontiers for applications of thermal infrared imaging devices: Computational psychophysiology in the neurosciences. *Sensors*, 17(5). doi: 10.3390/s17051042
- Cardone, D., Pinti, P., & Merla, A. (2015). Thermal infrared imaging-based computational psychophysiology for psychometrics. *Computational and Mathematical Methods in Medicine*, 2015, 984353. doi: 10.1155/2015/984353
- Caspi, A., McClay, J., Moffitt, T. E., Mill, J., Martin, J., Craig, I. W., ... Poulton, R. (2002). Role of genotype in the cycle of violence in maltreated children. *Science*, 297(5582), 851-4. doi: 10.1126/science.1072290
- Darwin, C. R. (1872). *The expression of the emotions in man and animals*. London: John Murray.
- de Boer, S. F. (2018). Animal models of excessive aggression: implications for human aggression and violence. *Current Opinion in Psychology*, 19, 81-87. doi: 10.1016/j.copsyc.2017.04.006
- Di Giacinto, A., Brunetti, M., Sepede, G., Ferretti, A., & Merla, A. (2014). Thermal signature

- of fear conditioning in mild post traumatic stress disorder. *Neuroscience*, 266, 216-23. doi: 10.1016/j.neuroscience.2014.02.009
- Drummond, P. D. (1999). Facial flushing during provocation in women. *Psychophysiology*, 36(3), 325-32. doi: 10.1017/s0048577299980344
- Drummond, P. D., & Su, D. (2012). The relationship between blushing propensity, social anxiety and facial blood flow during embarrassment. *Cognition & Emotion*, 26(3), 561-567. doi: 10.1080/02699931.2011.595775
- Engert, V., Merla, A., Grant, J. A., Cardone, D., Tusche, A., & Singer, T. (2014). Exploring the use of thermal infrared imaging in human stress research. *Plos One*, 9(3). doi: 10.1371/journal.pone.0090782
- Ermatinger, F. A., Brugger, R. K., & Burkart, J. M. (2019). The use of infrared thermography to investigate emotions in common marmosets. *Physiology & Behavior*, 211, 112672. doi: 10.1016/j.physbeh.2019.112672
- Fazel, S., Gulati, G., Linsell, L., Geddes, J. R., & Grann, M. (2009). Schizophrenia and violence: systematic review and meta-analysis. *PLOS Medicine*, 6(8), e1000120. doi: 10.1371/journal.pmed.1000120
- Fernández-Cuevas, I., Bouzas Marins, J. C., Arnáiz Lastras, J., Gómez Carmona, P. M., Piñonosa Cano, S., García-Concepción, M. n., & Sillero-Quintana, M. (2015). Classification of factors influencing the use of infrared thermography in humans: A review. *Infrared Physics & Technology*, 71, 28-55. doi: 10.1016/j.infrared.2015.02.007
- Gjendal, K., Franco, N. H., Ottesen, J. L., Sorensen, D. B., & Olsson, I. A. S. (2018). Eye, body or tail? thermography as a measure of stress in mice. *Physiology & Behavior*, 196, 135-143. doi: 10.1016/j.physbeh.2018.08.022
- Harro, J. (2018). Animals, anxiety, and anxiety disorders: How to measure anxiety in rodents and why. *Behavioural Brain Research*, 352, 81-93. doi: 10.1016/j.bbr.2017.10.016
- Heaton, K., Chelune, G., Talley, J., Kay, G., & Curtiss, G. (2003). *Wisconsin card sorting test: computer version 4 (wcst: Cv4) research edition*. San Antonio, TX: Harcourt Assessment.
- Hellhammer, D. H., Wust, S., & Kudielka, B. M. (2009). Salivary cortisol as a biomarker in stress research. *Psychoneuroendocrinology*, 34(2), 163-71. doi: 10.1016/j.psyneuen.2008.10.026

- Herborn, K. A., Jerem, P., Nager, R. G., McKeegan, D. E. F., & McCafferty, D. J. (2018). Surface temperature elevated by chronic and intermittent stress. *Physiology & Behavior*, *191*, 47-55. doi: 10.1016/j.physbeh.2018.04.004
- Herschel, W. (1800). Experiments on the refrangibility of the invisible rays of the sun. *Philosophical Transactions of the Royal Society of London*, *90*, 284-292. doi: 10.1098/rstl.1800.0015
- Hollon, N. G., Burgeno, L. M., & Phillips, P. E. (2015). Stress effects on the neural substrates of motivated behavior. *Nature Neuroscience*, *18*(10), 1405-12. doi: 10.1038/nn.4114
- Howes, O. D., & Murray, R. M. (2014). Schizophrenia: an integrated sociodevelopmental-cognitive model. *The Lancet*, *383*(9929), 1677-1687. doi: 10.1016/s0140-6736(13)62036-x
- Ioannou, S., Gallese, V., & Merla, A. (2014). Thermal infrared imaging in psychophysiology: potentialities and limits. *Psychophysiology*, *51*(10), 951-63. doi: 10.1111/psyp.12243
- Ioannou, S., Morris, P. H., Baker, M., Reddy, V., & Gallese, V. (2017). Seeing a blush on the visible and invisible spectrum: A functional thermal infrared imaging study. *Frontiers in Human Neuroscience*, *11*, 525. doi: 10.3389/fnhum.2017.00525
- Jarlier, S., Grandjean, D., Delplanque, S., N'Diaye, K., Cayeux, I., Velazco, M. I., ... Scherer, K. R. (2011). Thermal analysis of facial muscles contractions. *Ieee Transactions on Affective Computing*, *2*(1), 2-9. doi: 10.1109/T-Affc.2011.3
- Jian, B. L., Chen, C. L., Chu, W. L., & Huang, M. W. (2017). The facial expression of schizophrenic patients applied with infrared thermal facial image sequence. *BMC Psychiatry*, *17*(1), 229. doi: 10.1186/s12888-017-1387-y
- Joseph, D. N., & Whirledge, S. (2017). Stress and the hpa axis: Balancing homeostasis and fertility. *International Journal of Molecular Sciences*, *18*(10). doi: 10.3390/ijms18102224
- Juruena, M. F. (2014). Early-life stress and hpa axis trigger recurrent adulthood depression. *Epilepsy & Behavior*, *38*, 148-59. doi: 10.1016/j.yebeh.2013.10.020
- Keeney, A. J., Hogg, S., & Marsden, C. A. (2001). Alterations in core body temperature, locomotor activity, and corticosterone following acute and repeated social defeat of male nmri mice. *Physiology & Behavior*, *74*(1-2), 177-184. doi: 10.1016/s0031-9384(01)00541-8
- Kim-Cohen, J., Caspi, A., Taylor, A., Williams, B., Newcombe, R., Craig, I. W., & Moffitt, T. E. (2006). Maa, maltreatment, and gene-environment interaction predicting

- children's mental health: new evidence and a meta-analysis. *Molecular Psychiatry*, 11(10), 903-913. doi: 10.1038/sj.mp.4001851
- Kistler, A., Mariauzouls, C., Kuhr, C., Simmen, D., Maranta, C. A., Stratil, J., ... Suter, B. (1996). Acute sympathetic responses elicited by acupuncture are pain-related and non-specific. *Complementary Medicine Research*, 3(6), 269-278. doi: 10.1159/000210242
- Kistler, A., Mariauzouls, C., & von Berlepsch, K. (1998a). Fingertip temperature as an indicator for sympathetic responses. *International Journal of Psychophysiology*, 29(1), 35-41. doi: 10.1016/s0167-8760(97)00087-1
- Kistler, A., Mariauzouls, C., & von Berlepsch, K. (1998b). Saliva collection with salivettes® is a sympathetic stimulus. *Complementary Medicine Research*, 5, 12-17.
- Knapp, M., Mangalore, R., & Simon, J. (2004). The global costs of schizophrenia. *Schizophrenia Bulletin*, 30(2), 279-93. doi: 10.1093/oxfordjournals.schbul.a007078
- Kosonogov, V., De Zorzi, L., Honore, J., Martinez-Velazquez, E. S., Nandrino, J. L., Martinez-Selva, J. M., & Sequeira, H. (2017). Facial thermal variations: A new marker of emotional arousal. *Plos One*, 12(9). doi: 10.1371/journal.pone.0183592
- Krueger-Burg, D., Winkler, D., Mitkovski, M., Daher, F., Ronnenberg, A., Schluter, O. M., ... Ehrenreich, H. (2016). The sociobox: A novel paradigm to assess complex social recognition in male mice. *Frontiers in Behavioral Neuroscience*, 10, 151. doi: 10.3389/fnbeh.2016.00151
- Kulke, L., Janßen, L., Demel, R., & Schacht, A. (2017). Validating the goettingen faces database. *Open Science Framework*. doi: 10.17605/OSF.IO/4KNPF
- Lahiri, B. B., Bagavathiappan, S., Jayakumar, T., & Philip, J. (2012). Medical applications of infrared thermography: A review. *Infrared Physics & Technology*, 55(4), 221-235. doi: 10.1016/j.infrared.2012.03.007
- Lai, W. S., & Johnston, R. E. (2002). Individual recognition after fighting by golden hamsters: a new method. *Physiology & Behavior*, 76(2), 225-39. doi: 10.1016/s0031-9384(02)00721-7
- Martinez, R. C., Carvalho-Netto, E. F., Amaral, V. C., Nunes-de Souza, R. L., & Canteras, N. S. (2008). Investigation of the hypothalamic defensive system in the mouse. *Behavioural Brain Research*, 192(2), 185-90. doi: 10.1016/j.bbr.2008.03.042
- McEwen, B. S. (2007). Physiology and neurobiology of stress and adaptation: central role of the brain. *Physiological Reviews*, 87(3), 873-904. doi: 10.1152/physrev.00041.2006

- Meyer, C. W., Ootsuka, Y., & Romanovsky, A. A. (2017). Body temperature measurements for metabolic phenotyping in mice. *Frontiers in Physiology, 8*, 520. doi: 10.3389/fphys.2017.00520
- Mick, E., McGough, J., Deutsch, C. K., Frazier, J. A., Kennedy, D., & Goldberg, R. J. (2014). Genome-wide association study of proneness to anger. *PLoS One, 9*(1), e87257. doi: 10.1371/journal.pone.0087257
- Miczek, K. A., Fish, E. W., De Bold, J. F., & De Almeida, R. M. (2002). Social and neural determinants of aggressive behavior: pharmacotherapeutic targets at serotonin, dopamine and gamma-aminobutyric acid systems. *Psychopharmacology, 163*(3-4), 434-58. doi: 10.1007/s00213-002-1139-6
- Moline, A., Galvez-Garcia, G., Fernandez-Gomez, J., De la Fuente, J., Iborra, O., Tornay, F., ... Gomez Milan, E. (2017). The pinocchio effect and the cold stress test: Lies and thermography. *Psychophysiology, 54*(11), 1621-1631. doi: 10.1111/psyp.12956
- Mufford, J. T., Paetkau, M. J., Flood, N. J., Regev-Shoshani, G., Miller, C. C., & Church, J. S. (2016). The development of a non-invasive behavioral model of thermal heat stress in laboratory mice (*mus musculus*). *Journal of Neuroscience Methods, 268*, 189-95. doi: 10.1016/j.jneumeth.2015.12.011
- Nelson, R. J., & Trainor, B. C. (2007). Neural mechanisms of aggression. *Nature Reviews Neuroscience, 8*(7), 536-46. doi: 10.1038/nrn2174
- Palumbo, S., Mariotti, V., Iofrida, C., & Pellegrini, S. (2018). Genes and aggressive behavior: Epigenetic mechanisms underlying individual susceptibility to aversive environments. *Frontiers in Behavioral Neuroscience, 12*, 117. doi: 10.3389/fnbeh.2018.00117
- Perpetuini, D., Cardone, D., Chiarelli, A. M., Filippini, C., Croce, P., Zappasodi, F., ... Merla, A. (2019). Autonomic impairment in alzheimer's disease is revealed by complexity analysis of functional thermal imaging signals during cognitive tasks. *Physiological Measurement, 40*(3), 034002. doi: 10.1088/1361-6579/ab057d
- Piazza, P. V., & Le Moal, M. (1998). The role of stress in drug self-administration. *Trends in Pharmacological Sciences, 19*(2), 67-74. doi: 10.1016/s0165-6147(97)01115-2
- Raine, A. (2002). Biosocial studies of antisocial and violent behavior in children and adults: a review. *Journal of Abnormal Child Psychology, 30*(4), 311-26. doi: 10.1023/a:1015754122318

- Ribbe, K., Friedrichs, H., Begemann, M., Grube, S., Papiol, S., Kastner, A., ... Ehrenreich, H. (2010). The cross-sectional gras sample: a comprehensive phenotypical data collection of schizophrenic patients. *BMC Psychiatry, 10*, 91. doi: 10.1186/1471-244X-10-91
- Ring, E. F. (2010). Thermal imaging today and its relevance to diabetes. *Journal of Diabetes Science and Technology, 4*(4), 857-62. doi: 10.1177/193229681000400414
- Ring, E. F., & Ammer, K. (2012). Infrared thermal imaging in medicine. *Physiological Measurement, 33*(3), R33-46. doi: 10.1088/0967-3334/33/3/R33
- Rogalski, A. (2002). Infrared detectors: an overview. *Infrared Physics & Technology, 43*(3-5), 187-210. doi: 10.1016/s1350-4495(02)00140-8
- Rogalski, A. (2012). History of infrared detectors. *Opto-Electronics Review, 20*(3), 279-308. doi: 10.2478/s11772-012-0037-7
- Sariaslan, A., Lichtenstein, P., Larsson, H., & Fazel, S. (2016). Triggers for violent criminality in patients with psychotic disorders. *JAMA Psychiatry, 73*(8), 796-803. doi: 10.1001/jamapsychiatry.2016.1349
- Schoeler, T., Petros, N., Di Forti, M., Klamerus, E., Foglia, E., Ajnakina, O., ... Bhat-tacharyya, S. (2016). Effects of continuation, frequency, and type of cannabis use on relapse in the first 2 years after onset of psychosis: an observational study. *The Lancet Psychiatry, 3*(10), 947-953. doi: 10.1016/s2215-0366(16)30188-2
- Smith, S. M., & Vale, W. W. (2006). The role of the hypothalamic-pituitary-adrenal axis in neuroendocrine responses to stress. *Dialogues in Clinical Neuroscience, 8*(4), 383-95.
- Stepniak, B., Papiol, S., Hammer, C., Ramin, A., Everts, S., Hennig, L., ... Ehrenreich, H. (2014). Accumulated environmental risk determining age at schizophrenia onset: a deep phenotyping-based study. *The Lancet Psychiatry, 1*(6), 444-453. doi: 10.1016/s2215-0366(14)70379-7
- Österman, K., Björkqvist, K., Lagerspetz, K. M. J., Kaukiainen, A., Landau, S. F., Frączek, A., & Caprara, G. V. (1998). Cross-cultural evidence of female indirect aggression. *Aggressive Behavior, 24*(1), 1-8. doi: 10.1002/(sici)1098-2337(1998)24:1<1::aid-ab1>3.0.co;2-r
- Tattersall, G. J. (2016). Infrared thermography: A non-invasive window into thermal physiology. *Comparative Biochemistry and Physiology Part A: Molecular & Integrative Physiology, 202*, 78-98. doi: 10.1016/j.cbpa.2016.02.022

- Tiihonen, J., Rautiainen, M. R., Ollila, H. M., Repo-Tiihonen, E., Virkkunen, M., Palotie, A., ... Paunio, T. (2015). Genetic background of extreme violent behavior. *Molecular Psychiatry*, *20*(6), 786-92. doi: 10.1038/mp.2014.130
- Toth, I., & Neumann, I. D. (2013). Animal models of social avoidance and social fear. *Cell and Tissue Research*, *354*(1), 107-18. doi: 10.1007/s00441-013-1636-4
- Ulrich-Lai, Y. M., & Herman, J. P. (2009). Neural regulation of endocrine and autonomic stress responses. *Nature Reviews Neuroscience*, *10*(6), 397-409. doi: 10.1038/nrn2647
- Usamentiaga, R., Venegas, P., Guerediaga, J., Vega, L., Molleda, J., & Bulnes, F. G. (2014). Infrared thermography for temperature measurement and non-destructive testing. *Sensors*, *14*(7), 12305-48. doi: 10.3390/s140712305
- van Os, J., & Kapur, S. (2009). Schizophrenia. *The Lancet*, *374*(9690), 635-645. doi: 10.1016/s0140-6736(09)60995-8
- Veroude, K., Zhang-James, Y., Fernandez-Castillo, N., Bakker, M. J., Cormand, B., & Faraone, S. V. (2016). Genetics of aggressive behavior: An overview. *American Journal of Medical Genetics Part B: Neuropsychiatric Genetics*, *171B*(1), 3-43. doi: 10.1002/ajmg.b.32364
- Vianna, D. M., & Carrive, P. (2005). Changes in cutaneous and body temperature during and after conditioned fear to context in the rat. *European Journal of Neuroscience*, *21*(9), 2505-12. doi: 10.1111/j.1460-9568.2005.04073.x
- Waltes, R., Chiocchetti, A. G., & Freitag, C. M. (2016). The neurobiological basis of human aggression: A review on genetic and epigenetic mechanisms. *American Journal of Medical Genetics Part B: Neuropsychiatric Genetics*, *171*(5), 650-75. doi: 10.1002/ajmg.b.32388
- Won, E., & Kim, Y.-K. (2016). Stress, the autonomic nervous system, and the immune-kynurenine pathway in the etiology of depression. *Current Neuropharmacology*, *14*(7), 665-673. doi: 10.2174/1570159x14666151208113006
- Yaribeygi, H., Panahi, Y., Sahraei, H., Johnston, T. P., & Sahebkar, A. (2017). The impact of stress on body function: A review. *EXCLI Journal*, *16*, 1057-1072. doi: 10.17179/excli2017-480
- Yoshihara, K., Tanabe, H. C., Kawamichi, H., Koike, T., Yamazaki, M., Sudo, N., & Sadato, N. (2016). Neural correlates of fear-induced sympathetic response associated with the peripheral temperature change rate. *Neuroimage*, *134*, 522-531.

A APPENDIX

A.1 Accepted co-authorships

Co-author publication I

Ursini, G., Punzi, G., Chen, Q., Marengo, S., Robinson, J. F., Porcelli, A., Hamilton, E. G., Mitjans, M., Maddalena, G., Begemann, M., **Seidel, J.**, Yanamori, H., Jaffe, A. E., Berman, K. F., Egan, M. F., Straub, R. E., Colantuoni, C., Blasi, G., Hashimoto, R., Rujescu, D., Ehrenreich, H., Bertolino, A., Weinberger, D. R. (2018). Convergence of placenta biology and genetic risk for schizophrenia. *Nature Medicine* 24, 792-801.

Personal contribution:

I derived required phenotypical information of schizophrenia patients from the GRAS database to be used as an independent analysis sample. Further, I read and corrected the final version of the manuscript.

Co-author publication II

Pan, H.*, Oliveira, B.*, Saher, G.*, Dere, E., Tapken, D., Mitjans, M., **Seidel, J.**, Wesolowski, J., Wakhloo, D., Klein-Schmidt, C., Ronnenberg, A., Schwabe, K., Trippe, R., Mätz-Rensing, K., Berghoff, S., Al-Krinawe, Y., Martens, H., Begemann, M., Stöcker, W., Kaup, F. J., Mischke, R., Boretius, S., Nave, K. A., Krauss, J. K., Hollmann, M., Lühder, F., Ehrenreich, H. (2019). Uncoupling the widespread occurrence of anti-NMDAR1 autoantibodies from neuropsychiatric disease in a novel autoimmune model. *Molecular Psychiatry*, 24, 1489-1501.

*Equally contributing authors

Personal contribution:

I was responsible for the statistical analyses and graphical representation with respect to NMDA receptor antibody positivity and age in both animal and human (extended GRAS) samples. Additionally, I read, corrected, and approved the final version of the manuscript.

Convergence of placenta biology and genetic risk for schizophrenia

Gianluca Ursini^{1,2,3}, Giovanna Punzi^{1,2}, Qiang Chen¹, Stefano Marengo^{4,5}, Joshua F. Robinson⁶, Annamaria Porcelli², Emily G. Hamilton⁶, Marina Mitjans⁷, Giancarlo Maddalena², Martin Begemann⁷, Jan Seidel⁷, Hidenaga Yanamori⁸, Andrew E. Jaffe^{9,10}, Karen F. Berman⁴, Michael F. Egan¹⁰, Richard E. Straub¹, Carlo Colantuoni^{11,12,13}, Giuseppe Blasi^{10,2}, Ryota Hashimoto^{10,8,14}, Dan Rujescu¹⁵, Hannelore Ehrenreich⁷, Alessandro Bertolino² and Daniel R. Weinberger^{1,3,11,12,13,16*}

Defining the environmental context in which genes enhance disease susceptibility can provide insight into the pathogenesis of complex disorders. We report that the intra-uterine environment modulates the association of schizophrenia with genomic risk (in this study, genome-wide association study-derived polygenic risk scores (PRSs)). In independent samples from the United States, Italy, and Germany, the liability of schizophrenia explained by PRS is more than five times greater in the presence of early-life complications (ELCs) compared with their absence. Patients with ELC histories have significantly higher PRS than patients without ELC histories, which is confirmed in additional samples from Germany and Japan. The gene set composed of schizophrenia loci that interact with ELCs is highly expressed in placenta, is differentially expressed in placenta from complicated in comparison with normal pregnancies, and is differentially upregulated in placenta from male compared with female offspring. Pathway analyses reveal that genes driving the PRS-ELC interaction are involved in cellular stress response; genes that do not drive such interaction implicate orthogonal biological processes (for example, synaptic function). We conclude that a subset of the most significant genetic variants associated with schizophrenia converge on a developmental trajectory sensitive to events that affect the placental response to stress, which may offer insights into sex biases and primary prevention.

Schizophrenia is a complex disabling disorder that occurs in all populations, with a lifetime morbidity risk of around 0.7–0.8%¹ and a higher incidence in males compared with females². The high heritability of the disorder indicates a major role for genetic variants in its etiology^{3,4}; however, non-genetic influences involving the intra-uterine environment have been repeatedly implicated in explaining at least part of the non-shared environmental contribution to the disorder^{5,6}.

Animal studies have shown that exposure to environmental insults in utero leads to altered response to stress postnatally, with effects on brain development and behavior that are partly mediated by gene expression changes in placenta^{7,8}, a key environmentally sensitive organ during development^{9,10}. Studies in animals also reveal that males are more vulnerable than females to prenatal adversities^{8,9}.

An important role for the intra-uterine environment in the etiology of schizophrenia is consistent with the disorder's

putative neurodevelopmental origins¹¹ and is also supported by many epidemiological studies. For example, the prevalence of schizophrenia increases in offspring of mothers who were in the second trimester during influenza epidemics; in a prospective study, maternal respiratory infection during pregnancy increased the risk for schizophrenia in the offspring threefold to sevenfold¹². More generally, schizophrenia has been associated with a number of early-life complications (ELCs), that is, potentially adverse events that occur during pregnancy and labor, at delivery, and early in neonatal life^{5,12,13}. Meta-analyses of this body of literature have found that ELCs increase risk by 1.5- to 2-fold¹⁴, a greater effect than any common genetic variant. Studies of ELCs in high-risk individuals (that is, offspring of parents affected with schizophrenia) suggest an interactive role for genetic background¹⁵, which is consistent with preliminary evidence of a relationship between ELCs, hypoxia-related genes, and risk for schizophrenia^{15–19}.

¹Lieber Institute for Brain Development, Johns Hopkins Medical Campus, Baltimore, MD, USA. ²Group of Psychiatric Neuroscience, Department of Basic Medical Science, Neuroscience and Sense Organs, Aldo Moro University, Bari, Italy. ³Departments of Psychiatry and Behavioral Sciences, Johns Hopkins University School of Medicine, Baltimore, MD, USA. ⁴Clinical and Translational Neuroscience Branch, National Institute of Mental Health, Intramural Research Program, National Institutes of Health, Bethesda, MD, USA. ⁵Human Brain Collection Core, National Institute of Mental Health, Intramural Research Program, National Institutes of Health, Bethesda, MD, USA. ⁶Center for Reproductive Sciences, Department of Obstetrics, Gynecology and Reproductive Sciences, University of California, San Francisco, San Francisco, CA, USA. ⁷Clinical Neuroscience, Max Planck Institute of Experimental Medicine, DFG Research Center for Nanoscale Microscopy and Molecular Physiology of the Brain, Göttingen, Germany. ⁸Department of Psychiatry, Osaka University Graduate School of Medicine, Osaka, Japan. ⁹Department of Mental Health, Johns Hopkins Bloomberg School of Public Health, Baltimore, MD, USA. ¹⁰Merck Research Laboratories, Merck and Co., Inc., Whitehouse Station, NJ, USA. ¹¹Department of Neurology, Johns Hopkins University School of Medicine, Baltimore, MD, USA. ¹²Department of Neuroscience, Johns Hopkins University School of Medicine, Baltimore, MD, USA. ¹³Institute for Genome Sciences, University of Maryland School of Medicine, Baltimore, MD, USA. ¹⁴Molecular Research Center for Children's Mental Development, United Graduate School of Child Development, Osaka University, Osaka, Japan. ¹⁵Department of Psychiatry, Psychotherapy, and Psychosomatics, Martin Luther University of Halle-Wittenberg, Halle, Germany. ¹⁶McKusick Nathans Institute of Genetic Medicine, Johns Hopkins University School of Medicine, Baltimore, MD, USA. *e-mail: drweinberger@libd.org

Table 1 | Sample composition and summary statistics

	CONT			SCZ			ELCs and diagnosis			PRS1 and diagnosis			ELCs absence			ELCs presence			Whole sample			PRS1 and ELCs			PRSt*ELCs interaction		
	N	ELCs	N	N	R ²	P	N	R ²	P	N	R ²	P	N	R ²	P	N	R ²	P	t	P	t	P	t	P			
scz_lie_eur	267	0.67	234	0.66	-0.38	0.70	501	0.06	2e-07	167	0.01	0.28	334	0.11	5e-09	0.68	0.49	-0.68	0.50	2.21	0.028	2.87	0.004				
scz_barl_eur	182	0.51	91	0.47	-0.51	0.61	273	0.02	0.04	138	<.01	0.91	135	0.09	0.001	1.14	0.26	-0.57	0.57	2.88	0.003	2.17	0.015				
scz_mmc_eur	398	0.15	521	0.24	3.54	4e-04	919	0.04	5e-08	733	0.02	1e-04	186	0.11	2e-05	0.91	0.36	-1.64	0.10	1.60	0.055	2.12	0.017				
scz_osak_asi			172	0.60			172			69			103							1.79	0.047						
scz_gras_eur			1,020	0.32			1,020			690			330							1.70	0.044						
merged1	847	0.39	846	0.38	-0.33	0.74	1,693	0.04	1e-14	1,038	0.02	2e-04	655	0.10	2e-15	1.49	0.14	-1.58	0.10	3.25	0.001	4.02	6e-05				
merged2			2,038	0.37		(0.05)	2,038			1,281			757							3.86	1e-04						

Columns 2 and 4 report number (N) of healthy control subjects (CONT) and patients with schizophrenia (SCZ) in the discovery sample (scz_lie_eur), in the four replication samples, and in the merged samples (merged1; cases and controls; merged2; cases only); columns 3 and 5 report the proportion of ELCs in the discovery sample (scz_lie_eur), in the four replication samples, and in the merged samples (merged1; cases and controls; merged2; cases only); columns 6 and 8 report the Nagelkerke R² value for the association of ELCs with case-control status (scz_barl_eur, scz_mmc_eur, scz_osak_asi) and with the association of ELCs with case-control status (scz_lie_eur, scz_barl_eur, scz_mmc_eur, scz_osak_asi); columns 9 and 11 report the statistics of the association of ELCs with case-control status (scz_barl_eur, scz_mmc_eur, scz_osak_asi) and with the association of ELCs with case-control status (scz_lie_eur, scz_barl_eur, scz_mmc_eur, scz_osak_asi); columns 12 and 14 report the statistics of the association of ELCs with case-control status (scz_barl_eur, scz_mmc_eur, scz_osak_asi) and with the association of ELCs with case-control status (scz_lie_eur, scz_barl_eur, scz_mmc_eur, scz_osak_asi); columns 15 and 17 report the statistics of the association of ELCs with case-control status (scz_barl_eur, scz_mmc_eur, scz_osak_asi) and with the association of ELCs with case-control status (scz_lie_eur, scz_barl_eur, scz_mmc_eur, scz_osak_asi); columns 18 and 20 report the statistics of the association of ELCs with case-control status (scz_barl_eur, scz_mmc_eur, scz_osak_asi) and with the association of ELCs with case-control status (scz_lie_eur, scz_barl_eur, scz_mmc_eur, scz_osak_asi); columns 21 and 23 report the statistics of the association of ELCs with case-control status (scz_barl_eur, scz_mmc_eur, scz_osak_asi) and with the association of ELCs with case-control status (scz_lie_eur, scz_barl_eur, scz_mmc_eur, scz_osak_asi); columns 24 and 26 report the statistics of the association of ELCs with case-control status (scz_barl_eur, scz_mmc_eur, scz_osak_asi) and with the association of ELCs with case-control status (scz_lie_eur, scz_barl_eur, scz_mmc_eur, scz_osak_asi); columns 27 and 29 report the statistics of the association of ELCs with case-control status (scz_barl_eur, scz_mmc_eur, scz_osak_asi) and with the association of ELCs with case-control status (scz_lie_eur, scz_barl_eur, scz_mmc_eur, scz_osak_asi); columns 30 and 32 report the statistics of the association of ELCs with case-control status (scz_barl_eur, scz_mmc_eur, scz_osak_asi) and with the association of ELCs with case-control status (scz_lie_eur, scz_barl_eur, scz_mmc_eur, scz_osak_asi); columns 33 and 35 report the statistics of the association of ELCs with case-control status (scz_barl_eur, scz_mmc_eur, scz_osak_asi) and with the association of ELCs with case-control status (scz_lie_eur, scz_barl_eur, scz_mmc_eur, scz_osak_asi); columns 36 and 38 report the statistics of the association of ELCs with case-control status (scz_barl_eur, scz_mmc_eur, scz_osak_asi) and with the association of ELCs with case-control status (scz_lie_eur, scz_barl_eur, scz_mmc_eur, scz_osak_asi); columns 39 and 41 report the statistics of the association of ELCs with case-control status (scz_barl_eur, scz_mmc_eur, scz_osak_asi) and with the association of ELCs with case-control status (scz_lie_eur, scz_barl_eur, scz_mmc_eur, scz_osak_asi); columns 42 and 44 report the statistics of the association of ELCs with case-control status (scz_barl_eur, scz_mmc_eur, scz_osak_asi) and with the association of ELCs with case-control status (scz_lie_eur, scz_barl_eur, scz_mmc_eur, scz_osak_asi); columns 45 and 47 report the statistics of the association of ELCs with case-control status (scz_barl_eur, scz_mmc_eur, scz_osak_asi) and with the association of ELCs with case-control status (scz_lie_eur, scz_barl_eur, scz_mmc_eur, scz_osak_asi); columns 48 and 50 report the statistics of the association of ELCs with case-control status (scz_barl_eur, scz_mmc_eur, scz_osak_asi) and with the association of ELCs with case-control status (scz_lie_eur, scz_barl_eur, scz_mmc_eur, scz_osak_asi); columns 51 and 53 report the statistics of the association of ELCs with case-control status (scz_barl_eur, scz_mmc_eur, scz_osak_asi) and with the association of ELCs with case-control status (scz_lie_eur, scz_barl_eur, scz_mmc_eur, scz_osak_asi); columns 54 and 56 report the statistics of the association of ELCs with case-control status (scz_barl_eur, scz_mmc_eur, scz_osak_asi) and with the association of ELCs with case-control status (scz_lie_eur, scz_barl_eur, scz_mmc_eur, scz_osak_asi); columns 57 and 59 report the statistics of the association of ELCs with case-control status (scz_barl_eur, scz_mmc_eur, scz_osak_asi) and with the association of ELCs with case-control status (scz_lie_eur, scz_barl_eur, scz_mmc_eur, scz_osak_asi); columns 60 and 62 report the statistics of the association of ELCs with case-control status (scz_barl_eur, scz_mmc_eur, scz_osak_asi) and with the association of ELCs with case-control status (scz_lie_eur, scz_barl_eur, scz_mmc_eur, scz_osak_asi); columns 63 and 65 report the statistics of the association of ELCs with case-control status (scz_barl_eur, scz_mmc_eur, scz_osak_asi) and with the association of ELCs with case-control status (scz_lie_eur, scz_barl_eur, scz_mmc_eur, scz_osak_asi); columns 66 and 68 report the statistics of the association of ELCs with case-control status (scz_barl_eur, scz_mmc_eur, scz_osak_asi) and with the association of ELCs with case-control status (scz_lie_eur, scz_barl_eur, scz_mmc_eur, scz_osak_asi); columns 69 and 71 report the statistics of the association of ELCs with case-control status (scz_barl_eur, scz_mmc_eur, scz_osak_asi) and with the association of ELCs with case-control status (scz_lie_eur, scz_barl_eur, scz_mmc_eur, scz_osak_asi); columns 72 and 74 report the statistics of the association of ELCs with case-control status (scz_barl_eur, scz_mmc_eur, scz_osak_asi) and with the association of ELCs with case-control status (scz_lie_eur, scz_barl_eur, scz_mmc_eur, scz_osak_asi); columns 75 and 77 report the statistics of the association of ELCs with case-control status (scz_barl_eur, scz_mmc_eur, scz_osak_asi) and with the association of ELCs with case-control status (scz_lie_eur, scz_barl_eur, scz_mmc_eur, scz_osak_asi); columns 78 and 80 report the statistics of the association of ELCs with case-control status (scz_barl_eur, scz_mmc_eur, scz_osak_asi) and with the association of ELCs with case-control status (scz_lie_eur, scz_barl_eur, scz_mmc_eur, scz_osak_asi); columns 81 and 83 report the statistics of the association of ELCs with case-control status (scz_barl_eur, scz_mmc_eur, scz_osak_asi) and with the association of ELCs with case-control status (scz_lie_eur, scz_barl_eur, scz_mmc_eur, scz_osak_asi); columns 84 and 86 report the statistics of the association of ELCs with case-control status (scz_barl_eur, scz_mmc_eur, scz_osak_asi) and with the association of ELCs with case-control status (scz_lie_eur, scz_barl_eur, scz_mmc_eur, scz_osak_asi); columns 87 and 89 report the statistics of the association of ELCs with case-control status (scz_barl_eur, scz_mmc_eur, scz_osak_asi) and with the association of ELCs with case-control status (scz_lie_eur, scz_barl_eur, scz_mmc_eur, scz_osak_asi); columns 90 and 92 report the statistics of the association of ELCs with case-control status (scz_barl_eur, scz_mmc_eur, scz_osak_asi) and with the association of ELCs with case-control status (scz_lie_eur, scz_barl_eur, scz_mmc_eur, scz_osak_asi); columns 93 and 95 report the statistics of the association of ELCs with case-control status (scz_barl_eur, scz_mmc_eur, scz_osak_asi) and with the association of ELCs with case-control status (scz_lie_eur, scz_barl_eur, scz_mmc_eur, scz_osak_asi); columns 96 and 98 report the statistics of the association of ELCs with case-control status (scz_barl_eur, scz_mmc_eur, scz_osak_asi) and with the association of ELCs with case-control status (scz_lie_eur, scz_barl_eur, scz_mmc_eur, scz_osak_asi); columns 99 and 101 report the statistics of the association of ELCs with case-control status (scz_barl_eur, scz_mmc_eur, scz_osak_asi) and with the association of ELCs with case-control status (scz_lie_eur, scz_barl_eur, scz_mmc_eur, scz_osak_asi); columns 102 and 104 report the statistics of the association of ELCs with case-control status (scz_barl_eur, scz_mmc_eur, scz_osak_asi) and with the association of ELCs with case-control status (scz_lie_eur, scz_barl_eur, scz_mmc_eur, scz_osak_asi); columns 105 and 107 report the statistics of the association of ELCs with case-control status (scz_barl_eur, scz_mmc_eur, scz_osak_asi) and with the association of ELCs with case-control status (scz_lie_eur, scz_barl_eur, scz_mmc_eur, scz_osak_asi); columns 108 and 110 report the statistics of the association of ELCs with case-control status (scz_barl_eur, scz_mmc_eur, scz_osak_asi) and with the association of ELCs with case-control status (scz_lie_eur, scz_barl_eur, scz_mmc_eur, scz_osak_asi); columns 111 and 113 report the statistics of the association of ELCs with case-control status (scz_barl_eur, scz_mmc_eur, scz_osak_asi) and with the association of ELCs with case-control status (scz_lie_eur, scz_barl_eur, scz_mmc_eur, scz_osak_asi); columns 114 and 116 report the statistics of the association of ELCs with case-control status (scz_barl_eur, scz_mmc_eur, scz_osak_asi) and with the association of ELCs with case-control status (scz_lie_eur, scz_barl_eur, scz_mmc_eur, scz_osak_asi); columns 117 and 119 report the statistics of the association of ELCs with case-control status (scz_barl_eur, scz_mmc_eur, scz_osak_asi) and with the association of ELCs with case-control status (scz_lie_eur, scz_barl_eur, scz_mmc_eur, scz_osak_asi); columns 120 and 122 report the statistics of the association of ELCs with case-control status (scz_barl_eur, scz_mmc_eur, scz_osak_asi) and with the association of ELCs with case-control status (scz_lie_eur, scz_barl_eur, scz_mmc_eur, scz_osak_asi); columns 123 and 125 report the statistics of the association of ELCs with case-control status (scz_barl_eur, scz_mmc_eur, scz_osak_asi) and with the association of ELCs with case-control status (scz_lie_eur, scz_barl_eur, scz_mmc_eur, scz_osak_asi); columns 126 and 128 report the statistics of the association of ELCs with case-control status (scz_barl_eur, scz_mmc_eur, scz_osak_asi) and with the association of ELCs with case-control status (scz_lie_eur, scz_barl_eur, scz_mmc_eur, scz_osak_asi); columns 129 and 131 report the statistics of the association of ELCs with case-control status (scz_barl_eur, scz_mmc_eur, scz_osak_asi) and with the association of ELCs with case-control status (scz_lie_eur, scz_barl_eur, scz_mmc_eur, scz_osak_asi); columns 132 and 134 report the statistics of the association of ELCs with case-control status (scz_barl_eur, scz_mmc_eur, scz_osak_asi) and with the association of ELCs with case-control status (scz_lie_eur, scz_barl_eur, scz_mmc_eur, scz_osak_asi); columns 135 and 137 report the statistics of the association of ELCs with case-control status (scz_barl_eur, scz_mmc_eur, scz_osak_asi) and with the association of ELCs with case-control status (scz_lie_eur, scz_barl_eur, scz_mmc_eur, scz_osak_asi); columns 138 and 140 report the statistics of the association of ELCs with case-control status (scz_barl_eur, scz_mmc_eur, scz_osak_asi) and with the association of ELCs with case-control status (scz_lie_eur, scz_barl_eur, scz_mmc_eur, scz_osak_asi); columns 141 and 143 report the statistics of the association of ELCs with case-control status (scz_barl_eur, scz_mmc_eur, scz_osak_asi) and with the association of ELCs with case-control status (scz_lie_eur, scz_barl_eur, scz_mmc_eur, scz_osak_asi); columns 144 and 146 report the statistics of the association of ELCs with case-control status (scz_barl_eur, scz_mmc_eur, scz_osak_asi) and with the association of ELCs with case-control status (scz_lie_eur, scz_barl_eur, scz_mmc_eur, scz_osak_asi); columns 147 and 149 report the statistics of the association of ELCs with case-control status (scz_barl_eur, scz_mmc_eur, scz_osak_asi) and with the association of ELCs with case-control status (scz_lie_eur, scz_barl_eur, scz_mmc_eur, scz_osak_asi); columns 150 and 152 report the statistics of the association of ELCs with case-control status (scz_barl_eur, scz_mmc_eur, scz_osak_asi) and with the association of ELCs with case-control status (scz_lie_eur, scz_barl_eur, scz_mmc_eur, scz_osak_asi); columns 153 and 155 report the statistics of the association of ELCs with case-control status (scz_barl_eur, scz_mmc_eur, scz_osak_asi) and with the association of ELCs with case-control status (scz_lie_eur, scz_barl_eur, scz_mmc_eur, scz_osak_asi); columns 156 and 158 report the statistics of the association of ELCs with case-control status (scz_barl_eur, scz_mmc_eur, scz_osak_asi) and with the association of ELCs with case-control status (scz_lie_eur, scz_barl_eur, scz_mmc_eur, scz_osak_asi); columns 159 and 161 report the statistics of the association of ELCs with case-control status (scz_barl_eur, scz_mmc_eur, scz_osak_asi) and with the association of ELCs with case-control status (scz_lie_eur, scz_barl_eur, scz_mmc_eur, scz_osak_asi); columns 162 and 164 report the statistics of the association of ELCs with case-control status (scz_barl_eur, scz_mmc_eur, scz_osak_asi) and with the association of ELCs with case-control status (scz_lie_eur, scz_barl_eur, scz_mmc_eur, scz_osak_asi); columns 165 and 167 report the statistics of the association of ELCs with case-control status (scz_barl_eur, scz_mmc_eur, scz_osak_asi) and with the association of ELCs with case-control status (scz_lie_eur, scz_barl_eur, scz_mmc_eur, scz_osak_asi); columns 168 and 170 report the statistics of the association of ELCs with case-control status (scz_barl_eur, scz_mmc_eur, scz_osak_asi) and with the association of ELCs with case-control status (scz_lie_eur, scz_barl_eur, scz_mmc_eur, scz_osak_asi); columns 171 and 173 report the statistics of the association of ELCs with case-control status (scz_barl_eur, scz_mmc_eur, scz_osak_asi) and with the association of ELCs with case-control status (scz_lie_eur, scz_barl_eur, scz_mmc_eur, scz_osak_asi); columns 174 and 176 report the statistics of the association of ELCs with case-control status (scz_barl_eur, scz_mmc_eur, scz_osak_asi) and with the association of ELCs with case-control status (scz_lie_eur, scz_barl_eur, scz_mmc_eur, scz_osak_asi); columns 177 and 179 report the statistics of the association of ELCs with case-control status (scz_barl_eur, scz_mmc_eur, scz_osak_asi) and with the association of ELCs with case-control status (scz_lie_eur, scz_barl_eur, scz_mmc_eur, scz_osak_asi); columns 180 and 182 report the statistics of the association of ELCs with case-control status (scz_barl_eur, scz_mmc_eur, scz_osak_asi) and with the association of ELCs with case-control status (scz_lie_eur, scz_barl_eur, scz_mmc_eur, scz_osak_asi); columns 183 and 185 report the statistics of the association of ELCs with case-control status (scz_barl_eur, scz_mmc_eur, scz_osak_asi) and with the association of ELCs with case-control status (scz_lie_eur, scz_barl_eur, scz_mmc_eur, scz_osak_asi); columns 186 and 188 report the statistics of the association of ELCs with case-control status (scz_barl_eur, scz_mmc_eur, scz_osak_asi) and with the association of ELCs with case-control status (scz_lie_eur, scz_barl_eur, scz_mmc_eur, scz_osak_asi); columns 189 and 191 report the statistics of the association of ELCs with case-control status (scz_barl_eur, scz_mmc_eur, scz_osak_asi) and with the association of ELCs with case-control status (scz_lie_eur, scz_barl_eur, scz_mmc_eur, scz_osak_asi); columns 192 and 194 report the statistics of the association of ELCs with case-control status (scz_barl_eur, scz_mmc_eur, scz_osak_asi) and with the association of ELCs with case-control status (scz_lie_eur, scz_barl_eur, scz_mmc_eur, scz_osak_asi); columns 195 and 197 report the statistics of the association of ELCs with case-control status (scz_barl_eur, scz_mmc_eur, scz_osak_asi) and with the association of ELCs with case-control status (scz_lie_eur, scz_barl_eur, scz_mmc_eur, scz_osak_asi); columns 198 and 200 report the statistics of the association of ELCs with case-control status (scz_barl_eur, scz_mmc_eur, scz_osak_asi) and with the association of ELCs with case-control status (scz_lie_eur, scz_barl_eur, scz_mmc_eur, scz_osak_asi); columns 201 and 203 report the statistics of the association of ELCs with case-control status (scz_barl_eur, scz_mmc_eur, scz_osak_asi) and with the association of ELCs with case-control status (scz_lie_eur, scz_barl_eur, scz_mmc_eur, scz_osak_asi); columns 204 and 206 report the statistics of the association of ELCs with case-control status (scz_barl_eur, scz_mmc_eur, scz_osak_asi) and with the association of ELCs with case-control status (scz_lie_eur, scz_barl_eur, scz_mmc_eur, scz_osak_asi); columns 207 and 209 report the statistics of the association of ELCs with case-control status (scz_barl_eur, scz_mmc_eur, scz_osak_asi) and with the association of ELCs with case-control status (scz_lie_eur, scz_barl_eur, scz_mmc_eur, scz_osak_asi); columns 210 and 212 report the statistics of the association of ELCs with case-control status (scz_barl_eur, scz_mmc_eur, scz_osak_asi) and with the association of ELCs with case-control status (scz_lie_eur, scz_barl_eur, scz_mmc_eur, scz_osak_asi); columns 213 and 215 report the statistics of the association of ELCs with case-control status (scz_barl_eur, scz_mmc_eur, scz_osak_asi) and with the association of ELCs with case-control status (scz_lie_eur, scz_barl_eur, scz_mmc_eur, scz_osak_asi); columns 216 and 218 report the statistics of the association of ELCs with case-control status (scz_barl_eur, scz_mmc_eur, scz_osak_asi) and with the association of ELCs with case-control status (scz_lie_eur, scz_barl_eur, scz_mmc_eur, scz_osak_asi); columns 219 and 221 report the statistics of the association of ELCs with case-control status (scz_barl_eur, scz_mmc_eur, scz_osak_asi) and with the association of ELCs with case-control status (scz_lie_eur, scz_barl_eur, scz_mmc_eur, scz_osak_asi); columns 222 and 224 report the statistics of the association of ELCs with case-control status (scz_barl_eur, scz_mmc_eur, scz_osak_asi) and with the association of ELCs with case-control status (scz_lie_eur, scz_barl_eur, scz_mmc_eur, scz_osak_asi); columns 225 and 227 report the statistics of the association of ELCs with case-control status (scz_barl_eur, scz_mmc_eur, scz_osak_asi) and with the association of ELCs with case-control status (scz_lie_eur, scz_barl_eur, scz_mmc_eur, scz_osak_asi); columns 228 and 230 report the statistics of the association of ELCs with case-control status (scz_barl_eur, scz_mmc_eur, scz_osak_asi) and with the association of ELCs with case-control status (scz_lie_eur, scz_barl_eur, scz_mmc_eur, scz_osak_asi); columns 231 and 233 report the statistics of the association of ELCs with case-control status (scz_barl_eur, scz_mmc_eur, scz_osak_asi) and with the association of ELCs with case-control status (scz_lie_eur, scz_barl_eur, scz_mmc_eur, scz_osak_asi); columns 234 and 236 report the statistics of the association of ELCs with case-control status (scz_barl_eur, scz_mmc_eur, scz_osak_asi) and with the association of ELCs with case-control status (scz_lie_eur, scz_barl_eur, scz_mmc_eur, scz_osak_asi); columns 237 and 239 report the statistics of the association of ELCs with case-control status (scz_barl_eur, scz_mmc_eur, scz_osak_asi) and with the association of ELCs with case-control status (scz_lie_eur, scz_barl_eur, scz_mmc_eur, scz_osak_asi); columns 240 and 242 report the statistics of the association of ELCs with case-control status (scz_barl_eur, scz_mmc_eur, scz_osak_asi) and with the association of ELCs with case-control status (scz_lie_eur, scz_barl_eur, scz_mmc_eur, scz_osak_asi); columns 243 and 245 report the statistics of the association of ELCs with case-control status (scz_barl_eur, scz_mmc_eur, scz_osak_asi) and with the association of ELCs with case-control status (scz_lie_eur, scz_barl_eur, scz_mmc_eur, scz_osak_asi); columns 246 and 248 report the statistics of the association of ELCs with case-control status (scz_barl_eur, scz_mmc_eur, scz_osak_asi) and with the association of ELCs with case-control status (scz_lie_eur, scz_barl_eur, scz_mmc_eur, scz_osak_asi); columns 249 and 251 report the statistics of the association of ELCs with case-control status (scz_barl_eur, scz_mmc_eur, scz_osak_asi) and with the association of ELCs with case-control status (scz_lie_eur, scz_barl_eur, scz_mmc_eur, scz_osak_asi); columns 252 and 254 report the statistics of the association of ELCs with case-control status (scz_barl_eur, scz_mmc_eur, scz_osak_asi) and with the association of ELCs with case-control status (scz_lie_eur, scz_barl_eur, scz_mmc_eur, scz_osak_asi); columns 255 and 257 report the statistics of the association of ELCs with case-control status (scz_barl_eur, scz_mmc_eur, scz_osak_asi) and with the association of ELCs with case-control status (scz_lie_eur, scz_barl_eur, scz_mmc_eur, scz_osak_asi); columns 258 and 260 report the statistics of the association of ELCs with case-control status (scz_barl_eur, scz_mmc_eur, scz_osak_asi) and with the association of ELCs with case-control status (scz_lie_eur, scz_barl_eur, scz_mmc_eur, scz_osak_asi); columns 261 and 263 report the statistics of the association of ELCs with case-control status (scz_barl_eur, scz_mmc_eur, scz_osak_asi) and with the association of ELCs with case-control status (scz_lie_eur, scz_barl_eur, scz_mmc_eur, scz_osak_asi); columns 264 and 266 report the statistics of the association of ELCs with case-control status (scz_barl_eur, scz_mmc_eur, scz_osak_asi) and with the association of ELCs with case-control status (scz_lie_eur, scz_barl_eur, scz_mmc_eur, scz_osak_asi); columns 267 and 269 report the statistics of the association of ELCs with case-control status (scz_barl_eur, scz_mmc_eur, scz_osak_asi) and with the association of ELCs with case-control status (scz_lie_eur, scz_barl_eur, scz_mmc_eur, scz_osak_asi); columns 270 and 272 report the statistics of the association of ELCs with case-control status (scz_barl_eur, scz_mmc_eur, scz_osak_asi) and with the association of ELCs with case-control status (scz_lie_eur, scz_barl_eur, scz_mmc_eur, scz_osak_asi); columns 273 and 275 report the statistics of the association of ELCs with case-control status (scz_barl_eur, scz_mmc_eur, scz_osak_asi) and with the association of ELCs with case-control status (scz_lie_eur, scz_barl_eur, scz_mmc_eur, scz_osak_asi); columns 276 and 278 report the statistics of the association of ELCs with case-control status (scz_barl_eur, scz_mmc_eur, scz_osak_asi) and with the association of ELCs with case-control status (scz_lie_eur, scz_barl_eur, scz_mmc_eur, scz_osak_asi); columns 279 and 281 report the statistics of the association of ELCs with case-control status (scz_barl_eur, scz_mmc_eur, scz_osak_asi) and with the association of ELCs with case-control status (scz_lie_eur, scz_barl_eur, scz_mmc_eur, scz_osak_asi); columns 282 and 284 report the statistics of the association of ELCs with case-control status (scz_barl_eur, scz_mmc_eur, scz_osak_asi) and with the association of ELCs with case-control status (scz_lie_eur, scz_barl_eur, scz_mmc_eur, scz_osak_asi); columns 285 and 287 report the statistics of the association of ELCs with case-control status (scz_barl_eur, scz_mmc_eur, scz_osak_asi) and with the association of ELCs with case-control status (scz_lie_eur, scz_barl_eur, scz_mmc_eur, scz_osak_asi); columns 288 and 290 report the statistics of the association of ELCs with case-control status (scz_barl_eur, scz_mmc_eur, scz_osak_asi) and with the association of ELCs with case-control status (scz_lie_eur, scz_barl_eur, scz_mmc_eur, scz_osak_asi); columns 291 and 293 report the statistics of the association of ELCs with case-control status (scz_barl_eur, scz_mmc_eur, scz_osak_asi) and with the association of ELCs with case-control status (scz_lie_eur, scz_barl_eur, scz_mmc_eur, scz_osak_asi); columns 294 and 296 report the statistics of the association of ELCs with case-control status (scz_barl_eur, scz_mmc_eur,

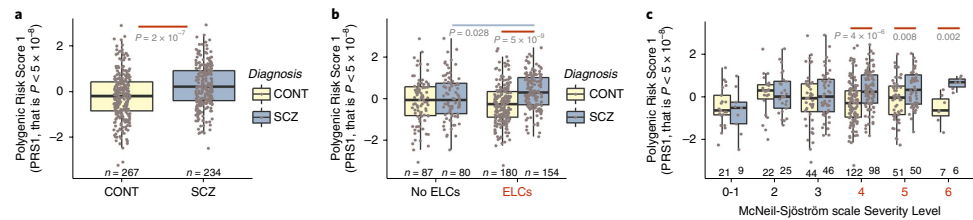


Fig. 1 | PRS1, ELC history, and schizophrenia in the *scz_lie_eur* sample ($N=501$). **a**, Association between genomic risk score (PRS1), constructed from alleles showing significant association with schizophrenia (with GWAS $P < 5 \times 10^{-9}$), and case-control status. **b**, Interaction between PRS1 and ELCs on case-control status: shown are genomic risk scores (PRS1) in the absence of ELCs (left) and in the presence of ELC history (right). **c**, Relation between PRS1 and case-control status in the context of ELCs with different severity levels; ELCs with severity scores ≥ 4 (in red) are considered harmful or relevant factors in fetal stress, whereas ELCs with severity scores of 0, 1, 2, and 3 (in black) are not. All of the statistics were generated using multiple logistic regression, adjusting for population stratification (ten PCs) (see also main text and Table 1 for detailed statistics). Boxplot centers depict median; lower and upper hinges correspond to 25th and 75th percentiles; whiskers extend from hinges to the smallest and larger values no further than $1.5 \times$ IQR from the 25th and 75th percentiles. Results in the other clinical samples are shown in Supplementary Figs. 3 and 4.

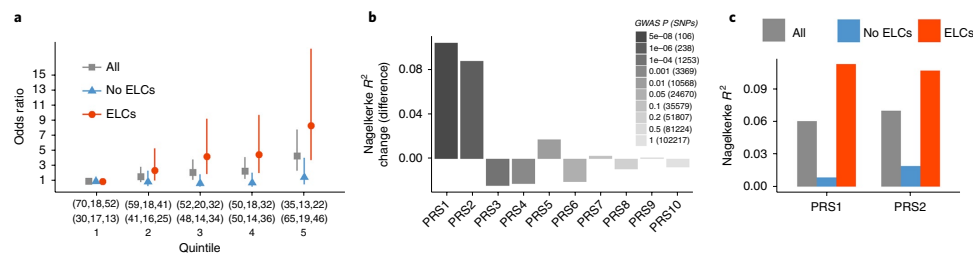


Fig. 2 | Liability of schizophrenia explained by genomic risk in the context of ELC history, in the *scz_lie_eur* sample ($N=501$). **a**, OR for schizophrenia by PRS1 quintile and ELC history: the PRSs constructed from alleles showing significant association with schizophrenia (with GWAS $P < 5 \times 10^{-9}$) were converted to quintiles (1 = lowest PRS1, 5 = highest PRS1), and the ORs were estimated for affected status for each quintile with reference to the lowest risk quintile, in the whole sample (gray square) and in the absence (blue triangles) and presence (orange dots) of ELCs. Bars correspond to 95% confidence intervals. The numbers within brackets on the x axis refer to the individuals within each quintile, in the whole sample, in the absence of ELCs and in the presence of ELCs, in controls (first row) and in patients with schizophrenia (second row). **b**, Change of variance explained by genomic risk in the presence of ELCs compared with the absence of ELCs: proportion of variance (Nagelkerke R^2) of schizophrenia risk was calculated, by comparison of a full model (covariates + PRS) with a reduced model (covariates only), in the presence and absence of ELC history, for each of the ten different PRSs constructed from alleles showing association with schizophrenia at different threshold of significance (GWAS P value threshold and number of SNPs contributing to each PRS are reported in the grayscale legend). Shown is the difference (y axis) between Nagelkerke R^2 in the presence of ELCs and Nagelkerke R^2 in the absence of ELC history, for each PRS (x axis). **c**, Proportion of variance of schizophrenia by PRS1 and PRS2, and ELC history: shown is variance of case-control status (Nagelkerke R^2 , y axis) explained by PRS1 and PRS2, in the whole sample (gray bars), in the absence of ELCs (blue bars), and in the presence of ELCs (orange bars). All of the statistics were generated using multiple logistic regression, adjusting for population stratification (ten PCs). Results in the other clinical samples are shown in Supplementary Figs. 3 and 4.

significant variant in the extended major histocompatibility complex (MHC) region (chr6: 25–34 Mb; Supplementary Table 4).

We then grouped individuals in quintiles based on their PRS1 levels, and we determined odds ratios (ORs) of being affected with schizophrenia associated with being in each PRS1 quintile, compared with the lowest PRS1 quintile. We also stratified our sample by ELC history to further represent the capacity of PRS1 to predict risk for schizophrenia in the context of ELCs. The OR increased with higher PRS1 quintiles only in the sample with ELCs, so that having the highest PRS1 quintile corresponded to an OR of 8.36 (95% confidence interval [CI]: 3.79–18.47, $P=3.22 \times 10^{-6}$) in the presence of ELCs, and only 1.55 (95% CI: 0.59–4.07, $P=0.37$) in the absence of ELCs (Fig. 2a), compared with having the lowest PRS1 quintile.

We further analyzed whether the interaction between genomic risk and ELCs was specific for the PRS constructed with GWAS significant alleles (PRS1) or was also found with other PRS levels (that is, PRS2–10) constructed from alleles showing association with schizophrenia at lesser statistical thresholds (that is, not GWAS significant). Interestingly, the ELC-dependent change in schizophrenia risk variance, explained by PRS, gradually decreased when considering different PRSs constructed from variants showing association with schizophrenia at the lower thresholds of significance (Fig. 2b). Specifically, only the first two scores, constructed from the alleles showing the strongest clinical association with schizophrenia (PRS1: $P < 5 \times 10^{-9}$; PRS2: $P < 1 \times 10^{-6}$), interact with ELCs on case-control status, and the variance in risk explained by them is much

higher in individuals with a history of ELCs, compared with those without (Fig. 2b,c and Supplementary Figs. 1 and 2). The other scores, PRS3–10, do not show any interaction with ELCs, and the variance explained by them is not influenced by a history of ELCs (Fig. 2b and Supplementary Figs. 1 and 2). This is consistent with the possibility that the latter scores, involving a greater number of putative susceptibility genes, capture a greater number of genetic risk variants acting in a simply cumulative way, whereas the aggregate effect of the GWAS significant SNPs (PRS1) and the almost GWAS significant SNPs (PRS2) is more conditioned on the history of ELCs. These results raise the possibility that the reason PRS1 and PRS2 loci achieve their privileged statistical significance status in this heterogeneous clinical sample is because of this interaction. From another perspective, the data show that patients with a history of ELCs have greater PRS1 than patients without ELCs ($N=234$, $t=2.21$, $P=0.028$), whereas this relationship is not seen in healthy subjects ($N=267$, $t=-0.68$, $P=0.50$). Maternal PRSs were available on a subsample of healthy mothers ($N=160$) of schizophrenic offspring and were not associated with ELCs in their offspring ($t=0.08$, $P=0.94$; Supplementary Table 5). Similarly, paternal PRSs were available only for a subsample of fathers ($N=136$) and were also not significantly associated with ELCs in the offspring ($t=1.40$, $P=0.16$; Supplementary Table 5). These results suggest that the interaction between genomic risk and ELCs is mainly driven by the fetal genome and is relatively independent of gene-environment interactions related to parental genomes per se.

We sought to replicate our findings in several additional, independent samples. We first analyzed two case-control samples: an Italian sample of 273 subjects (*scz_bari_eur*) and a German sample of 919 subjects (*scz_munc_eur*) (see Table 1 and Supplementary Table 2 for sample information). As in the discovery sample, PRS1 was positively associated with case-control status in both samples (*scz_bari_eur*: $N=273$, $R^2=0.02$, $t=2.11$, $P=0.036$; *scz_munc_eur*: $N=919$, $R^2=0.04$, $t=5.51$, $P=5 \times 10^{-8}$; Supplementary Table 3). ELCs were not differentially distributed between healthy subjects and patients with schizophrenia in the *scz_bari_eur* sample ($z=-0.51$, $P=0.61$), but there was a significant association of ELC history with schizophrenia in the larger *scz_munc_eur* sample ($z=3.54$, $P=0.0004$, OR = 1.85, 95% CI: 1.32–2.61). In both case-control samples, PRS again showed a significant interaction with ELCs in predicting case-control status (*scz_bari_eur*: $t=2.17$, $P_{one-sided}=0.015$; *scz_munc_eur*: $t=2.12$, $P_{one-sided}=0.017$; Table 1 and Supplementary Fig. 3a,b). When analyzing the relationship between PRS1 and case-control status in the context of ELCs, this PRS was once again associated with schizophrenia only in the presence of ELCs in the *scz_bari_eur* sample ($N=135$, $t=3.38$, $P=0.001$), and not in their absence ($N=138$, $t=-0.11$, $P=0.91$), whereas in the *scz_munc_eur* sample, the association between PRS1 and case-control status was significant both in the absence ($N=733$, $t=3.88$, $P=0.0001$) and in the presence of ELCs ($N=186$, $t=4.45$, $P=2 \times 10^{-5}$; Table 1 and Supplementary Fig. 3a,b). However, in both samples the variance of case-control status explained by PRS1 was much higher in individuals with a history of ELCs (*scz_bari_eur*: $R^2=0.09$; *scz_munc_eur*: $R^2=0.11$) than in those without such history (*scz_bari_eur*: $R^2=0.0001$; *scz_munc_eur*: $R^2=0.02$; Supplementary Fig. 3c,d), and again subjects who experienced ELCs who were in the upper quintile for PRS1 had the highest OR (*scz_bari_eur*: OR = 6.67, 95% CI: 1.6–27.6, $P=0.005$; *scz_munc_eur*: OR = 14.17, 95% CI: 4.0–49.9, $P=5.03 \times 10^{-6}$; Supplementary Fig. 3e,f). These replication analyses also confirmed that PRS1 was positively associated with ELCs only in cases (*scz_bari_eur*: $N=91$, $t=2.88$, $P_{one-sided}=0.003$; *scz_munc_eur*: $N=521$, $t=1.60$, $P_{one-sided}=0.0547$), but not in controls (*scz_bari_eur*: $N=182$, $t=-0.57$, $P=0.57$; *scz_munc_eur*: $N=398$, $t=-1.64$, $P=0.10$; Table 1 and Supplementary Fig. 3a,b).

We further tested the relationship between genomic risk for schizophrenia and ELC history in two more samples of only patients (total

$N=1,192$): another independent German sample of 1,020 patients with schizophrenia, namely, the Göttingen Research Association for Schizophrenia (GRAS) data collection (*scz_gras_eur*), and a Japanese sample of 172 patients with schizophrenia (*scz_osak_asi*) (Table 1 and Supplementary Table 2). In regard to the latter, it should be noted that the PRS derived from the European Caucasian sample of the recent GWAS study of schizophrenia has much less association with schizophrenia in Asian samples¹⁶, as would be expected because the correlation between genotypes at nearby markers (that is, the linkage disequilibrium structure) is different across populations¹⁶. However, because many of the alleles comprising the score likely monitor ancient haplotypes, an association with ELCs might still be expected. As in the three other samples, we again found that PRS1 was associated with ELCs in both samples of patients with schizophrenia (*scz_gras_eur*: $N=1,020$, $t=1.70$, $P_{one-sided}=0.044$; *scz_osak_asi*: $N=172$, $t=1.79$, $P_{one-sided}=0.047$; Supplementary Fig. 4), so that patients with a history of complications had higher PRSs than patients who did not experience ELCs.

We also performed analyses in merged samples of cases and controls (*scz_lie_eur*, *scz_bari_eur*, *scz_munc_eur*) and of only cases (*scz_lie_eur*, *scz_bari_eur*, *scz_munc_eur*, *scz_osak_asi*, *scz_gras_eur*), after normalization of PRSs in each population. In these merged samples, we confirmed the interaction of PRS1 and ELCs on case-control status ($N=1,693$, $t=4.02$, $P=6.18 \times 10^{-5}$; Supplementary Fig. 5) and the relationship between PRS1 and ELCs in patients with schizophrenia ($N=2,038$, $t=3.86$, $P=0.0001$; Supplementary Figs. 5 and 6). Also, in the merged samples, only PRS1 and PRS2 interact with ELCs on case-control status, and only PRS1 and PRS2 are positively associated with ELCs in patients with schizophrenia (Supplementary Figs. 5 and 6). Again, the positive association between genomic risk and ELCs was not present in controls, where the trend was actually negative ($P=0.10$; Table 1), which is compatible with a pattern of a gene-environment interaction. Sensitivity analyses with sex, age, paternal and maternal ages, maternal stress, socioeconomic status, and substance use as covariates and related interaction terms (in addition to genetic principal components) confirmed the same results (Supplementary Tables 6–8). These consistent results in five independent samples support the hypothesis that these top PRSs are relevant for the etiopathogenesis of schizophrenia, particularly in the context of ELCs, whereas other PRSs (that is, PRS3–10) may capture polygenic mechanisms of schizophrenia not directly related to ELCs.

Expression of schizophrenia risk-associated genes in placenta.

Even though several recent studies show preferential regulation of many schizophrenia risk genes in fetal brain^{27–29}, the relationship between the PRSs and ELCs that we found in five independent clinical samples from diverse ancestries points to the intra-uterine context as a likely place where some risk genes for schizophrenia and environmental adversity intersect, with implications not limited to the brain. Because PRS1 and PRS2 risk SNPs are associated with expression of nearby genes across many different tissues (Supplementary information, see “Screening of PRS1 and PRS2 SNPs for eQTLs across different tissues” note), we tested whether the genes mapping to the loci showing the strongest association with schizophrenia and interacting with ELCs (that is, PRS1 and PRS2 genes; Fig. 2b and Supplementary Table 9) were more highly expressed in the placenta, compared with randomly selected genes contributing to PRSs constructed from alleles showing association with schizophrenia at lesser thresholds of significance ($P > 1 \times 10^{-6}$), which do not show an interaction with ELCs (that is, PRS3–10). We analyzed RNA sequencing data from placental tissue, generated in the Epigenome Roadmap Project (GSE16368), and found relatively greater expression of the PRS1 and PRS2 genes ($N=1,643$ genes), compared with same size set of genes randomly selected from PRS3–10 genes ($N=18,029$ genes), in multiple placental tissue

Table 2 | Differential expression of schizophrenia risk genes in placenta from complicated pregnancies

Dataset	Condition	Tissue	N	P value of gene set test	χ^2 test	
					P value	χ^2
GSE24129	Pre-eclampsia	Chorionic villi	16	3.5e-04	0.002	7.93
GSE24129	IUGR	Chorionic villi	16	0.019	0.0007	10.21
GSE35574	Pre-eclampsia	Chorionic tissue	59	0.04	0.062	2.36
GSE35574	IUGR	Chorionic tissue	75	0.007	0.03	3.56
GSE10588	Pre-eclampsia	Chorionic tissue	43	0.003	0.002	8.46
GSE25906	Pre-eclampsia	Chorionic tissue	60	0.02	0.03	3.40
GSE12216	Pre-eclampsia	Chorionic tissue	16	0.01	0.01	4.82
GSE40182	Pre-eclampsia	CTB	20	0.009	0.04	3.04
GSE12767	Pre-eclampsia	First trimester chorionic villi	12	0.003	0.005	6.78
GSE25861	Pre-eclampsia/IUGR	Microvascular endothelium	8	0.006	0.04	3.002
GSE65271	CTB invasiveness	CTB	7	0.005	0.002	8.30
GSE28619	Hepatitis (liver)	Liver	22	0.136	0.10	1.70
GSE41804	Hepatitis (liver)	Liver	40	0.285	0.20 (opposite direction)	0.69
GSE27411	HP gastritis (corpus)	Stomach corpus	9	0.377	0.45	0.01
GSE27411	HP gastritis (antrum)	Stomach antrum	9	0.453	0.34	0.17
GSE42955	Dilatative cardiomyopathy	Heart	17	0.172	0.40	0.07
GSE3586	Dilatative cardiomyopathy	Heart	28	0.283	0.10 (opposite direction)	1.63
GSE4172	Dilatative cardiomyopathy	Heart	12	0.246	0.42	0.04
GSE4483	Hypoxia	Second trimester astrocytes	6	0.470	0.18	0.85
GSE26420	MIBP1 overexpression	HEK293 cells	6	0.263	0.002 (opposite direction)	8.01
GSE64699	IUGR	Adipocytes from UC-MSC lines	28	0.109	0.37	0.12

Genes mapping to loci showing the strongest association with schizophrenia (GWAS $P < 5 \times 10^{-6}$; PRS1; $P < 1 \times 10^{-4}$; PRS2) and interacting with ELCs were tested for enrichment among the differentially expressed genes in pre-eclamptic and IUGR placental samples compared with controls, and in non-invasive cytotrophoblasts (CTBs), in nine independent datasets (11 differential expression analyses: rows 1–11), and in datasets from liver, stomach (HP: *Helicobacter pylori*), heart, and cells of embryonic origins (last 10 rows). Sample sizes are reported in the fourth column. The table shows the results of the gene set test (Wilcoxon test) analysis using the moderated t -statistics from each differential expression analysis, and the χ^2 test results from the gene set enrichment analyses (see also Supplementary information, “Differential expression of schizophrenia risk genes in placenta” and “Sensitivity analyses for placental enrichment” notes). Significant results ($P < 0.05$) with consistent directionality are highlighted in bold.

compartments: amnion ($N=4$ samples, $P=1 \times 10^{-4}$), basal plate ($N=4$, $P=1 \times 10^{-4}$), chorion ($N=4$, $P=3 \times 10^{-4}$), villi ($N=4$, $P=1 \times 10^{-5}$), trophoblast ($N=4$, $P=1 \times 10^{-5}$; second trimester: $N=2$, $P=3 \times 10^{-5}$; third trimester: $N=2$, $P=1.6 \times 10^{-4}$; Supplementary Table 10). These results indicate that, as predicted, genes mapping to GWAS significant loci that interact with ELCs are more abundantly expressed in placenta than are genes in the other GWAS loci, which do not interact with ELCs.

Differential expression of schizophrenia risk-associated genes in placenta from complicated pregnancies. To elaborate on a specific role for the placenta in mediating the interaction between schizophrenia risk genes and ELCs, we next analyzed whether the PRS1 and PRS2 genes were differentially expressed in placenta from pregnancies complicated with pre-eclampsia and/or intra-uterine growth restriction (IUGR) compared with normal placental controls, and in contrast with the PRS3–10 genes. The ELCs interacting with genomic risk for schizophrenia represent heterogeneous conditions, spanning pregnancy, labor, delivery, and early neonatal life; however, ischemic disease processes, with impaired trophoblast invasion and deficient remodeling of the maternal spiral arteries, as well as an altered inflammatory response, may represent common denominators in the mechanisms underlying many ELCs^{30–32} (also including perinatal complications that are often the result of pathological processes starting during pregnancy^{30,33}). We therefore analyzed gene expression data from placenta with pre-eclampsia and IUGR, because they represent two paradigmatic placental diseases, characterized by ischemic processes, with

impaired migration of extravillous trophoblasts and impaired spiral artery remodeling^{32,34,35}, and often associated with an altered inflammatory response of the placenta^{31,36,37}. Pre-eclampsia and IUGR are multifactorial syndromes and indeed are frequently linked with many other ELCs detected in our samples, including diabetes, obesity, alcohol use, vaginal bleeding, maternal smoking, preterm birth and other adverse birth outcomes, and perinatal morbidity^{38–41}. They are themselves classic severe ELCs (severity level ≥ 4 in the McNeil–Sjöström scale) that have been linked with increased risk for schizophrenia, and also where the primary affected cells have been isolated and studied ex vivo^{38,42,43}. In analyzing eight publicly available datasets, we consistently detected enrichment of the PRS1 and PRS2 genes (Table 2 and Supplementary Table 9) among the genes differentially expressed in the fetal portion of placenta from pregnancies complicated with pre-eclampsia and IUGR, specifically in pre-eclamptic (GSE24129: $P=3.5 \times 10^{-4}$; GSE35574: 0.04; GSE10588: 0.003; GSE25906: 0.02) and IUGR (GSE24129: $P=0.019$; GSE35574: 0.007; GSE12216: 0.01) chorionic tissue from term placenta, in pre-eclamptic cytotrophoblast (GSE40182: $P=0.009$) and first trimester chorionic villi (GSE12767: $P=0.003$), and in microvascular endothelium from IUGR/pre-eclamptic pregnancies (GSE25861: $P=0.006$). We observed that PRS1 and PRS2 genes tend to be upregulated (positive t -statistics) in multiple placental samples from pre-eclampsia and IUGR, compared with placental controls (Supplementary information, see “Differential expression of schizophrenia risk genes in placenta” note). Because the PRS1 and PRS2 genes were among the highly expressed placental genes, we then performed a

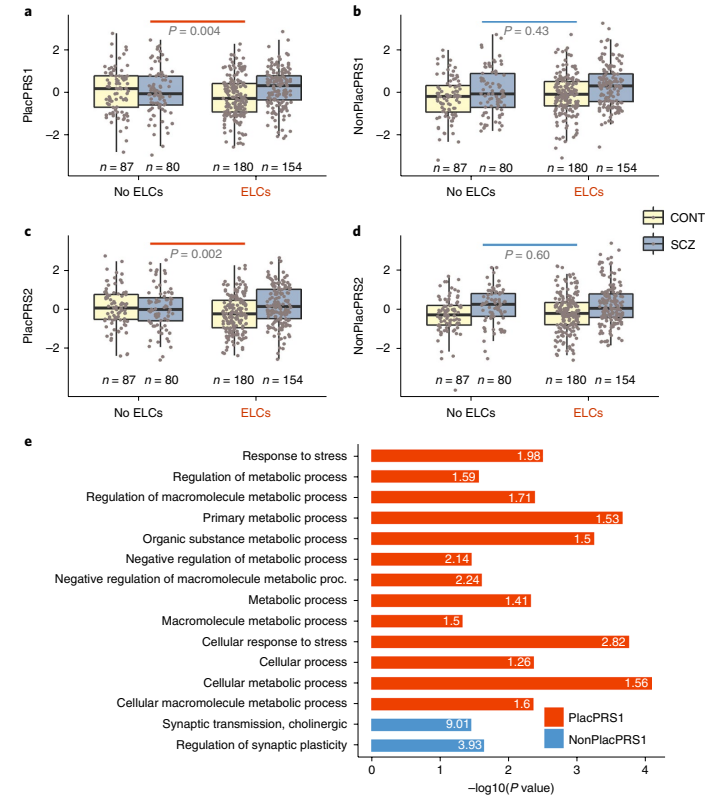


Fig. 3 | Placental and non-placental genomic risk for schizophrenia. a–d, Using GWAS SNPs marking loci containing genes highly and differentially expressed in pre-eclamptic/IUGR placental samples, we created new PRSs (PlacPRSs) and compared their interaction with ELCs with PRSs derived from the SNPs marking the remaining GWAS significant loci (NonPlacPRSs). The figure shows the interaction between PRSs and ELCs on case-control status in the US discovery sample (*scz_lie_eur*; $N=501$): shown are PlacPRS1 (**a**), NonPlacPRS1 (**b**), PlacPRS2 (**c**), and NonPlacPRS2 (**d**) of controls (CONT) and patients with schizophrenia (SCZ), in the absence of ELCs (left side of each boxplot) and in the presence of ELC history (right). Results in the other clinical samples are shown in Supplementary Figs. 7–9. All the statistics were generated using multiple logistic regression, adjusting for population stratification (ten PCs); the P values refer to the significance of the interaction of ELCs with PlacPRSs (orange lines, **a,c**) and with NonPlacPRSs (blue lines, **b,d**); boxplot centers depict median; lower and upper hinges correspond to 25th and 75th percentiles; whiskers extend from hinges to smallest and larger values no further than 1.5*IQR from the 25th and 75th percentiles. **e**, Biological processes Gene Ontology terms enriched for PlacPRS1 genes ($N=130$, orange bars) and NonPlacPRS1 genes ($N=707$, blue bars) (see also Supplementary Tables 9, 15–18 and Supplementary Figs. 10–20); bars depict negative logarithm of the P values, and white numbers within bars correspond to fold enrichment.

sensitivity analysis controlling for average gene expression level, and the results were consistent (Supplementary Table 11).

We considered the possibility that differential expression of PRS1 and PRS2 genes in complicated placenta might be a nonspecific response to pathology or stress in adult or fetal tissue. We therefore performed the same differential expression analyses on datasets from tissues with diseases likely unrelated to schizophrenia, such as hepatitis (GSE28619, GSE41804), *Helicobacter pylori* (HP) gastritis infection (GSE27411), and dilatative cardiomyopathy (GSE42955, GSE4172), as well as in datasets from embryonic cells (GSE4483, GSE26420, GSE64699). The PRS1 and PRS2 genes were not enriched among the genes

differentially expressed in the pathological compared with normal condition in any of these datasets, from adult tissues and embryonic cells (Table 2; Supplementary Table 9; and Supplementary information, see “Sensitivity analyses for placental enrichment” note).

Taken together, these results converge on the conclusion that schizophrenia GWAS significant risk-associated genes that interact with ELCs are highly expressed in the placenta during early life and dynamically modulated in the placenta during biological stress, as reflected in their differential expression in placenta from complicated pregnancies, and that these associations are relatively placental specific.

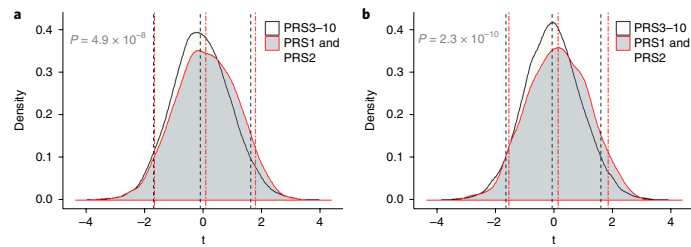


Fig. 4 | Upregulation of schizophrenia risk genes in male compared with female placentae. **a, b**, PRS1 and PRS2 genes were tested for enrichment among the differentially expressed genes in placentae from male compared with female offspring in two placental datasets (**a**: GSE35574: $N=40$, 17 females and 23 males; **b**: GSE25906: $N=37$, 16 females and 21 males). Shown are the density plots of the t -statistics, from the differential expression analysis, of PRS1 and PRS2 genes (dark gray area), and of all of the other genes in PRSs (PRS3-10, ivory area) constructed from lesser statistical thresholds (negative t -statistics = more expressed in females; positive t -statistics = more expressed in males; $P_{\text{unmoderated}}$ from the Wilcoxon 'geneSetTest' statistics at the top of the graphic). Dotted lines depict 95% confidence intervals and median of the moderated t -statistics from the differential expression analysis (multiple regression) of PRS1 and PRS2 genes (red double-dotted lines) and of PRS3-10 genes (black dotted lines).

Genes highly and differentially expressed in placenta drive the interaction between polygenic risk scores and early-life complications on schizophrenia risk.

The enrichment of expression in the placenta of genes in schizophrenia GWAS significant loci provides circumstantial evidence that the interaction of these loci with ELCs on risk for schizophrenia arises at least in part because of primary effects in the placenta. To achieve a more direct test of this possibility, we created new PRSs based on the GWAS SNPs marking loci-containing genes highly expressed in normal placentae and dynamically modulated in placentae from complicated pregnancies (Table 2 and Supplementary Table 9), and compared their interaction with ELCs with PRSs derived from the SNPs marking the remaining GWAS significant loci, first in our discovery sample (*scz_lie_eur*; Fig. 3a–d). The PRSs from the former group significantly interact with ELCs in increasing risk for schizophrenia (PlacPRS1 (PRS1 “placental” subset based on 56 SNPs): $t=2.86$, $P=0.004$; PlacPRS2 (PRS2 “placental” subset based on 112 SNPs): $t=3.10$, $P=0.002$; Fig. 3a,c), whereas those from the latter do not (NonPlacPRS1 (PRS1 “non-placental” subset based on 49 SNPs): $t=0.78$, $P=0.43$; NonPlacPRS2 (PRS2 “non-placental” subset based on 125 SNPs): $t=-0.53$, $P=0.60$; Fig. 3b,d). Similar results were found in both other case–control samples (Supplementary Figs. 7 and 8). Analyses on the merged samples of cases and controls (*scz_lie_eur*, *scz_bari_eur*, *scz_munc_eur*: $N=1,693$) confirm these results; PlacPRS1 ($t=3.19$, $P=0.0014$) and PlacPRS2 ($t=3.28$, $P=0.0011$) significantly interact with ELCs on case–control status, whereas NonPlacPRS1 and NonPlacPRS2 do not (Supplementary Fig. 9).

To verify the specificity of these interactions to placenta gene expression, we calculated PRSs based on the genes highly expressed in various adult and fetal tissues/embryonic cells, and differentially expressed in these organs during pathological/stress compared with the normal condition, employing the same procedure that we used for the computation of PlacPRSs and NonPlacPRSs (Supplementary information, see “Sensitivity analyses for placental enrichment” note). We also calculated brain PRSs, based on SNPs in PRS1 and PRS2 loci associated with methylation quantitative trait loci in adult brain²⁹ and with chromatin interaction in fetal brain²⁷. In all of these sensitivity analyses, the PRSs comprising SNPs marking loci having genes highly expressed in these diverse adult and fetal tissues, and dynamically regulated in adult and fetal brain, as in the pathology of heart, liver, and stomach, and in pathological cells of embryonic origins, do not significantly interact with ELCs on risk for schizophrenia (all $P>0.16$ after false discovery rate correction; results are

in Supplementary Tables 12–14), whereas only the SNPs mapping to the loci highly expressed and differentially expressed in placenta do.

Biological insights about placental-enriched genes associated with ELCs. Both PlacPRS1 and PlacPRS2 genes are significantly enriched for many pathways related to metabolic and cellular stress and hypoxia, particularly to “unfolded protein response”, “mitochondrial dysfunction”, and “HIF1 α signaling” (Supplementary Figs. 10 and 11; Supplementary Table 15), whereas not a single significant pathway enrichment could be obtained from the remaining PRS1 and PRS2 genes (NonPlacPRS1 and NonPlacPRS2), as well as from the whole PRS1 and PRS2 gene sets, consistent with the analogously negative results of the original analysis of the GWAS significant loci¹⁶ (Supplementary information, see “Pathway, functional and co-expression analyses” note). Notably, the pathways (Supplementary Figs. 10 and 11; Supplementary Table 15), biological functions and processes (Fig. 3e; Supplementary Figs. 12–14; Supplementary Tables 16, 17), and cellular compartments (Supplementary Figs. 15 and 16; Supplementary Table 17) implicated in PlacPRS genes are virtually orthogonal to those highlighted in other analyses of schizophrenia loci, such as synaptic function, calcium signaling, fragile X-associated proteins, and chromatin remodeling¹⁶. Interestingly, and in contrast, genes in the NonPlacPRSs do tend to implicate some of these brain-relevant functions. These results suggest that the loci containing the schizophrenia-associated genes dynamically modulated and most enriched in the placenta contribute to schizophrenia risk at least in part by influencing the fetal/placental response to stress (Supplementary Figs. 17–19), as exemplified by the cellular stress response factor HSF1^{44,45} being the main transcriptional regulator of genes in PlacPRS2 (Supplementary Fig. 18 and Supplementary Table 18). Moreover, co-expression analyses reveal that the PlacPRS1 and PlacPRS2 genes are significantly co-expressed with immune response genes, in contrast with NonPlacPRS1 and NonPlacPRS2 genes, as well as similarly sized gene sets of non-schizophrenia-associated genes in the same datasets (Supplementary Tables 19 and 20; Supplementary Fig. 20; Supplementary information, see “Pathway, functional and co-expression analyses” note).

The suggestion of a distinct and orthogonal biology for the placental component of genomic risk raises the question whether genetic prediction might be enhanced by deconstructing genomic risk into discrete subcomponents that represent alternate risk biologies. An exploratory analysis revealed that the aggregate effect on prediction accuracy of the SNPs contributing to PRS3-10

(which include PRS1 loci) is higher when separating the contribution of PRS1 (Supplementary Fig. 21; Supplementary information, see “Variance of schizophrenia liability explained by ‘decomposed’ PRSs” note for details). This is particularly true in the context of a history of ELCs, for each PRS. These results suggest that decomposing PRSs based on early environmental exposure and placental genetic risk may increase the prediction accuracy of genetic variation for schizophrenia.

Sex-specific analyses. The interaction between ELCs and genetic risk for schizophrenia is consistent with a body of literature pointing to the placenta as a mediator of stress effects on the developing brain^{7–9}. Animal studies also have shown that the outcomes of altered placental functioning on neurodevelopment are substantially sex-specific, with males more vulnerable than females to prenatal adversity⁶³. Epidemiological studies of schizophrenia suggest that incidence is higher in males than in females^{64,67}, despite the prevalence being similar across sexes², likely because of higher mortality in males⁶⁸. Consistently, most evidence suggests that males have an earlier age of onset of schizophrenia^{69,70}, which is also a predictor of a worse prognosis^{69,71}, and is plausibly linked with a higher sensitivity to early developmental risk factors. These observations raise the possibility that expression of schizophrenia risk-associated genes may be different in placentae of male compared with female offspring, and this might relate to the greater incidence of developmental disorders like schizophrenia among males^{2,32}. We therefore tested whether PRS1 and PRS2 genes, which interact with ELCs on case–control status, are differentially expressed in placentae from male compared with female offspring. Analyses on placental samples from the two datasets with sex information revealed that PRS1 and PRS2 genes are highly significantly enriched among the genes differentially expressed, and specifically upregulated, in placentae from male compared with female offspring (GSE35574: $N=40$, 17 females and 23 males, $P=4.9 \times 10^{-8}$, Fig. 4a; GSE25906: $N=37$, 16 females and 21 males, $P=2.3 \times 10^{-10}$; Fig. 4b). In the same datasets, the relative upregulation was also present in male pre-eclamptic placentae (GSE35574: $P=0.01$; GSE25906: $P=0.001$). Analogous analyses in a heart dataset (GSE4172) and a fetal lung dataset (GSE14334) with sex information did not reveal upregulation of the PRS1 and PRS2 genes in males compared with females ($P>0.40$; Supplementary information, see “Sensitivity analyses for placental enrichment” note). These data suggest a sex-biased role for the placenta in expressing genetic risk for schizophrenia.

Discussion

In this study, we show that exposure to ELCs represents an early environmental context that influences cumulative genomic risk for schizophrenia derived from GWAS significant loci. More to the point, the set of genes within these genomic loci that show interaction with intra-uterine and perinatal complications is highly expressed in placenta, and the same set of genes displays differential enrichment in this organ in abnormal invasive placental states. These results suggest that the most significant genetic variants detected by current GWASs¹⁶ contribute to risk for schizophrenia at least partly by converging on a developmental trajectory sensitive to intra-uterine and perinatal adversity, and linked with abnormal placental. Moreover, the strikingly relative enrichment of expression of schizophrenia risk genes in placenta from male compared with female offspring suggests that gene–environment interactions influencing placental biology may contribute to the higher incidence of schizophrenia in males compared with females⁶.

Our results indicate a link between placental biology, ELCs, and schizophrenia, even as the syndrome is diagnosed during early adult life, which resonates with a broader evolutionary perspective and the developmental trajectory of schizophrenia. Schizophrenia is thought to be a condition on which the human species has a

monopoly, and the delayed emergence of the clinical disorder has been posited to reflect the relatively late maturation of highly evolved neural functions, such as prefrontal cortical circuitry¹¹. Interestingly, the evolutionary complexity of the primate placenta shows parallels with the phylogenetically remarkable expansion of the human brain, particularly prefrontal cortical regions that are among the most affected in schizophrenia^{33,34}; both placental complexity and brain expansion come with higher rates of ELCs in humans than in other species^{33,35}. Our results are consistent with the possibility that some of the common genes implicated in schizophrenia risk—through diverse biological mechanisms—regulate the physiology of the placenta, the risk of ELCs, and thereby secondarily the development of the brain, potentially interacting with other mechanisms of gene regulation acting primarily within fetal brain^{27,36}.

Despite many studies that have stressed the role of prenatal development and early-life events in affecting risk for brain disorders like schizophrenia^{3,12,13,37}, as well as autism^{38,39}, the mechanisms by which this may have been elusive. Genetic research has been successfully focused on detecting GWAS significant variants, but the difficulty of collecting environmental data has hindered defining the developmental context in which these common variants may have their critical effects. Our results underscore the importance of assessing early environmental factors such as obstetrical complications, in addition to genetic risk, to fully investigate their joint effect on susceptibility to neurodevelopmental disorders. Our results also point to the placenta as a crucial mediator of this interaction in relation to schizophrenia in particular, but likely to other neurodevelopmental disorders in general, underscoring the need for further research on placenta physiology in the context of brain development and genomic risk. Pursuing this path should advance the role of prenatal care for reducing the burden of psychiatric illness and may identify new strategies⁶⁰ for placental health as a form of primary prevention of schizophrenia, perhaps particularly in males with high genetic risk.

Methods

Methods, including statements of data availability and any associated accession codes and references, are available at <https://doi.org/10.1038/s41591-018-0021-y>.

Received: 30 August 2017; Accepted: 16 March 2018;

Published online: 28 May 2018

References

- Saha, S., Chant, D., Welham, J. & McGrath, J. A systematic review of the prevalence of schizophrenia. *PLoS Med.* **2**, e141 (2005).
- McGrath, J., Saha, S., Chant, D. & Welham, J. Schizophrenia: a concise overview of incidence, prevalence, and mortality. *Epidemiol. Rev.* **30**, 67–76 (2008).
- Sullivan, P. F. The genetics of schizophrenia. *PLoS Med.* **2**, e212 (2005).
- Lichtenstein, P. et al. Common genetic determinants of schizophrenia and bipolar disorder in Swedish families: a population-based study. *Lancet* **373**, 234–239 (2009).
- Patterson, P. H. Neuroscience. *Maternal effects on schizophrenia risk.* *Science* **318**, 576–577 (2007).
- Gottesman, I. I. & Wolfgram, D. L. *Schizophrenia Genesis: The Origins of Madness* (Freeman, 1991).
- Mikaelsson, M. A., Constancia, M., Dent, C. L., Wilkinson, L. S. & Humby, T. Placental programming of anxiety in adulthood revealed by Igf2-null models. *Nat. Commun.* **4**, 2311 (2013).
- Bronson, S. L. & Bale, T. L. Prenatal stress-induced increases in placental inflammation and offspring hyperactivity are male-specific and ameliorated by maternal antiinflammatory treatment. *Endocrinology* **155**, 2635–2646 (2014).
- Bronson, S. L. & Bale, T. L. The placenta as a mediator of stress effects on neurodevelopmental programming. *Neuropsychopharmacology* **41**, 207–218 (2016).
- Bonnin, A. & Levitt, P. Placental source for 5-HT that tunes fetal brain development. *Neuropsychopharmacology* **37**, 299–300 (2012).
- Weinberger, D. R. From neuropathology to neurodevelopment. *Lancet* **346**, 552–557 (1995).

12. Brown, A. S. & Derkots, E. J. Prenatal infection and schizophrenia: a review of epidemiologic and translational studies. *Am. J. Psychiatry* **167**, 261–280 (2010).
13. Cannon, M., Jones, P. B. & Murray, R. M. Obstetric complications and schizophrenia: historical and meta-analytic review. *Am. J. Psychiatry* **159**, 1080–1092 (2002).
14. Nicodemus, K. K. et al. Serious obstetric complications interact with hypoxia-regulated/vascular-expression genes to influence schizophrenia risk. *Mol. Psychiatry* **13**, 873–877 (2008).
15. Schmidt-Kastner, R., van Os, J., Esquivel, G., Steinbusch, H. W. & Rutten, B. P. An environmental analysis of genes associated with schizophrenia: hypoxia and vascular factors as interacting elements in the neurodevelopmental model. *Mol. Psychiatry* **17**, 1194–1205 (2012).
16. Schizophrenia Working Group of the Psychiatric Genomics Consortium. Biological insights from 108 schizophrenia-associated genetic loci. *Nature* **511**, 421–427 (2014).
17. Stefansson, H. et al. Common variants conferring risk of schizophrenia. *Nature* **460**, 744–747 (2009).
18. Ingason, A. et al. Copy number variations of chromosome 16p13.1 region associated with schizophrenia. *Mol. Psychiatry* **16**, 17–25 (2011).
19. Purcell, S. M. et al. A polygenic burden of rare disruptive mutations in schizophrenia. *Nature* **506**, 185–190 (2014).
20. International Schizophrenia Consortium et al. Common polygenic variation contributes to risk of schizophrenia and bipolar disorder. *Nature* **460**, 748–752 (2009).
21. Wray, N. R., Goddard, M. E. & Visscher, P. M. Prediction of individual genetic risk to disease from genome-wide association studies. *Genome Res.* **17**, 1520–1528 (2007).
22. McNeil, T. F. et al. Obstetric complications in histories of monozygotic twins discordant and concordant for schizophrenia. *Acta Psychiatr. Scand.* **89**, 196–204 (1994).
23. McNeil, T. F., Cantor-Graae, E. & Sjöström, K. Obstetric complications as antecedents of schizophrenia: empirical effects of using different obstetric complication scales. *J. Psychiatr. Res.* **28**, 519–530 (1994).
24. Ursini, G. et al. Stress-related methylation of the catechol-O-methyltransferase Val 158 allele predicts human prefrontal cognition and activity. *J. Neurosci.* **31**, 6692–6698 (2011).
25. Verdoux, H., Sutter, A. L., Glatigny-Dallay, E. & Minisini, A. Obstetrical complications and the development of postpartum depressive symptoms: a prospective survey of the MATQUID cohort. *Acta Psychiatr. Scand.* **106**, 212–219 (2002).
26. Wall, J. D. & Pritchard, J. K. Haplotype blocks and linkage disequilibrium in the human genome. *Nat. Rev. Genet.* **4**, 587–597 (2003).
27. Won, H. et al. Chromosome conformation elucidates regulatory relationships in developing human brain. *Nature* **538**, 523–527 (2016).
28. Jaffe, A. E. et al. Developmental regulation of human cortex transcription and its clinical relevance at single base resolution. *Nat. Neurosci.* **18**, 154–161 (2015).
29. Jaffe, A. E. et al. Mapping DNA methylation across development, genotype and schizophrenia in the human frontal cortex. *Nat. Neurosci.* **19**, 40–47 (2016).
30. Burton, G. J. & Jauniaux, E. The cytotrophoblastic shell and complications of pregnancy. *Placenta* **60**, 134–139 (2017).
31. Cotichini, T. & Graham, C. H. Aberrant maternal inflammation as a cause of pregnancy complications: a potential therapeutic target?. *Placenta* **36**, 960–966 (2015).
32. Maltepe, E. & Fisher, S. J. Placenta: the forgotten organ. *Annu. Rev. Cell Dev. Biol.* **31**, 523–552 (2015).
33. Maltepe, E., Bakardjiev, A. I. & Fisher, S. J. The placenta: transcriptional, epigenetic, and physiological integration during development. *J. Clin. Invest.* **120**, 1016–1025 (2010).
34. Leavey, K. et al. Unsupervised placental gene expression profiling identifies clinically relevant subclasses of human preeclampsia. *Hypertension* **68**, 137–147 (2016).
35. Redman, C. Pre-eclampsia: a complex and variable disease. *Pregnancy Hypertens.* **4**, 241–242 (2014).
36. Ferguson, K. K., Meeker, J. D., McElrath, T. F., Mukherjee, B. & Cantonwine, D. E. Repeated measures of inflammation and oxidative stress biomarkers in pre-eclamptic and normotensive pregnancies. *Am. J. Obstet. Gynecol.* **216**, 527.e521–527.e529 (2017).
37. Redman, C. W., Sacks, G. P. & Sargent, I. L. Preeclampsia: an excessive maternal inflammatory response to pregnancy. *Am. J. Obstet. Gynecol.* **180**, 499–506 (1999).
38. Hwang, S. S. et al. Maternal substance use disorders and infant outcomes in the first year of life among Massachusetts singletons, 2003–2010. *J. Pediatr.* **191**, 69–75 (2017).
39. Mol, B. W. J. et al. Pre-eclampsia. *Lancet* **387**, 999–1011 (2016).
40. Lisonkova, S. & Joseph, K. S. Incidence of preeclampsia: risk factors and outcomes associated with early- versus late-onset disease. *Am. J. Obstet. Gynecol.* **209**, 544.e541–544.e512 (2013).
41. Wollmann, H. A. Intrauterine growth restriction: definition and etiology. *Horm. Res.* **49** (Suppl. 2), 1–6 (1998).
42. Dalman, C., Allebeck, P., Cullberg, J., Grunevald, C. & Koster, M. Obstetric complications and the risk of schizophrenia: a longitudinal study of a national birth cohort. *Arch. Gen. Psychiatry* **56**, 234–240 (1999).
43. Byrne, M., Agerbo, E., Bennedson, B., Eaton, W. W. & Mortensen, P. B. Obstetric conditions and risk of first admission with schizophrenia: a Danish national register based study. *Schizophr. Res.* **97**, 51–59 (2007).
44. Xiao, X. et al. HSF1 is required for extra-embryonic development, postnatal growth and protection during inflammatory responses in mice. *EMBO J.* **18**, 5943–5952 (1999).
45. Hashimoto-Torii, K. et al. Roles of heat shock factor 1 in neuronal response to fetal environmental risks and its relevance to brain disorders. *Neuron* **82**, 560–572 (2014).
46. McGrath, J. et al. A systematic review of the incidence of schizophrenia: the distribution of rates and the influence of sex, urbanicity, migrant status and methodology. *BMC Med.* **2**, 13 (2004).
47. Aleman, A., Kahn, R. S. & Selten, J. P. Sex differences in the risk of schizophrenia: evidence from meta-analysis. *Arch. Gen. Psychiatry* **60**, 565–571 (2003).
48. Hjorthøj, C., Sturup, A. E., McGrath, J. J. & Nordentoft, M. Years of potential life lost and life expectancy in schizophrenia: a systematic review and meta-analysis. *Lancet Psychiatry* **4**, 295–301 (2017).
49. Ochoa, S., Usall, J., Cobo, J., Labad, X. & Kulkarni, J. Gender differences in schizophrenia and first-episode psychosis: a comprehensive literature review. *Schizophr. Res. Treatment* **2012**, 916198 (2012).
50. Abel, K. M., Drake, R. & Goldstein, J. M. Sex differences in schizophrenia. *Int. Rev. Psychiatry* **22**, 417–428 (2010).
51. Angermeyer, M. C., Kühn, L. & Goldstein, J. M. Gender and the course of schizophrenia: differences in treated outcomes. *Schizophr. Bull.* **16**, 293–307 (1990).
52. Bloom, B., Cohen, R. A. & Freeman, G. Summary health statistics for U.S. children: National Health Interview Survey, 2010. *Vital Health Stat.* **10**, 1–80 (2011).
53. Burton, G. J., Moffett, A. & Keverne, B. Human evolution: brain, birthweight and the immune system. *Philos. Trans. R. Soc. Lond. B Biol. Sci.* **370**, 20140061 (2015).
54. Teffer, K. & Semendeferi, K. Human prefrontal cortex: evolution, development, and pathology. *Prog. Brain Res.* **195**, 191–218 (2012).
55. Rosenberg, K. R. & Trevathan, W. R. An anthropological perspective on the evolutionary context of preeclampsia in humans. *J. Reprod. Immunol.* **76**, 91–97 (2007).
56. Sekar, A. et al. Schizophrenia risk from complex variation of complement component 4. *Nature* **530**, 177–183 (2016).
57. Niemela, S. et al. Prenatal nicotine exposure and risk of schizophrenia among offspring in a national birth cohort. *Am. J. Psychiatry* **73**, 799–806 (2016).
58. Glasson, E. J. et al. Perinatal factors and the development of autism: a population study. *Arch. Gen. Psychiatry* **61**, 618–627 (2004).
59. Stoner, R. et al. Patches of disorganization in the neocortex of children with autism. *N. Engl. J. Med.* **370**, 1209–1219 (2014).
60. Ross, R. G. et al. Perinatal phosphatidylcholine supplementation and early childhood behavior problems: evidence for CHRNA7 moderation. *Am. J. Psychiatry* **173**, 509–516 (2016).

Acknowledgements

We are grateful to the Lieber and Maltz families for their visionary support that funded the analytic work of this project. We thank all of the participants in the study and their families. We thank Joo Heon Shin for help with the gene expression analyses, and Barbara Gelao, Marina Mancini, Raffaella Romano, Rita Masellis, and Grazia Caforio for help with data acquisition. We also thank Sally Cheung and John Meyer for data management, and Susan Fisher for guidance with placental datasets and review of the manuscript. We thank the Psychiatric Genomics Consortium for providing the statistics for PRS calculation, and Thomas F. McNeil for providing the scale for ELC scoring. We also thank all of the authors of the publicly available placental datasets that have been used in this study. The collection of the ELC and genetic data for the American samples was supported by direct funding from the Intramural Research Program of the NIMH to the Clinical Brain Disorders Branch (D.R.W., PI, protocol 95-M-0150, NCT00001486, annual report number: ZIA MH002942-05), with supplemental analytic support from the Clinical and Translational Neuroscience Branch (K.F.B., PI). G.U. received partial support from P50MH094268. The collection of ELCs and genetic data for the Italian sample has been supported by the NARSAD grant no. 20337 and the “Ricerca Finalizzata” grant no. PE-2011-02347951 (both awarded to A.B.). The GRAS data collection has been supported by funding from the Max Planck Society, the Max Planck Förderstiftung, the DFG (CNMPB), EXTRABRAIN EU-FP7, and the Niedersachsen-Research Network on Neuroinfectology (N-RENNT) (to H.E.).

Author contributions

G.U., G.P., and D.R.W. designed the study and interpreted the results. G.U., G.P., J.E.R., E.G.H., A.E.J., and C.C. carried out statistical analyses. G.U., Q.C., M.M., R.E.S., H.E., and D.R.W. organized and performed genotyping, imputation, and risk profile scoring. G.U., S.M., M.B., J.S., K.F.B., M.F.E., R.E.S., G.B., R.H., D.R., H.E., A.B., and D.R.W. organized and carried out subject recruitment and biological material collection in the discovery sample and in the replication samples, whereas G.U., G.P., S.M., A.P., G.M., M.B., H.Y., R.H., D.R., and H.E. carried out ELC assessment. J.E.R. and E.G.H. contributed to the collection of the placental tissue used in the RNA-sequencing analysis and, together with G.U., G.P., C.C., and D.R.W., interpreted the results of the gene set enrichment analyses in placental samples from complicated pregnancies compared with controls. G.U., G.P., and D.R.W. drafted the manuscript, and all authors contributed to the final version of the paper.

Competing interests

The authors declare no competing interests.

Additional information

Supplementary information is available for this paper at <https://doi.org/10.1038/s41591-018-0021-y>.

Reprints and permissions information is available at www.nature.com/reprints.

Correspondence and requests for materials should be addressed to D.R.W.

Publisher's note: Springer Nature remains neutral with regard to jurisdictional claims in published maps and institutional affiliations.

Methods

Compliance with ethical requirements All procedures performed in the clinical samples were in accordance with the ethical standards of the institutional research committees and with the 1964 Declaration of Helsinki and its later amendments or comparable ethical standards. Informed consent was obtained from all individual participants included in this study.

Samples and genotyping.

- Discovery sample (USA):** *scz_lie_eur*. A total of 501 Caucasian unrelated adult subjects, with good-quality genetics data and ELC history information (as described later), were selected from participants in the Clinical Brain Disorders Branch Sibling Study of Schizophrenia at the National Institute of Mental Health (NIMH; Clinical Brain Disorders Branch, protocol 95-M-0150, NCT00001486, Annual Report number: ZIA MH002942-05). The sample included 234 patients who met *Diagnostic and Statistical Manual of Mental Disorders*, Fourth Edition (DSM-IV) criteria for schizophrenia and 267 healthy subjects (see Supplementary Table 2 for details). The Institutional Review Board of the NIMH Intramural Program approved the study, and written informed consent was obtained from the participants after complete description of the study. Exclusion and inclusion criteria have been previously reported⁴¹. Genotyping was done using Illumina BeadChips (510/610/660/2.5).
- First replication sample (Italy):** *scz_lie_eur*. A total number of 273 Italian Caucasian unrelated adult subjects from the Region of Puglia, Italy (91 schizophrenia cases and 182 controls; see Supplementary Table 2 for details) with availability of genetics data and ELC history information, similar to the discovery sample, entered the study. The Institutional Review Board of University of Bari ‘Aldo Moro’, Bari (Italy), approved protocols and procedures, and written informed consent was obtained from the participants after complete description of the study. Exclusion and inclusion criteria were similar to the discovery sample, as reported elsewhere⁴². Genotyping was done using Illumina BeadChips (510/610/660/2.5).
- Second replication sample (Germany):** *scz_munc_eur*. A total of 919 Caucasian unrelated adult subjects entered the study (521 schizophrenia cases and 298 controls; see Supplementary Table 2 for details). Cases were ascertained from the Munich area of Germany, as described previously⁴³. The controls were unrelated volunteers randomly selected from the general population of Munich. All were screened to exclude a history of psychosocial/central neurological disease either personally or in a first-degree relative. All participants gave written informed consent, and the ethic committee of the Ludwig Maximilians University, Munich (Germany), approved the human subjects protocols. Genotyping was done with the Illumina 317 K array.
- Third replication sample (Germany):** *scz_gras_eur*. The GRAS collection included 1,020 unrelated adult patients with schizophrenia (see Supplementary Table 2 for details), recruited across 23 German hospitals. Cases completed a structured clinical interview and were diagnosed with DSM-IV schizophrenia or schizoaffective disorder⁴⁴. The study was approved by the Georg-August-University ethics committee and Ethics Committee of the University of Göttingen, Göttingen (Germany). All participants gave written informed consent. Genotyping was done with a semiautomated Axiom myDesign genotyping array (Affymetrix, Santa Clara, CA, USA), based on a CEU (Caucasian residents of European ancestry from Utah, USA) marker backbone and a custom marker set.
- Fourth replication sample (Eastern Asia):** *scz_osak_asi*. A total of 172 Japanese unrelated adult patients who met DSM-IV criteria for schizophrenia (see Supplementary Table 2 for details) with availability of genetics data and ELC exposure information, similar to the discovery sample, entered the study. The Institutional Review Board of University of Osaka, Osaka (Japan), approved protocols and procedures, and written informed consent was obtained from the participants after complete description of the study. Exclusion and inclusion criteria were similar to the other samples⁴⁵. Genotyping of this sample was done using the Affymetrix Genome-Wide Human SNP Array 6.0 (Affymetrix, Santa Clara, CA, USA).

Quality control for genotyping. Quality control was performed using PLINK (version 1.07; <http://pngu.mgh.harvard.edu/purcell/plink/>), consistent with previous reference, for the *scz_lie_eur*, *scz_bari_eur*, *scz_munc_eur*, and *scz_osak_asi* samples⁴⁶. Participants with missing rate higher than 2% and extreme heterozygosity values (± 3 s.d.) were removed. SNPs with missing rate higher than 2% and difference in missingness between cases and controls > 0.02 were also removed. In addition, SNPs were excluded if they failed Hardy–Weinberg equilibrium ($P < 10^{-4}$ in controls or $P < 10^{-10}$ in cases) and if they had minor allele frequency less than 1%. Prephasing was done before imputation using SHAPEIT, and imputation was done using IMPUTE2 with Phase 1 1000 genome as the reference panel^{47,48}. The quality-control procedure in the *scz_gras_eur* sample was consistent with the other samples, as described previously⁴⁹.

Derivation of polygenic risk profile scores. Cumulative genetic risk profile scores (PRSs)⁵¹ were calculated for each individual, as described elsewhere⁵². In brief, PRSs are a measure of genomic risk⁵¹ calculated as the weighted sum of risk alleles

for schizophrenia from the recent GWAS study^{49,50}. We thus multiplied the natural log of the OR of each index SNP, from this recent schizophrenia GWAS⁴⁹, by the imputation probability for the corresponding reference allele at each variant, and summed the products over all variants, so that each subject had whole genome PRSs as originally described for this measure^{51,52}. The PGC provided ORs and index SNPs for each sample. For the *scz_lie_eur* sample, ORs and 102K index SNPs were derived from a meta-analysis of PGC GWAS datasets excluding our discovery sample (PGC 2014, non-*scz_lie_eur* PGC GWAS⁴⁹). Consistently, for the *scz_munc_eur* and the *scz_gras_eur* samples (also included in the PGC GWAS⁴⁹), ORs and index SNPs were derived from a meta-analysis of PGC GWAS datasets, excluding, respectively, the *scz_munc_eur* and the *scz_gras_eur* samples. For the *scz_bari_eur* and *scz_osak_asi* samples, ORs and index SNPs were derived from the PGC GWAS datasets, because these samples are not included in the PGC GWAS dataset⁴⁹. Consistent with the standard procedure for PRS calculation^{51,52}, only autosomal SNPs were included in the analysis, to prevent any bias related to sex in the PRS calculation. We performed a linkage disequilibrium (LD) pruning and clumping of the SNPs, discarding variants within 500 kb of, and in $r^2 \geq 0.1$ with, another (more significant) marker, as reported elsewhere^{53,54}. Ten PRSs (PRS1–10) were calculated using subsets of SNPs selected according to the GWAS P value thresholds of association with schizophrenia: 5e–08 (PRS1), 1e–06 (PRS2), 1e–04 (PRS3), 0.001 (PRS4), 0.01 (PRS5), 0.05 (PRS6), 0.1 (PRS7), 0.2 (PRS8), 0.5 (PRS9), and 1 (PRS10). SNPs in sets with lower P values are also in sets with higher P values (for example, SNPs in PRS1 are included in PRS2, SNPs in PRS2 are included in PRS3, and so on). A detailed list of SNPs included in PRS1 and PRS2 is provided in Supplementary Table 1. We performed all of the analyses both including and excluding the top GWAS significant SNP in the extended MHC locus (hg19 coordinates: chr6: 25–34 Mb), with similar results (Supplementary Table 4). For additional analyses (Supplementary Fig. 21; Supplementary information, see ‘‘Variance of schizophrenia liability explained by decomposed PRSs’’ note), we also calculated PRSs from sets of SNPs with higher P values (PRS2–10) without including SNPs in sets with the lowest P values (PRS1).

Assessment of early-life complications. ELCs are here referred to as ‘‘somatic complications and conditions occurring during pregnancy, labor-delivery and the neonatal period’’ potentially harmful for the offspring, with special focus on the central nervous system⁵⁵. These events are also referred to elsewhere as ‘‘obstetric complications’’^{14,22,23} and, despite their potential frequent occurrence⁵⁶, do not lead to negative outcomes in most cases. We assessed ELCs through medical records, when available, and personal interviews, described as follows:

- scz_lie_eur*, and *scz_bari_eur*.** We used mainly manual recall based on an extensive personal interview, which was repeatedly shown to represent a reliable method for obtaining ELC history, when used in a careful and detailed manner^{27,72}. Specifically, we used a well-standardized and validated questionnaire⁵⁷, based on all the items scored with the McNeil–Sjöström scale for obstetric complications^{22,53}. It covers the entire duration of pregnancy and early neonatal life, and also contains indicators of reliability and an assessment of the seriousness of each complication.
- scz_osak_asi*.** We used mainly medical records. When medical records were not exhaustive, we interviewed the mothers of the patients; the histories were again scored directly based on the McNeil–Sjöström metrics⁵³.
- scz_munc_eur* and *scz_gras_eur*.** We used medical records, including all the discharge letters of patients, and personal interviews. Differently from the questionnaires used in the other samples, these interviews did not contain all the items included in the McNeil–Sjöström scale⁵³, thus increasing the risk for incomplete information. History of ELCs from the available information was again scored using the McNeil–Sjöström scale⁵³.

In the McNeil–Sjöström scale^{22,53} each ELC is assigned a severity level of 1–6, based on the degree of inferred potential harm to the offspring central nervous system. ELCs with severity weight ≥ 4 are considered potentially clearly harmful or relevant factors in fetal stress. The McNeil–Sjöström scale in the context of maternal recollection has been well validated in comparison with hospital records⁵⁷. As in other reports^{22,23,53}, we defined a positive history of ELCs based on the presence of at least one serious ELC (severity level ≥ 4), and we identified the severity level of each individual as the highest severity level of all of the ELCs occurring in that individual. GWAS-derived PRSs were unknown to both the individuals who provided the information about ELCs and to the researchers who collected and evaluated them. Individuals were excluded if the information provided was incomplete or inconsistent (for example, contradictory answers to related questions), or if the presence of a complication was certain but a severity weight could not be confidently determined. The frequency of ELCs in our samples may be not representative of the general populations (Supplementary information, see ‘‘Considerations about the assessment and the frequency of early life complications (ELCs)’’ note). Supplementary Table 21 contains a list of the ELCs detected in each sample.

Statistical analysis of the interaction between polygenic risk scores and early-life complications on case–control status. All statistical analyses were performed in the ‘R’ environment⁵⁸. To test the central hypothesis of this study (that is, the interaction between PRS1 and ELCs on case–control status),

we used multiple logistic regression, with the following model: Diagnosis ~ PRS + ELCs + PRS * ELCs + covariates. We also used multiple logistic regressions to confirm the association of each PRS with case–control status in our samples (Diagnosis ~ PRS + covariates) and to verify whether ELCs were associated with schizophrenia (Diagnosis ~ ELCs + covariates). In the presence of an interaction between PRS and ELCs, we performed post hoc analyses to evaluate the relationship between PRS and case–control status, in the presence and absence of ELC history (that is, stratifying the sample, based on ELC history), using the same model described earlier (Diagnosis ~ PRS + covariates). For all of these analyses, we report in the main text the P values and the t -statistics associated with our variable of interest (that is, PRS * ELCs, or PRS). To evaluate goodness of fit of these logistic models (Diagnosis ~ PRS + covariates) in the whole sample, in the absence and presence of ELC history, we calculated the Nagelkerke R^2 , by comparison of a full model (covariates + PRS) with a reduced model (covariates only). Similarly, in the presence of an interaction between PRS and ELCs on case–control status, we performed post hoc analyses to test the relation between PRS and ELCs, separately in controls and in patients with schizophrenia (that is, after stratifying the sample for diagnosis), using multiple logistic regression (ELC history ~ PRS + covariates). Consistently with the interaction between PRS and ELCs, we found a positive relation between PRS and ELCs only in patients with schizophrenia; we further explored this relationship in the two replication samples of only patients (*scz_gras_eur*, *scz_osak_asi*). In each analysis, we used 10 ancestry-based principal components as covariates, to avoid potential confounding effects of population stratification, consistent with previous work⁴⁹. We performed sensitivity analyses adding sex, age, maternal and paternal ages, maternal stress, history of substance use, and socioeconomic status, as covariates, and also their interaction with PRS and ELCs, as recommended to properly exclude the role of confounders⁵⁹. We also performed sensitivity analyses, in each sample, by excluding the individuals with mothers with a history of substance use. Results were consistent and are reported in Supplementary Tables 6–8. For the analyses in the merged sample, PRS scores were normalized by subtracting the mean and dividing for the s.d. in each sample; for this analysis, we added the sample as a covariate.

Selection of PRS1 and PRS2 genes. To define genes mapping to the PRS1 and PRS2 loci for gene set analyses, we used two alternative criteria:

- PGC LD regions:** We considered, as PRS1 and PRS2 genes, all of the University of California, Santa Cruz (UCSC) genes overlapping the LD regions associated with each SNP ($R^2 > 0.6$), as reported in a previous reference⁶⁰ and on the PGC website (<http://www.med.unc.edu/pgc/downloads/>);
- Distance:** We considered, as PRS1 and PRS2 genes, all of the UCSC genes mapping 500 kb \pm the index SNPs of each PRS in the discovery sample (*scz_lie_eur*). We use this criterion, in addition to the ‘‘traditional’’ LD criterion, on the grounds that LD differs among populations, as we analyzed multiple samples. Moreover, the LD regions associated with each SNP have a huge variability; for example, 2 out of the 108 GWAS significant schizophrenia-risk SNPs have an LD region that spans only 1 bp (rs4766428, rs117074560)⁶⁰. Further, it has been shown that GWAS SNPs are often associated with expression of genes that are not their nearest genes and are outside the associated LD regions^{60,73}. Finally, the distance of 500 kb \pm the index SNPs is within the range commonly used for detection of cis-expression quantitative trait loci (eQTLs)⁷⁴ and is the same dimension used to calculate PGC loci eQTL in the original PGC report⁴⁹. This criterion allowed us to distribute 21,028 out of 23,056 UCSC genes among the 10 PRSs.

Differences between the two list of genes (reported in Supplementary Table 9a,b) are related not only to the criterion adopted for SNP selection (distance or LD), but also to the fact that the PGC loci associated with schizophrenia at $P < 5 \times 10^{-8}$ are defined based on combining the primary GWAS and the supplementary deCODE data, whereas SNPs for PRS calculation are derived from the primary GWAS only⁴⁹. Because only SNPs mapping to autosomal chromosomes are used for schizophrenia PRS construction^{49,50}, we excluded from our analysis genes that were irrelevant to our question, that is, genes mapping to mitochondrial DNA, and X- and Y-chromosome genes or other genes mapping to loci not used for PRS calculation. After exclusion of the genes on sex chromosomes and on mitochondrial DNA, and genes undetected in the expression datasets analyzed, the final number of PRS1 and PRS2 genes was 1,643 in the list based on distance (matching 325 out of the 348 genes assigned to the 108 schizophrenia GWAS significant loci⁴⁹), and 589 in the gene list based on LD (matching 334 out of the 348 genes assigned to the 108 schizophrenia GWAS significant loci⁴⁹). In both gene lists, PRS1 genes are a subset of PRS2 genes (therefore referred in the text as PRS1 and PRS2 genes). We performed all of the gene set analyses, with PRS1 and PRS2 genes defined with both criteria (LD and distance), and found consistent results (Supplementary Table 9). In the main text, we report results with the PRS1 and PRS2 genes defined based on the distance criterion (Table 2).

Expression of PRS1 and PRS2 genes in placenta. The proprietary placental tissue used for this analysis was collected at the University of California, San Francisco. Methods of collection were approved by the University of California, San Francisco Institutional Review Board, and informed consent was obtained from all donors. The RNA-sequencing datasets related to second trimester and term placental tissues (amion, basal plate, chorion, villi) and isolated cells (trophoblasts) are

publicly available (GSE16368) on the National Institutes of Health Roadmap Epigenomics Project website (<http://www.roadmapepigenomics.org/>). Expression levels of each gene were quantified by determining reads per kilobase of transcript per million values⁷⁵. Based on our primary hypothesis and on the fact that PRS1 and PRS2 risk SNPs are associated with expression of nearby genes across many different tissues (Supplementary information, see ‘‘Screening of PRS1 and PRS2 SNPs for eQTLs across different tissues’’), we tested whether the genes mapping to the loci showing the strongest association with schizophrenia and interacting with ELCs are more expressed in placenta compared with randomly selected genes contributing to the other PRSs constructed from alleles showing association with schizophrenia at lesser thresholds of significance, which do not show an interaction with ELCs. To perform this analysis, we used the function ‘geneSetTest’ in the R package ‘limma’⁷⁶, using the gene expression data from the RNA-sequencing analysis in placenta. With this function, we calculated a P value from a Wilcoxon test to verify the hypothesis that the selected set of genes (PRS1 and PRS2) tends to be more highly ranked in expression compared with randomly selected sets of genes of the same size (from the PRS3–10 genes). Results are reported in Supplementary Table 10. We also performed a further analysis testing the enrichment of the genes overlapping the PRS1 and PRS2 loci using the function ‘findOverlaps’ in the R package ‘GenomicRanges’⁷⁷ (either including or excluding genes with reads per kilobase of transcript per million expression > 0.01) and, as predictable, we obtained similar results.

Differential expression of PRS1 and PRS2 genes in placenta from complicated pregnancies. We searched for enrichment of the PRS1 and PRS2 genes among genes differentially expressed in placental samples from complicated pregnancies compared with controls. We interrogated placental datasets from the Gene Expression Omnibus public repository. Datasets were chosen for analysis if they included all of the following: a comparison between placental samples from complicated pregnancies and controls, more than one sample per group (that is, comparisons between pooled RNA samples were discarded), and expression data for at least half of the PRS genes. We found eight datasets that met these criteria, comparing control versus diseased (pre-eclampsia and IUGR) placenta cells. A dataset on normal cultured cytotrophoblasts was also chosen as cells were induced into different states of invasiveness. Because two of these datasets contain a comparison of controls versus pre-eclamptic and controls versus IUGR placenta, we were able to perform 11 differential expression analyses. In each dataset, we dropped probes that map to multiple genes and, when more than one probe per gene was present, we selected the one with the highest mean expression. We used the function ‘eBayes’ in the R package ‘limma’⁷⁶ to attribute a moderated t -statistic to each gene related to differential expression (using the covariates provided by each reporting group); then we applied the ‘geneSetTest’ function on the moderated t -statistics (results are reported in Table 2) testing whether the selected set of genes (that is, those related to PRS1 and PRS2) tends to be more highly ranked in differential expression compared with randomly selected genes of the same size from the other GWAS loci (PRS3–10). We also used a χ^2 test to confirm whether PRS1 and PRS2 genes were enriched for differentially expressed genes compared with the remaining genes (Table 2).

We chose different thresholds for gene expression to exclude that low-expressed genes could affect the significance of the results. Also, because PRS1 and PRS2 genes are relatively highly expressed in placenta, we performed sensitivity analysis, adjusting for average gene expression: for this purpose, we assigned each gene a moderated t -statistic from the differential expression analyses, an ‘in-set’ value ‘1’ to PRS1 and PRS2 genes, and an ‘inset’ value ‘0’ to the remaining genes (PRS3–PRS10); we then analyzed the relationship between the t -statistics and the ‘in-set’ variable, after covarying for average gene expression (see results in Supplementary Table 11). Importantly, in addition to an enrichment analysis of PRS1 and PRS2 genes based on genes mapping 500 kb \pm the index SNPs of PRS1 and PRS2, we also calculated the enrichment results for the PRS1 and PRS2 genes, defined as the UCSC genes overlapping the LD regions associated with each SNP ($R^2 > 0.6$), as reported on the PGC website (<http://www.med.unc.edu/pgc/downloads/>) (Supplementary Table 9). We finally tested whether the PRS1 and PRS2 genes are enriched among the genes that are differentially expressed in placenta from male compared with female offspring. Among the placental datasets selected in our study, only three (“GSE25861”, “GSE35574”, “GSE25906”) contained sex information; one of them (“GSE25861”) included one female sample. Therefore, we limited this analysis to the remaining two datasets, “GSE35574” and “GSE25906” (Fig. 4). Also, in this case, we performed sensitivity analyses adjusting for average gene expression (Supplementary Table 11).

To confirm the specificity of our findings in the placenta from complicated pregnancies, we performed similar analyses in available datasets from normal/affected organs and in embryonic cells under distress (results for all of these sensitivity analyses are reported in Table 2, Supplementary Tables 9 and 11, and Supplementary information, see ‘‘Sensitivity analyses for placental enrichment’’ note).

Placental-enriched risk profile scoring. We calculated PRSs based on the GWAS SNPs marking loci-containing genes highly expressed in placenta and differentially expressed in placenta from complicated pregnancies, and compared their interaction with ELCs to PRSs derived from the SNPs marking the remaining

GWAS significant loci. For this purpose, we selected the loci-containing genes differentially expressed ($P < 0.05$) in at least four of the eight datasets analyzed and the loci containing genes with expression in the upper decile both in trophoblast and in villi. This gave us a list of 56 SNPs for PRS1 and 112 SNPs for PRS2, as marking loci with genes dynamically modulated and enriched in placenta; we then calculated PRSs based on these SNPs ("Placental" risk profile scores, PlacPRS1 and PlacPRS2) and on the remaining SNPs in these PRS1 and PRS2 loci that did not show high or differential expression in placental tissues (NonPlacPRS1 and NonPlacPRS2), as described earlier (see earlier "Derivation of polygenic risk profile scores" section). In an analogous way and to address the organ specificity of the PlacPRS interaction with ELCs, we calculated "TissuePRSs" and "NonTissuePRSs" based on SNPs marking PRS1 and PRS2 loci-containing genes highly and differentially expressed in adult and fetal tissues, or associated with methylation quantitative trait loci in postmortem human dorsolateral prefrontal cortex²⁸, or with chromatin interactions in fetal brain²⁹. We then analyzed the interaction of these TissuePRSs and NonTissuePRSs with ELCs on case-control status. Results of these sensitivity analyses are reported in Supplementary Tables 12–14 and in the Supplementary information (see "Sensitivity analyses for placental enrichment" note).

Pathway and functional analyses. We investigated whether the placenta-enriched genes mapping to the loci of PlacPRS1 and PlacPRS2 are enriched for particular biological features, compared with the remaining genes mapping to the PRS1 and PRS2 loci (NonPlacPRS1 and NonPlacPRS2). Data were analyzed through QIAGEN's Ingenuity Pathway Analysis (QIAGEN, Redwood City, CA, USA; <http://www.qiagen.com/ingenuity>). The software determines the pathways and biological processes enriched for a given set of genes by considering the number of focus genes that participate in each process and the total number of genes that are known to be associated with that process in the selected reference set. We performed the Ingenuity Pathway Analysis "core" analysis, using default parameters (reference set: Ingenuity Knowledge Base; relationships: direct and indirect; node types: all; data sources: all; confidence: experimentally observed and high; species: human, mouse, and rat; tissues and cell lines: all; mutations: all). We chose a P value calculation based on the Benjamini–Hochberg method of accounting for multiple testing in the canonical pathway and functional analyses. In addition, we used the Panther tool³⁰ on the Gene Ontology database (<http://geneontology.org>) for statistical overrepresentation testing, to further explore whether PlacPRS1 and PlacPRS2 genes and NonPlacPRS1 and NonPlacPRS2 genes show differences in enrichment among Gene Ontology terms associated with molecular functions, biological processes, and cellular components. In this analysis, the P value calculation is based by default on the Bonferroni method of accounting for multiple testing.

Reporting Summary. Further information on experimental design is available in the Nature Research Reporting Summary linked to this article.

Data and code availability. To protect the privacy of the study participants, the genetic and ELC data generated and analyzed during this study are available from the corresponding author on reasonable request, together with the codes used for the analyses. The placental datasets and the other gene expression datasets analyzed in this study are available on the Gene Expression Omnibus

repository (<https://www.ncbi.nlm.nih.gov/geo/>) under the accession codes provided in this article.

References

- Rasetti, R. et al. Altered cortical network dynamics: a potential intermediate phenotype for schizophrenia and association with ZNF804A. *Arch. Gen. Psychiatry* **68**, 1207–1217 (2011).
- Ursini, G. et al. BDNF rs6265 methylation and genotype interact on risk for schizophrenia. *Epigenetics* **11**, 1–13 (2016).
- Begemann, M. et al. Modification of cognitive performance in schizophrenia by complexin 2 gene polymorphisms. *Arch. Gen. Psychiatry* **67**, 879–888 (2010).
- Ribbe, K. et al. The cross-sectional GRAS sample: a comprehensive phenotypical data collection of schizophrenic patients. *BMC Psychiatry* **10**, 91 (2010).
- Ohi, K. et al. Glutamate networks implicate cognitive impairments in schizophrenia: genome-wide association studies of 52 cognitive phenotypes. *Schizophr. Bull.* **41**, 909–918 (2015).
- Purcell, S. et al. PLINK: a tool set for whole-genome association and population-based linkage analyses. *Am. J. Human Genet.* **81**, 559–575 (2007).
- Howie, B., Marchini, J. & Stephens, M. Genotype imputation with thousands of genomes. *G3 (Bethesda)* **1**, 457–470 (2011).
- Delaneau, O., Marchini, J. & Zagury, J. F. A linear complexity phasing method for thousands of genomes. *Nat. Methods* **9**, 179–181 (2012).
- Stepniak, B. et al. Accumulated environmental risk determining age at schizophrenia onset: a deep phenotyping-based study. *Lancet Psychiatry* **1**, 444–453 (2014).
- Damilack, V. A., Nunes, A. P. & Phipps, M. G. Unexpected complications of low-risk pregnancies in the United States. *Am. J. Obstet. Gynecol.* **212**, 809.e1–809.e6 (2015).
- Hewson, D. & Bennett, A. Childbirth research data: medical records or women's reports? *Am. J. Epidemiol.* **125**, 484–491 (1987).
- O'Callaghan, E., Larkin, C. & Waddington, J. L. Obstetric complications in schizophrenia and the validity of maternal recall. *Psychol. Med.* **20**, 89–94 (1990).
- R Development Core Team. *R: A Language and Environment for Statistical Computing* (R Foundation for Statistical Computing, 2008).
- Keller, M. C. Gene x environment interaction studies have not properly controlled for potential confounders: the problem and the (simple) solution. *Biol. Psychiatry* **75**, 18–24 (2014).
- Zhu, Z. et al. Integration of summary data from GWAS and eQTL studies predicts complex trait gene targets. *Nat. Genet.* **48**, 481–487 (2016).
- Roadmap Epigenomics Consortium et al. Integrative analysis of 111 reference human epigenomes. *Nature* **518**, 317–330 (2015).
- Ritchie, M. E. et al. limma powers differential expression analyses for RNA-sequencing and microarray studies. *Nucleic Acids Res.* **43**, e47 (2015).
- Lawrence, M. et al. Software for computing and annotating genomic ranges. *PLoS Comput. Biol.* **9**, e1003118 (2013).
- Mi, H., Muruganujan, A., Casagrande, J. T. & Thomas, P. D. Large-scale gene function analysis with the PANTHER classification system. *Nat. Protoc.* **8**, 1551–1566 (2013).

ARTICLE



Uncoupling the widespread occurrence of anti-NMDAR1 autoantibodies from neuropsychiatric disease in a novel autoimmune model

Hong Pan¹ · Bárbara Oliveira¹ · Gesine Saher² · Ekrem Dere¹ · Daniel Tapken³ · Marina Mitjans¹ · Jan Seidel¹ · Janina Wesolowski¹ · Debja Wakhloo¹ · Christina Klein-Schmidt³ · Anja Ronnenberg¹ · Kerstin Schwabe⁴ · Ralf Trippel³ · Kerstin Mätz-Rensing⁵ · Stefan Berghoff² · Yazeed Al-Krinawe⁴ · Henrik Martens⁶ · Martin Begemann¹ · Winfried Stöcker⁷ · Franz-Josef Kaup⁵ · Reinhard Mischke⁸ · Susann Boretius⁹ · Klaus-Armin Nave^{2,10} · Joachim K. Krauss⁴ · Michael Hollmann¹⁰ · Fred Lühder¹¹ · Hannelore Ehrenreich^{1,10}

Received: 29 August 2017 / Revised: 20 October 2017 / Accepted: 30 October 2017 / Published online: 9 February 2018
© The Author(s) 2018. This article is published with open access

Abstract

Autoantibodies of the IgG class against N-methyl-D-aspartate-receptor subunit-NR1 (NMDAR1-AB) were considered pathognomonic for anti-NMDAR encephalitis. This view has been challenged by the age-dependent seroprevalence (up to >20%) of functional NMDAR1-AB of all immunoglobulin classes found in >5000 individuals, healthy or affected by different diseases. These findings question a merely encephalitogenic role of NMDAR1-AB. Here, we show that NMDAR1-AB belong to the normal autoimmune repertoire of dogs, cats, rats, mice, baboons, and rhesus macaques, and are functional in the NMDAR1 internalization assay based on human iPSC-derived cortical neurons. The age dependence of seroprevalence is lost in nonhuman primates in captivity and in human migrants, raising the intriguing possibility that chronic life stress may be related to NMDAR1-AB formation, predominantly of the IgA class. Active immunization of *ApoE*^{-/-} and *ApoE*^{+/+} mice against four peptides of the extracellular NMDAR1 domain or ovalbumin (control) leads to high circulating levels of specific AB. After 4 weeks, the endogenously formed NMDAR1-AB (IgG) induce psychosis-like symptoms upon MK-801 challenge in *ApoE*^{-/-} mice, characterized by an open blood–brain barrier, but not in their *ApoE*^{+/+} littermates, which are indistinguishable from ovalbumin controls. Importantly, NMDAR1-AB do not induce any sign of inflammation in the brain. Immunohistochemical staining for microglial activation markers and T lymphocytes in the hippocampus yields comparable results in *ApoE*^{-/-} and *ApoE*^{+/+} mice, irrespective of immunization against NMDAR1 or ovalbumin. These data suggest that NMDAR1-AB of the IgG class shape behavioral phenotypes upon access to the brain but do not cause brain inflammation on their own.

Introduction

Autoantibodies (AB) of the immunoglobulin G (IgG) class against the N-methyl-D-aspartate-receptor subunit-NR1 (NMDAR1) were originally interpreted as pathognomonic for a condition called “anti-NMDAR encephalitis”, characterized by high serum and cerebrospinal fluid (CSF) titers

of these AB, as well as a variably favorable response to immunosuppressive therapy. The reported syndrome, reflecting typical NMDAR1 antagonistic actions, consisted of psychosis, epileptic seizures, dyskinesia, cognitive decline, reduced consciousness, and autonomic dysregulation [1–4]. However, work on >5000 individuals, healthy or affected by different diseases, consistently revealed overall comparable age-dependent seroprevalence of functional NMDAR1-AB of all Ig classes, nurturing serious doubts regarding a purely pathological role of NMDAR1-AB of any Ig class [5–10].

NMDAR1-AB apparently belong to a pre-existing autoimmune repertoire [11–17], where Ig isotypes are determined by extracellular vs. intracellular antigen location [6]. This may explain the rarity of the IgG class among AB directed against extracellular epitopes, e.g., NMDAR1,

MOG, and CASPR2. In contrast, AB that recognize intracellular antigens, e.g., amphiphysin, ARHGAP26, or GAD65, show predominance of IgG [6]. Despite this apparent “physiological autoimmunity”, no report exists that systematically screened mammals other than humans for the presence of NMDAR1-AB. In recent work, we found that all naturally occurring NMDAR1-AB are functional and thus have pathogenic potential irrespective of epitope and Ig class [10]. Pathophysiological significance may emerge in conditions of compromised blood–brain barrier (BBB), for instance, upon injury, infection, inflammation, or genetic predisposition (*APOE4* haplotype), which then allows substantial access of circulating NMDAR1-AB to the brain where they act as NMDAR antagonists [5, 9, 18–20]. Alternatively, AB-specific plasma cells may reside or settle in the brain and produce large amounts of AB intrathecally [14, 21]. The question whether abundant endogenously produced NMDAR1-AB of the IgG class can—upon access to the brain—induce inflammation and thus “anti-NMDAR1 encephalitis” has never been experimentally addressed.

The present paper has therefore been designed to (i) systematically screen mammals other than humans for seroprevalence of functional NMDAR1-AB and (ii) study mice with open BBB behavioral and morphological consequences of high circulating levels of endogenous NMDAR1-AB of the IgG class formed in response to immunization.

Materials and methods

Ethical approvals

Ethics committees of Georg-August University, Göttingen, and collaborating centers approved the Göttingen Research Association for Schizophrenia (GRAS) data collection and other studies “extended GRAS” acquiring human data, serum samples, and iPSC [5, 6, 8, 9, 22, 23]. Hannover Medical School Ethics Committee approved the neurosurgical specimen collection. Studies comply with Helsinki Declaration. Patients gave written informed consent. Mouse studies were approved by Animal Ethics (LAVES, Oldenburg) following German Animal Protection Law.

Notes: All experiments were performed by researchers unaware of group assignment. The new nomenclature GluN1 for NMDAR1 is mostly disregarded here for consistency with the respective literature.

Human samples

GRAS and “extended GRAS”

The GRAS [22, 23] subsample used here consists of deep-phenotyped patients ($N = 970$; age 39.29 ± 0.40 years; 66.3%

men), diagnosed with schizophrenia or schizoaffective disorder according to DSM-IV-TR [24]. Subjects of “extended GRAS” ($N = 4933$; age 43.29 ± 0.24 years; 56.9% men) comprise healthy individuals and patients with different neuropsychiatric diagnoses, including schizophrenia, affective disorders, multiple sclerosis, Parkinson, ALS, stroke, and personality disorders (detailed description in [5, 6, 8, 9]). For this study, subjects are dichotomously classified as nonmigrants or migrants comprising first (patient migrated) and second generation (parents migrated). Identified migrants ($N = 301/N = 4933$) are from Europe (49.8%), Asia (36.9%), Africa (9%), North America (2%), South America (0.7%), or mixed (1.6%).

Neurosurgical patients

A total of $N = 72$ paired samples of serum and ventricular CSF were available from patients ($N = 45$ women; age 55.9 ± 2.2 years; $N = 27$ men; age 60.2 ± 2.7 years) undergoing neurosurgery for various reasons: meningiomas, metastases, and other brain tumors ($N = 25$); intracerebral/subarachnoid hemorrhages ($N = 20$); hydrocephalus ($N = 12$); arterial aneurysms ($N = 7$); trigeminal neuralgia ($N = 4$); and others ($N = 4$). Most pairs were taken simultaneously at the time point of surgery, i.e., <5 min ($N = 64$) or <30 min ($N = 8$) apart.

Other mammals

Dogs and cats

Serum samples from dogs and cats of different breeds were prospectively collected during routine (health check/vaccination) or diagnostic (spectrum of different disorders) workup of outpatients in the Small Animal Clinic, University of Veterinary Medicine, Hannover.

Monkeys

Serum samples from healthy baboons and rhesus macaques were obtained through routine checkups at the Leibniz Institute for Primate Research, Göttingen.

Rodents

Serum samples from healthy rats and mice were obtained at the Max Planck Institute of Experimental Medicine and the Institute for Multiple Sclerosis Research, Göttingen.

Serological analyses

NMDAR1-AB determination by clinical standard procedures

Human serum and ventricular CSF were tested for NMDAR1-AB positivity using commercially available kits,

Hong Pan, Bárbara Oliveira, and Gesine Saher contributed equally to this work.

✉ Hannelore Ehrenreich
ehrenreich@em.mpg.de

Extended author information available on the last page of the article

based on HEK293T cells transfected with NMDAR1 and secondary AB against human IgG, IgM, or IgA (Euroimmun, Lübeck, Germany) [2, 25]. Mouse serum was analyzed using the same assay with secondary AB against mouse IgG, IgM, or IgA (M31001, A-31570, A-21042; Thermo Fisher, Rockford, USA).

NMDAR1-AB IgM screening in monkey samples

HEK293T cells (50,000) cultured at 37 °C/8% CO₂ in DMEM (high glucose, Life Technologies, Carlsbad, USA) were seeded on a 35-mm dish, grown for 3 days, and transfected with 3 µg of myc-His-tagged GluN1-1b cloned into pcDNA4/TO/myc-His A (Invitrogen, Carlsbad, USA) using Metafectene-Pro (Biontex, Munich, Germany) [10]. One day post transfection, cells were split onto five poly-D-lysine-coated coverslips in a 35-mm dish and 1 day later, they were fixed with 5% paraformaldehyde (PFA) for 20 min, washed 5× (PBS), permeabilized with 0.1% Triton X-100 for 5 min, again washed 5× (PBS), and blocked with 5% normal goat serum (NGS; Sigma-Aldrich, Munich, Germany) for 1 h. After five PBS washes, cells were incubated with serum and monoclonal mouse anti-myc IgG (clone 9E10, Hollmann-Lab, Bochum) for 1 h, washed with 10× (PBS), incubated for 1 h with fluorescein-labeled goat anti-monkey IgM (072-11-031; KPL, Gaithersburg, USA) and AlexaFluor®594-labeled goat anti-mouse IgG (A11005; Thermo Fisher) secondary AB, and PBS washed 5×. Cells were mounted in Fluoromount-G (Southern Biotech, Birmingham, USA) and analyzed via TCS-SP2-AOBS confocal microscope (63× oil immersion objective; Leica-Microsystems, Wetzlar, Germany). The results were independently assessed by three investigators.

Protein-A assay

Human serum (for cross-validating clinical standard procedure and protein-A method), as well as dog, cat, rat, and monkey serum were labeled with protein-A from *Staphylococcus aureus*, binding the Fc portion of immunoglobulins of different species [26]. Plasma (50 µl) and 25 µg of FITC-conjugated protein-A (Sigma-Aldrich) were incubated for 2 h in the dark at room temperature (RT). The mixture was then diluted to 250 µl (PBS) and unbound FITC-Protein-A was removed using 100-kDa Amicon filter units (Sartorius, Göttingen, Germany), reconcentrating to ~50 µl [27]. NMDAR1-AB seropositivity was determined using Euroimmun assay combined with commercial monoclonal mouse NMDAR1-AB (114011; M68, SYSY, Göttingen, Germany). Samples showing distinct double labeling were rated "positive" (>98% consensus of three investigators).

Endocytosis assay

Functional studies were conducted with sera following ammonium-sulfate precipitation of immunoglobulins [28] and dialysis (Slide-A-Lyzer® Mini Dialysis Units, 10,000 MWCO Plus Float, Thermo Fisher). To assess AB functionality, human iPSC-derived neurons were exposed to dialyzed serum [10]. For each species, arbitrarily selected seronegative ($N = 1$) and seropositive samples ($N = 2-3$) were analyzed. Briefly, cells were precooled on ice and washed prior to incubation in cold HBSS with 1:50 diluted dialyzed sera, control NMDAR1-AB (M68-SYSY), or HBSS alone (negative control) for 30 min/4 °C. After washing to remove unbound AB, neurons were returned to their media and incubated for 20 min at 37 °C (three coverslips/sample, endocytosis) or 4 °C (one coverslip/sample, endocytosis control). The remaining surface NMDAR1 was exposed to mouse anti-human NMDAR1-AB (N-terminal; ab134308; Abcam, Cambridge, UK, 1:100), followed by labeling with secondary donkey anti-mouse IgG (A10036; Life Technologies, AlexaFluor®546, 1:100). Neurons were fixed with ice-cold 4% PFA and double stained with chicken anti-NeuN-AB (266006; SYSY, 1:500) and secondary donkey anti-chicken AB (703-546-155; Life Technologies, AlexaFluor®488, 1:250). Nuclei were visualized using DAPI (Sigma-Aldrich, 0.01 µg/ml). After PBS wash, coverslips were mounted on SuperFrost®-Plus slides with Mowiol mounting media (Sigma-Aldrich). Confocal laser-scanning microscopy was used to quantify NMDAR1 density at the membrane (63× glycerol objective; TCS-SP5 Leica-Microsystems, Mannheim, Germany). From each coverslip, Z series of optical sections (0.5 µm apart) covering the three-dimensional extension of neurons were acquired (sequential scanning mode, identical acquisition parameters). FIJI-ImageJ software [29] was used to randomly select NeuN⁺ cells and determine soma profile. Fluorescence intensity/cell surface area (AlexaFluor546) was automatically measured as readout of NMDAR1 surface expression. After background subtraction, the mean intensity for each coverslip was determined and fluorescence intensity ratio (37/4 °C) was calculated.

BBB-integrity testing

BBB integrity of 12-month-old *ApoE*^{-/-} ($N = 5$) and *ApoE*^{+/+} ($N = 5$) mice was determined using two different fluorescent tracers, Evans blue (50 mg/g body weight) [30] and sodium fluorescein (200 mg/g body weight). A detailed description of this method will be published elsewhere [31]. Briefly, for tracer quantification in the brain at 4 h after intravenous injection in the tail vein, animals were PBS perfused to remove the circulating tracer. Brains were dissected, immediately frozen on dry ice, weighed, and stored

at -80 °C. Tissue was lyophilized at -56 °C for 24 h under vacuum of 0.2 mBar (Christ LMC-1-BETA-1-16, Osterode, Germany). For tracer extraction, hemispheres were incubated with shaking in 10 ml formamide/mg brain at 57 °C for 24 h. Integrated density of tracer fluorescence was determined in triplicates on a fluorescent microscope (Observer Z2, Zeiss, Germany), equipped with Axio-CamMrc3, 1×Camera-Adapter, and ZEN2012 blue-edition software, recorded at 10× magnification (Plan-Apochromat 10×/0.45M27). Tracer concentration was calculated using a standard curve and normalized to controls (set to 1).

Mouse immunization

Mice (12-month-old C57BL/6 littermates: *ApoE*^{-/-} $N = 20$ and *ApoE*^{+/+} $N = 23$; genders balanced) were immunized with a mixture of GluN1 extracellular peptides and/or chicken ovalbumin (Sigma-Aldrich), and emulsified in equal volume of complete Freund's Adjuvant (*Mycobacterium tuberculosis* H37RA plus incomplete Freund's Adjuvant; Becton-Dickinson, Sparks, USA) at a final concentration of 1 mg/ml [32]. At the tail base, 50 µg of GluN1 peptides and/or 20 µg of ovalbumin were injected subcutaneously (each side one).

Enzyme-linked immunosorbent assay (ELISA)

Orbital sinus blood of immunized mice was stored as EDTA plasma at -80 °C. ELISA plates (96 well) were coated with 0.5 µg of GluN1 peptide mixture or 0.2 µg of chicken ovalbumin in 50 µl PBS/well overnight at 4 °C and blocked with 5% BSA/PBS (Carl Roth, Karlsruhe, Germany). Mouse plasma (1:1000 or 1:50,000 5% BSA/PBS 50 µl/well) was added for 2 h at RT. The signal was amplified with horseradish peroxidase-linked anti-IgG (Sigma-Aldrich), and 3,3',5,5'-Tetramethylbenzidine as colorimetric substrate (BD Biosciences, San Jose, USA). Absorbance at 450 nm was measured by microplate reader (Tecan-Trading AG, Männedorf, Switzerland).

Basic behavioral screening

The behavioral test battery was performed as described previously [33-36]. Starting at age 5 months, experimentally naïve *ApoE*^{-/-} and *ApoE*^{+/+} littermates underwent (during light phase) tests of anxiety, activity and exploratory behavior (elevated plus-maze, open field, hole-board), motor (rotarod, grip strength) and sensory function (visual cliff, olfaction, hearing, hot plate), sensorimotor gating (prepulse inhibition), pheromone-based social preference, and cognitive performance (IntelliCage place/reversal learning). Males and females were tested separately.

Baseline and post MK-801 locomotion in the open field

The open-field apparatus consisted of a gray circular Perspex-arena (120 cm diameter; wall height 25 cm). Indirect white light illumination ensured constant light intensity of 120 lux in the center. Locomotion was measured using automated tracking software (Viewer2-Biobserve, Bonn, Germany). *ApoE*^{-/-} and *ApoE*^{+/+} littermates received four baseline measurements preimmunization and post immunization (15 min each), the last followed by intraperitoneal MK-801 (Dizocilpine-[5S,10R]-(+)-5-methyl-10,11-dihydro-5H-dibenzo[a,d]cyclohept-5,10-imine hydrogen maleate; 0.3 µg/10 µl PBS/g Sigma-Aldrich). MK-801 is a noncompetitive NMDAR antagonist, acting as a use-dependent ion-channel blocker, and known to induce psychosis-like hyperactivity in the open field (loss of inhibition) [37]. Directly post injection, locomotor activity in open field was analyzed (4 min intervals), with the first 4 min defined as reference locomotion to express changes over 120 min as % reference.

Immunohistochemistry

Mice were anesthetized with Avertin (2,2,2-Tribromoethanol, Sigma-Aldrich), and transcardially perfused with 4% PFA/Ringer solution (Braun-Melsungen, Germany). Brains were removed, postfixed in 4% PFA overnight at 4 °C, and incubated in 30% sucrose/PBS for 2 days at 4 °C. Brains were cryosectioned coronally into 30 µm slices and stored in 25% ethylene glycol and 25% glycerol/PBS at -20 °C. Frozen sections (three/mouse; rostral hippocampus), mounted on SuperFrost®-Plus slides (Thermo Fisher, Waltham, USA), were used for cell quantification. For CD3 staining, sections were microwaved 3× for 4 min in citrate buffer (1 mM, pH 6) and blocked with 5% normal horse serum (NHS), and 0.5% Triton X-100/PBS for 1 h at RT. Incubation with rat anti-mouse CD3 (MCA1477; BioRad, Hercules, USA; 1:100) diluted in 5% NHS, and 0.5% Triton X-100/PBS was performed for two nights/4 °C, followed by incubation with goat anti-rat AlexaFluor®647 (A-21247; Thermo Fisher, Schwerte, Germany; 1:1000) diluted in 5% NHS, and 0.5% Triton X-100/PBS for 2 h at RT. For Iba1, GFAP, CD68, and MHC-II staining, sections were blocked with 5% NGS and/or 5% NHS in 0.5% Triton X-100/PBS for 1 h at RT. Incubation with rabbit anti-mouse Iba1 (019-19741; Wako-Chemicals GmbH, Neuss, Germany; 1:1000), or mouse anti-mouse GFAP (NCL-GFAP-GA5; Novocastra-Leica, Newcastle upon Tyne, UK; 1:500), diluted in 3% NGS or 3% NHS, and 0.5% Triton X-100/PBS, was performed overnight, and incubation with rat anti-mouse CD68 (MCA1957GA; BioRad GmbH, München, Germany, 1:400) and rat

anti-mouse MHC-II (14-5321; eBioscience, San Diego, USA, 1:100) diluted in 3% NGS and 3% NHS, and 0.5% Triton X-100/PBS, was performed over two nights, all at 4 °C. Incubation with secondary antibodies was performed with goat anti-rabbit AlexaFluor®555 (A-21428; Thermo Fisher; 1:500) diluted in 3% NGS, 0.5% Triton X-100/PBS, or donkey anti-rabbit AlexaFluor®488 (A-21206; Thermo Fisher; 1:500) or goat anti-rat AlexaFluor®647 (A-21247; Thermo Fisher; 1:500), diluted in 3% NGS or 3% NHS, and 0.5% Triton X-100/PBS for 1.5 h at RT. Nuclei were counterstained with DAPI (Sigma-Aldrich, 0.01 µg/ml) and sections were mounted using Aqua-Poly/Mount (Polysciences, Warrington, USA). Tile scans of hippocampus were acquired using Leica-DMI6000 epifluorescence microscope (20× objective; Leica) and Iba1⁺ and CD3⁺ cells were counted using cell counter plug-in of FIJI-ImageJ software [29]. GFAP⁺ cells in the hippocampus were quantified densitometrically upon uniform thresholding (expressed as % respective area).

Statistical analyses

Statistical analyses were performed using SPSSv.17 (IBM-Deutschland-GmbH, Munich, Germany) or Prism4 (GraphPad Software, San Diego, California, USA). Group differences in categorical and continuous variables were assessed using χ^2 , Mann–Whitney U, or Student's *t*-tests depending on data distribution/variance homogeneity. ANOVA was employed as indicated in display item legends. All *p*-values are two tailed; significance is set to *p* < 0.05; data are presented as mean ± S.E.M.

Results

Cross-validation of NMDAR1-AB detection methods

To determine NMDAR1-AB seropositivity in mammals other than humans, we had to validate the protein-A detection method [27]. For that, *N* = 72 paired human serum and ventricular CSF samples, prospectively collected from random neurosurgical patients, were analyzed by the usual cell-based assay, employing specific secondary AB for all Ig classes. A total of *N* = 5 sera turned out NMDAR1-AB positive (titers ≤ 1:100; 3 × IgM; 2 × IgA; 0 × IgG). Ventricular CSF samples were all negative. For cross-validation of NMDAR1-AB of the IgG class, we used serum of a seropositive stroke patient [8]. Application of protein-A method combined with double labeling for NMDAR1-AB M68 confirmed positive and negative results (Fig. 1a).

High seroprevalence of NMDAR1-AB across mammalian species

We next analyzed by protein-A method serum samples of dogs, cats, rats, baboons, and rhesus macaques. Strikingly, all mammalian species, independent of their respective life expectancy, show high NMDAR1-AB seropositivity (Fig. 1b). Mouse samples were analyzed using specific AB against murine IgA, IgM, and IgG. As known for humans [6], NMDAR1-AB of the IgG class were the rarest. For another cross-validation, all monkey samples (*N* = 100) were analyzed in blinded fashion by an independent lab (Bochum; using specific anti-monkey IgM). IgM-positive results coincided with the protein-A positivity by >97% (76 of 78). The fraction of protein-A positive but IgM-negative monkey samples (total 22%) likely presents NMDAR1-AB of IgA class and IgG class where specific AB were not available.

Age-dependent NMDAR1-AB seroprevalence except for nonhuman primates and human migrants

All species revealed age dependence of NMDAR1-AB seroprevalence (χ^2 test; dogs: $\chi^2(1) = 11.5$, *p* = 0.01; cats: $\chi^2(1) = 4.8$, *p* = 0.03; rats: $\chi^2(1) = 9.5$, *p* = 0.002; and mice: Fisher's exact test *p* = 0.032) as for humans [5, 8] with the exception of baboons ($\chi^2(1) = 1.0$, *p* = 0.3), where already >50% of young animals were seropositive. This surprising result made us investigate another monkey species, rhesus macaques, showing again high seroprevalence in old and young animals ($\chi^2(1) = 0.2$, *p* = 0.6) (Fig. 1b). We wondered what the difference between humans, dogs, cats, mice, and rats, on one hand, and monkeys, on the other hand, could be, leading to loss of the usual age pattern regarding seroprevalence. Postulating that captivity/non-domestication of young monkeys might induce chronic life stress due to maladaptation to the environment, we investigated in a hypothesis-driven way whether young human migrants would display a similar increase in NMDAR1-AB seropositivity. Of the GRAS data collection, detailed information on migration was available in a subsample of *N* = 970 individuals. While nonmigrants show the typical age association of NMDAR1-AB seroprevalence ($\chi^2(1) = 10.7$, *p* = 0.001), migrants do not ($\chi^2(1) = 0.6$, *p* = 0.4) (Fig. 1c). Seroprevalence in young migrants is significantly higher as compared to young nonmigrants ($\chi^2(1) = 5.381$, *p* = 0.020). In both monkey species and migrants, the IgM fraction still follows the expected age trend, while IgA seems to account for the early increase in NMDAR1-AB seroprevalence (Fig. 1c). Presentation of NMDAR1-AB by Ig class in the extended GRAS sample (*N* = 4933), with *N* = 4632 of likely nonmigrants (available information less detailed) and *N* = 301 known migrants, illustrates the

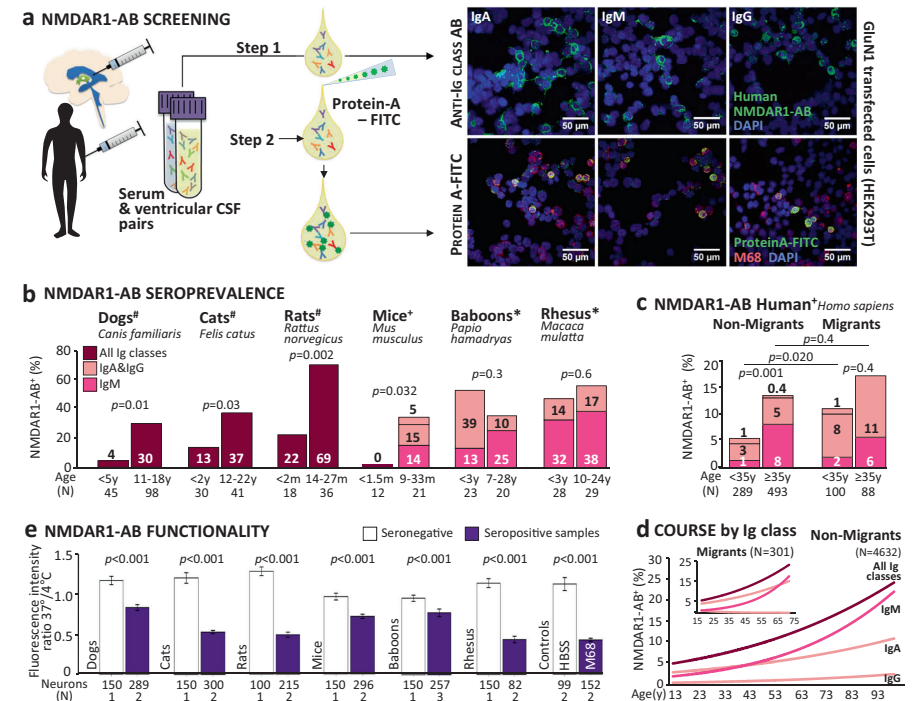


Fig. 1 NMDAR1-AB seropositivity and functionality across mammalian species. **a** Cross-validation of assays: paired serum and intra-ventricular CSF samples from neurosurgical patients were tested using a HEK293T cell-based clinical standard assay for NMDAR1-AB seropositivity (Euroimmun biochip). For step 1, fluorescently labeled IgA-specific, IgM-specific, and IgG-specific secondary AB were used; for method cross-validation (step 2), NMDAR1-AB seropositive and seronegative samples of each Ig class from step 1 were labeled with protein-A-FITC conjugate and tested for colocalization (yellow) of protein-A-FITC⁺ (green) and M68⁺ (monoclonal mouse NMDAR1-AB followed by Alexa555 donkey anti-mouse IgG red). Representative pictures of both methods using the same seropositive samples (IgA, IgM, and IgG) are displayed on the right: upper row step 1/lower row step 2. **b** NMDAR-AB seropositivity (%) of young and old

abnormal course of IgA vs. IgM/IgG seroprevalence over age in migrants (Fig. 1d).

Functionality of NMDAR1-AB from different mammalian species

To assess whether NMDAR1-AB of the tested species are functional, our endocytosis assay using IPSC-derived human cortical neurons [10] was employed. All positive

mammals for all Ig classes combined (*protein-A-FITC/Euroimmun) or for individual classes (†Euroimmun; *protein-A-FITC/Euroimmun and cross-validation with Euroimmun/monkey IgM) presented in the bars; color codes used for consistency and kept also in c and d; age given in months (m) or years (y); χ^2 or Fisher's exact test. **c** NMDAR-AB seropositivity of subjects with migration (first and second generation) vs. nonmigration history (GRAS data collection); all Ig classes presented; age split at 35 years; χ^2 test. **d** NMDAR1-AB course by Ig classes in serum over age groups in migrants vs. nonmigrants of the extended GRAS data collection. Note the different course particularly for IgA. **e** Functionality testing of NMDAR1-AB in human IPSC-derived cortical neurons: degree of internalization expressed as a ratio of fluorescence intensity measured at 37 and 4 °C; number of neurons and sera (*N*) given; Mann–Whitney U test

sera provoked NMDAR1 internalization, verifying functionality (Mann–Whitney U; all *p* < 0.001) (Fig. 1e).

BBB dysfunction but normal behavior of *ApoE*^{-/-} mice

We next induced endogenous NMDAR1-AB formation in a mouse model of BBB dysfunction, *ApoE*^{-/-} mice vs. WT littermates. *ApoE*^{+/+}. Before that, we confirmed in 12-

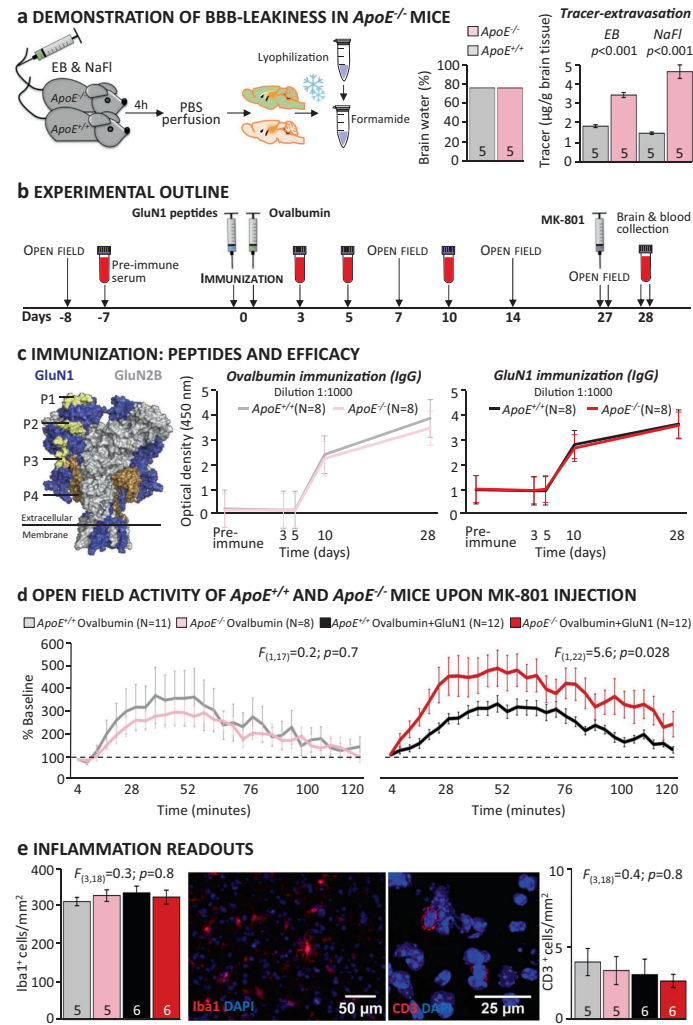


Fig. 2 Behavioral and morphological effects of endogenous NMDAR1-AB of the IgG class in a mouse model with open BBB. **a** Demonstration of BBB leakiness in *ApoE*^{-/-} mice using an intravenously injected mixture of Evans blue (EB) and sodium fluorescein (NaFl): After brain cryopreservation/lyophilization, tracers were extracted with formamide and quantified; Student's *t*-test; **b** Experimental outline; **c** Immunization: Left: GluN1 peptides (P1–P4) located in the extracellular part of the receptor were used for immunization (compare Fig. 3); middle and right: Time course of anti-ovalbumin and anti-GluN1-AB (IgG) upon immunization in *ApoE*^{-/-} and *ApoE*^{+/+} mice; optical density at dilution 1:1000 shown; titers after day 10 reach up to 1:50,000; **d** Effect of MK-

801 injection on activity in the open field; results presented as % change from baseline (first 4 min post MK-801 set to 100%); no difference in MK-801-induced hyperactivity between genotypes after ovalbumin immunization (one-way repeated measures ANOVA: treatment × group interaction: $F_{(1,17)}=0.2; p=0.7$); increase in hyperactivity (during rise, plateau, decline, and after-effect phases) upon MK-801 in *ApoE*^{-/-} but not *ApoE*^{+/+} mice immunized against GluN1 (one-way repeated measures ANOVA: treatment × group interaction: $F_{(1,22)}=5.6; p=0.028$). **e** Quantification of Iba1⁺ and CD3⁺ cells in the hippocampus to assess inflammation in the brain: one-way ANOVA; representative pictures of Iba1 (left) and CD3 (right) stainings in the middle

Table 1 Basic behavioral screening of male and female *ApoE*^{+/+} and *ApoE*^{-/-} mice

Behavioral paradigms	Males				Females			
	Age (month)	<i>ApoE</i> ^{+/+} (N)	<i>ApoE</i> ^{-/-} (N)	<i>p</i> -value	Age (month)	<i>ApoE</i> ^{+/+} (N)	<i>ApoE</i> ^{-/-} (N)	<i>p</i> -value
Anxiety and activity								
Elevated plus-maze (time open [%])	5	12.6±3.2 (10)	19.5±4.0 (10)	<i>p</i> =0.14 <i>U</i> =30.0	5	17.5±2.9 (13)	14.8±1.3 (11)	<i>p</i> =0.98 <i>U</i> =71.0
Exploratory behavior								
Hole-board (holes visited [#])	5	15.2±2.3 (10)	11.9±1.9 (10)	<i>p</i> =0.30 <i>t</i> (18)=1.07	5	15.5±1.8 (13)	15.6±2.9 (13)	<i>p</i> =0.96 <i>t</i> (22)=0.96
Open-field								
Locomotion [m]	5	31.8±1.7 (10)	32.7±1.5 (10)	<i>p</i> =0.70 <i>t</i> (18)=0.39	5	42.7±1.3 (13)	43.7±3.2 (13)	<i>p</i> =0.76 <i>t</i> (22)=0.31
Motor learning and coordination								
Rotarod day 1 (latency to fall [s])	6	89.3±11.6 (10)	130.0±15.3 (10)	<i>p</i> =0.06 <i>t</i> (18)=2.01	5	130.9±14.0 (13)	133.3±16.0 (11)	<i>p</i> =0.91 <i>t</i> (22)=0.11
Rotarod day 2 (latency to fall [s])	6	140.3±9.4 (10)	145.6±17.8 (10)	<i>p</i> =0.81 <i>t</i> (18)=0.25	5	179.0±16.8 (13)	160.5±19.9 (11)	<i>p</i> =0.5 <i>t</i> (22)=0.69
Muscle strength								
Grip-strength [au]	6	110.2±5.4 (10)	122.0±5.0 (10)	<i>p</i> =0.15 <i>t</i> (18)=1.52	6	108.8±3.0 (13)	115.1±4.4 (11)	<i>p</i> =0.26 <i>t</i> (22)=1.16
Heat/pain perception								
Hot-plate (latency to lick [s])	5	12.8±0.4 (10)	11.9±0.7 (10)	<i>p</i> =0.22 <i>t</i> (18)=1.26	5	13.7±0.5 (12)	12.4±0.5 (10)	<i>p</i> =0.15 <i>t</i> (20)=1.5
Vision								
Visual-cliff (time on "air" side [%])	5	26.5±7.2 (10)	22.0±5.6 (10)	<i>p</i> =0.85 <i>U</i> =47.0	5	21.7±5.1 (13)	29.0±3.9 (11)	<i>p</i> =0.13 <i>U</i> =45.0
Olfaction								
Buried food-test (latency to find cookie [s])	5	59.4±9.2 (10)	50.6±8.5 (9)	<i>p</i> =0.52 <i>t</i> (17)=0.66	5	47.8±12.9 (12)	50.7±10.7 (11)	<i>p</i> =0.87 <i>t</i> (21)=0.16
Hearing								
Acoustic startle at 65dB [AU]	6	0.5±0.04 (10)	0.5±0.04 (10)	<i>p</i> =0.53 <i>F</i> (1,18)=0.42	8	0.4±0.1 (13)	0.5±0.04 (11)	<i>p</i> =0.19 <i>F</i> (1,22)=1.82
Acoustic startle at 120dB [AU]		4.5±1.0 (10)	4.8±1.0 (10)			3.3±0.5 (13)	4.2±0.6 (11)	
Sensorimotor gating								
Mean pre-pulse inhibition [%]	6	44.8±6.7 (10)	40.6±7.4 (10)	<i>p</i> =0.69 <i>F</i> (1,18)=0.16	8	57.7±4.1 (13)	50.4±6.3 (11)	<i>p</i> =0.35 <i>F</i> (1,22)=0.91
Pheromone-based social preference								
Time spent in pheromone box [s]	15	1213±50.8 (12)	1115±83.7 (12)	<i>p</i> =0.33 <i>t</i> (22)=1.0				
Time spent in control box [s]		780.5±75.4 (12)	751.1±83.5 (12)	<i>p</i> =0.84 <i>t</i> (22)=0.21				
Cognitive performance in IntelliCage								
Place-learning [% target corner visits] ^a	15	34.2±1.3 (12)	34.2±1.8 (13)	<i>p</i> =0.76 <i>U</i> =72.0				
Reversal-learning [% target corner visits] ^a		34.2±1.3 (12)	34.2±1.8 (13)	<i>p</i> =0.17 <i>U</i> =52.0				

^aas previously described in Netrakanti et al. 2015

Note: All data in the table are mean ± S.E.M.

month-old mice (age of immunization) BBB leakiness using two fluorescent tracers. While brain water content was similar in both genotypes, pointing against inflammation, *ApoE*^{-/-} mice showed increased tracer extravasation, confirming BBB dysfunction (Student's *t*-test: EB: *t*(8) =

-10.66, *p* < 0.001; NaFl: *t*(8) = -8.97, *p* < 0.001) (Fig. 2a). We wondered whether this compromised BBB would by itself lead to behavioral abnormalities in *ApoE*^{-/-} mice. A comprehensive behavioral battery, including tests for anxiety, activity, exploratory behavior,

motor and sensory function, sensorimotor gating, pheromone-based social preference, and cognitive performance did not reveal any differences between genotypes (Table 1).

Immunization of *ApoE*^{-/-} and *ApoE*^{+/+} mice against NMDAR1-peptides

To explore whether endogenously formed NMDAR1-AB would lead to measurable behavioral and morphological effects, we immunized 12-month-old *ApoE*^{-/-} and *ApoE*^{+/+} littermates against four peptides of the extracellular NMDAR1/GluN1-domain (including NTD-G7; N368/G369) and ovalbumin or against ovalbumin alone as immunization control (Fig. 2b–c). GluN1 shows >99% sequence homology among all here-tested mammalian species, with immunizing peptides being 100% homologous (Fig. 3). Immunization led to high circulating levels of specific IgG (titers up to 1:50,000). Efficacy of immunization and time course of IgG appearance as determined by ELISA were comparable for NMDAR1-peptides and ovalbumin across genotypes, making a simple boosting effect of NMDAR1-peptides on pre-existing NMDAR1-specific B cell clones rather improbable (Fig. 2c).

Psychosis-related behavior of *ApoE*^{-/-} mice upon MK-801 challenge

Open-field tests measuring baseline preimmunization and postimmunization locomotion did not reveal any differences between genotypes and/or immunization groups (Fig. 2b; not shown). After 4 weeks, the endogenously formed NMDAR1-AB of the IgG class induced strong hyperactivity (psychosis-like symptoms [37]) upon MK-801 challenge in *ApoE*^{-/-} mice only. In contrast, *ApoE*^{+/+} mice behaved comparably to ovalbumin-only immunized mice of both genotypes (Fig. 2d; all *p* > 0.5). Thus, an open BBB together with sufficiently high titers of AB (to reach a threshold loss of NMDAR1 surface expression) is a prerequisite for the observed behavioral perturbation upon MK-801.

No inflammation in hippocampus of immunized *ApoE*^{-/-} and *ApoE*^{+/+} mice

Immunohistochemistry did not show any evidence of inflammation in either genotype and/or immunization group. Numbers of Iba1⁺ and CD3⁺ cells as markers of microglia and T cells, respectively, were comparable for total hippocampus (one-way ANOVA: Iba1: *F*(3,18) = 0.3; *p* = 0.8; CD3: *F*(3,18) = 0.4; *p* = 0.8) (Fig. 2e) and for all hippocampal subfields separately (all *p*-values > 0.2; not shown). Also, staining for microglial activity markers,

CD68 and MHCII, was essentially negative and identical across groups. Moreover, staining for GFAP did not reveal any appreciable density increase in the hippocampus, and thus no sign of astrogliosis (data not shown).

Discussion

The present work demonstrates high seroprevalence of functional NMDAR1-AB of all Ig classes across mammals, indicating that these AB are part of a pre-existing auto-immune repertoire [11–17]. As in humans, NMDAR1-AB of the IgG class are the least frequent [6, 20]. The age related up to >50% NMDAR1-AB seropositivity is independent of the respective species' life expectancy, indicating that the aging process itself rather than years of exposure to a certain environment triggers NMDAR1-AB formation. However, our knowledge on predisposing factors and inducing mechanisms is limited. Specific auto-immune-reactive B cells may get repeatedly boosted by, e.g., infections, neoplasms, or the microbiome, and less efficiently suppressed over a lifespan likely owing to a gradual loss of immune tolerance upon aging [14].

Unexpectedly, we find the age-dependence lost in non-human primates and in human migrants that all display an early-life rise in NMDAR1-AB seropositivity, mainly of IgA. The intriguing possibility that chronic life stress, known to be present in human migrants [38] and animals in captivity [39], acts as a trigger of early NMDAR1-AB formation is worth pursuing experimentally in the future. A large proportion of migrants in our human samples are suffering from neuropsychiatric illness. This may additionally support our chronic stress hypothesis since migration is recognized as an environmental stressor predisposing to mental disease [40]. Further studies should screen wild-life monkeys and species in zoos for NMDAR1-AB. Experimental confirmation of our findings provided, NMDAR1-AB (IgA) may even serve as stress markers. In fact, earlier reports show that total serum-Ig of all classes, most prominently IgA, respond to psychological stress [41]. NMDAR1-AB might thus belong to a set of stress-boosted AB. Interestingly, we also find accumulated seroprevalence of 23 other brain-directed AB [6] in young migrants vs. nonmigrants increased (data not shown), suggesting a global inducer role of chronic stress in humoral autoimmunity. Earlier work has shown that AB against brain antigens in general are common among mammals [42], but no study has so far systematically screened nonhuman mammals for NMDAR1-AB. As an exception, a recent report described "anti-NMDAR1 encephalitis" in the young polar bear Knut [27]. Based on the present findings, Knut may have belonged to those nondomesticated species in captivity—

		Peptide 1	
Homo sapiens	MSTRRLTLALLFSCSVAARAADPKPVIIGAVLSTRKHEQHFREAVNQANKRHGSKVQLNATSVTHKPNAIQALSVCELDL15SQVAYLVSHPPPTND		100
Macaca mulatta	MSTRRLTLALLFSCSVAARAADPKPVIIGAVLSTRKHEQHFREAVNQANKRHGSKVQLNATSVTHKPNAIQALSVCELDL15SQVAYLVSHPPPTND		
Papio anubis	MSTRRLTLALLFSCSVAARAADPKPVIIGAVLSTRKHEQHFREAVNQANKRHGSKVQLNATSVTHKPNAIQALSVCELDL15SQVAYLVSHPPPTND		
Canis lupus fam.	MSTRRLTLALLFSCSVAARAADPKPVIIGAVLSTRKHEQHFREAVNQANKRHGSKVQLNATSVTHKPNAIQALSVCELDL15SQVAYLVSHPPPTND		
Felis catus	MSTRRLTLALLFSCSVAARAADPKPVIIGAVLSTRKHEQHFREAVNQANKRHGSKVQLNATSVTHKPNAIQALSVCELDL15SQVAYLVSHPPPTND		
Rattus norvegicus	MSTRMLTLFALLFSCSVAARAADPKPVIIGAVLSTRKHEQHFREAVNQANKRHGSKVQLNATSVTHKPNAIQALSVCELDL15SQVAYLVSHPPPTND		
Mus musculus	MSTRMLTLFALLFSCSVAARAADPKPVIIGAVLSTRKHEQHFREAVNQANKRHGSKVQLNATSVTHKPNAIQALSVCELDL15SQVAYLVSHPPPTND		
		—SP	
		—S1	
		—TMD A	
		—S2	
		—TMD B	
		—TMD C	
		—P	
		—S2	
		—S1	
		—TMD A	
		—TMD B	
		—TMD C	
		—P	
		—S2	
		—S1	
		—TMD A	
		—TMD B	
		—TMD C	
		—P	
		—S2	
		—S1	
		—TMD A	
		—TMD B	
		—TMD C	
		—P	
		—S2	
		—S1	
		—TMD A	
		—TMD B	
		—TMD C	
		—P	
		—S2	
		—S1	
		—TMD A	
		—TMD B	
		—TMD C	
		—P	
		—S2	
		—S1	
		—TMD A	
		—TMD B	
		—TMD C	
		—P	
		—S2	
		—S1	
		—TMD A	
		—TMD B	
		—TMD C	
		—P	
		—S2	
		—S1	
		—TMD A	
		—TMD B	
		—TMD C	
		—P	
		—S2	
		—S1	
		—TMD A	
		—TMD B	
		—TMD C	
		—P	
		—S2	
		—S1	
		—TMD A	
		—TMD B	
		—TMD C	
		—P	
		—S2	
		—S1	
		—TMD A	
		—TMD B	
		—TMD C	
		—P	
		—S2	
		—S1	
		—TMD A	
		—TMD B	
		—TMD C	
		—P	
		—S2	
		—S1	
		—TMD A	
		—TMD B	
		—TMD C	
		—P	
		—S2	
		—S1	
		—TMD A	
		—TMD B	
		—TMD C	
		—P	
		—S2	
		—S1	
		—TMD A	
		—TMD B	
		—TMD C	
		—P	
		—S2	
		—S1	
		—TMD A	
		—TMD B	
		—TMD C	
		—P	
		—S2	
		—S1	
		—TMD A	
		—TMD B	
		—TMD C	
		—P	
		—S2	
		—S1	
		—TMD A	
		—TMD B	
		—TMD C	
		—P	
		—S2	
		—S1	
		—TMD A	
		—TMD B	
		—TMD C	
		—P	
		—S2	
		—S1	
		—TMD A	
		—TMD B	
		—TMD C	
		—P	
		—S2	
		—S1	
		—TMD A	
		—TMD B	
		—TMD C	
		—P	
		—S2	
		—S1	
		—TMD A	
		—TMD B	
		—TMD C	
		—P	
		—S2	
		—S1	
		—TMD A	
		—TMD B	
		—TMD C	
		—P	
		—S2	
		—S1	
		—TMD A	
		—TMD B	
		—TMD C	
		—P	
		—S2	
		—S1	
		—TMD A	
		—TMD B	
		—TMD C	
		—P	
		—S2	
		—S1	
		—TMD A	
		—TMD B	
		—TMD C	
		—P	
		—S2	
		—S1	
		—TMD A	
		—TMD B	
		—TMD C	
		—P	
		—S2	
		—S1	
		—TMD A	
		—TMD B	
		—TMD C	
		—P	
		—S2	
		—S1	
		—TMD A	
		—TMD B	
		—TMD C	
		—P	
		—S2	
		—S1	
		—TMD A	
		—TMD B	
		—TMD C	
		—P	
		—S2	
		—S1	
		—TMD A	
		—TMD B	
		—TMD C	
		—P	
		—S2	
		—S1	
		—TMD A	
		—TMD B	
		—TMD C	
		—P	
		—S2	
		—S1	
		—TMD A	
		—TMD B	
		—TMD C	
		—P	
		—S2	
		—S1	
		—TMD A	
		—TMD B	
		—TMD C	
		—P	
		—S2	
		—S1	
		—TMD A	
		—TMD B	
		—TMD C	
		—P	
		—S2	
		—S1	
		—TMD A	
		—TMD B	
		—TMD C	
		—P	
		—S2	
		—S1	
		—TMD A	
		—TMD B	
		—TMD C	
		—P	
		—S2	
		—S1	
		—TMD A	
		—TMD B	
		—TMD C	
		—P	
		—S2	
		—S1	
		—TMD A	
		—TMD B	
		—TMD C	
		—P	
		—S2	
		—S1	
		—TMD A	
		—TMD B	
		—TMD C	
		—P	
		—S2	
		—S1	
		—TMD A	
		—TMD B	
		—TMD C	
		—P	
		—S2	
		—S1	
		—TMD A	
		—TMD B	
		—TMD C	
		—P	
		—S2	
		—S1	
		—TMD A	
		—TMD B	
		—TMD C	
		—P	
		—S2	
		—S1	
		—TMD A	
		—TMD B	
		—TMD C	
		—P	
		—S2	
		—S1	
		—TMD A	
		—TMD B	
		—TMD C	
		—P	
		—S2	
		—S1	
		—TMD A	
		—TMD B	
		—TMD C	
		—P	
		—S2	
		—S1	
		—TMD A	
		—TMD B	
		—TMD C	
		—P	
		—S2	
		—S1	
		—TMD A	
		—TMD B	
		—TMD C	
		—P	
		—S2	
		—S1	
		—TMD A	
		—TMD B	
		—TMD C	
		—P	
		—S2	
		—S1	
		—TMD A	
		—TMD B	
		—TMD C	
		—P	
		—S2	
		—S1	
		—TMD A	
		—TMD B	
		—TMD C	
		—P	
		—S2	
		—S1	
		—TMD A	
		—TMD B	
		—TMD C	
		—P	
		—S2	
		—S1	
		—TMD A	
		—TMD B	
		—TMD C	
		—P	
		—S2	
		—S1	
		—TMD A	
		—TMD B	
		—TMD C	
		—P	
		—S2	
		—S1	

comparable to monkey species investigated here—that are affected by chronic early-life stress, inducing NMDAR1-AB seropositivity. Pre-existing NMDAR1-AB of this bear may have ultimately shaped the clinical picture of an encephalitis of unexplained origin (likely infectious according to the zoo's pathology reports) where an epileptic seizure led to drowning [27].

This interpretation is supported by our novel auto-immune model, namely, mice immunized against NMDAR1-peptides. Even high titers of endogenously formed NMDAR1-AB (IgG; up to 1:50,000) that induce psychosis-like behavior upon MK-801 challenge in *ApoE*^{-/-} mice, with here-confirmed open BBB, do not lead to any appreciable signs of encephalitis. This dissociation of behavioral/symptomatic consequences and inflammation in the brain is of major importance for clinicians [14]. For instance, earlier studies reported an influence of NMDAR1-AB infusions into the hippocampus on learning and memory in mice [43], and others found increased NMDAR1-AB seroprevalence in patients with mild cognitive impairment and Alzheimer's disease [44, 45]. However, while all naturally occurring NMDAR1-AB that have pathogenic potential irrespective of epitope and Ig class [10], and upon entry to the brain (or via intrathecal production) can shape brain functions in the sense of NMDAR antagonism, only a fraction of individuals happens to have underlying encephalitis of various etiologies, which is then called anti-NMDAR encephalitis. The highly variable neuropathology and response to immunosuppression of this condition [2, 3, 46] may point to a broad range of possible encephalitogenic mechanisms (from infection to oncology or genetics) which need to be diagnosed and specifically treated [14].

Even though it is unclear how NMDAR1-AB are generated by chronic stress, it should be considered that NMDAR1 are not only expressed in the brain but also by peripheral organs and tissues, including adrenal glands and gut [47] which may be involved in triggering NMDAR1-AB formation but may also be functionally modulated by them. Since NMDAR antagonists are increasingly recognized as antidepressant, anxiolytic, and anti-inflammatory agents [48–52], we speculate that stress-induced NMDAR1-AB could serve as endogenous stress protectants. Remarkably, also in stroke, NMDAR1-AB can be protective [8].

In conclusion, the widespread occurrence of NMDAR1-AB across mammals, as well as the failure of even high titers of endogenously formed NMDAR1-AB of the IgG class to induce any signs of brain inflammation should lead to rethinking current concepts that link NMDAR1-AB to neuropsychiatric disease including encephalitis.

Acknowledgements This work was supported by the Max Planck Society, the Max Planck Förderstiftung, the DFG (CNMPB),

EXTRABRAIN EU-FP7, and the Niedersachsen-Research Network on Neuroinfectiology (N-RENNT). The authors thank all subjects for participating in the study, and the many colleagues who have contributed over the past decade to the extended GRAS data collection.

Author contributions Concept, design, and supervision of the study: HE; Data acquisition/analysis/interpretation: HP, BO, ED, DT, MM, JS, JW, DW, CKS, AR, KS, RT, KMR, StB, YAK, HM, MB, WS, GS, FJK, RM, SB, KAN, JKK, MH, FL, and HE; Drafting manuscript: HE, with the help of BO and HP; Drafting display items: HE and BO, with the help of HP, MM, DT, and JS. All authors read and approved the final version of the manuscript.

Compliance with ethical standards

Conflict of interest WS is a member of the board and holds stocks in Euroimmun AG. HM is a full-time employee of Synaptic Systems GmbH. The remaining authors declare that they have no conflict of interest.

Open Access This article is licensed under a Creative Commons Attribution-NonCommercial-ShareAlike 4.0 International License, which permits any non-commercial use, sharing, adaptation, distribution and reproduction in any medium or format, as long as you give appropriate credit to the original author(s) and the source, provide a link to the Creative Commons license, and indicate if changes were made. If you remix, transform, or build upon this article or a part thereof, you must distribute your contributions under the same license as the original. The images or other third party material in this article are included in the article's Creative Commons license, unless indicated otherwise in a credit line to the material. If material is not included in the article's Creative Commons license and your intended use is not permitted by statutory regulation or exceeds the permitted use, you will need to obtain permission directly from the copyright holder. To view a copy of this license, visit <http://creativecommons.org/licenses/by-nc-sa/4.0/>.

References

- Dalmau J, Tuzun E, Wu HY, Masjuan J, Rossi JE, Voloschin A, et al. Paraneoplastic anti-N-methyl-D-aspartate receptor encephalitis associated with ovarian teratoma. *Ann Neurol*. 2007;61:25–36.
- Dalmau J, Gleichman AJ, Hughes EG, Rossi JE, Peng X, Lai M, et al. Anti-NMDA-receptor encephalitis: case series and analysis of the effects of antibodies. *Lancet Neurol*. 2008;7:1091–8.
- Dalmau J, Lancaster E, Martinez-Hernandez E, Rosenfeld MR, Balice-Gordon R. Clinical experience and laboratory investigations in patients with anti-NMDAR encephalitis. *Lancet Neurol*. 2011;10:63–74.
- Titulaer MJ, McCracken L, Gabilondo I, Armanig T, Glaser C, Iizuka T, et al. Treatment and prognostic factors for long-term outcome in patients with anti-NMDA receptor encephalitis: an observational cohort study. *Lancet Neurol*. 2013;12:157–65.
- Hammer C, Stepniak B, Schneider A, Papiol S, Tantra M, Begemann M, et al. Neuropsychiatric disease relevance of circulating anti-NMDA receptor autoantibodies depends on blood-brain barrier integrity. *Mol Psychiatry*. 2014;19:1143–9.
- Dahl M, Ott C, Steiner J, Stepniak B, Teegen B, Saschenbrecker S, et al. Seroprevalence of autoantibodies against brain antigens in health and disease. *Ann Neurol*. 2014;76:82–94.

- Steiner J, Teegen B, Schiltz K, Bernstein HG, Stoecker W, Bogerts B. Prevalence of N-methyl-D-aspartate receptor autoantibodies in the peripheral blood: healthy control samples revisited. *JAMA Psychiatry*. 2014;71:838–9.
- Zerche M, Weissenborn K, Ott C, Dere E, Asif AR, Worthmann H, et al. Preexisting serum autoantibodies against the NMDAR subunit NR1 modulate evolution of lesion size in acute ischemic stroke. *Stroke*. 2015;46:1180–6.
- Castillo-Gomez E, Kastner A, Steiner J, Schneider A, Hettling B, Poggi G, et al. The brain as immunoprecipitator of serum autoantibodies against N-Methyl-D-aspartate receptor subunit NR1. *Ann Neurol*. 2016;79:144–51.
- Castillo-Gomez E, Oliveira B, Tapken D, Bertrand S, Klein-Schmidt C, Pan H et al. All naturally occurring autoantibodies against the NMDA receptor subunit NR1 have pathogenic potential irrespective of epitope and immunoglobulin class. *Mol Psychiatry*. 2016;22:1776–178.
- Abramson J, Husebye ES. Autoimmune regulator and self-tolerance—molecular and clinical aspects. *Immunol Rev*. 2016; 271:127–40.
- Cohen I, Young D. Autoimmunity, microbial immunity and the immunological holonculus. *Immunol Today*. 1991;12:105–10.
- Coutinho A, Kazatchkine MD, Avrameas S. Natural autoantibodies. *Curr Opin Immunol*. 1995;7:812–8.
- Ehrenreich H. Autoantibodies against the N-methyl-d-aspartate receptor subunit NR1: untangling apparent inconsistencies for clinical practice. *Front Immunol*. 2017;8:181.
- Lobo PI. Role of natural autoantibodies and natural IgM anti-leucocyte autoantibodies in health and disease. *Front Immunol*. 2016;7:198.
- Mader S, Brimberg L, Diamond B. The role of brain-reactive autoantibodies in brain pathology and cognitive impairment. *Front Immunol*. 2017;8:1101.
- Nguyen TT, Baumgarth N. Natural IgM and the development of b cell-mediated autoimmune diseases. *Crit Rev Immunol*. 2016; 36:163–77.
- Coutinho E, Harrison P, Vincent A. Do neuronal autoantibodies cause psychosis? A neuroimmunological perspective. *Biol Psychiatry*. 2014;75:269–75.
- Diamond B, Huerta P, Mina-Osorio P, Kowal C, Volpe B. Losing your nerves? Maybe it's the antibodies. *Nat Rev Immunol*. 2009;9:449–56.
- Hammer C, Zerche M, Schneider A, Begemann M, Nave KA, Ehrenreich H. Apolipoprotein E4 carrier status plus circulating anti-NMDAR1 autoantibodies: association with schizoaffective disorder. *Mol Psychiatry*. 2014;19:1054–6.
- Kreye J, Wenke NK, Chayka M, Leubner J, Murugan R, Maier N, et al. Human cerebrospinal fluid monoclonal N-methyl-D-aspartate receptor autoantibodies are sufficient for encephalitis pathogenesis. *Brain*. 2016;139:2641–52.
- Begemann MGS, Papiol S, Malzahn D, Krampe H, Ribbe K, et al. Modification of cognitive performance in schizophrenia by complexin 2 gene polymorphisms. *Arch Gen Psychiatry*. 2010;67: 879–88.
- Ribbe K, Friedrichs H, Begemann M, Grube S, Papiol S, Kästner A, et al. The cross-sectional GRAS sample: a comprehensive phenotypical data collection of schizophrenic patients. *BMC Psychiatry*. 2010;10:20.
- American Psychiatric Association. (2000) Diagnostic and statistical manual of mental disorders. 4th edn American Psychiatric Press, Washington, DC.
- Wandering KP, Saschenbrecker S, Stoecker W, Dalmau J. Anti-NMDA-receptor encephalitis: a severe, multistage, treatable disorder presenting with psychosis. *J Neuroimmunol*. 2011;231:86–91.
- Boyle MDP, Reis KJ. Bacterial Fc receptors. *Nat Biotechnol*. 1987;5:697–703.
- Pruss H, Leubner J, Wenke NK, Czirkaj GA, Szentiks CA, Greenwood AD. Anti-NMDA receptor encephalitis in the polar bear (*Ursus maritimus*) Knut. *Sci Rep*. 2015;5:1–7.
- Toyka KBD, Pestronk A, Kao I. Myasthenia gravis: passive transfer from man to mouse. *Science*. 1975;190:397–9.
- Schindelin J, Arganda-Carreras I, Frise E, Kaynig V, Longair M, Pietzsch T, et al. Fiji: an open-source platform for biological-image analysis. *Nat Methods*. 2012;9:676–82.
- Berghoff SA, Gerndt N, Winchenbach J, Stumpf SK, Hosang L, Odoardi F, et al. Dietary cholesterol promotes repair of demyelinated lesions in the adult brain. *Nat Commun*. 2017;8:1–15.
- Berghoff SA, Dikig T, Spieth L, Winchenbach J, Stumpf SK, Gerndt N, et al. Blood-brain barrier hyperpermeability precedes demyelination in the cuprizone model. *Acta Neuropathol Commun*. 2017;5:94.
- Wust S, van den Brandt J, Tischner D, Kleiman A, Tuckermann JP, Gold R, et al. Peripheral T cells are the therapeutic targets of glucocorticoids in experimental autoimmune encephalomyelitis. *J Immunol*. 2008;180:8434–43.
- Dere E, Dahl M, Lu D, Hammerschmidt K, Ju A, Tantra M, et al. Heterozygous ambral deficiency in mice: a genetic trait with autism-like behavior restricted to the female gender. *Front Behav Neurosci*. 2014;8:181.
- Dere E, Winkler D, Ritter C, Ronnenberg A, Poggi G, Patzig J, et al. Gpm6b deficiency impairs sensorimotor gating and modulates the behavioral response to a 5-HT2A/C receptor agonist. *Behav Brain Res*. 2015;277:254–63.
- Netrakanti PR, Cooper BH, Dere E, Poggi G, Winkler D, Brose N, et al. Fast cerebellar reflex circuitry requires synaptic vesicle priming by munc13-3. *Cerebellum*. 2015;14:264–83.
- Winkler D, Daher F, Wustefeld L, Hammerschmidt K, Poggi G, Seelbach A et al. Hypersocial behavior and biological redundancy in mice with reduced expression of PSD95 or PSD93. *Behav Brain Res*. 2017. <https://doi.org/10.1016/j.bbr.2017.02.011> (e-pub ahead of print).
- Radyushkin K, El-Kordi A, Boretius S, Castaneda S, Ronnenberg A, Reim K, et al. Complexin2 null mutation requires a 'second hit' for induction of phenotypic changes relevant to schizophrenia. *Genes Brain Behav*. 2010;9:592–602.
- Akdeniz C, Tost H, Streit F, Haddad L, Wust S, Schafer A, et al. Neuroimaging evidence for a role of neural social stress processing in ethnic minority-associated environmental risk. *JAMA Psychiatry*. 2014;71:672–80.
- Jacobson SL, Ross SR, Bloomsmith MA. Characterizing abnormal behavior in a large population of zoo-housed chimpanzees: prevalence and potential influencing factors. *PeerJ*. 2016;4: e2225.
- Stepniak B, Papiol S, Hammer C, Ramin A, Everts S, Hennig L, et al. Accumulated environmental risk determining age at schizophrenia onset: a deep phenotyping-based study. *Lancet Psychiatry*. 2014;1:444–53.
- Maes M, Hendriks D, Gastel AV, Demedts P, Wauters A, Neels H, et al. Effects of psychological stress on serum immunoglobulin, complement and acute phase protein concentrations in normal volunteers. *Psychoneuroendocrinology*. 1997;22: 397–409.
- Nagele EP, Han M, Acharya NK, DeMarshall C, Kosciuk MC, Nagele RG. Natural IgG autoantibodies are abundant and ubiquitous in human sera, and their number is influenced by age, gender, and disease. *PLoS ONE*. 2013;8:4.
- Planaguma J, Leyboldt F, Mannara F, Gutierrez-Cuesta J, Martin-Garcia E, Aguilar E, et al. Human N-methyl-D-aspartate receptor antibodies alter memory and behaviour in mice. *Brain*. 2015;138:94–109.
- Busse S, Brix B, Kunschmann R, Bogerts B, Stoecker W, Busse M. N-methyl-d-aspartate glutamate receptor (NMDA-R)

- antibodies in mild cognitive impairment and dementias. *Neurosci Res.* 2014;85:58–64.
45. Doss S, Wandinger KP, Hyman BT, Panzer JA, Synofzik M, Dickerson B, et al. High prevalence of NMDA receptor IgA/IgM antibodies in different dementia types. *Ann Clin Transl Neurol.* 2014;1:822–32.
 46. Tuzun E, Zhou L, Baehring JM, Bannykh S, Rosenfeld MR, Dalmau J. Evidence for antibody-mediated pathogenesis in anti-NMDAR encephalitis associated with ovarian teratoma. *Acta Neuropathol.* 2009;118:737–43.
 47. Du J, Li XH, Li YJ. Glutamate in peripheral organs: biology and pharmacology. *Eur J Pharmacol.* 2016;784:42–8.
 48. Gerhard DM, Wohleb ES, Duman RS. Emerging treatment mechanisms for depression: focus on glutamate and synaptic plasticity. *Drug Discov Today.* 2016;21:454–64.
 49. Abdallah CG, Adams TG, Kelmendi B, Esterlis I, Sanacora G, Krystal JH. Ketamine's mechanism of action: a path to rapid-acting antidepressants. *Depress Anxiety.* 2016;33:689–97.
 50. Alexander JK, DeVries AC, Kigerl KA, Dahlman JM, Popovich PG. Stress exacerbates neuropathic pain via glucocorticoid and NMDA receptor activation. *Brain Behav Immun.* 2009;23:851–60.
 51. Rubio-Casillas A, Fernandez-Guasti A. The dose makes the poison: from glutamate-mediated neurogenesis to neuronal atrophy and depression. *Rev Neurosci.* 2016;27:599–622.
 52. Nair A, Hunzeker J, Bonneau RH. Modulation of microglia and CD8(+) T cell activation during the development of stress-induced herpes simplex virus type-1 encephalitis. *Brain Behav Immun.* 2007;21:791–806.

Affiliations

Hong Pan¹ · Bárbara Oliveira¹ · Gesine Saher² · Ekrem Dere¹ · Daniel Tapken³ · Marina Mitjans¹ · Jan Seidel¹ · Janina Wesolowski¹ · Debia Wakhloo¹ · Christina Klein-Schmidt³ · Anja Ronnenberg¹ · Kerstin Schwabe⁴ · Ralf Trippe³ · Kerstin Mätz-Rensing⁵ · Stefan Berghoff² · Yazeed Al-Krinawe⁴ · Henrik Martens⁶ · Martin Begemann¹ · Winfried Stöcker⁷ · Franz-Josef Kaup⁵ · Reinhard Mischke⁸ · Susann Boretius⁹ · Klaus-Armin Nave^{2,10} · Joachim K. Krauss⁴ · Michael Hollmann¹⁰ · Fred Lühder¹¹ · Hannelore Ehrenreich^{1,10}

¹ Clinical Neuroscience, Max Planck Institute of Experimental Medicine, Göttingen, Germany

² Department of Neurogenetics, Max Planck Institute of Experimental Medicine, Göttingen, Germany

³ Department of Biochemistry I—Receptor Biochemistry, Ruhr University, Bochum, Germany

⁴ Department of Neurosurgery, Hannover Medical School, Hannover, Germany

⁵ Department of Pathology, Leibniz Institute for Primate Research, Göttingen, Germany

⁶ Synaptic Systems GmbH, Göttingen, Germany

⁷ Institute for Experimental Immunology, affiliated to Euroimmun, Lübeck, Germany

⁸ Small Animal Clinic, University of Veterinary Medicine, Hannover, Germany

⁹ Functional Imaging Laboratory, Leibniz Institute for Primate Research, Göttingen, Germany

¹⁰ DFG Research Center for Nanoscale Microscopy and Molecular Physiology of the Brain (CNMPB), Göttingen, Germany

¹¹ Department of Neuroimmunology, Institute for Multiple Sclerosis Research and Hertie Foundation, University Medicine Göttingen, Göttingen, Germany

A.2 List of publications

Seidel, J.*, Bockhop, F.*, Mitkovski, M.*, Martin, S., Ronnenberg, A., Krueger-Burg, D., Schneider, K., Röhse, H., Wüstefeld, L., Cosi, F., Bröking, K., Schacht, A., Ehrenreich, H. (2020). Vascular response to social cognitive performance measured by infrared thermography: A translational study from mouse to man. *FASEB BioAdvances*, 2, 18-32.

Seidel, J. & Ehrenreich, H. (2018). Frühe Risikoakkumulation und Kriminalität im Erwachsenenalter. *Schweizer Zeitschrift für Psychiatrie & Neurologie*, 04, 7-9.

Mitjans, M.*, **Seidel, J.***, Begemann, M.*, Bockhop, F., Moya-Higueras, J., Bansal, V., Wesolowski, J., Seelbach, A., Ibáñez, M. I., Kovacevic, F., Duvar, O., Fañanás, L., Wolf, H.-U., Ortet, G., Zwanzger, P., Klein, V., Lange, I., Tänzer, A., Dudeck, M., Penke, L., Tebartz van Elst, L., Bittner, R. A., Schmidmeier, R., Freese, R., Müller-Isberner, R., Wiltfang, J., Bliesener, T., Bonn, S., Poustka, L., Müller, J. L., Arias, B., Ehrenreich, H. (2018). Violent aggression predicted by multiple pre-adult environmental hits. *Molecular Psychiatry*, 24(10), 1549-1564.

Ursini, G., Punzi, G., Chen, Q., Marengo, S., Robinson, J. F., Porcelli, A., Hamilton, E. G., Mitjans, M., Maddalena, G., Begemann, M., **Seidel, J.**, Yanamori, H., Jaffe, A. E., Berman, K. F., Egan, M. F., Straub, R. E., Colantuoni, C., Blasi, G., Hashimoto, R., Rujescu, D., Ehrenreich, H., Bertolino, A., Weinberger, D. R. (2018). Convergence of placenta biology and genetic risk for schizophrenia. *Nature Medicine* 24, 792-801.

Pan, H.*, Oliveira, B.*, Saher, G.*, Dere, E., Tapken, D., Mitjans, M., **Seidel, J.**, Wesolowski, J., Wakhloo, D., Klein-Schmidt, C., Ronnenberg, A., Schwabe, K., Trippe, R., Mätz-Rensing, K., Berghoff, S., Al-Krinawe, Y., Martens, H., Begemann, M., Stöcker, W., Kaup, F. J., Mischke, R., Boretius, S., Nave, K. A., Krauss, J. K., Hollmann, M., Lühder, F., Ehrenreich, H. (2019). Uncoupling the widespread occurrence of anti-NMDAR1 autoantibodies from neuropsychiatric disease in a novel autoimmune model. *Molecular Psychiatry*, 24, 1489-1501.

*Equally contributing authors